THIA-ARENES AS POLLUTION SOURCE TRACERS IN URBAN AIR PARTICULATE

By

L.M. ALLAN, B.Sc.

A Thesis

Submitted to the School of Graduate Studies

in Partial Fulfilment of the Requirements

for the Degree

Doctor of Philosophy

McMaster University

THIA-ARENES AS POLLUTION SOURCE TRACERS IN URBAN AIR

DOCTOR OF PHILOSOPHY (1999) McMaster University

(Chemistry) Hamilton, Ontario

TITLE: Thia-Arenes as Pollution Source Tracers in Urban Air Particulate

AUTHOR: Laurie M. Allan, B.Sc. (McMaster University)

SUPERVISOR: Professor B.E. McCarry

NUMBER OF PAGES: xxiv, 214

ABSTRACT

A method to distinguish coke oven emissions from diesel exhaust emissions in ambient samples has been developed. Sulfur-containing polycyclic aromatic compounds (thia-arenes) and polycyclic aromatic hydrocarbons (PAH) were determined in source samples, standard reference samples and ambient samples using gas chromatography/mass spectrometry.

A total of 92 ambient respirable air particulate samples that were collected at four locations upwind and downwind of the steel industries in Hamilton, Ontario in 1995, were analyzed for their total particulate mass, 15 PAH and a number of thia-arene compounds. The steel industries were found to contribute the majority of PAH pollution in Hamilton air particulate above the urban background of approximately 1.5 ng/m^3. Particulate concentrations in Hamilton air indicate several major sources of particulate, including vehicle emissions.

Profiles of alkylated dibenzothiophene isomers, 234 amu thia-arene isomers and 258 amu thia-arene isomers were examined in Hamilton air particulate, Toronto air particulate, coke oven condensate, Diesel Exhaust Particulate Standard Reference Material (SRM 1650), Urban Dust Standard Reference Material (SRM 1649) and Coal Tar Standard Reference Material (SRM1597). Selected thia-arenes were also examined in a variety of other environmental samples. Principal component analysis (PCA) was

used to select suitable thia-arene tracer compounds and examine the relationship between a variety of environmental samples.

A thia-arene index was developed using a combination of ratios of selected 234 amu and 258 amu isomers. The suitability of thia-arene tracers for distinguishing coke oven emissions from diesel emissions is demonstrated with Hamilton air particulate and source samples. Ambient samples with particulate bound PAH levels below 1.6 ng/m^3 were classified as petrogenic in origin in all cases, while samples with PAH levels above about 3.6 ng/m^3 were shown to have significant coke oven impacts. The quality of the thia-arene criteria is discussed in comparison to PAH criteria found in the literature.

Four gas chromatography stationary phases were evaluated for the separation of thia-arenes and PAH. Retention index values are reported for 49 PAH and 66 thia-arene compounds. The 50% phenyl-substituted methylpolysiloxane stationary phase provided the best overall separation of thia-arenes and PAH.

ACKNOWLEDGEMENTS

I wish to express my gratitude to my supervisor, Dr. Brian E. McCarry, who always made time to provide guidance and support for this project. I am also grateful to the other members of my supervisory committee, Dr. P. Brassard and Dr. J.K. Terlouw, for sharing their knowledge and providing advice throughout the course of my study. Helpful discussions with Dr. W.H. Morris and Dr. D.W. Bryant are also greatly appreciated.

The study of such a large variety of samples would not have been possible without the help of Ms. Adrienne Boden, Dr. Chris Marvin, Dr. Arnold Legzdins, Ms. Tanya Mayer of Canada Center for Inland Waters, Mr. Paul Thompson of the Ontario Ministry of Environment, and the Atmospheric Environment Service who either assisted with sample collection or provided sample extracts. I also wish to thank Dr. M.L. Lee of Brigham Young University, Provo, UT for his generous donation of authentic thia-arene standards.

I am thankful for the opportunity to work in a supportive lab group with John Villella, Arnold Legzdins, Adrienne Boden, Chun-ling Li, Krista Barfoot Kinsie, Suzanne Ackloo and Lena Andrew.

Maps created by Mr. Norm Finkelstein are very much appreciated. Technical and financial provided by the Ontario Ministry of the Environment is gratefully acknowledged.

TABLE OF CONTENTS

LIST OF FIGURES

LIST OF TABLES

LIST OF MAPS

LIST OF ABBREVIATIONS

17DMP	1,7-dimethylphenanthrene
26DMP	2,6-dimethylphenanthrene
AES	Atmospheric Environment Service
amu	atomic mass unit
B[def]DBT	benzo[def]dibenzothiophene
B12T	benzo[b]naphtho[1,2-d]thiophene
B21T, BN21dT	benzo[b]naphtho[2,1-d]thiophene
B23T	benzo[b]naphtho[2,3-d]thiophene
BAA	benz[a]anthracene
BAP, B[a]P	benzo[a]pyrene
BBF	benzo[b]fluoranthene
BCP	benzo[c]phenanthrene
BEP	benzo[e]pyrene
BFs	benzofluoranthenes
BGP	benzo[ghi]perylene
BJF	benzo[j]fluoranthene
BKF	benzo[k]fluoranthene
C	coke oven designation
C.I.	confidence interval

C1	methyl
C2	dimethyl
C3	trimethyl
CCIW	Canada Center for Inland Waters
CHR	chrysene
cm	centimeter
CO	coke oven emissions
COR	coronene
CPP	cyclopenta[cd]pyrene
D	diesel designation
DBT	dibenzothiophene
DCA	dibenz[a,c]anthracene
DE	diesel emissions
DiMePASH	dimethyl substituted thia-arene
DW	downwind
EI	electron impact
EPA	Environmental Protection Agency
FPD	flame photometric detector
ft^3	cubic feet
GC	gas chromatography

GC/MS	gas chromatography/mass spectrometry
hr	hour
i.d.	internal diameter
IND	indeno[1,2,3-cd]pyrene
km	kilometer
L	liter
LC	liquid chromatography
LC50	concentration that will kill 50% of the test subjects
M	molecular mass
m	meter
m/z	mass to charge ratio
m^3	cubic meter
MCPBA	m-chloroperoxybenzoic acid
MePASH	methyl substituted thia-arene
mg	milligram
mg	microgram
min	minute
mL	milliliter
mL	microliter
mm	millimeter

mm	micrometer
MOE	Ontario Ministry of the Environment
ng	nanogram
NIST	National Institute of Standards and Technology
nm	nanometer
NWRI	National Water Research Institute
PAC	polycyclic aromatic compound
PAH	polycyclic aromatic hydrocarbon
PASH	sulfur-containing polycyclic aromatic compound
PCA	principal component analysis
PER	perylene
pg	picogram
PLS	partial least squares
PM_{10}, PM10	respirable particulate matter, < 10 micrometers in diameter
R	correlation coefficient
R234	234 amu thia-arene ratio
R258	258 amu thia-arene ratio
RBG	Royal Botanical Gardens
RI	retention index
RSD	relative standard deviation

S	indicates filter was analyzed but not classified as upwind or downwind
SIM	selected ion monitoring
SRM	Standard Reference Material
TI	thia-arene index
TIC	total ion chromatogram
TSP	total suspended particulate
US, U.S.A.	United States of America
UV	ultraviolet
UW	upwind
v/v	volume to volume ratio

1.0 INTRODUCTION

1.1 Major Emission Sources in Hamilton, Ontario, Canada

Hamilton, Ontario is a large industrial city located on the southwest end of Lake Ontario. Two major steel manufacturing companies with coking operations are situated on the north end of the city next to a large natural harbour. The city is highly populated (population: 320,000) and located between two major highways. Emissions from the steel industries and motor vehicles are major sources of ambient air pollution in Hamilton. Levels of airborne pollutants in this area have caused concern for some time.

A significant correlation was found between industrial air pollution and morbidity and mortality rates for respiratory diseases, lung cancer and some other cancers in the Northeast area of Hamilton [1]. Studies on excess cancer deaths in the late 1960s revealed highest mortality rates closest to the main sources of industrial emissions in Hamilton [1]. In the 1970s, standardized lung cancer mortality ratios, which account for age, sex, and smoking habits, were approximately 15% higher in the industrial area of Hamilton than in the residential area on the escarpment [2]. Hospital admissions in Hamilton for acute respiratory disease were found to be associated with levels of particulate in the air in areas closest to the industry [3].

The industrial area also contains heavy traffic particularly from large diesel-fueled trucks. Many of the same types of pollutants emitted from the steel industries are also

emitted from motor vehicles. It would be useful to determine the extent to which traffic emissions contribute to pollutant levels in ambient air near the industries.

One class of pollutants, the polycyclic aromatic hydrocarbons (PAH), contain compounds that are known carcinogens. PAH are chemically composed of benzene rings fused together on one or more sides. The chemical structures of a variety of PAH are shown in Appendix I. PAH exist in the environment as complex mixtures containing many structural isomers and alkylated derivatives. PAH are widespread environmental contaminants produced by the combustion of fossil fuels for industry, residential heating, power generation, incineration, and vehicle engines [4]. Concentrations of PAH were significantly higher in Hamilton air than in the air of New York City or Los Angeles [5,6]. Extracts of Hamilton air particulate [7-9] and Hamilton Harbour sediment [10] were found to be mutagenic.

Studies of sediments in other areas, also located near industries, have suggested that PAH contamination occurs mainly by atmospheric deposition rather than from runoff or industrial effluent [11,12]. Airborne pollutants may also travel hundreds of miles, contaminating remote environments. Toxicity of pollutants in the air is a major concern because humans receive direct exposure to the pollutants through inhalation. For these reasons, the present study will focus mainly on ambient air pollution.

Efforts made to reduce emissions from industries and vehicles are ongoing. Improvements are currently being made to emission control technology, coke oven design and maintenance practices to reduce PAH emissions from the steel industries [13].

The Province of Ontario has recently developed a program designed to regulate and reduce emissions from motor vehicles.

1.2 Source Apportionment

1.2.1 General Approach

The development of air pollution control regulations requires an understanding of the origin of pollutants and the relative contribution of individual sources to ambient pollutant levels. The main objective of this thesis is to develop a source apportionment model that can be used to differentiate coke oven emissions from vehicle emissions in Hamilton air particulate, based on differences in the chemical profiles of these emission sources.

Two basic approaches to air pollution modeling are source-oriented and receptor-oriented [14]. The source-oriented approach, also referred to as a dispersion model, uses source emission rates and dispersion factors to calculate pollutant concentrations at a receptor located some distance from the source. Traditionally, government agencies have used emissions inventories as input for dispersion models that estimate ambient concentrations [15,16]. Source oriented models do not adequately describe the complicated random nature of dispersion in the atmosphere and do not include fugitive emissions or emissions from accidental events [17]. Emission inventories quickly become outdated as changes are made to fuel composition, emission controls and analytical technology.

Receptor models use observed ambient pollutant concentrations to apportion the pollutants between several sources. Ambient concentrations of pollutants are monitored at the receptor, or sampling site, and these observations are used to calculate the contribution of individual sources. Receptor-oriented models have recently gained more interest because they do not require previous knowledge of the source emission profile. Receptor models are commonly used in conjunction with dispersion models to increase the reliability of source apportionment [15]. This approach, combining source and receptor modeling will be adopted for the present study. Chemical data from source samples and receptor samples will be used to characterize pollutant sources.

1.2.2 Chemical Tracers

If sources of pollutants contained unique tracer compounds, it would be possible to characterize pollution sources. Trace elements have been used to characterize sources, such as the use of lead as a tracer for gasoline emissions [19-21]. Since the use of lead-containing gasoline additives has been discontinued and many sources do not emit trace elements, researchers have begun to rely on organic chemical data for source characterization [22]. Polycyclic aromatic hydrocarbons (PAH) have been popular as source tracers. A large amount of data exists for PAH because many of these compounds are mutagenic and/or carcinogenic.

1.2.3 PAH as Source Tracers

Individual PAH and PAH ratios have been suggested and used as potential source apportionment tracers for ambient air analysis [20-34]. A summary of these individual PAH and PAH ratios is presented chronologically in Tables 1.1 and 1.2, respectively. In early reports, individual PAH compounds were identified in source samples and proposed as source indicators, however, it was soon realized that the majority of PAH were common to multiple sources. Scientists then recognized that although sources had common PAH compounds, the relative amounts of various isomers often differed. Patterns of PAH in several sources have been published as source inventories [35,36]. Variations in source profiles have been used to try to distinguish between different pollution sources. Ratios between specific PAH compounds were examined and proposed as source tracers. Problems including volatility, reactivity and source variability complicate this approach. These and other difficulties encountered with the use of PAH ratios in source apportionment studies will be discussed in Section 1.2.4.

Principal component analysis (PCA) is another popular receptor modeling technique used with ambient PAH concentrations to identify major sources of emissions and select source tracers [25,37-45]. PCA is used to extract information from data sets containing concentrations of several PAH measured in a large number of samples (typically 40-60 samples). This technique works on the basis that a smaller number of variables can be chosen to explain the majority of variance in a data set. PCA extracts information in the form of components that are linear combinations of the measurements in the data set (e.g., PAH concentrations). The components are independent of one

Table 1.1. Summary of individual PAH compounds suggested as source tracers in ambient air.

PAH Indicator[1]	Sources Studied	No. of Samples		Location (Year)	Ref.
		Source	Ambient		
COR	traffic		4	Los Angeles (1973)	20
Alkylated PAH DBT B[def]DBT	combustion of coal, wood, and kerosene	3	2	Indianapolis Boston (1977)	30
BN21dT CPP BCP BGP COR	diesel exhaust gasoline exhaust	4		(1980)	34
BGP COR	traffic		4	New Jersey (1981)	21
CPP BGP COR	traffic			(1982)	33
BBF BKF	diesel exhaust	2		California (1984)	24
CHR BKF BGP	diesel comb. gasoline comb.	2		California (1994)	23

[1]For full PAH name refer to List of Abbreviations

Table 1.2. Summary of PAH ratios suggested as source tracers in ambient air.

PAH Ratio[1]	Sources Studied	No. of Samples		Location (Year)	Ref.
		Source	Ambient		
BGP:BAP	coal combustion traffic		16	New York, Essen, Beijing (1983)	32
BKF:BGP IND:BGP	traffic	2		California (1984)	31
ln(1+BFs/PAH)- ln(1+BGP/PAH)	domestic fires traffic	21	27	New Zealand (1985)	25
BAP:BEP BGP:BEP BCP:BEP BKF:BEP	coke oven/coal comb. traffic	35	1	(1986)	22
BGP:BAP BKF:BGP IND:BGP	traffic		22	Rio de Janiero (1987)	26
BKF:IND BGP:IND	traffic	10	7	Rio de Janeiro (1989)	28
BGP:COR BBF:COR	gasoline comb. diesel comb. wood comb. gasoline comb. diesel comb. wood comb.	22		(1993)	29
17DMP:26DMP	wood comb. traffic	50	36	Boise (1995)	27

[1]For full PAH name refer to List of Abbreviations

another and, in receptor modeling, often represent pollution sources. The use of PCA in receptor modeling has been described in detail elsewhere [17,46-51].

Past PCA receptor models have indicated that the majority of the variability in the ambient sample PAH profile was due to volatility of low molecular mass isomers and reactivity of certain PAH, rather than differences in source profiles [40,52]. The inclusion of additional data, such as trace element concentrations, with PAH concentrations was often required to adequately distinguish between pollution sources [24,39]. Alternatively, when a relationship between PAH concentrations and pollution sources was indicated by PCA, a useful model that could be applied to a single sample was not developed.

New criteria continue to appear in the literature due to the limitations associated with current source apportionment models. There is no general consensus as to the best criteria to use for PAH-based source apportionment models. Although many criteria have been suggested as possible source indicators, studies rarely evaluate the suggested criteria or result in the development of a useful model that can be applied elsewhere. Solid criteria need to be established for the determination of source identity.

PCA will be investigated in the present study as a tool for the selection of source apportionment criteria. A useful model will be developed that can be applied to other samples. The research presented in this study will differ from past work in that a different class of polycyclic aromatic compounds will be examined. This class of compounds, the thia-arenes, will be introduced in Section 1.3.

1.2.4 Difficulties with Source Apportionment using PAH

It is important to understand the difficulties encountered in previous source apportionment studies before attempting to develop a new model. The limitations of past source apportionment models using PAH as source tracers will be outlined in the following subsections. Structures for compounds discussed in the text can be found in Appendix I.

1.2.4.1 Certain models only work when one major source is present

In the earliest source apportionment studies, individual PAH were used as source tracers. Concentrations of coronene and benzo[ghi]perylene correlate with traffic emissions and have been used as source tracers to estimate traffic density [20-23,33]. This approach was found later to be useful only when traffic is the major pollution source due to the presence of coronene and benzo[ghi]perylene in coal and oil combustion emissions. Daisey *et al.* [22] suggested the use of benzo[b]naphtho[2,1-d]thiophene (B21T) as a tracer for diesel emissions. This tracer was used in PCA to help distinguish between diesel and gasoline combustion emissions [42]. B21T is also produced by the combustion of coal, so it can not unambiguously be attributed to diesel exhaust when emissions from coal sources are present [33]. It was expected that B21T would occur in both diesel exhaust and coke oven emissions in the Hamilton area. Benzo[b]fluoranthene and benzo[k]fluoranthene levels increased with increasing diesel component in the traffic and were suggested by Hering *et al.* [24] as possible tracers for diesel exhaust. Due to the widespread occurrence of PAH, individual compounds are not usually suitable for

differentiating pollution sources. Often it is necessary to examine the whole profile of PAH.

Source profiles have been compared by normalizing each PAH concentration to the concentration of one standard PAH compound [22,23,53]. PAH concentrations are typically, but not exclusively, normalized to benzo[e]pyrene, a stable and non-volatile PAH. This led to the investigation of several PAH ratios and some were found to vary from source to source. Daisey *et al.* [26], Miguel *et al.* [31] and Greenberg *et al.* [54] report consistent ratios of benzo[ghi]perylene to benzo[a]pyrene, benzo[k]fluoranthene to benzo[ghi]perylene and indeno[1,2,3-cd]pyrene to benzo[ghi]perylene in areas where vehicle emissions are the principal source of PAH. Again, these ratios were found to be appropriate source tracers when traffic was the only PAH source present [28].

1.2.4.2 Although differences exist in source profiles, ambient samples appear similar

Source samples have been used to determine characteristic PAH profiles in combustion emissions from motor vehicles, wood, coal and kerosene [27,30]. However, characteristic profiles are sometimes difficult to identify in ambient samples. Greenberg *et al.* [54] measured PAH concentrations at three urban sites in New Jersey near a variety of different industries during winter and summer months. Profiles of PAH were not found to vary significantly from site to site or between seasons. Similarly, Cretney *et al.* [25] report almost identical PAH profiles in air particulate from three locations in New Zealand impacted by different pollution sources. De Raat *et al.* [52] found only a slight

indication for the influence of sources on PAH profiles at five locations in the Netherlands. Remarkably similar PAH profiles were reported by Simcik *et al.* [55] in Lake Michigan sediments from different locations despite great variability in source profiles.

1.2.4.3 There may be variability among a single source.

It has been observed that profiles for some sources are highly variable, particularly for low-temperature combustion sources [46]. Emission rates of PAH from vehicles are dependent on engine type, driving conditions, and fuel composition [36,56]. Coal used for residential heating was found to produce more PAH than coal used for coal-fired power plants [57]. High temperature combustion of fossil fuels favours the formation of unsubstituted aromatic compounds [58]. A reduction in the proportion of methyl-substituted PAH was also reported with increased temperature in coke ovens [59].

The origin of PAH in combustion emissions is controversial. Some studies suggest that PAH in combustion emissions are mainly produced in the combustion process, while other studies indicate preservation of PAH from the original fuel. Westerholm *et al.* [43] found that although greater than 99% of the PAH in diesel fuel were found to decompose in the combustion process, PAH content in fuel was the major factor influencing PAH emissions. Brown *et al.* [36] and Candeli *et al.* [56] also agreed that increasing emissions of PAH were observed with increasing PAH content of the fuel [36,56]. This is a concern because the aromatic content was increased in some fuels after regulations reduced the content of lead in gasoline [60]. PAH in emissions can also be

formed from the smaller aromatic compounds during the combustion process (pyrosynthetic reactions). A study using radiolabelled B[a]P found that >99% of B[a]P in diesel fuel was combusted, consistent with the previous studies, but also found that the majority of B[a]P in the exhaust was derived from the unburned fuel [61]. Regardless of the origin of the PAH, there is clearly an increase in PAH content in emissions with increasing PAH content of the fuel.

1.2.4.4 Source samples may not be representative

It is difficult to obtain a representative sample from mobile pollution sources such as cars and trucks. Traffic emissions are typically represented by air sampled in tunnels [23,24,27,28]. These samples are not exposed to sunlight and may not be representative of ambient air. Humidity, temperature, sunlight and particle organic composition have been shown to influence the lifetime of PAH bound to air particulate [62,63].

1.2.4.5 Reactivity or volatility of compounds may influence the model.

Differences exist in the reactivities of various PAH compounds. The use of reactive PAH in source apportionment studies may lead to inaccurate results. Cyclopenta[cd]pyrene has been identified as a tracer for vehicle emissions, but the usefulness of this compound in source apportionment studies is limited due to the high reactivity of the compound [25]. Benzo[a]pyrene and benz[a]anthracene are also very reactive, and for this reason, many studies have eliminated these species from the analysis. Pistikopoulos *et al.* [64] and Li *et al.* [29] have applied a correction to the PAH

profile for the reactive species to allow for the use of reactive species in a source apportionment model. It was pointed out that to estimate the lifetime of a PAH it is also important to consider the concentration of the reacting species, which can be difficult to measure [29].

Several studies have investigated chemical reactivity of PAH in the laboratory and show that PAH are susceptible to chemical oxidation by ozone [65,66], nitration [67,68] and photochemical degradation [62]. Researchers agree, however, that true atmospheric conditions cannot be simulated in the laboratory so it is difficult to predict the reactivity of PAH in ambient conditions. Photochemical degradation of PAH was found to depend on the substrate to which the PAH is adsorbed [54,69,70]. Substrates that were dark in colour inhibited photochemical degradation which suggests that this process might not be as significant for PAH adsorbed to air particulate.

Consistency of PAH profiles at different sites or during different seasons has led some researchers to conclude that PAH decomposition in the atmosphere is negligible [54,64]. Other studies have found variability in the ratio of reactive to non-reactive species with particle age, but agree it is difficult to determine which factors, reactivity, volatility, source composition or sampling artifacts are responsible for the variability [40,52].

It is difficult to assess the degree to which atmospheric transformations affect the PAH profile of ambient samples, however, the potential for preferential losses of certain PAH exists and should not be ignored. The relative reactivity of many PAH have been estimated using half-lives [31,35,62,67], ionization potentials [71] and bond localization

parameters [54,71]. Half-lives between one hour and several weeks have been measured in laboratory studies for various PAH. Air particulate may travel hundreds of miles over a period of weeks before reaching the sampler so this time frame is significant.

The distribution of PAH between the particulate and vapour phases will also affect the PAH profile determined for air particulate. The distribution of PAH between vapour and particulate depends on ambient temperature, particle age, meteorological conditions and sampling conditions [54,60,72,73]. PAH concentrations on particulate were found to be 4-6 times higher in the winter than the summer months, but it was uncertain if this was due to volatility effects or differences in emissions or reactivity [54]. It is generally agreed that PAH with four or fewer rings may partition significantly into the vapour phase while five-ring PAH are found almost exclusively in the particulate phase [52]. Many studies have restricted the analysis of particulate-bound PAH to compounds with four or more rings to minimize the effect of volatility on PAH profiles.

1.2.4.6 Few studies account for coal combustion.

Few studies have developed source apportionment models that account for coal combustion, even though the two main sources of PAH in air have been identified as the burning of coal and the combustion of oil-based fuels [60]. In areas where coal combustion is absent, vehicle emissions are often identified as the major source of PAH. Coal combustion is still a major source of pollution in areas where it is used in power plants or coke ovens. Coal combustion was reported to be the major source of PAH in Beijing, China [32], and Indianapolis, U.S.A. [30]. Based on this information, emissions

from coke ovens in Hamilton are expected to be a significant source of PAH and must be accounted for by the source apportionment model.

1.2.4.7 Relevance of limitations to the current study

The use of chemical tracers for source apportionment purposes is extremely complex. The work presented in this thesis was not intended to fully address each of the limitations presented in this section. The source apportionment model developed in this study will attempt to minimize some of these problems by the following:

- The presence of more than one pollution source will be considered.
- Profile differences will be evaluated in ambient samples and source samples.
- More than one sample of a single source type will be analyzed when possible to examine source variability
- Efforts will be made to obtain representative source samples.
- Volatility effects will be minimized by choice of compounds in the development of the source apportionment model.

1.3 Thia-Arenes (Sulfur-Containing PAH, or PASH)

In the present study, the class of polycyclic aromatic compounds proposed for a source apportionment study are the thia-arenes. Thia-arenes are polycyclic aromatic

hydrocarbons that contain a thiophene ring. Structures and names for a large number of thia-arenes can be found in Appendix I.

1.3.1 Sources

Thia-arenes have been identified in crude oils [74-78], lubricating oils [79], shale oils [78,80,81], petroleum vacuum residue [82], carbon black [83-86], diesel exhaust particulate matter [33,87,88], cigarette smoke [89], coal and coal-derived products [30,78,81,90-102], and coal-fired residential stove emissions [103,104]. Thia-arenes are emitted to the environment by the combustion of sulfur-containing fuels, such as coal or diesel fuel, and have been detected in sediments [105-108], marine organisms [107] and air particulate [26,109].

I chose the sulfur heterocycles as source tracers because they are produced by fewer sources than PAH. The two major pollution sources studied in this thesis, coke oven emissions and motor vehicle emissions, are expected to contain significant levels of thia-arenes due to the presence of thia-arenes in coal and diesel fuels. Other sources of PAH that do not emit thia-arenes, such as gasoline exhaust, are not expected to interfere with the source apportionment model. Thia-arenes were not detected in gasoline-fueled automobile emissions [34,42] or emissions from the combustion of kerosene or wood [30]. The combustion of oil or wood for space heating has been shown to contribute to the total PAH burden but the contribution was negligible in summer months [110].

1.3.2 Interest in Thia-arenes

In the past, interest in thia-arenes has arisen mainly from the potential mutagenic and/or carcinogenic nature of these compounds [27,28,35,64], and the desire to remove these compounds from fuels [29,30]. The presence of sulfur in heavy oils interferes with the desulfurization process, and contributes to environmental sulfur dioxide concentrations so it is beneficial to remove sulfur compounds from fossil fuels [82,98]. Thia-arenes have not been studied as widely as PAH so there is a need to characterize sulphur compounds in fossil fuels.

The toxicity of thia-arenes has been investigated due to the known carcinogenicity and mutagenicity of certain homocyclic PAH. An early report suggested that high carcinogenic activity of certain thia-arenes, when tested on mice, was due to the presence of a phenanthrene bridge (the 9,10-double bond in the phenanthrene moiety of the molecule) rather than the presence of the sulfur heteroatom [111]. Eastmond *et al.* compared a series of thia-arenes to structurally similar PAH for toxicity in *Daphnia magna* [112]. Thia-arenes tested generally had lower LC_{50} values (higher toxicity) than the corresponding PAH.

After the development of the Ames assay [113,114], several thia-arene isomers were tested for mutagenic response. One 3-ring thia-arene isomer, and seven 4-ring thia-arene isomers showed significant mutagenic responses in the Ames test [115]. Phenanthro[3,4-b]thiophene gave the highest response, comparable to that of widely-studied carcinogen, benzo[a]pyrene. McFall *et al.* [116] determined high mutagenic responses from 4- and 6-methylbenzo[b]naphtho[2,1-d]thiophene, but the mutagenic

responses were lower than that of benzo[a]pyrene. Nishioka *et al.* determined that the presence of a sulfur heteroatom had little effect on mutagenicity of polycyclic aromatic compounds [117]. These studies indicate that certain thia-arene isomers have toxic properties comparable to those of certain PAH isomers. Thia-arenes, however, are found at much lower levels in the environment (many are < 1% relative to the concentration of PAH) so their toxicity is generally not as great a concern.

1.4 Analysis of Thia-Arenes and PAH in Air Particulate

1.4.1 Sampling

Polycyclic aromatic hydrocarbons exist in the vapour phase and adsorbed to particles in the air. An air sample is collected by pumping air through a sampling device containing a filter or solid sorbent. Particles are trapped by the filter while vapour-phase pollutants are trapped by the solid sorbent. Gas-particle partitioning of PAH is dependent on ambient temperature, particle age, meteorological conditions, and sampling conditions [54,60,72]. The sampling and analysis of airborne PAH has recently been reviewed [124,125]. Only particulate-bound PAH will be considered in this study.

The size of the particles that transport PAH in the air is also important. Only particles below about 7 μm are transported into human lungs and are considered a health hazard [5]. Samplers used in this study filtered out particulate less than 10 μm in diameter to result in the collection of particles in the respirable size range.

PAH are not uniformly adsorbed over the entire particle size range. Katz and Chan [5] found up to 89% of PAH on particles less than 3.3 μm. Data published by

Poster *et al.* [126] were in agreement with the study by Katz and Chan. Venkataraman and Friedlander [127] observed a bimodal distribution of PAH on particles with peaks in the 0.05-0.12 μm and 0.5-1.0 μm size ranges. A greater proportion of the smaller PAH were found in the larger particle size range which may be explained by differences in their sources or by differences in volatility. Allen *et al.* [128] found a higher concentration of high molecular mass PAH in rural air particulate than in urban air particulate indicating a slow mass transfer process. Miguel *et al.* [129] observed a source-dependent distribution of PAH on particles of various size ranges. All studies reviewed indicate that the PAH are predominately found on the low or sub-micron particle size range and will be collected by the PM_{10} samplers used in this study.

1.4.2 Separation

Gas and liquid chromatography are both popular methods for the analysis of PAH [130-133]. A number of GC and LC analytical methods have been reported for the analysis of PAH in air particulate [134-140]. Liquid chromatographic retention characteristics of thia-arenes have been investigated on both normal- and reversed-phase columns [141]. Gas chromatographic retention characteristics of thia-arene isomers have also been studied [142]. Gas chromatography can provide higher resolution than liquid chromatography, but LC allows greater optimization of method parameters. Gas chromatography was chosen for the analysis of thia-arene isomers in this study.

1.4.2.1 Gas chromatography retention indices

The presence of a sulfur atom in the molecular structure of thia-arenes leads to a greater variety of isomers than exist for the homocyclic PAH. Identification of thia-arene isomers is difficult because standards are not available for many of the isomers. Retention indices are helpful for the identification of compounds when standards do not exist, because retention indices are more reproducible than elution times. The retention index of a compound is calculated based on the elution time of the compound relative to selected reference compounds. This reduces the variability of results due to differences in column manufacturing and allows interlaboratory comparisons to be made. Reference compounds are chemically similar to the solute to produce consistent retention indices [143].

Several studies have investigated the relationship between PAH structure and chromatographic retention to enable the prediction of retention indices when pure standards are not available [144-145]. The structure-retention relationship of thia-arenes has not been widely studied but the retention behaviour of thia-arenes is found to be different than that of PAH [90]. A GC retention index system has been developed for the identification of PAH, based on the PAH reference compounds naphthalene, phenanthrene, chrysene and picene [143]. A large number of PAH and thia-arene compounds were analyzed and assigned retention indices. This retention index system has been applied to the analysis of lubricating oils [146], diesel fuel [87,147], cigarette smoke [89], coal products [81,90,92,94,97], and shale oils [81,92]. A similar system was

introduced, using a series of benzene homologues of thiophene as reference compounds, for the analysis of thia-arenes by sulfur-specific detection [148].

Some of the PAH retention index data reported in the literature were produced almost 20 years ago. Developments have since been made in the production of GC columns and the types of stationary phases now available commercially. There is a need to determine retention indices on currently available columns, and new stationary phases need to be evaluated for their ability to separate PAH and thia-arenes. In the present study, five different capillary columns will be evaluated for the separation of PAH and thia-arenes. Retention indices will be calculated for standard compounds and compared to data previously reported in the literature. The column that provides the best overall separation of the thia-arenes will be selected for determination of source apportionment criteria.

1.4.2.2 Separation from interferences in complex mixtures

Thia-arenes are typically found at low levels in environmental samples compared to PAH so it is necessary to either separate the thia-arenes from the PAH before analysis, or selectively detect the thia-arenes in the presence of the more abundant PAH. Several fractionation procedures have been reported for the separtion of thia-arenes from PAH.

An oxidation-reduction procedure [81,149] gave reasonable yields for thia-arenes with fusion on two or three sides of the thiophene ring, but thia-arenes with fusion on only one side of the ring gave very low recoveries due to the occurrance of additional oxidation reactions which were not reversed with the subsequent reduction, or reduction

of the non-fused side to produce dihydrothiophenes [81,92]. Several ligand exchange chromatography procedures have been developed using copper [150], silver [151], or palladium [152-154] salts to separate PASH from PAH. The evaluation of these procedures revealed difficulties in separating PASH with terminal thiophene rings or PASH containing more than three rings. None of these procedures have resulted in a complete separation of the thia-arenes from PAH. The present study will employ selective detection techniques for the analysis of thia-arenes.

1.4.3 Detection

Sulfur-specific detectors have been developed for use with the gas chromatograph. The flame photometric detector (FPD) has been popular, but it suffers from the disadvantages of non-linearity and hydrocarbon quenching effects [155-156]. The sulfur chemiluminescence detector [157-158], and the atomic emission detector [80,159] both provide linear responses. The mass selective detector has the advantage of providing molecular mass and structural information for thia-arenes. The mass selective detector was chosen for the analyses in the present study.

Electron impact (EI) mass spectra of thia-arenes show intense molecular ions (M+). EI mass spectra of parent thia-arenes contain fragmentation peaks at mass (M-45) due to the loss of a (CH=S)- unit and mass (M-32) caused by the elimination of the sulfur heteroatom [160]. Monomethyl-substituted thia-arenes produce these fragments shifted by one mass unit, i.e., (M-46) and (M-33). The fragmentation pattern can be helpful for the identification of thia-arenes. Other ions commonly observed in thia-arene spectra are

(M-2) due to elimination of a hydrogen molecule, and doubly charged (M+/2e) ions. The mass spectrum of benzo[b]naphtho[2,1-d]thiophene is shown in Figure 1.1.

1.5 Thia-Arenes as Source Tracers

The few previous studies that used thia-arenes as source markers examined sediments and crude oils. Alkylthiophenes have been used as source tracers in sediments [118-120] and as indicators for the maturity of crude oils [121,122]. Thiophenes with long alkyl chains were found in sediments and immature oils, but in mature oils, the thiophenes have been incorporated into larger aromatic structures with much shorter side chains [121]. A wide variation in thia-arene profiles was observed in different oils [123]. Douglas *et al.* [123] found that C_2-DBT and C_2-phenanthrene degrade at the same rate, and that the ratio of the two species may be used as a source indicator [123].

Sporstol *et al.* [119] conducted a study in Norway in the early 1980s using PAH profiles to distinguish coal soot from petroleum pollution in sediments. Profiles for C_1 to C_3 alkylated dibenzothiophene isomers were reported in these sediments and the two source samples, relative to dibenzothiophene. Similar profiles were observed in the two source samples, so no further evaluation was performed with the thia-arenes. However, what the authors did not point out was the dissimilarity of the thia-arene profiles in the various sediments analyzed. This indicated to me that the approach may be useful for the analysis of contaminated sediment in Hamilton Harbour and coke-oven contaminated air particulate.

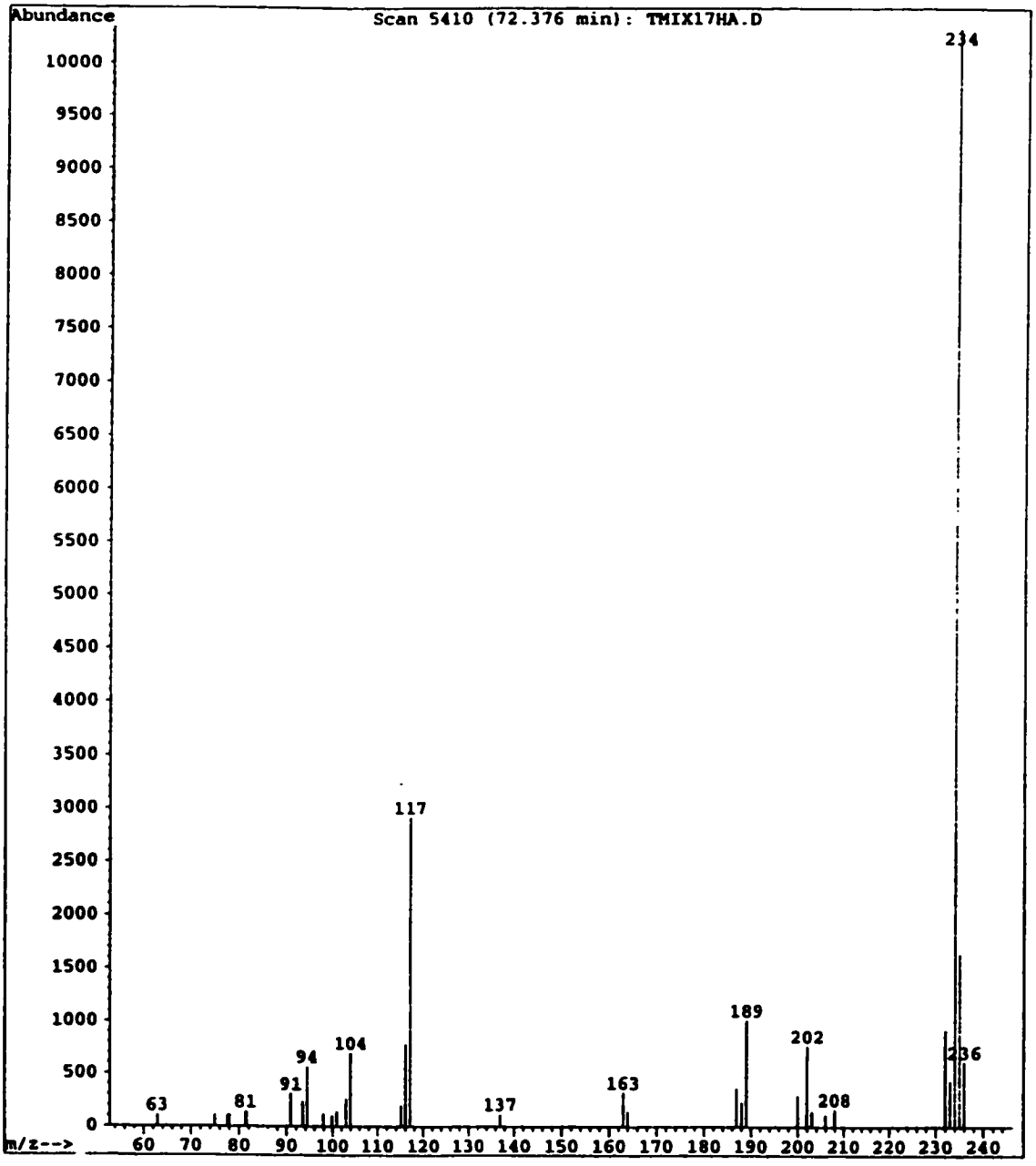

Figure 1.1. Electron impact mass spectrum of benzo[b]naphtho[2,1-d]thiophene.

In 1991-92, I completed an undergraduate thesis project under the supervision of Dr. B. E. McCarry to investigate patterns of thia-arenes in environmental samples. Contaminated sediment from Hamilton Harbour, Diesel Exhaust Particulate (NIST SRM 1650) and one 24-hour air particulate sample collected in Hamilton were examined. The alkylated dibenzothiophene isomer profiles were measured for each of the samples. The thia-arene profile of the coal tar contaminated sediment differed from the thia-arene profiles of diesel exhaust particulate. Not enough samples were available at that time to further investigate thia-arenes as source tracers.

Since the time of the undergraduate thesis, a large number of air particulate and sediment samples were collected by other graduate students for other projects. Results of the present work will begin in Chapter 3 with the analysis of the alkylated dibenzothiophene isomers in these samples. In the following chapters, a new air particulate sampling strategy will be used to obtain samples primarily for source apportionment applications and additional thia-arene compounds will be investigated as source tracers. The best criteria determined from this study will then be used to create an index which can be used to distinguish coke oven emissions from diesel emissions.

1.6 Summary of Objectives

The main objectives of the present study are summarized:

1. To obtain and analyze a variety of ambient samples in the Hamilton area and source samples representative of the major pollution sources.

2. To optimize analytical methodology by evaluating several gas chromatography stationary phases for the separation of thia-arenes and PAH.
3. To characterize emission sources using thia-arene profiles and PAH concentrations in source and ambient samples.
4. To identify the best thia-arene criteria for use in source apportionment studies.
5. To develop a source apportionment model that can distinguish coke oven emissions from diesel exhaust emissions in Hamilton air particulate.
6. To compare the thia-arene source apportionment model to currently available models which use PAH as source tracers.

2.0 METHODS

2.1 Samples

2.1.1 Air Particulate Samples

2.1.1.1 Hamilton Sampling Station, 1990-1991

This site (MOE Station 29000) is located at the corner of Kelly and Elgin Streets, just east of downtown Hamilton. This location is shown on the map in Map 2.1. Sampling of air particulate was carried out for 24-hour periods every second day from May, 1990 to June 1991, with a few exceptions for holidays and instrument maintenance. A total of 155 filters were collected at this site. A Hamilton composite air particulate sample was made by combining portions of extracts from 10 filters collected at Station 29000 and 12 filters collected at the Canada Centre for Inland Waters (CCIW) in Burlington, Ontario beside the Burlington Skyway Bridge. Station 29000 samples were collected by Dr. A. E. Legzdins and CCIW samples were collected by Dr. C. H. Marvin.

2.1.1.2 Hamilton Sampling Stations, 1995

A map of the air particulate sampling sites selected in Hamilton is shown in Map 2.1. Station 29000 is an MOE air monitoring station; the same location that was used in the 1990-1991 study of Legzdins. We sampled at this station in the 1995 study because the results would be directly comparable to those from the previous study. Stations 29113, 29547 and 29102 were also MOE air monitoring stations. These sites provided sample collections closer to the steel mills and since they were already established, they

Map 2.1. Air particulate sampling stations (⊙) in Hamilton, Ontario.

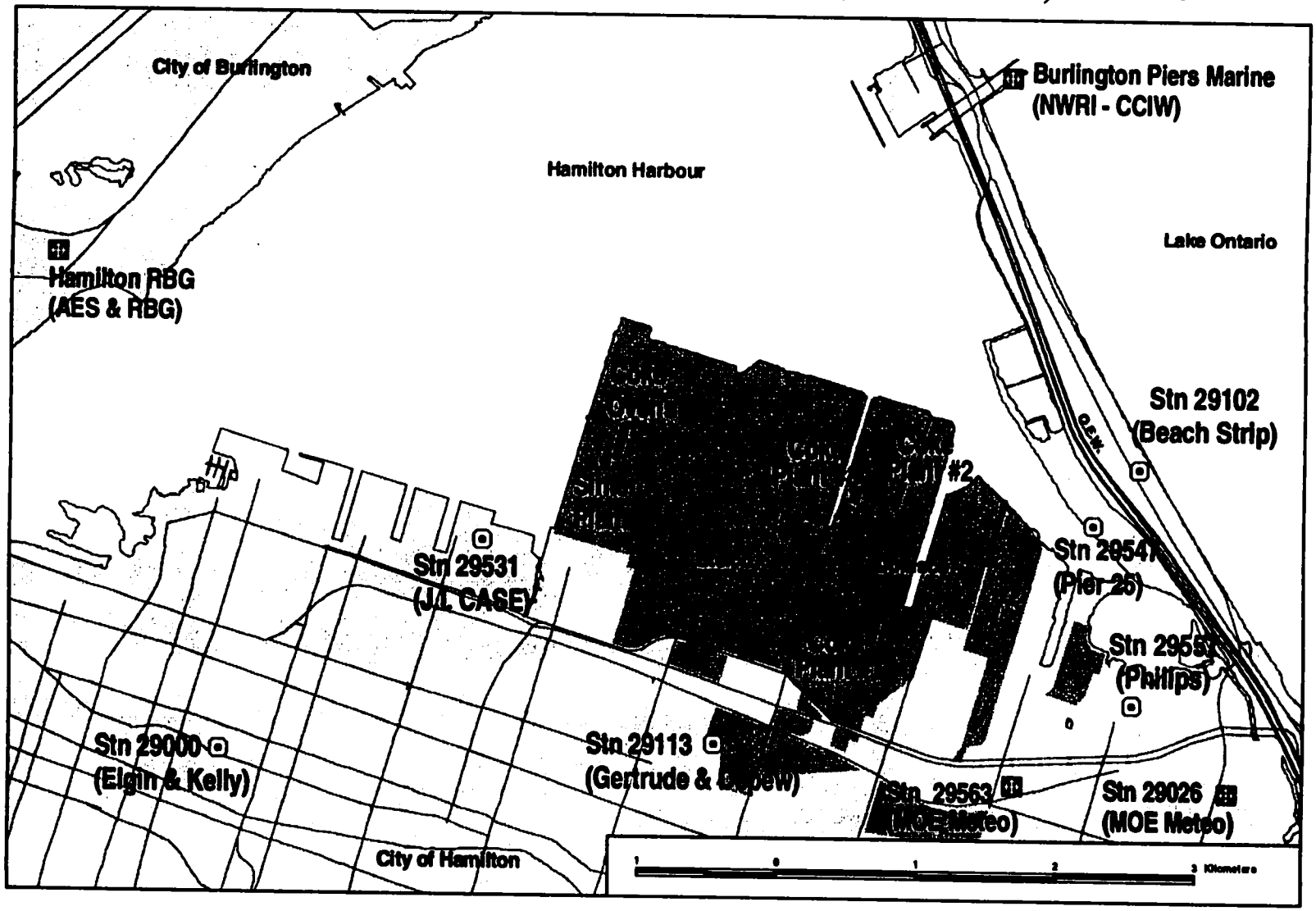

were easy to access and provided protection for sample integrity. Stations 29531 and 29557 were established by our group. Station 29531 is located close to a current MOE monitoring site so I have used the MOE station number to refer to this site. The MOE set up their own equipment at this Station in the year following this study. For our purposes, a PM_{10} sampler was located on the roof of the Hamilton Harbour Commission building near the end of Hillyard Street. Station 29557 was located on the roof of a one-story building which served as a weigh station for a scrap metal recycling plant. This station was located near a carbon black plant and the bulk of the samples collected at this site were used in another study.

Respirable air particulate (PM_{10}) was collected every day from July 10th to August 20th, 1995 at Stations 29000, 29113, 29557, and 29547, and from July 20th to August 20th, 1995 at Station 29531. The sampler at Station 29102 was shared with the MOE so samples were collected for four sequential days, followed by two days off, from July 10th to August 20th, 1995. At Stations 29547 and 29557, a second sampler used to collect total suspended particulate (TSP) was co-located with the PM_{10} sampler. Some of the samples were invalidated due to power interruptions or instrument failures. A total of 219 valid respirable air particulate filters were obtained. Samples were collected by Ms. A. R. Boden and myself. This study will focus primarily on samples collected at Stations 29000, 29113, 29531 and 29547.

Respirable airborne particulate was collected using an Anderson PM_{10} modified high volume air sampler (General Metal Works Ltd., Village of Cleves, OH) equipped with a flow controller operating at a flow rate of 40 ft^3/min. Flow controllers were

calibrated before the sampling period and every two weeks during the sampling period. Total suspended particulate was collected using a Hi-Vol sampler (General Metal Works Ltd., Village of Cleves, OH). The flow rate for the Hi-Vol samplers was measured on a rotometer before and after each sample collection and the average flow rate was used to determine total sample volume. Timers were used to start sample collection at 8:00 a.m. on the sample date and stop sample collection at 6:00 a.m. the following morning. Filters were changed between 6:00 a.m. and 8:00 a.m. every day during the sampling period.

Air particulate was collected on Teflon-coated glass fibre filters (Pallflex 8 x 10 inch, type TX40H120WW, Pall Corp., Putnam, Connecticut). Filters were weighed on an analytical balance before and after sample collection. Filters were stored in a desiccator for five days before weighing to reduce the moisture content. After weighing, filters were stored in individual envelopes in the freezer prior to extraction.

2.1.1.3 The Highway 404 Sampling Sites

Sampling was carried out at the boundary fences on both the east and west sides of Highway 404 in Toronto, Ontario. One site was on the grounds of Highland Memorial Gardens Cemetery (on the west side of Highway 404) and the other site was on the east side on Gordon Baker Road in a light industrial area. Samples were collected by workers from Rowan, Williams, Davies and Irwin, who were subcontracted by the Ontario Ministry of Transport. Equal portions of extracts from ten of these samples were combined to produce a composite Toronto Highway sample (Toronto Composite A).

2.1.1.4 The Downtown Toronto Sampling Site

Sixteen 24-hour air particulate filters were collected on Bay Street in downtown Toronto in 1989. These filters were combined to produce a composite air particulate sample (Toronto Composite B).

2.1.1.5 Arctic Region Sampling Sites

Air particulate was collected at two sites in the Canadian Arctic (Alert on Ellesmere Island, and Tagish in the western Yukon) and one site in the Russian Arctic (Dunai Island in eastern Siberia) between the months of January and March, 1994. Sampling was carried out by Bovar Environmental (Toronto, Ontario) and dichloromethane extracts were provided to us by the Atmospheric Environment Service (Environment Canada). PM_{10} particulate was collected on 20 cm diameter glass fibre filters at a sampling rate of 1.13 m^3/min continuously for seven days (11400 m^3 total air volume sampled).

2.1.2 Hamilton Harbour Samples

Centrifuged sediments were collected in October, 1993 at a depth of 0.5 m to 1 m using two Westfalia flow-through centrifuges operated in tandem. Each centrifuge was operated at 5 L/min to sample a total volume of 1000 L of water per site. Zebra mussels were removed from buoys near the water surface. Samples were collected by Dr. C. H. Marvin and Mr. Murray Charlton of the National Water Research Institute, CCIW (Burlington, Ontario).

2.1.3 Roadway Runoff Samples

Three roadway runoff samples were collected by placing large vessels directly under the QEW Skyway Bridge during rain episodes. These samples were provided by Ms. T. Mayer from the Canada Centre for Inland Waters.

2.1.4 Hamilton Creek Samples

Suspended sediment samples were collected during flow events from seven different creeks that drain into Hamilton Harbour. Five of the eight samples contained high enough levels of thia-arenes for quantification of the major thia-arene isomers. These samples were extracted and analyzed for PAH by C-I. Li.

2.1.5 Source Samples

Diesel Exhaust Particulate Standard Reference Material (SRM 1650), Urban Dust Standard Reference Material (SRM 1649) and Coal Tar Standard Reference Material (SRM 1597) were obtained from the National Institute of Standards and Technology (NIST, Gaithersburg, MD). Coke oven condensate was collected at a Hamilton steel company by Mr. P. Thompson of the Ontario Ministry of the Environment.

2.2 Meteorological Data

Wind direction and wind speed was measured at the Hamilton Sewage Treatment Plant (Station 29026, Map 2.1) and supplied by the Ontario Ministry of Environment.

Twenty-two hour averages and standard deviations of the wind directions were calculated using Oriana software (version 1.1).

2.3 Equipment and Chemicals

2.3.1 GC/MS Instrumentation

Samples were analyzed by a Hewlett-Packard Model 5890 Series II Gas Chromatograph equipped with either a DB-5ms capillary column (Analysis A, 60 m x 0.25 mm i.d. x 0.25 μm film) or a DB-17ht capillary column (Analysis B, 30 m x 0.25 mm i.d. x 0.15 μm film, J&W Scientific, Folson, CA) and an on-column injector. The detection system was a Hewlett-Packard Model 5971A Mass Selective Detector operated in the selected ion monitoring mode. Samples were quantified by the internal standard method. Two internal standards, pyrene-d_{10} and perylene-d_{12} were added to the samples prior to injection.

2.3.2 Chemicals

High purity helium carrier gas (>99.999%) was purchased from VitalAir (Hamilton, Ontario). HPLC grade solvents were purchased from Caledon Laboratories (Georgetown, Ontario). A Milli-Q purification system (Waters Associates, Millford, Massachusetts) was used to further purify the distilled water.

PAH standards, except for the thia-arenes, were purchased from Aldrich Chemical Company Inc. (Milwaukee, WI). Thia-arene standards were a generous gift from Dr. M.

L. Lee (Brigham Young University, Provo, UT). Deuterated PAH standards were purchased from Cambridge Isotope Labs Ltd. (Woburn, MA).

2.4 Sample Preparation

The procedure for particulate sample preparation is summarized in a flowchart (Figure 2.1).

2.4.1 Extraction Method

The following extraction method is adapted from that of Schuetzle *et al.* [161] and McCalla *et al.* [162]. Individual Teflon-coated glass fibre filters were folded in half and manipulated with clean tongs to fit inside a clean, glass Soxhlet apparatus. Each filter was spiked with 500 μL of a solution containing phenanthrene-d_{10} (732 ng/mL), chrysene-d_{12} (852 ng/mL) and dibenz[a,h]anthracene-d_{14} (820 ng/mL) in dichloromethane to monitor the recovery of PAH. The Soxhlet extraction vessels (approximately 80 mL volume) were fitted with 250 mL round bottom flasks filled with 180 mL dichloromethane and a few boiling chips. The flasks were wrapped with aluminum foil to reduce light exposure and placed on a heating mantle. Solvent was cycled at a rate of six cycles per hour for a total extraction time of 18-24 hours.

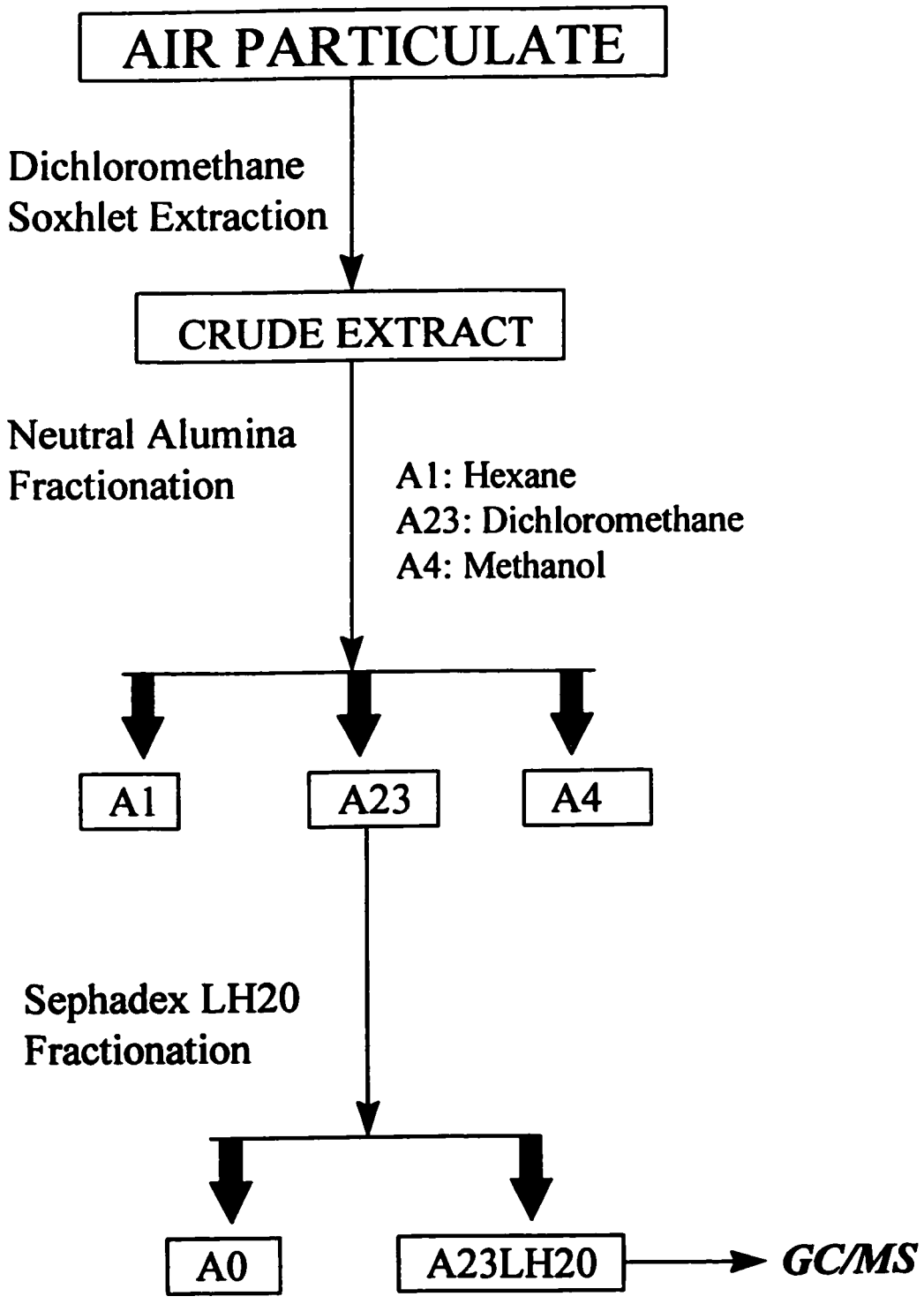

Figure 2.1. Analytical scheme for preparation of particulate samples.

2.4.2 Open-Column Alumina Chromatography

This procedure has been modified from the original method, first described by Lee *et al.* [163]. The procedure has been scaled down by Legzdins in our research group for smaller sample sizes.

Neutral alumina (Fisher, Brockman activity I, 80-200 mesh), was heated for at least 48 hours at 170°C and allowed to cool to room temperature immediately before weighing for use in the following protocol. The dichloromethane extract from one air particulate filter was reduced in volume, using a Rotovap evaporator, to ~2 mL and transferred quantitatively to a 50 mL round bottom flask containing 1 g of neutral alumina. The sample was adsorbed onto the alumina by evaporating the solvent on a Rotovap evaporator and added to the top of 2 g of alumina in a glass column (1 cm diameter). Elution of the column with 20 mL of hexane afforded fraction A1; elution with 25 mL of dichloromethane afforded fraction A23, which contained the non-polar aromatic compounds; and a final elution with 20 mL of methanol afforded fraction A4. The A23 fractions were further purified using Sephadex LH20 chromatography. The A1 and A4 fractions were reduced in volume and transferred to glass vials for storage in the refrigerator. Only the A23 fractions were analyzed in this study.

2.4.2 Sephadex LH20 Chromatography

The Sephadex LH20 procedure has been published by our lab group [164]. Sephadex LH20 gel was allowed to soak overnight in the eluent (hexane:methanol:dichloromethane, 6:4:3, v/v) followed by degassing under vacuum. A

portion of the slurry was poured into a glass column (1 inch diameter). The column was packed by pumping eluent through the column, removing excess solvent and adding more slurry when required, producing a packed column about 15 cm in length. The column was allowed to equilibrate by pumping eluent through the column at a flow rate of 3 mL/min. A Beckman model 153 analytical UV detector (254 nm) connected to a strip-chart recorder was used to monitor the eluate. The column was tested by injecting 250 μL of a 1 mg/mL solution of naphthalene dissolved in eluent to observe peak shape and elution time. Symmetrical peak shape and consistent elution time for two sequential injections indicated a ready system.

The A23 sample fraction was reduced in volume to < 250 μL and drawn into the syringe. The A23 collection flask was rinsed twice with small portions of dichloromethane and the rinses were also drawn up in the syringe. A total sample volume of 250 μL was injected onto the Sephadex LH20 column. The column eluate was collected beginning at the elution time determined for naphthalene measured at the start of the peak on the strip-chart recording, and ending when the UV signal returned to the baseline. The collected fraction is the A23LH20 fraction.

The A23LH20 fraction was reduced in volume to about 1 mL and transferred quantitatively to a 4 mL glass vial. Internal standard (70 μL of a solution containing 5.00 μg/mL pyrene-d_{10} and 4.01 μg/mL perylene-d_{12} in toluene) was added to the sample vial. The sample was reduced in volume to approximately 70 μL using the Reacti-Vap evaporator. If the sample was deep yellow in colour, a 5 to 10-fold dilution was

performed using toluene. A 10 μL aliquot of the sample was transferred to a 1.5 mL autosampler vial, equipped with a 100 μL insert, for GC/MS analysis.

2.5 GC/MS Methods

Two sets of conditions were used for GC/MS analysis of sample extracts (Table 2.1). Initially, a 60m DB-5ms column (5% phenylmethylpolysiloxane stationary phase) was used for PAH and thia-arene analysis reported in Chapter 3 (Conditions A, Table 2.1). A selected ion monitoring program was set up to monitor the ions listed in Table 2.2. Method development discussed in Chapter 4 led to changes that included the use of a different column (30m DB-17ht, 50% phenylmethylpolysiloxane; Conditions B, Table 2.1). A new selected ion monitoring program was also designed to include a greater number of ions to allow the detection of a greater number of compounds or to confirm compound identity by allowing the detection of characteristic fragments (Table 2.3).

A calibration standard containing 45 polycyclic aromatic compounds and 5 deuterated PAH was prepared for compound quantification. The calibration concentrations of the 50 compounds are listed in Table 2.4. Peak numbers are used to identify the compounds in a total ion chromatogram of the calibration standard analyzed using Conditions B (Figure 2.2). Compounds 1 to 23, and Compounds 51, 80 and 86 were quantified using pyrene-d_{10} as the internal standard. Compounds 24 to 49 were quantified using perylene-d_{12} as the internal standard.

Table 2.1. Instrument parameters used for GC/MS analysis.

Property	Conditions A (Chapter 3)	Conditions B (Chapters 5-7)
Stationary Phase	DB-5ms	DB-17ht
Column Length (m)	60	30
Column I.D. (mm)	0.25	0.25
Film Thickness (μm)	0.25	0.15
Oven Temperature Program:		
Initial Temp. (C)	130	90
Rate (C/min)	1.6	2.5
Final Temp. (C)	300	300
Final Time (min)	30	20
Injector Type	Cool on-column	Cool on-column
Detector Temp. (C)	300	300
Carrier Gas	He	He
Flow Rate (mL/min)	1.0	1.0

Table 2.2. Selected ion monitoring program used with GC/MS Conditions A.

Group #	Start Time (min)	Ions Monitored
1	8	128,134,142,152,154,166,181
2	29	139,152,178,180,184,192,197,198,208,211,212
3	50	163,202,208,216,221,222,230
4	64	117,189,228,230,234,247,248,258,261,262
5	85	129,142,213,239,252,258,266,284
6	98	142,239,276,278,284,300,302

Table 2.3. Selected ion monitoring program used with GC/MS Conditions B.

Group #	Start time (min)	Ions Monitored
1	10	128,129,139,141,142,151,152,153,154,165,166, 178,179,184,188,189,191,192,197,198
2	35	152,180,191,192,197,198,202,203,205,206,208, 211,212,219,220,225,226,229,230
3	43	163,191,202,203,205,206,208,212,213,215,216, 219,220,221,222,225,226,229,230,231
4	50	117,189,202,215,216,221,222,226,227,228,229, 230,234,235,236,243,244
5	56	117,189,202,226,227,228,229,230,234,235,236, 239,240,241,242,243,244,247,248,255,256
6	59	117,189,201,202,217,230,234,239,240,241,242, 243,244,247,248,255,256,261,262,275,276
7	61	201,217,230,239,240,241,242,247,248,253,254, 255,256,258,261,262,269,270,275,276
8	63	201,217,230,239,240,241,242,247,253,254,255, 256,258,261,262,267,268,269,270,275,276
9	65	213,252,253,254,255,256,258,261,262,265,266, 267,268,269,270,271,272,275,276
10	69	213,252,253,254,258,260,264,265,266,267,268, 269,270,271,272,275,276,285,286,280
11	70	213,252,253,258,260,264,265,266,268,269,270, 271,272,275,276,279,280,285,286,299,300
12	72	239,252,265,266,268,269,270,271,272,275,276, 278,279,280,284,285,286,293,294,299,300
13	76	239,271,272,276,277,278,279,280,284,285,286, 288,289,290,292,293,294,299,300,303,304
14	79	239,271,272,276,277,278,279,280,284,285,286, 289,290,292,293,294,299,300,303,304,306
15	81	150,239,276,277,278,284,285,286,289,290,292, 293,294,299,300,302,303,304,306,317,318

Table 2.4. Concentrations of PAC in GC/MS calibration standard.

Peak #	Compound Name	Mass (g/mol)	Conc. (μg/mL)
1	Naphthalene	128	4.20
2	2-Methylnaphthalene	142	3.90
3	1-Methylnaphthalene	142	3.51
4	Biphenyl	154	4.93
5	Acenaphthylene	152	4.08
6	Acenaphthene	154	4.23
7	Fluorene	166	4.23
8	Phenanthrene	178	8.00
9	Anthracene	178	9.82
10	*o*-Terphenyl	230	4.15
11	Anthraquinone	208	9.84
12	Fluoranthene	202	6.84
13	Pyrene	202	7.35
14	*m*-Terphenyl	230	4.18
15	*p*-Terphenyl	230	4.17
16	Benzo[*a*]fluorene	216	4.24
18	Benzo[*b*]fluorene	216	4.46
19	Benzo[*ghi*]fluoranthene	226	6.61
20	Benzo[*c*]phenanthrene	228	4.21
21	Cyclopenta[*cd*]pyrene	226	4.80
22	Benz[*a*]anthracene	228	6.90
23	Chrysene	228	7.61
24	Benzanthrone	230	9.00
25	2-Nitrofluoranthene	247	5.65
26	Benz[*a*]anthracene-7,12-dione	258	9.23
27	1-Nitropyrene	247	7.19
28	2-Nitropyrene	247	7.25
29	Benzo[*b*]fluoranthene	252	6.47
30	Benzo[*j*]fluoranthene	252	4.65
31	Benzo[*k*]fluoranthene	252	4.75
33	Benzo[*e*]pyrene	252	6.91
34	Benzo[*a*]pyrene	252	5.27
35	Perylene	252	5.99
36	3-Methylcholanthrene	268	4.79
38	Indeno[1,2,3-*cd*]pyrene	276	3.32
39	Dibenz[*a,c*]anthracene	278	7.45
42	Picene	278	2.06
43	Benzo[*ghi*]perylene	276	6.33
46	Coronene	300	4.29
47	Dibenzo[*a,e*]pyrene	302	4.42
48	Dibenzo[*a,i*]pyrene	302	4.52
49	Dibenzo[*a,h*]pyrene	302	5.09
51	Dibenzothiophene	184	6.04
80	Benzo[*b*]naphtho[2,1-*d*]thiophene	234	2.21
86	Benzo[*b*]naphtho[2,3-*d*]thiophene	234	4.53
120	Pyrene-d_{10}	212	5.00
121	Perylene-d_{12}	264	4.01
122	Phenanthrene-d_{10}	188	3.66
123	Chrysene-d_{12}	240	4.26
124	Dibenz[a,h]anthracene-d_{14}	292	4.10

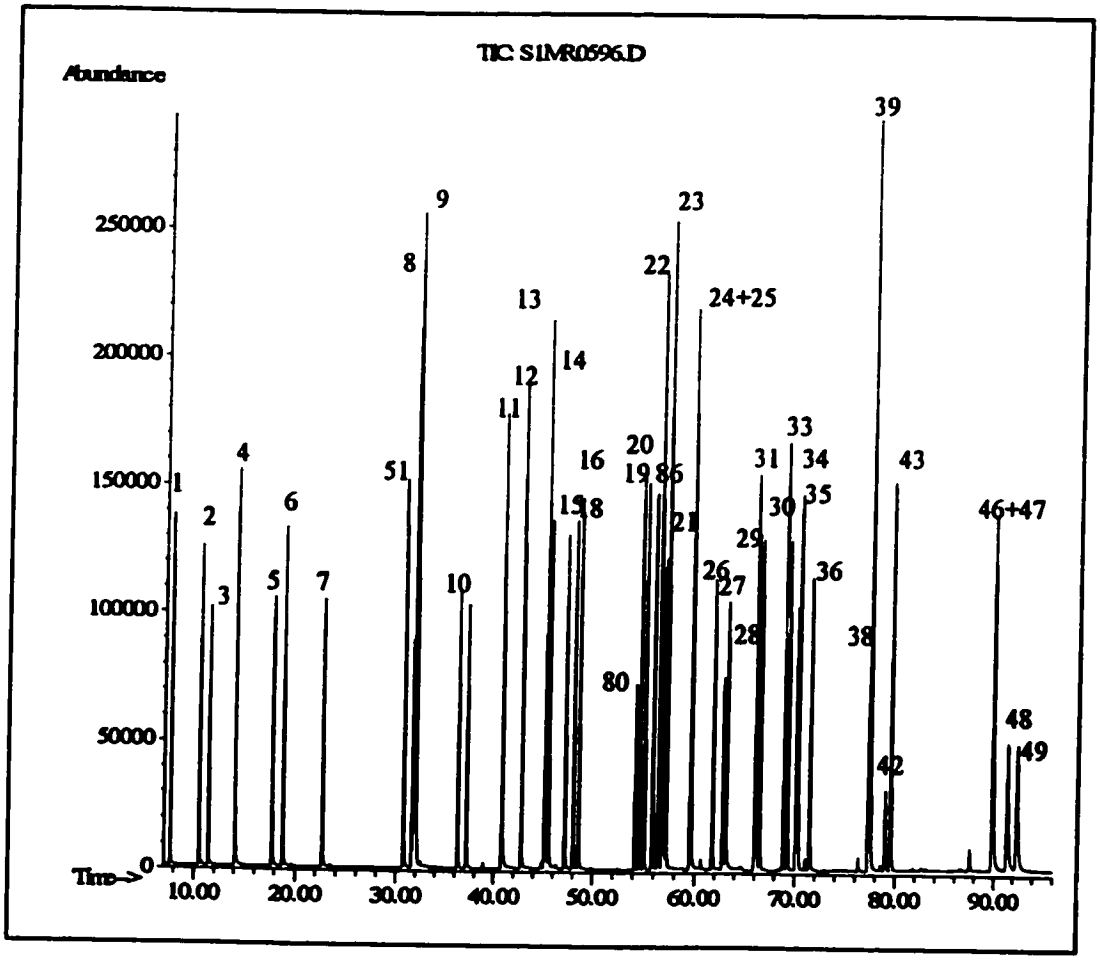

Figure 2.2. GC/MS chromatogram (SIM) of the calibration standard. Numbers refer to compounds listed in Table 2.4.

3.0 DIBENZOTHIOPHENES AS SOURCE TRACERS

3.1 OVERVIEW

In this chapter, selected thia-arenes were examined in source samples and ambient samples to determine the potential of thia-arenes as source apportionment tracers. This work follows from my undergraduate thesis project that was completed in 1992. During the two years between that time and the start of my Ph. D. work, graduate students in my lab had extracted a large number of source and ambient samples for other projects. These samples were re-analyzed for the present study. The source samples were analyzed first, followed by Hamilton respirable air particulate samples and then Hamilton Harbour sediments and zebra mussels. These samples were analyzed to investigate the use of thia-arenes as source apportionment tracers and determine what changes to the analytical method were required.

All samples were extracted using dichloromethane in a Soxhlet apparatus, then cleaned up on an alumina column followed by a Sephadex LH20 column to afford a non-polar aromatic fraction as described in Chapter 2. The total concentrations of PAH (in ng/m3 or μg/g) were determined in ambient samples using GC/MS with selected ion monitoring. The extraction, clean-up and PAH analysis for samples discussed in this chapter were completed by other graduate students as indicated in the relevant sections. The GC/MS analyses were repeated, by the author, for the source samples and selected

ambient samples to include ion parameters necessary for the analysis of thia-arenes and in some cases to obtain chromatograms of better quality.

The first class of thia-arenes examined consists of dibenzothiophene (DBT; Compound 51, Appendix I), naphthothiophene (Compounds 50, 52 and 53, Appendix I) and their alkylated derivatives. Four DBT and naphthothiophene isomers (184 amu) occur in environmental samples. A large number of monomethyl (198 amu) and dimethyl/ethyl (212 amu) derivatives of DBT and naphthothiophene also exist. These compounds were selected for this first investigation because they are the most widely studied group of thia-arenes. In the early 1980s, alkylated dibenzothiophenes were examined as source tracers in Norwegian and Swedish sediments [119]. The thia-arenes were rejected as source tracers because the DBT alkyl homologue distribution did not differ significantly in two source samples. However, spatial variation of the DBT alkyl homologue distribution in sediments was greater than the spatial variation of the PAH source tracers used in the study, indicating that the thia-arenes may provide greater discrimination among ambient samples than the PAH.

The relative abundances (peak areas) of the parent (184 amu), monomethyl (198 amu) and dimethyl/ethyl (212 amu) thia-arenes were determined for a variety of source samples and ambient samples. The alkyl homologue distribution (relative amount of the 184, 198 and 212 amu isomers) will be referred to as the DBT thia-arene profile in this chapter. DBT thia-arene profiles in the source samples were compared to DBT thia-arene profiles in air particulate, sediment and zebra mussel extracts to evaluate the use of thia-arenes as source tracers. The dependence of DBT thia-arene profiles on wind direction

(air samples) or location (harbour samples) and total concentration of PAH was also investigated.

3.2 Thia-arene Profiles in Source Samples

A selection of source samples and Standard Reference Materials (SRMs) were selected to represent two major pollution sources in Hamilton, Ontario: mobile emissions and coke oven emissions. A Hamilton coke oven condensate, Hamilton coal tar, and Coal Tar Standard Reference Material (NIST SRM 1597) were chosen to represent sources of coal-derived industrial emissions (i.e., coke oven emissions). Diesel Exhaust Particulate Standard Reference Material (NIST SRM 1650) was chosen to represent diesel emission sources. Urban Dust Standard Reference Material (NIST SRM 1649) was chosen to represent an urban air sample and will be discussed in Section 3.2 with other composite air particulate samples.

Standard Reference Materials were selected because other researchers can use these samples for evaluation of the current work or for comparison to other studies. Standard Reference Materials are also useful for evaluating new or existing analytical methodologies in a laboratory because selected chemical components have been certified by the National Institute of Standards and Technology (NIST). Local source samples (e.g., coke oven condensate and coal tar) were compared to the Standard Reference Materials and to local ambient samples, partially as a check for source profile reproducibility. Thia-arene profiles were determined for each of the reference standards and local samples.

A chromatogram of the non-polar aromatic fraction of an extract of Urban Dust Standard Reference Material (SRM 1649) is shown in Figure 3.1. Numbered peaks correspond to compound identities listed in Table 2.4 or Appendix I. Compound 51, dibenzothiophene (DBT), is one of the most abundant thia-arene compounds in this extract. The abundance of this compound is approximately 100-fold lower than the abundance of major PAH.

Mass selective detection is used to detect low-level thia-arenes in the presence of PAH. Single ion chromatograms were extracted from the total ion chromatogram (TIC) to reveal chromatographic peaks that may be indistinguishable from the background in the TIC. Ion chromatograms corresponding to the molecular ions of the dibenzothiophene or naphthothiophene isomers (*m/z* 184), the monomethyl derivatives (*m/z* 198) and the dimethyl or ethyl derivatives (*m/z* 212) for Diesel Exhaust Particulate (SRM 1650) and coke oven condensate are shown in Figure 3.2. The ion abundances of the *m/z* 198 and *m/z* 212 ions equal or exceed that of the parent compounds (*m/z* 184) in the diesel exhaust particulate source sample (Figure 3.2(a)). In contrast, the ion abundance of the alkylated derivatives in Hamilton coke oven condensate is significantly less than the ion abundance of the parent compounds (Figure 3.2(b)).

The sum of the areas under the four chromatographic peaks at *m/z* 184, corresponding to the parent thia-arenes, was determined. The sum of the peak areas of the monomethylated derivatives (*m/z* 198) and the sum of the peak areas of the dimethylated/ethylated derivatives (*m/z* 212) were also determined. The abundances of the monomethyl and dimethyl/ethyl derivatives were normalized to the abundance of the

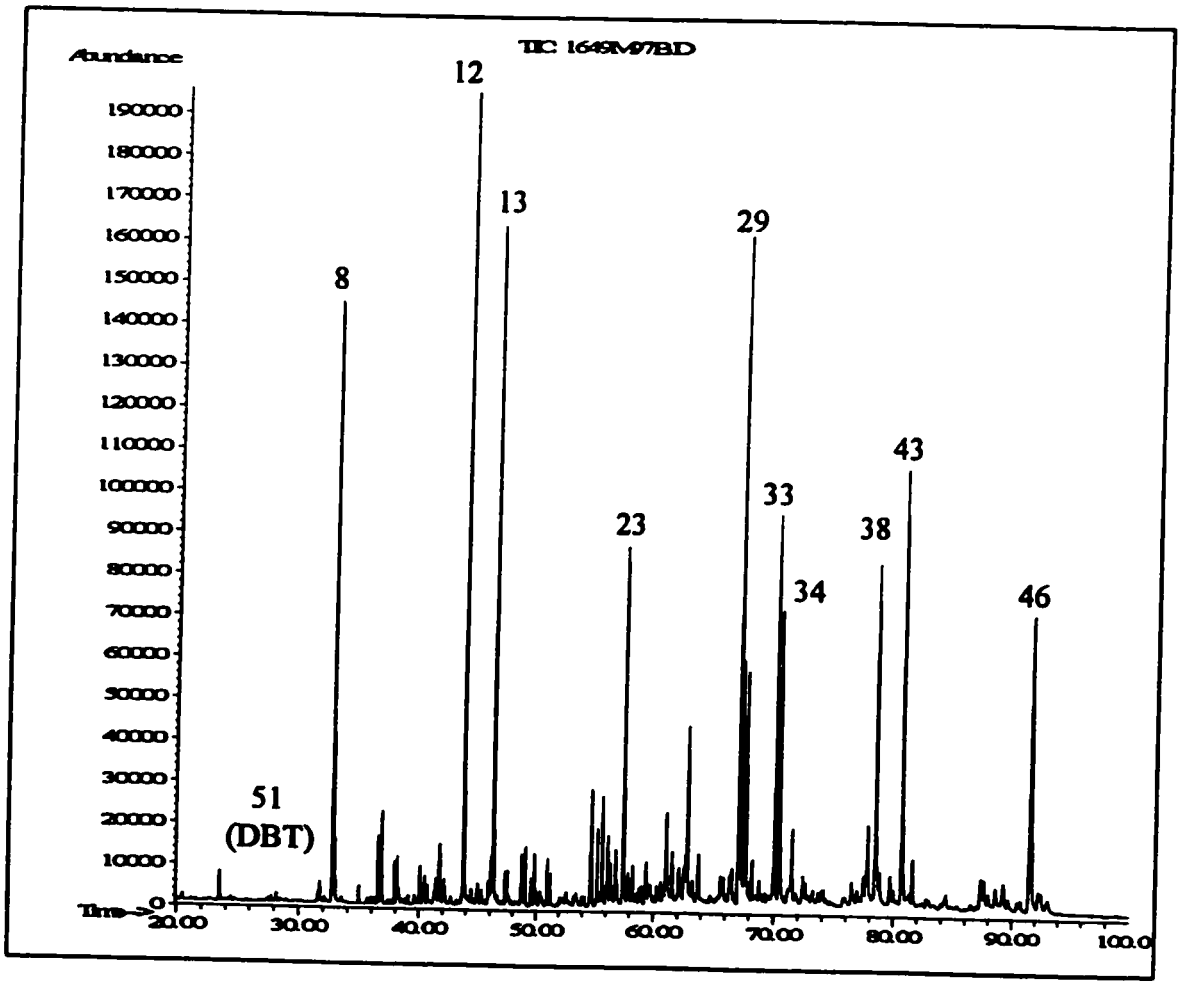

Figure 3.1. GC/MS chromatogram of an extract of Urban Dust Standard Reference Material (SRM 1649). Chromatogram obtained using Conditions A (Table 2.1).

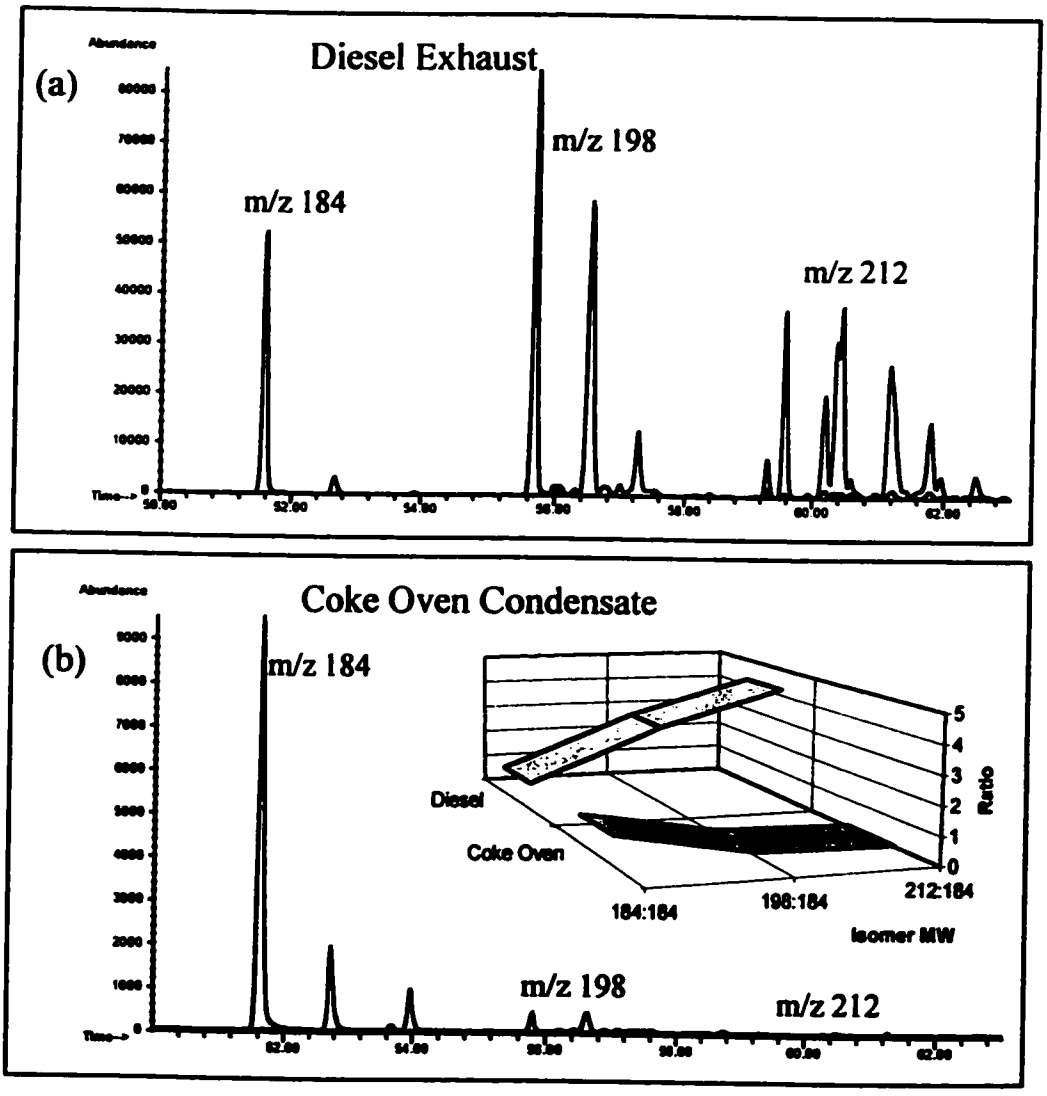

Figure 3.2. Ion chromatograms of the molecular ions of the parent (*m/z* 184) and alkylated (*m/z* 198 and *m/z* 212) dibenzothiophene compounds in (a) Diesel Exhaust Particulate (SRM 1650) and (b) coke oven condensate. Analysis performed on a 60 m DB-5ms column (column conditions A). Inset shows plot of relative ratios of peak areas.

parent compounds by dividing the total area under the *m/z* 198 peaks or *m/z* 212 peaks by the total area under the *m/z* 184 peaks. Two ratios, *m/z* 212:*m/z* 184 and *m/z* 198:*m/z* 184, are obtained and the sum of the areas under the parent compounds is assigned a value of 1.0. The DBT thia-arene profile is obtained by plotting the normalized parent value (1.0) and the two thia-arene ratios for each sample (see Figure 3.2, inset).

The *m/z* 198:*m/z* 184 and *m/z* 212:*m/z* 184 ratios for seven source samples, reference standards and composite air samples are listed in Table 3.1. Monomethyl and parent dibenzothiophene isomers have previously been quantified in diesel exhaust particulate extracts [87] and coal tar [78,96]. The ratios of the monomethyl to parent dibenzothiophenes (*m/z* 198:*m/z* 184) were calculated from reported concentrations for three diesel particulate samples and two coal tar samples (Table 3.1). Ratios calculated for the diesel samples (*m/z* 198:*m/z* 184 = 3.1, 4.0, and 4.2) compare favourably to the ratio value of 2.9 determined in the present work for the diesel exhaust particulate (SRM 1650). Two different ratios were calculated for the coal tar samples from concentrations reported in the literature, *m/z* 198:*m/z* 184 = 0.013 [78] and *m/z* 198:*m/z* 184 = 0.18 [96]. The latter ratio is consistent with the ratios determined for Hamilton coke oven condensate (*m/z* 198:*m/z* 184 = 0.16), Coal Tar Standard Reference Material (SRM 1597, *m/z* 198:*m/z* 184 = 0.12) and Hamilton coal tar (*m/z* 198:*m/z* 184 = 0.11).

DBT thia-arene profiles in a diesel exhaust particulate extract are significantly different from DBT thia-arene profiles in coal tars and Hamilton coke oven condensate, indicating that thia-arenes may be useful source tracers. Ambient air particulate samples were then analyzed to further explore this trend.

Table 3.1. Thia-arene ratios in source samples, Standard Reference Materials and composite air sample extracts compared to literature values.

Sample Type	Thia-arene Ratios	
	m/z 198:m/z 184	m/z 212:m/z 198
SRM 1597 (Coal Tar)	0.12	0.027
Hamilton Coal Tar	0.11	0.026
Coke Oven Condensate	0.16	0.043
Composite Hamilton Air	0.86	1.9
Composite Toronto Air	2.1	3.7
SRM 1649 (Urban Dust)	1.5	2.7
SRM 1650 (Diesel)	2.9	4.2
Coal Tar[1]	0.013	n/a
Coal Tar[2]	0.18	n/a
Diesel Particulate 1[3]	3.1	n/a
Diesel Particulate 2[3]	4.0	n/a
Diesel Particulate 3[3]	4.2	n/a

[1]Reference 78
[2]Reference 82
[3]Reference 87
n/a = not available

3.3 Composite Air Particulate Samples

The Urban Dust Standard Reference Material (NIST SRM 1649) was collected in a baghouse as total particulate material in the late 1970s in a large American city. Since the present study focused on inhalable particulate (PM_{10}) collected almost twenty years later, it seemed necessary to compare data for SRM 1649 to modern samples of urban air particulate in Canada. To achieve this, two local composite ambient air particulate samples were prepared, one from air particulate collected in Toronto, Ontario and one from air particulate collected in Hamilton, Ontario.

Toronto is a large urban centre (population: 2,100,000) with little heavy industry while Hamilton (population: 320,000) has two major steel mills and other associated industries. Pollutant emissions from motor vehicles are widespread in both cities. The Toronto samples were collected in 1994 at the fence-line bordering a four-lane expressway (Highway 404) where vehicle emissions (particularly cars) were expected to dominate these particulate samples. The Hamilton composite air particulate sample contains air particulate from two different locations on opposite sides of the industrial area. The composite Hamilton air sample is expected to contain a mixture of emissions from motor vehicles and industrial sources.

The DBT thia-arene profiles of the composite air particulate samples are compared to the thia-arene profiles of the source samples in Figure 3.3. The Toronto composite air particulate extract has a thia-arene profile similar to that of the diesel exhaust particulate (SRM 1650). The thia-arene profile of the Hamilton composite air particulate extract is intermediate between that of diesel exhaust particulate (SRM 1650)

and Hamilton coke oven condensate. The thia-arene profiles observed in Figure 3.3 support the assumption that the Hamilton sample contains a mixture of vehicle emissions and industrial emissions while the Toronto sample contains primarily vehicle emissions. The thia-arene profile of urban dust (SRM 1649) is also intermediate between diesel exhaust particulate (SRM 1650) and coke oven condensate indicating that this sample contains some contribution from coke oven or coal tar sources.

3.4 Hamilton Air Particulate Samples (24-hour collection)

3.4.1 Dependence of DBT Thia-arene Ratios in Air Particulate on Wind Direction

A former Ph. D. student, A. E. Legzdins, collected a large number of 24-hour respirable air particulate samples in Hamilton between May 1990 and May 1991 at a Ministry of the Environment (MOE) sampling station, Station 29000. This station is located in downtown Hamilton approximately 4 kilometers southwest of the nearest steel mill. This site may be impacted by coke oven emissions during periods of northeasterly winds. Legzdins determined the concentrations of selected PAH in these samples by GC/MS. The ions required for thia-arene analysis were included as part of Legzdins selected ion monitoring program, however, Legzdins did not evaluate this data. I re-examined the chromatograms of thirty-six of Legzdins' samples to determine the thia-arene ratios and to examine the daily variability of these ratios as a function of mean wind direction.

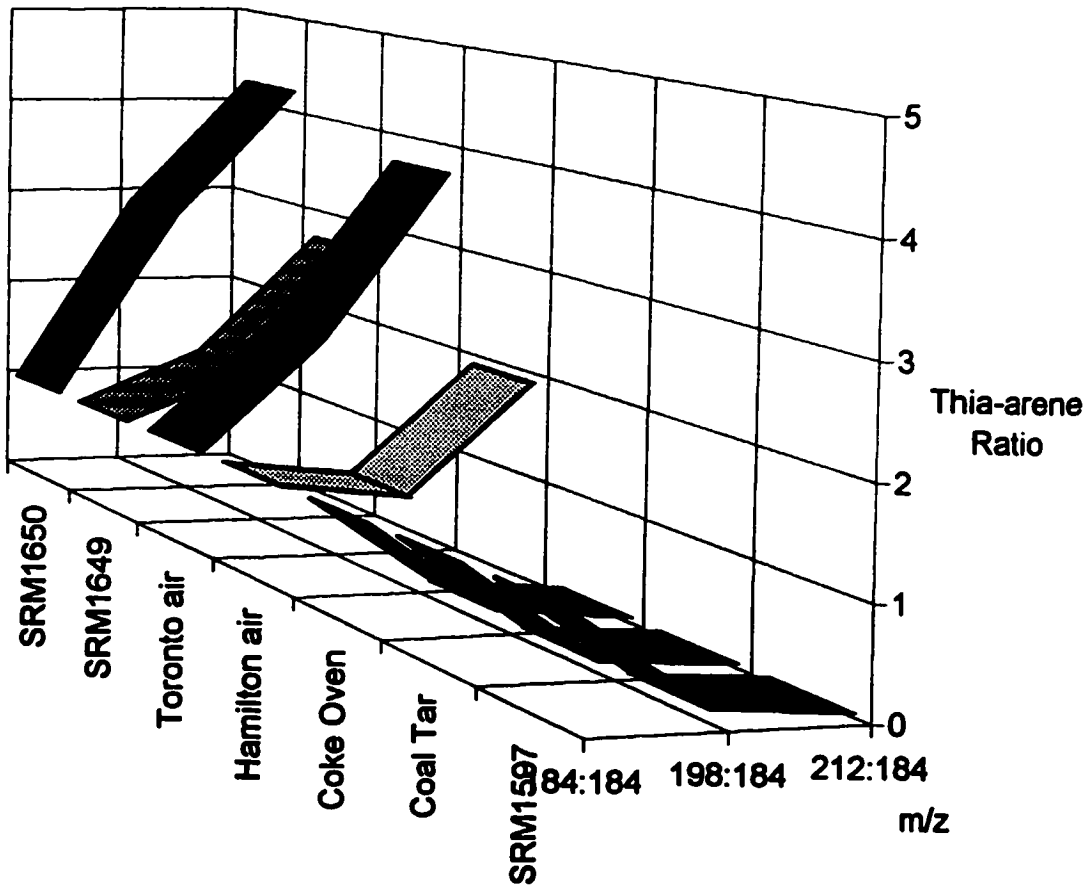

Figure 3.3. Thia-arene profiles in source samples, Standard Reference Materials and composite air sample extracts.

The *m/z* 212:*m/z* 184 ratio determined for each air particulate sample is plotted against the mean wind direction for the sampling period (Figure 3.4). Three samples were excluded because the variation in wind direction for the sampling period was large (C. I. > 100 degrees) or because wind direction information was not available for that sample. With a few exceptions, the data in Figure 3.4 are divided into two subsets. A *m/z* 212:*m/z* 184 ratio of 2.4 (shown as a dotted line) divides the data set in two. The majority of samples collected when the mean wind direction was between approximately 15° and 140° (northeasterly) had *m/z* 212:*m/z* 184 thia-arene ratios less than 2.4. The majority of samples collected when the mean wind direction was between 210° and 310° had *m/z* 212:*m/z* 184 ratios greater than 2.4. Winds from the east or northeast (from approximately 45° to 90°) are predicted to transport emissions from the steel mills toward the sampling site, resulting in a lower ratio. Thia-arene ratios (*m/z* 212:*m/z* 184) determined for all but one air particulate sample collected during these periods are below the dotted line and range from 1.4 to 2.4. Only one sample had a large ratio with a value equal to 4.3. The wind direction varied significantly during some of the sampling periods so it is difficult to estimate the source contributions for certain samples. Winds from the west or southwest (approximately 210° to 270°) are predicted to transport industrial emissions away from the sampling site, leaving mainly vehicular impacts in the air collected by the sampler. Thia-arene ratios range from 2.6 to 7.5 during periods of west or southwest winds. These values are consistent with the thia-arene ratios determined for mobile emission reference samples and Toronto air (Table 3.1). While motor vehicle emissions are assumed to impact the sampling site at all times and from all directions,

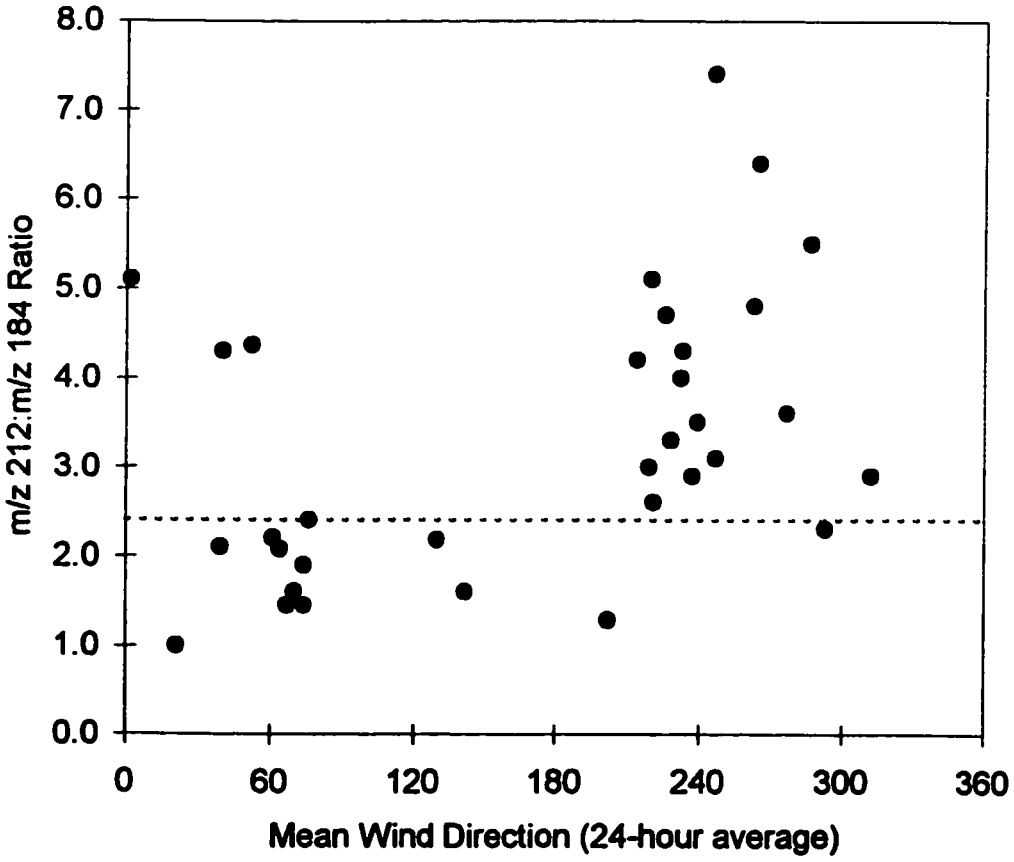

Figure 3.4. Dependence of thia-arene ratio (*m/z* 212:*m/z* 184) on mean wind direction of 24-hour air particulate samples collected near downtown Hamilton.

coke oven impacts (when present) tend to dominate the profile because of the significantly higher levels of PAH contaminants. Similar results were observed for the dependence of the *m/z* 198:*m/z* 184 ratio with wind direction (data not shown), but a larger range of values and a clearer pattern was observed for the *m/z* 212:*m/z* 184 ratios.

3.4.2 Relationship between DBT Thia-arene Ratios and PAH Concentrations in Urban Air

The *m/z* 212:*m/z* 184 thia-arene ratio is plotted against the total concentration of PAH for all 36 samples (Figure 3.5). The total concentration of PAH in each 24-hour air particulate sample is defined as the sum of the concentrations of the major PAH compounds in the samples (178 to 278 amu). In Figure 3.4, it was shown that air particulate collected downwind of the coke ovens tends to have *m/z* 212:*m/z* 184 ratios less than 2.4, while air particulate upwind of the coke ovens tends to have *m/z* 212:*m/z* 184 ratios greater than 2.4. Air particulate samples with *m/z* 212:*m/z* 184 ratios less than 2.4 (downwind of the steel industries) have total PAH concentrations greater than 40 ng/m^3 for all but one sample, indicating that samples impacted by coke oven emissions contain high concentrations of PAH. Air particulate samples with *m/z* 212:*m/z* 184 ratios that exceeded 2.8 have total PAH concentrations less than about 6 ng/m^3, indicating that samples collected upwind of the coke ovens have low PAH loadings. A third group of air particulate samples with total PAH concentrations between 6 and 30 ng/m^3 showed intermediate values for thia-arene ratios (2.3 to 5.2). Samples with intermediate thia-arene ratios and PAH concentrations likely contain some contribution due to coke oven

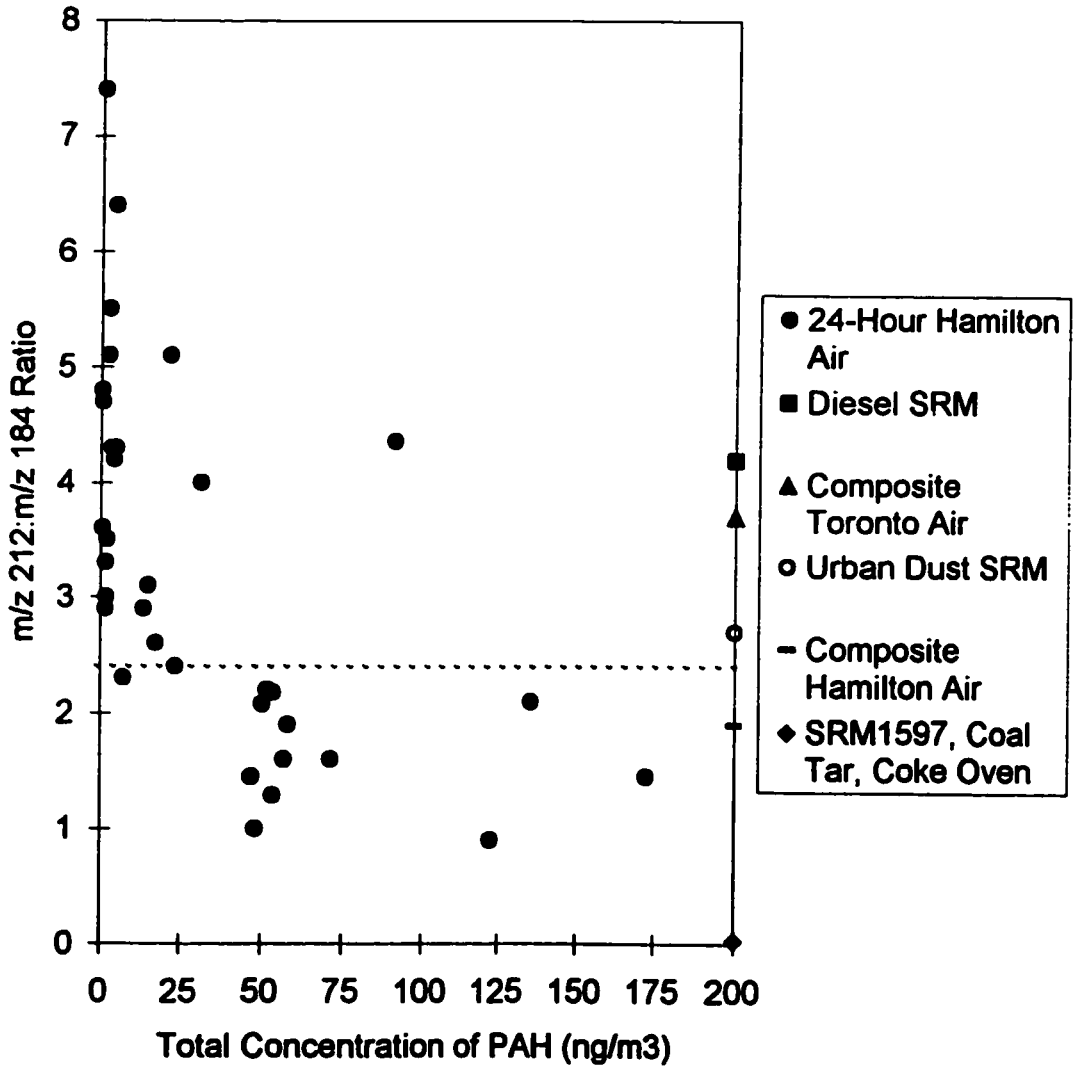

Figure 3.5. Relationship between thia-arene ratio (*m/z* 212:*m/z* 184) and total concentration of PAH in ambient air samples collected in downtown Hamilton.

emissions, but were probably not directly downwind of the industries for the entire sampling period.

The *m/z* 212:*m/z* 184 ratios for the five source samples (Table 3.1) are indicated on the right axis in Figure 3.4. The *m/z* 212:*m/z* 184 ratios in diesel particulate (4.2) and Toronto air (3.7) fall within the range of ratios determined for air particulate with <6 ng/m^3 of PAH. The composite Hamilton air sample has a *m/z* 212:*m/z* 184 ratio (1.9) that falls within the range of ratios determined for air particulate with >40 ng/m^3 of PAH. The *m/z* 212:*m/z* 184 ratio in the urban dust reference standard (2.7) is intermediate between these two groups. The very low *m/z* 212:*m/z* 184 ratios determined for coal tar and coke oven source samples (0.03-0.04) are not observed in any of the ambient air particulate samples.

A few of the *m/z* 212:*m/z* 184 ratios in Hamilton air particulate exceeded the values of the source samples. This is not surprising since the diesel source sample (SRM 1650) was obtained from a single diesel engine only, and profiles of polycyclic aromatic compounds in exhausts will vary depending on the source of fuel, the type of engine, and the operating conditions [36,56]. The stability of thia-arene profiles in ambient samples will be discussed in Section 3.6. Generally, PAH formation at high temperatures (e.g. the coking of coal) favour unsubstituted aromatics, while lower formation temperatures (e.g. in diesel engines) favour a greater degree of alkylation [58]. DBT thia-arene profiles determined for source samples and ambient samples follow this pattern in the present study.

3.5 Thia-Arene Profiles in Hamilton Harbour Samples

DBT thia-arene profiles were also examined in sediments and zebra mussels in Hamilton Harbour to evaluate the use of this source apportionment approach in matrices other than air particulate. Hamilton Harbour is situated on the north end of the city next to two major steel mills. Randle Reef in Hamilton Harbour is an area heavily contaminated by coal tar. Another pollution source nearby is a major highway that runs along the eastern side of the harbour, separating Hamilton Harbour from the rest of Lake Ontario.

C. H. Marvin and J. Villella were involved in studies on the mutagenicity and PAH concentrations in bottom sediments, suspended sediments and zebra mussels collected in Hamilton Harbour. Suspended sediments and zebra mussels were sampled near the surface of the water, and bottom sediments were sampled at various depths in the harbour, at several locations by Marvin. Sampling locations are indicated on the map of Hamilton Harbour (Map 3.1). Samples were collected west of the steel mills at Randle Reef, and at Sites 1 to 4, northeast of the steel mills.

Suspended sediments, collected one meter below the surface of the water, may enter the water column via creek runoff from the watershed, direct industrial discharges, atmospheric deposition, or resuspension of bottom sediments. Suspended sediments represent a snapshot of material present in the water column at the time of collection. Zebra mussels, on the other hand, feed on suspended material in the water column and process about one liter of water per day per mussel. As a result of this feeding, zebra

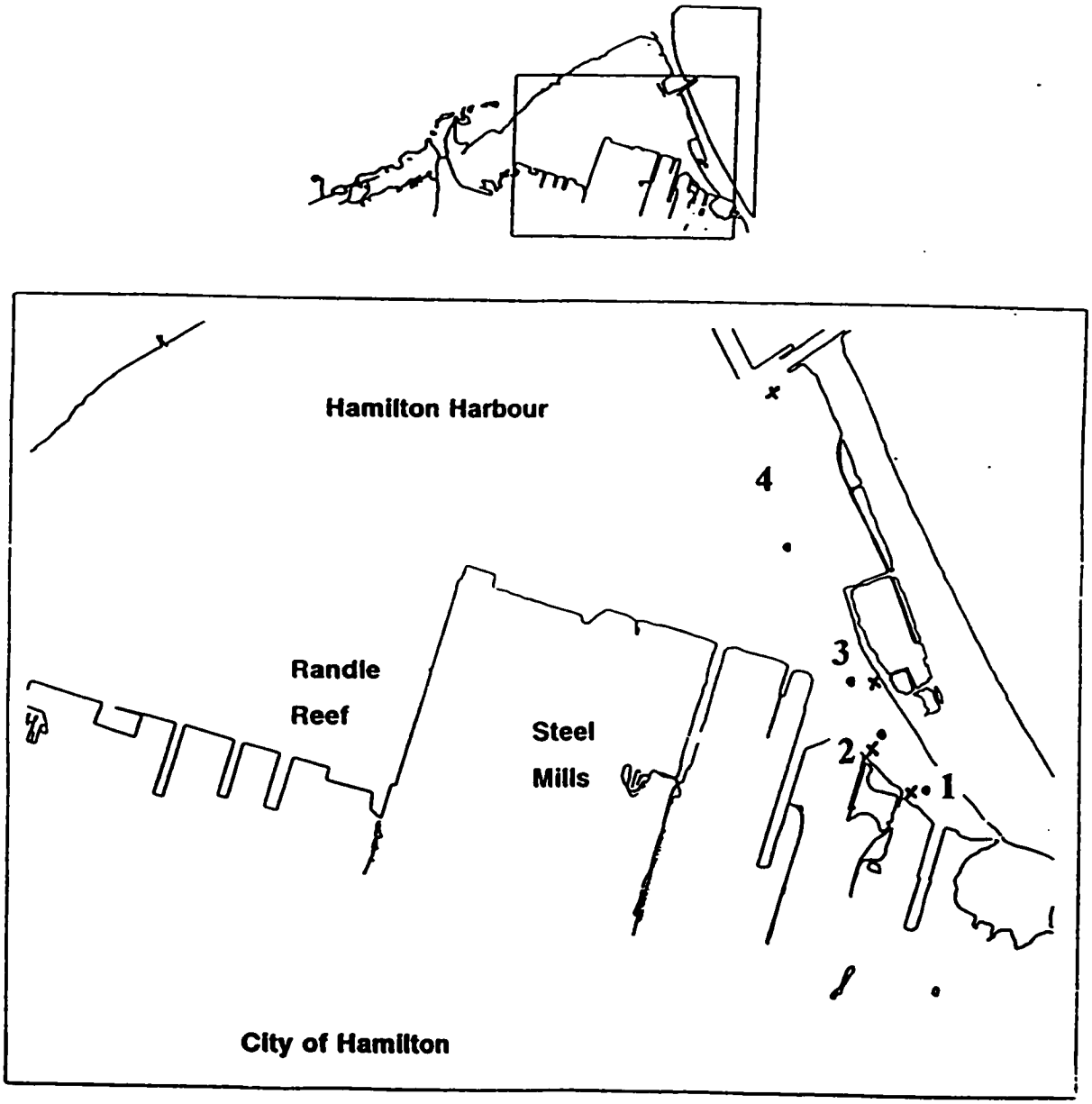

Map 3.1. Map of Hamilton Harbour showing suspended sediment and zebra mussel sampling locations. The dots show locations of suspended sediment sampling sites while the x indicate locations of marker buoys from which zebra mussels were collected.

mussels absorb contaminants from the suspended sediments in the water column and provide a time-integrated picture of organic contaminants in the water column. Harbour sediments and zebra mussel samples were examined to determine whether or not thia-arene profiles could be used to differentiate pollution sources in matrices other than air particulate.

The samples were collected, prepared and analyzed for PAH by Marvin and Villella. Chromatographic data for the zebra mussel extracts and Randle Reef bottom sediment was provided from Marvin. Data obtained from the zebra mussel samples was sufficient for the determination of thia-arene profiles. The Randle Reef bottom sediment and suspended sediment extracts from Sites 1 to 4, provided by Villella, were re-analyzed by GC/MS to determine DBT thia-arene profiles for this study.

Thia-arene profiles were determined in a Randle Reef bottom sediment extract and a Randle Reef zebra mussel extract from mussels collected from the marker buoy above the reef and were compared to thia-arene profiles in coal tar and diesel exhaust particulate (Figure 3.7). The profiles in the bottom sediment and zebra mussel samples closely resemble the profiles from coal tar or coke oven condensate. These data indicate that Randle Reef bottom sediment and zebra mussel extracts are contaminated by coal tar. The coal tar thia-arene signature in suspended material in the water column (analyzed in zebra mussels) is due to either resuspension of coal tar contaminated bottom sediments, atmospheric deposition of new particulate from coke oven emissions, or a combination of the two processes.

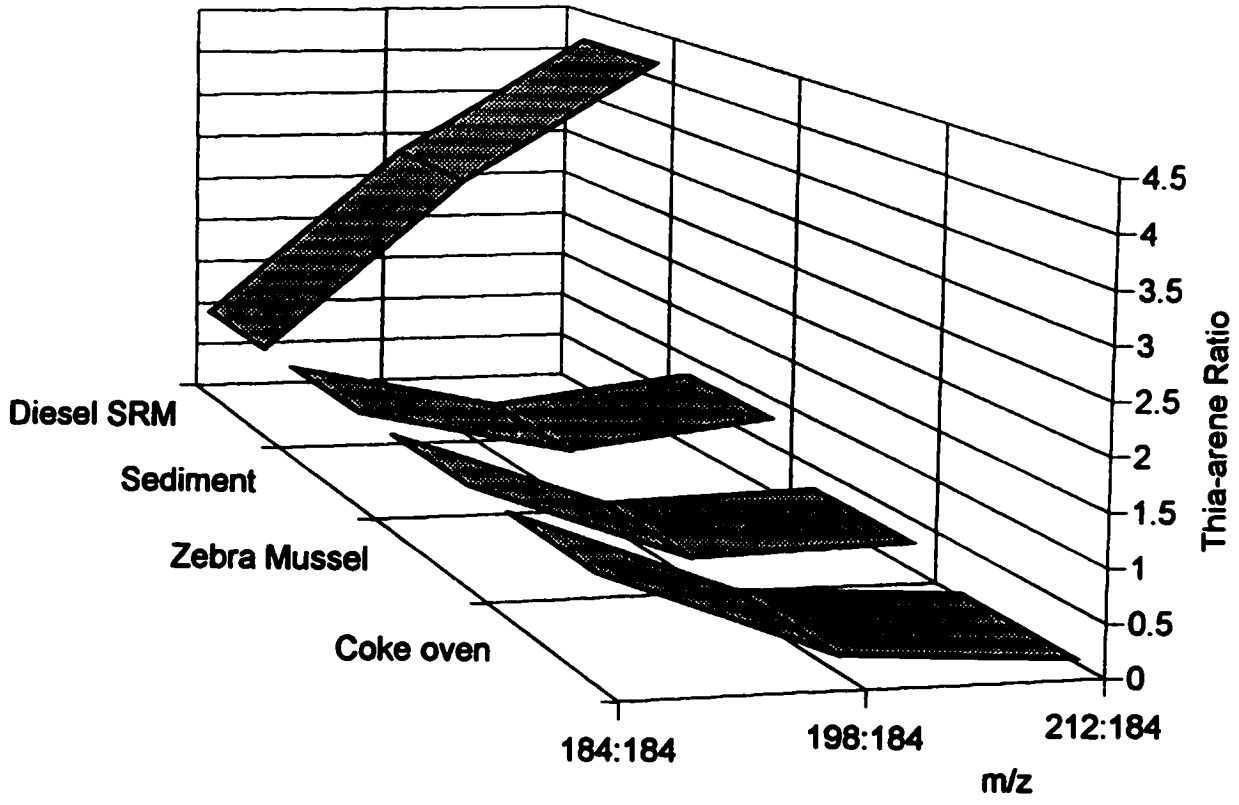

Figure 3.7. Alkyldibenzothiophene profiles in Randle Reef bottom sediment and Randle Reef zebra mussel extracts.

Four sets of suspended sediments and zebra mussels were sampled in the eastern end of Hamilton Harbour and in Windemere Arm (Map 3.1, Sites 1, 2, 3, and 4). Thia-arene profiles determined in each of the four sediment and mussel samples are shown in Figure 3.8. Sediments and zebra mussels at Sites 2, 3 and 4 have *m/z* 212:*m/z* 184 ratios ranging from 3.2 to 13. This range is similar to the range of *m/z* 212:*m/z* 184 ratios in Hamilton air particulate collected upwind of the coke ovens, implicating sources other than coal tar or coke oven emissions. Diesel particulate emissions entering the harbour via atmospheric deposition may be the primary source of thia-arene contamination at these locations; however, samples of other possible sources were not available for comparison. Thia-arene ratios (*m/z* 212:*m/z* 184) at Site 1 were determined to be 0.5 for the zebra mussel extract and 2.2 for the suspended sediment extract. These ratios compare favourably to the *m/z* 212:*m/z* 184 ratios in air particulate collected downwind of the industries, implicating a coal tar or coke oven source of contamination. The lower thia-arene ratios observed at Site 1 are likely due to the presence of coal tar contaminated material from a ship canal nearby.

The relationship between the *m/z* 212:*m/z* 184 ratio and total concentration of PAH was also examined in the zebra mussel extracts (Figure 3.9). A decrease in *m/z* 212:*m/z* 184 ratio was found with increasing total PAH concentration. The same trend observed in Figure 3.9 for the zebra mussels was observed in Figure 3.5 for the air particulate extracts. A similar relationship was observed between thia-arene ratio and total concentration of PAH in the suspended sediments (data not shown).

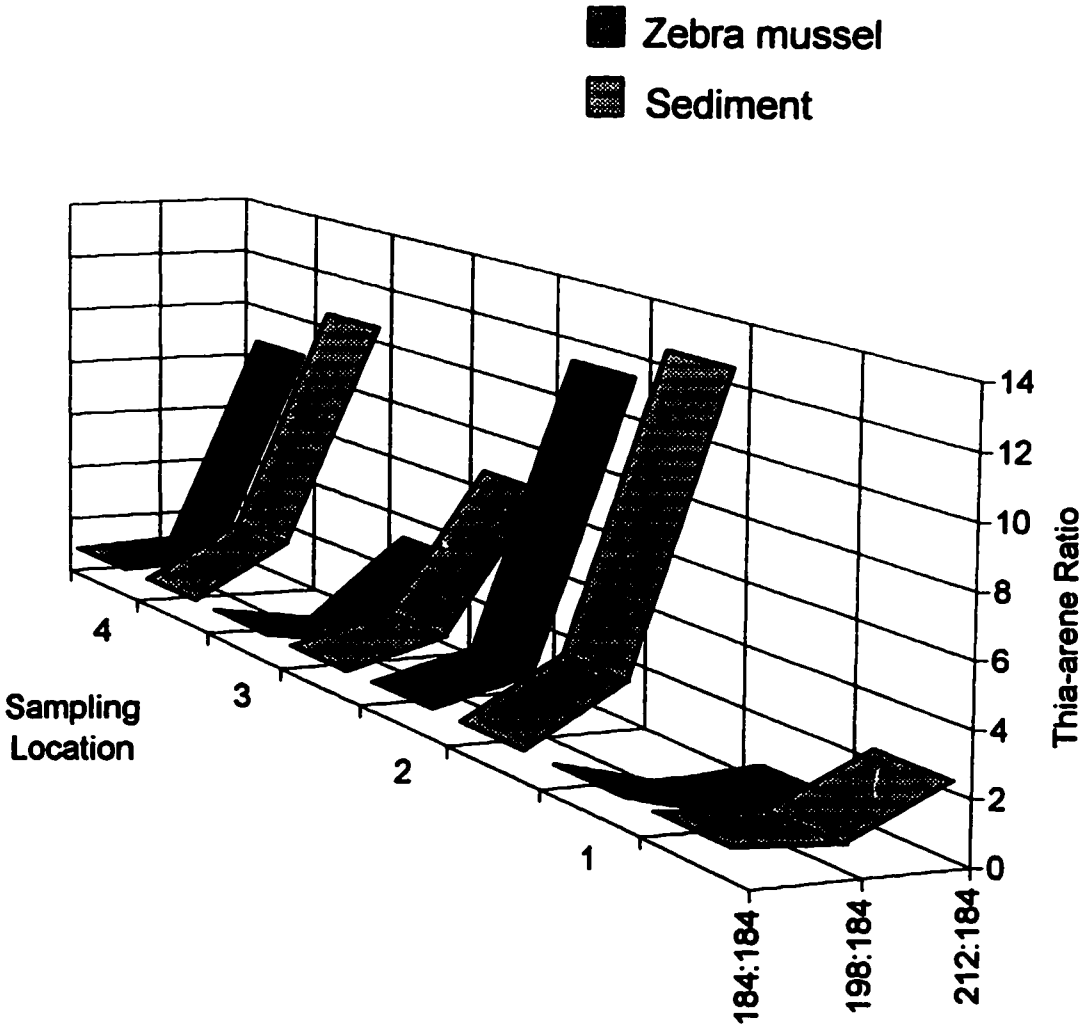

Figure 3.8. Alkyldibenzothiophene profiles in suspended sediments and zebra mussel extracts of samples collected at four locations in Hamilton Harbour. The dark bands correspond to zebra mussel extracts and the lighter bands correspond to suspended sediment extracts.

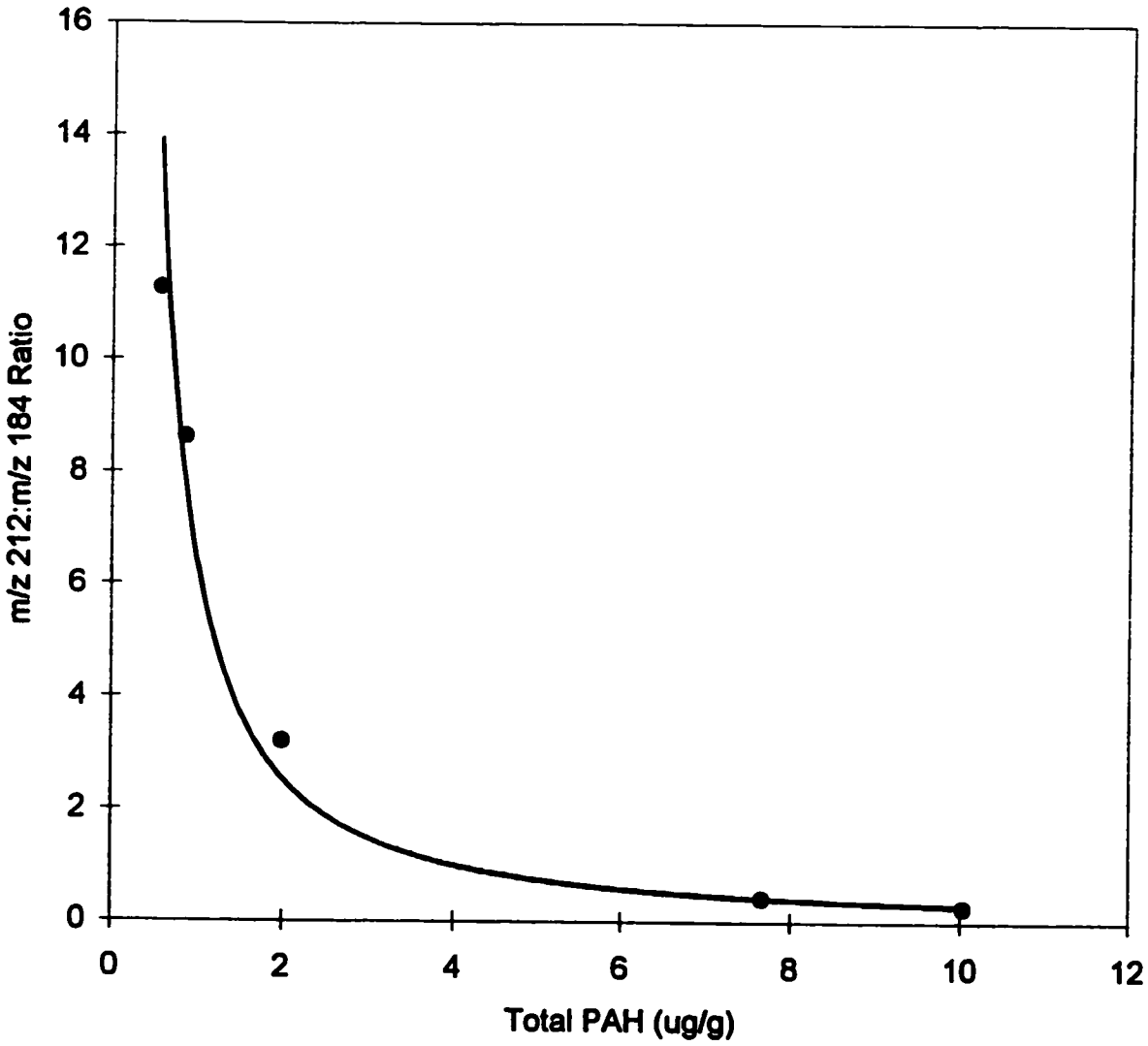

Figure 3.9. Relationship between thia-arene ratio (*m/z* 212:*m/z* 184) and total concentration of PAH in Hamilton Harbour zebra mussels.

3.6 Summary of DBT Thia-Arene Ratios as Source Tracers

A lesser degree of alkylation is observed in the thia-arene profiles of coke oven and coal tar samples than in the thia-arene profiles of diesel exhaust and urban air samples. Air particulate collected downwind of the coke ovens tended to have lower *m/z* 212:*m/z* 184 thia-arene ratios and greater PAH concentrations than air particulate collected upwind of the coke ovens. These results indicate that DBT thia-arene ratios can distinguish between coke oven emissions and diesel exhaust emissions and that coke oven emissions contribute significantly greater amounts of PAH to Hamilton air particulate than motor vehicle emissions. High levels of PAH on respirable air particulate are a concern because several PAH are mutagenic and/or carcinogenic and exposure to the pollutants can occur by inhalation.

Thia-arene profiles in sediments and zebra mussels vary with location and indicate that emissions from both mobile sources and the steel industries contribute to PAH contamination in Hamilton Harbour. Thia-arene profiles examined in Hamilton Harbour samples indicate that PAH contamination at Randle Reef and Windermere Arm Site 1 originates from coal tar or coke oven sources while at Windermere Arm Sites 2, 3 and 4, sources other than coal tar or coke oven emissions are responsible for PAH contamination. Coal-derived sources appear to contribute the greatest amount of PAH contamination to Hamilton Harbour.

3.7 Stability of Thia-Arene Ratios in the Environment

The use of chemical profiles as source tracers requires that these profiles are stable in ambient samples. Profiles of PAH in environmental samples may potentially be altered due to a variety of physical or chemical processes. PAH adsorbed to air particulate may partition into the vapour phase, react with other chemical species in the atmosphere, or undergo photochemical degradation [165]. In the aquatic environment, PAH may undergo volatilization from the water surface, photooxidation, chemical oxidation or microbial metabolism [166]. Atmospheric transformations might favour certain PAH compounds, leading to altered ratio values. This may be a problem for source apportionment studies which rely on PAH profiles for source identification.

It is difficult to estimate the importance of chemical transformations of PAH adsorbed to air particulate. Many PAH show significant reactivity in laboratory experiments with simulated atmospheric conditions [73], but ambient studies show varying effects of reactivity. PAH adsorbed to air particulate may be more persistent in the atmosphere than would be predicted from laboratory studies [166].

The reactivities of the sulfur heterocycles have not been studied to the same extent as the PAH. It would be of interest to determine the relative reactivity of the thia-arenes compared to PAH. It is expected that different thia-arene isomers will exhibit different reactivities. Oxidations of thia-arenes in a coal tar extract using MCPBA were performed in the present study for the purpose of investigating alternative analysis methods. This oxidation procedure was previously used to separate thia-arenes from PAH in crude oil [74]. It was observed that DBT (Compound 51) and Compound 53

were more easily oxidized than Compound 50 and Compound 52 in the sample (Figure 3.10). Differences were also observed in the relative reactivities of the 234 amu thia-arenes and the PAH. Following the oxidation procedure, 91% of benzo[a]pyrene was destroyed, but 98% of benzo[b]fluoranthene remained. It is possible that compounds included in DBT thia-arene ratios will have varying reactivities in ambient air. For example, if the parent (unsubstituted) thia-arenes were more reactive than the alkylated derivatives, then the m/z 212:m/z 184 ratio would increase with time.

Processes that degrade PAH in the aquatic environment include photooxidation, chemical oxidation and biodegradation. The solubilities of PAH also affect chemical profiles in sediments. The effects of these processes have been studied to some extent due to the presence of PAH and alkyl PAH in sediments contaminated by crude oils.

Certain thia-arene compounds appear to be preferentially degraded in the environment. Biodegradation may alter the alkyl homologue distribution of PAH and the relative ratios of PAH isomers. The susceptibility of thia-arenes to biodegradation was found to decrease with increasing alkyl substitution [123,167-169]. A decrease in concentration of selected PAH relative to their alkylated derivatives has also been observed with increasing maturity of crude oils [170,171]. The rate of PAH biodegradation in the environment was also found to decrease with increasing number of aromatic rings [123,169]. Certain methyldibenzothiophene isomers were found to be preferentially removed by bacteria, altering the distribution of the 198 amu isomers [172].

Some evidence has indicated that alkyl PAH are more sensitive to photooxidation than the parent PAH [166]. Chemical oxidation reactions of PAH in sediment are similar

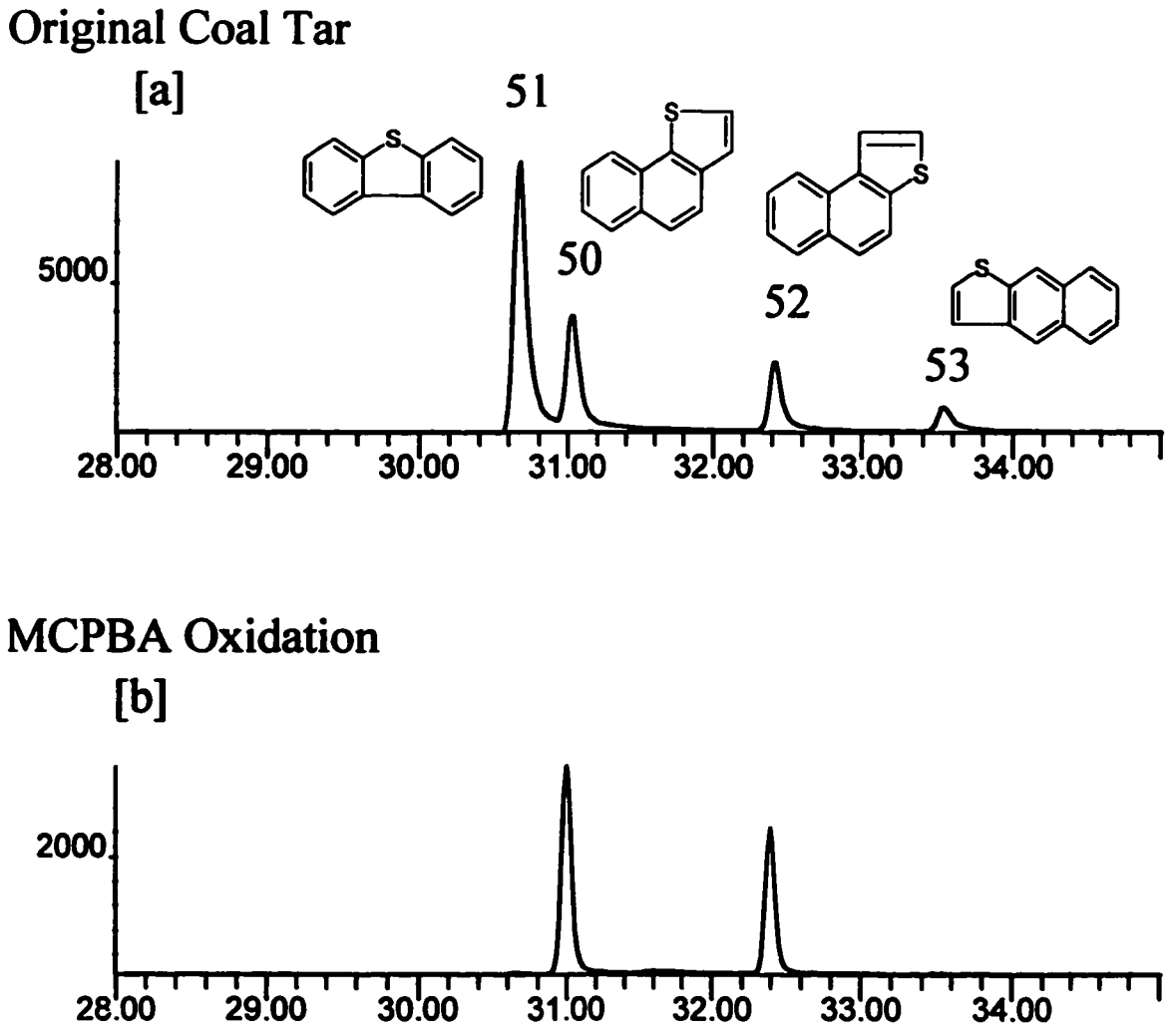

Figure 3.10. Thia-arene isomers (184 amu) in a coal tar extract, (a) before oxidation and (b) after oxidation with MCPBA.

to those of airborne PAH, but photooxidation is less significant for PAH in the harbour than in air particulate due to reduced sunlight, oxygen and temperature.

The solubility of PAH can also affect their distribution in sediments [166]. PAH generally have low solubilities in water, but the presence of other organic compounds or humic substances can increase solubility. Alkyl PAH were found to have lower solubilities in water than non-alkylated parent PAH. The solubility of PAH also decreases with increasing molecular mass.

Evaporative losses of thia-arenes from oil spills have been investigated [171]. Most homologous PAH groups show a trend for increasing evaporative loss with decreasing alkyl substitution. Evaporative losses of PAH from Harbour sediments are not expected to be large, but volatilization will likely be significant for air particulate. It is possible that a similar trend would be observed for volatilization losses from air particulate.

Biodegradation, solubility and evaporation all preferentially remove non-alkylated parent PAH and would be expected to increase the *m/z* 212:*m/z* 184 ratio. In contrast, photooxidation preferentially degrades the alkyl PAH, in effect reducing the *m/z* 212:*m/z* 184 ratio. Thia-arene ratios (*m/z* 212:*m/z* 184) were sometimes greater in ambient samples than in the diesel source sample and the lowest ratios were higher than the ratios for coke oven and coal tar source samples. It is possible that biodegradation and/or solubility have a significant effect on the thia-arene ratio in sediments, while volatilization may alter the *m/z* 212:*m/z* 184 ratio in air particulate. Preferential

degradation of the alkylated thia-arenes due to photooxidation is not observed in these ambient samples.

The observed DBT thia-arene profiles in ambient samples may also differ from the source samples due to chemical reactivity (as described earlier) or the presence of other sources not accounted for in this study. The source samples chosen for this study were selected mainly for the representation of air pollution sources. Petroleum spillage was found to be a major source of PAH to the aquatic environment [166]. Petroleum sources, formed at low temperatures, would be expected to contain dibenzothiophenes with a high degree of alkylation.

3.8 Future Direction of Source Apportionment Method

The results obtained at this point indicate that thia-arenes can be used to distinguish coke oven emissions from traffic emissions in Hamilton air particulate. A limited number of thia-arene compounds were analyzed in this set of ambient samples because the samples were originally analyzed for a different purpose. The initial results from these samples were promising so a new study was designed to further investigate thia-arenes as source apportionment tracers in air particulate. Changes will be made to the method to improve the analysis as a result of current limitations that will be discussed in the following paragraphs.

A new set of respirable air particulate samples were collected, and the placement of sampling sites was decided based on the following discussion. In Section 3.3, thia-arene ratios in air particulate collected downwind of the coke ovens were greater than

thia-arene ratios determined for the coke oven condensate. The difference between the ratios may exist because the downwind air particulate samples contain significant amounts of diesel emissions that increase the thia-arene ratio. Increased dispersion and dilution of coke oven emissions occurs with distance from the source, so it was thought that lower thia-arene ratios might be observed in air particulate collected closer to the coke ovens. Another possibility is that the thia-arene profile of the coke oven condensate source sample is not be representative of particulate emissions from the source. In future sampling, a sampler will be located closer to the coke ovens to determine if the thia-arene profile collected at a closer site will more closely resemble the thia-arene profile for coke oven condensate. A sampler will also be located on the opposite side of the steel mills to collect particulate upwind and downwind of the coke ovens, simultaneously. This will reduce the possibility of contamination from another source upwind of the steel mills.

The alkylated dibenzothiophene isomers (184, 198 and 212 amu) have shown to be useful source tracers in air particulate and sediment samples in this chapter. Many other thia-arene compounds exist in environmental samples and may also be useful as source tracers. Benzo[b]naphtho[2,1-d]thiophene (B21T, 234 amu) has been suggested as a tracer for diesel emissions [22]. This compound is not unique to diesel emissions as it is detected in both the coke oven condensate and diesel reference samples, however, relative amounts of the isomers of BNT are found to differ in the two reference samples. Profiles of higher mass thia-arenes (258 amu) also differed in the two reference samples. It would be useful to examine 234 and 258 amu thia-arenes in these ambient samples but insufficient mass spectral data were collected to permit a re-analysis of these thia-arenes

in the 1990-1991 air particulate samples. PAH with four or more rings are also less volatile than the smaller PAH and will be found predominately in the particulate phase. Only air particulate is analyzed in this study, so it is suitable to examine thia-arenes with four or more rings. For this reason, the 234 and 258 amu thia-arenes may be more appropriate source tracers.

Evaporative processes were not found to discriminate among structural isomers for four methyldibenzothiophenes in crude oil [171]. Rather than examining the alkyl homologue distribution, which was shown to be altered by evaporative processes, the pattern of the relative amounts of structural isomers (m/z 234 or m/z 258) will be studied.

A large number of thia-arene isomers exist and the number of isomers increases as the size of the molecule increases. As the analysis is extended to the 234 amu and 258 amu thia-arenes, a larger number of isomers will occur. It is desirable to chromatographically resolve as many isomers as possible to obtain the maximum source profile information from the sample. The larger number of thia-arene isomers at higher masses are difficult to resolve even with high resolution gas chromatography. The GC analyses to this point were performed using a 5% phenylmethylpolysiloxane (DB-5ms) stationary phase for the separation of compounds. The mass selective detector can resolve compounds that differ in mass, but an efficient chromatographic separation is required to resolve isomers of the same mass. Many thia-arene isomers co-elute on the DB-5ms column, so it would be useful to determine if another stationary phase allows the separation of a greater number of isomers.

In the next chapter, improvements made to the analytical method will be discussed. As a result of the work presented in this chapter, the method changes will include further air particulate sampling at a greater number of locations, the evaluation of several GC stationary phases, and validation of the analytical method for the analysis of 234 amu and 258 amu thia-arenes. After completion of the method development, determination of source apportionment criteria will resume in subsequent chapters.

4.0 METHOD DEVELOPMENT

4.1 Overview

The clean-up procedures and analytical methods used in our research group was evaluated several years ago and had been shown to be applicable to a wide range of environmental matrices including air particulate material, sediments, zebra mussels and neat organic matrices such as oils. In order to improve sample handling and throughput newer clean-up methods were investigated and the need for the Sephadex LH20 chromatographic procedure was evaluated. The optimal stationary phase for GC analysis of PAH and thia-arenes was also chosen. The reproducibility of the revised analytical method was then determined. It was not my intention to undertake a thorough validation of the method at this time, however, this chapter will address: (1) the evaluation of the clean-up procedures; (2) the selection of an optimal GC stationary phase; and (3) the determination of the reproducibility of the method.

4.2 Evaluation of Clean-Up Procedures

The standard method used in this laboratory for fractionating or cleaning up environmental sample extracts has involved the use of open-column alumina chromatography followed by Sephadex LH20 chromatography to isolate a non-polar aromatic fraction for GC/MS analysis. The details of these procedures are given in previous publications and theses from our group [10,173,174]. The alumina procedure involves adsorption of the crude organic extract onto alumina (1.0g) and packing this

alumina on top of freshly activated alumina (2.0g, activated at 170°C for at least 48 hours). This column is eluted with volumes of hexane, benzene, dichloromethane, methanol and methanol:water (3:1). The benzene (A2) and dichloromethane (A3) fractions contained non-polar aromatics (PAH and high mass PAH/PAC, respectively); the methanol (A4) and methanol/water (A5) fractions contained polar aromatics. The non-polar aromatic fractions (A2 and A3) were combined (A23) and further fractionated on Sephadex LH20 to afford an aliphatic fraction (A0) and an aromatic fraction (A23/LH20); the latter fraction was then analyzed by GC/MS.

4.2.1 Comparison of Chromatographic Clean-Up Methods

The procedures used to clean up samples prior to GC/MS analysis are time-consuming and labour-intensive. Other laboratories, such as the Ontario Ministry of the Environment employ sample clean-up procedures that involve a single silica chromatography step using pre-packed, disposable cartridges to remove polar compounds. It seemed appropriate to compare the silica cartridge method to our open column alumina method and, furthermore, to determine the need for performing the Sephadex LH20 chromatography step after the alumina or silica separation. A large number of samples were to be processed by these procedures so it was worthwhile to investigate or eliminate any unnecessary steps.

To address this problem it was necessary to prepare a single sample for clean-up and analysis by the different methods. A composite air particulate sample was prepared from sixteen filters collected on Bay Street in downtown Toronto, Ontario. The filters

were extracted together by A. R. Boden for 24 hours with dichloromethane using a large Soxhlet apparatus to afford a single extract. A portion was fractionated by the standard alumina clean-up procedure to afford a non-polar aromatic (A23) fraction. A second identical portion was cleaned up using dichloromethane elution through a silica Sep-pak cartridge to afford a non-polar fraction (S1). The non-polar fractions (A23 and S1) were each divided into two equal portions (two halves). One half of each fraction was solvent exchanged with toluene and analyzed by GC/MS in selected ion monitoring mode. The second half of each fraction was cleaned up further on a Sephadex LH20 column before GC/MS analysis.

Total ion current chromatograms for the four fractions of the composite air particulate extract are shown in Figures 4.1 and 4.2. The alumina only and alumina + Sephadex LH20 fractions are shown in Figure 4.1. The chromatographic performance of the alumina + Sephadex LH20 fraction was clearly superior to the alumina only fraction. Several peaks in the chromatogram of the alumina only fraction are not present in the chromatogram of the fraction cleaned up with alumina and Sephadex LH20. These peaks likely included smaller aromatic compounds and other substances that eluted before naphthalene from the Sephadex LH20 column, but the identities of these peaks were not determined. Gas chromatographic resolution improved when the Sephadex LH20 procedure was applied to the sample. Improvement in resolution was observed for several peaks that eluted close together (Figure 4.1(a)). The baseline was almost flat in the sample on which the Sephadex LH20 procedure was used, indicating the removal of interfering substances.

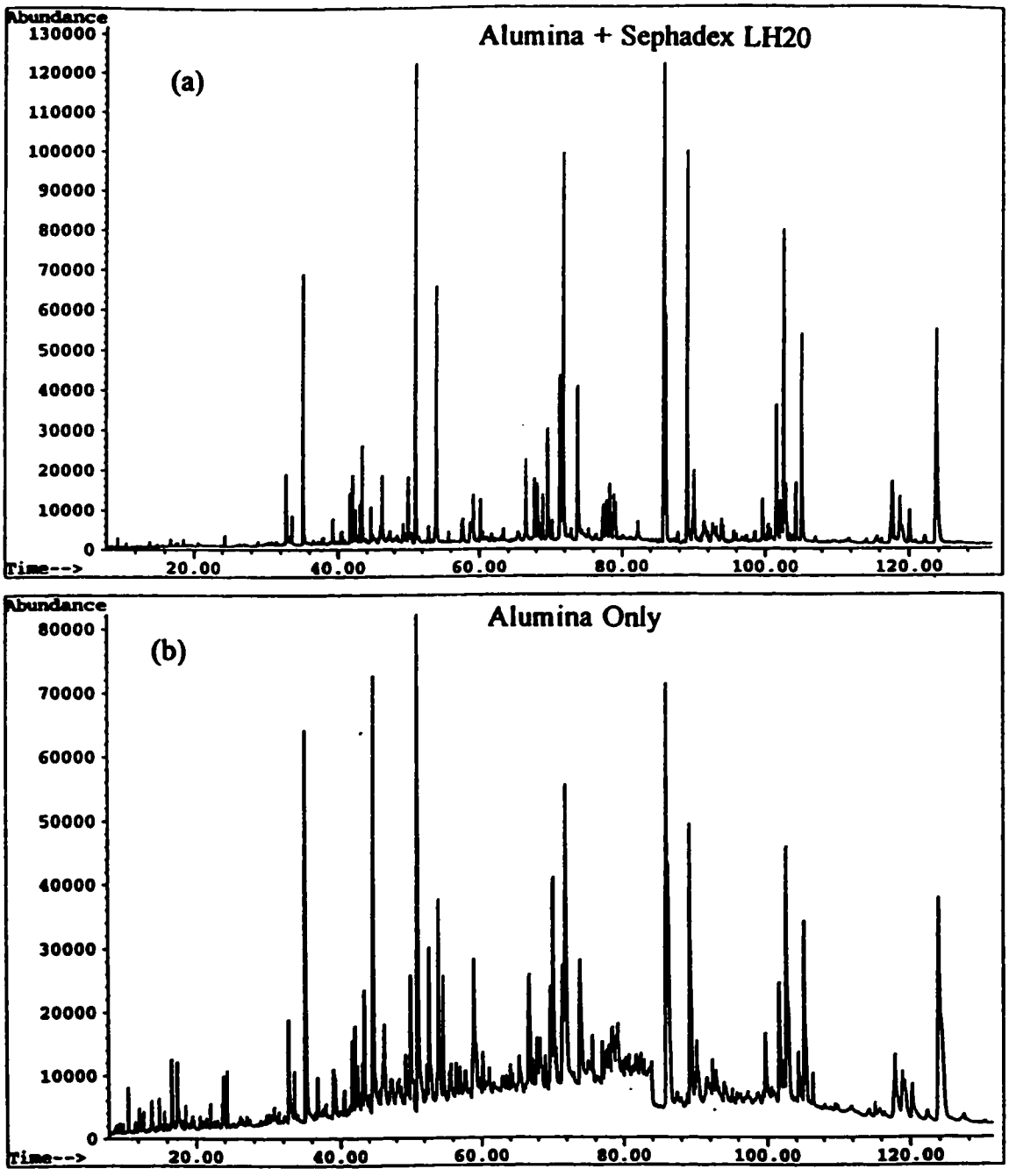

Figure 4.1. Chromatograms of a Toronto air particulate extract (Toronto Composite B) prepared by two different clean-up procedures: (a) alumina and Sephadex LH20 and (b) alumina only. Analyses performed using GC/MS Conditions A.

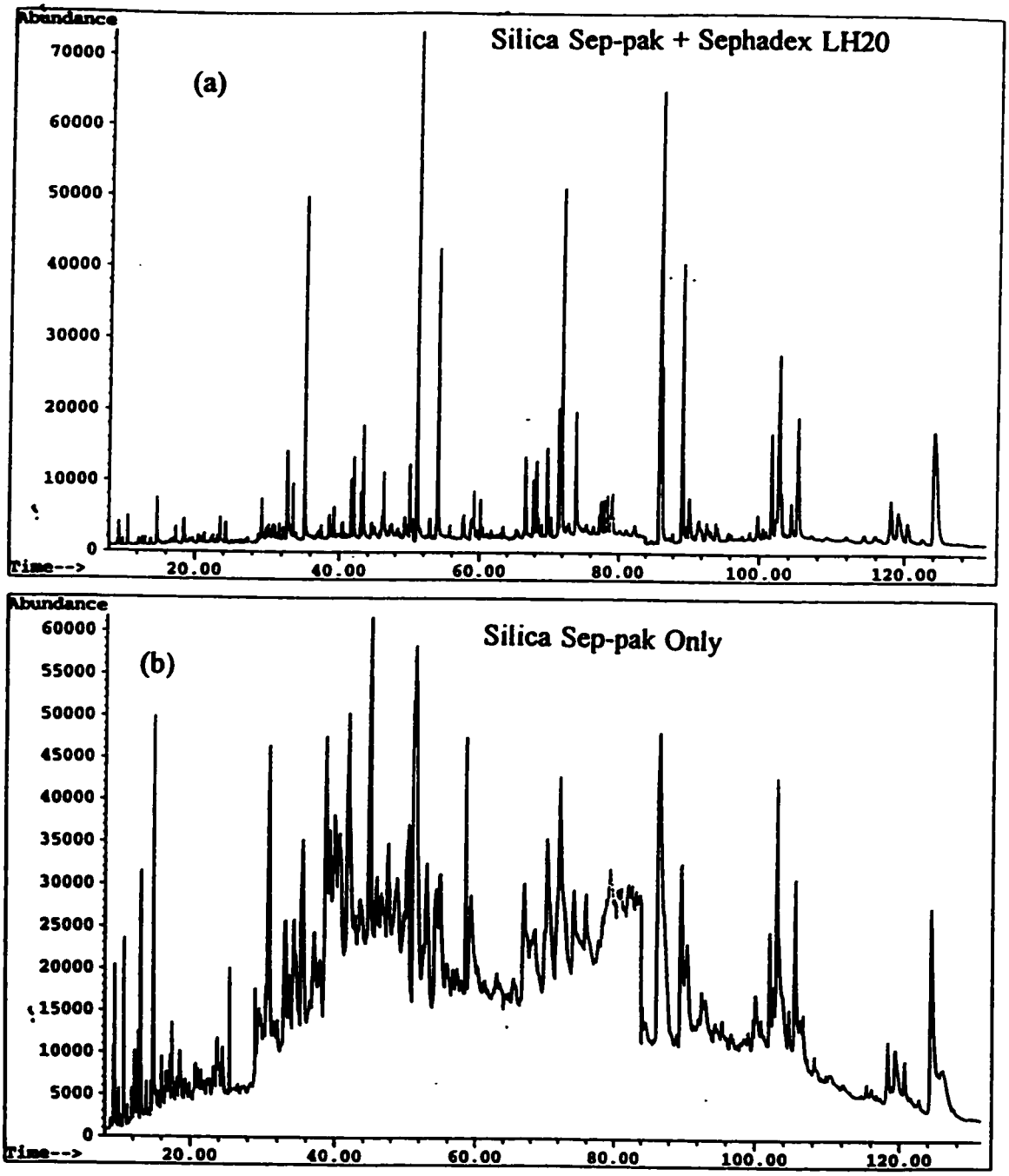

Figure 4.2. Chromatograms of a Toronto air particulate extract (Toronto Composite B) prepared by two different clean-up procedures: (a) silica Sep-pak and Sephadex LH20 and (b) silica Sep-pak only. Analyses performed using GC/MS Conditions A.

Total ion chromatograms for fractions prepared using the silica only and silica + Sephadex LH20 methods are shown in Figure 4.2. The baseline of the total ion chromatogram (TIC) of the silica only fraction (Figure 4.2(b)) was much higher in abundance than the baseline for the alumina only fraction (Figure 4.1(b)). More components seem to be removed from the air particulate extract using the alumina procedure compared to the silica Sep-pak procedure. After the silica sample was fractionated by Sephadex LH20, the chromatographic performance improved dramatically. Few differences exist in the chromatographic performance of samples following a Sephadex LH20 clean-up using either silica or alumina as the first step.

The first conclusion that can be drawn from these experiments is that the Sephadex LH20 step, while tedious, leads to a significant improvement in chromatographic performance by GC/MS. It is probable that maintenance of the GC column and retention gap is reduced when samples cleaned up using the Sephadex step are analyzed. While major PAH peaks can be quantified in the silica only and alumina only chromatograms, minor peaks posed a significant problem. Since thia-arene peaks have peak areas 10-fold to 1000-fold lower than the areas of the major PAH peaks, I decided that inclusion of the Sephadex LH20 was critical to the proper analysis and quantification of thia-arenes.

Careful analysis of the GC/MS chromatograms following the silica + Sephadex LH20 and alumina + Sephadex LH20 showed some minor differences (Figures 4.3 and 4.4). For example, an additional peak was observed in the m/z 198 extracted ion chromatogram of the silica + Sephadex LH20 fraction (Figure 4.3(b)) compared to the

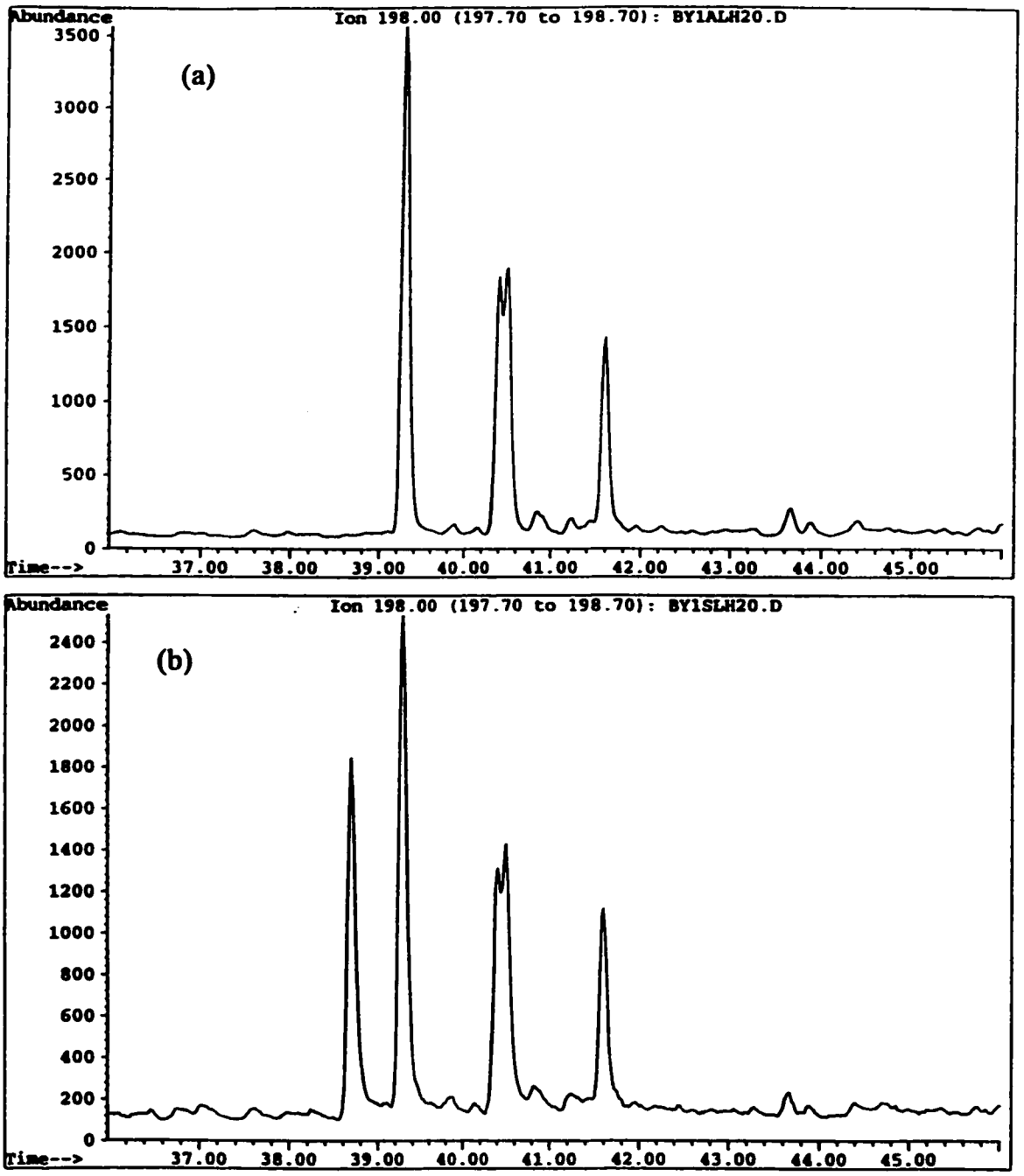

Figure 4.3. Ion chromatograms (m/z 198) of a Toronto air particulate extract (Toronto Composite B) prepared by two different clean-up procedures: (a) alumina + Sephadex LH20 and (b) silica Sep-pak + Sephadex LH20. Analyses performed using GC/MS Conditions A.

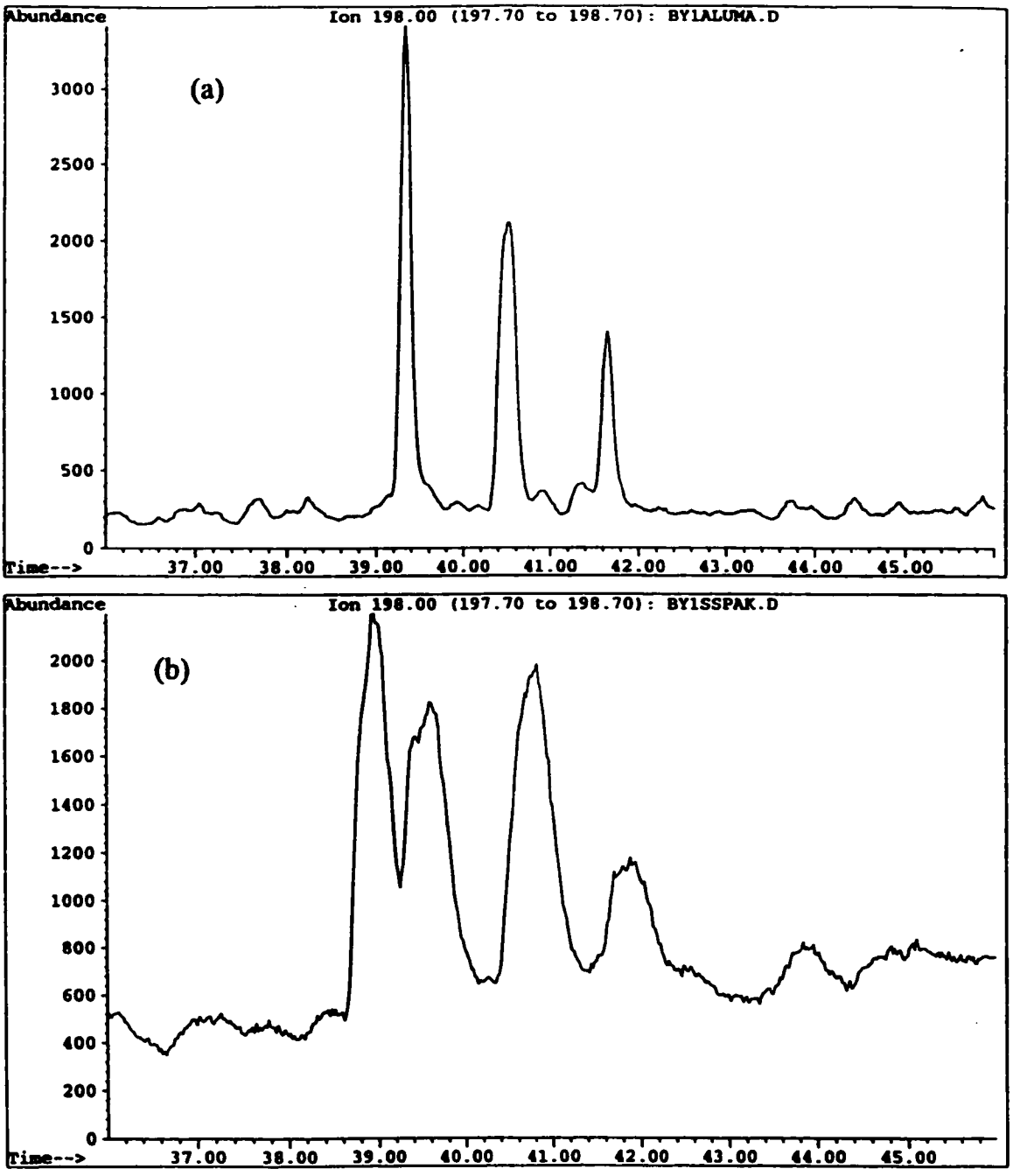

Figure 4.4. Ion chromatograms (m/z 198) of a Toronto air particulate extract (Toronto Composite B) prepared by two different clean-up procedures: (a) alumina only and (b) silica Sep-pak only. Analyses performed using GC/MS Conditions A.

alumina + Sephadex LH20 fraction (Figure 4.3(a)). The peak widths of the peaks in these chromatograms were comparable. The fractions which had not undergone Sephadex clean-up showed much poorer resolution and increased background compared to the fractions which had undergone Sephadex LH20 fractionation (Figure 4.4). The unidentified peak in Figure 4.3(a) may interfere with thia-arene analyses, particularly when different stationary phases are tested and the elution pattern of chromatographic peaks is altered. For this reason, it was decided to process all sample extracts using the standard alumina + Sephadex LH20 procedure.

Although not employed in the present study, the silica Sep-pak procedure was faster and simpler than the alumina step. The increased ease of the silica Sep-pak step prompted us to change our methodology for other applications to save time, effort and sample handling.

4.3 Recovery of Deuterated PAH Standards

The purpose of this series of experiments was to evaluate the recoveries of standards at each stage of the clean-up procedure separately and then to evaluate the whole procedure. A preliminary experiment was performed as follows. Three deuterated PAH recovery standards (phenanthrene-d_{10}, chrysene-d_{12}, and dibenz[a,h]anthracene-d_{14}) were taken through the alumina, Sephadex LH20 and solvent evaporation procedures separately to evaluate the percent recovery at each step of the clean-up procedure. For Trial 1, 0.5 mL recovery standard was placed in each of three 50 mL round bottom flasks (Flasks 1-3). Flask 1 was used to test the recovery after solvent evaporation using the

rotary evaporator then the Reacti-vap evaporator. The standard was quantitatively transferred to a vial and reduced to a volume of 175 μL. A 25 μL aliquot was transferred to a GC autosampler vial and evaporated to dryness. The residue was taken up in 10 μL of internal standard solution and analyzed and quantified by GC/MS.

Flask 2 was used to test the recovery of PAH from the alumina column. The solution containing the recovery standard was fractionated on alumina. The A23 fraction was prepared and reduced in volume to 175 μL, and processed in the same manner as Flask 1. Flask 3 was taken through the Sephadex LH20 procedure, then processed in the same manner as Flask 1.

The percent recoveries of the deuterated standards from each procedure are listed in Table 4.1. The recovery of phenanthrene-d_{10} was low for all procedures, ranging from 10-48 %. Volatilization of phenanthrene-d_{10} during solvent evaporation has likely contributed to these losses in all cases. Recoveries for chrysene-d_{12} and dibenz[a,h]anthracene-d_{14} are highest for the solvent evaporation procedure (94 and 98 %), followed by the alumina procedure (84 and 85 %) and the Sephadex LH20 procedure (69 and 71 %). This corresponds to average losses of 228-278 amu PAH of 4%, 16%, and 30% for the solvent evaporation, alumina, and Sephadex LH20 procedures respectively.

Evaporating the sample to dryness appears to cause a major loss of d10-phenanthrene, but negligible losses of the other two standards. Changes were made to the procedures to minimize recovery losses. Internal standard (70 μL) in toluene was added to the entire sample before evaporation of the LH20 solvent so that the sample would

Table 4.1. Percent recovery for three deuterated PAH standards for sample preparation procedures.

Procedure	%Recovery		
	Phenanthrene-d10	Chrysene-d12	Dibenz[a,h]anthracene-d14
Trial 1			
Evaporation (Flask 1)	10	94	98
Alumina (Flask 2)	48	84	85
Sephadex LH20 (Flask 3)	25	69	71
Trial 2			
Entire Procedure (blank filters)	76	89	90

never evaporate to dryness. The sample extract was then reduced in volume to approximately 70 μL and a 10 μL aliquot was transferred to an autosampler vial for GC/MS analysis. The recoveries of all standards increased, particularly the recoveries of phenanthrene-d_{10}.

Another potential source of samples loss occurs in the alumina column procedure when the sample adsorbed to alumina is transferred to the alumina column. Alumina powder adheres to the sides of the flask and is not completely transferred to the column. To minimize these losses, all flasks were rinsed three times with small portions of the column eluent and the rinses were added to the column. Another source of sample loss occurs when the sample extract is applied to the Sephadex LH20 column; some sample remains in the syringe needle. To minimize this sample loss, a larger injection volume was used so that a more dilute solution would be left in the syringe needle. In addition, the flask containing the alumina column eluent was rinsed twice with dichloromethane and these rinses were also taken up in the syringe before injection onto the Sephadex LH20 column.

To evaluate these modifications two blank filters were extracted and taken through the full clean-up procedure (Trial 2). Average recoveries for the deuterated standards were 76% for phenanthrene-d_{10}, 89% for chrysene-d_{12} and 90% for dibenz[a,h]anthracene-d_{14} (Table 4.1). Concentrations of other PAH were below the detection limit. These changes were incorporated into the standard procedure and all Hamilton air particulate filters collected in 1995 were extracted and cleaned up using this revised procedure. Average recoveries for the deuterated standards added to real samples

were 65% for phenanthrene-d10, 82% for chrysene-d12 and 84% for dibenz[a,h]anthracene-d14. Recoveries for individual samples are listed in Appendix II.

4.4 Instrument Performance: Linearity and Reproducibility

The linearity of the analytical system was tested by analyzing a PAH mixture on the DB-17ht column at six concentrations which spanned three orders of magnitude. The solutions were prepared by serial dilution of a concentrated mixture and each solution was analyzed three times in random order. Calibration curves for the five PAH components are shown in Figure 4.5. The phenanthrene curve was linear over the entire concentration range. The four remaining curves were linear up to 20 ng injected. Peak areas for injections of 30 ng for pyrene, chrysene, benzo[e]pyrene, and benzo[ghi]perylene were slightly lower than would be expected due to overloading of this thin film column. Samples analyzed in the present study that contained amounts of individual compounds above 20 ng were diluted and reanalyzed. The detection limit for these PAH was estimated to be approximately10 pg at a signal-to-noise ratio of 3:1.

To test the precision of the instrument, eight replicate analyses were performed using a PAH calibration standard. The amounts and retention times for the eight replicate analyses are listed in Table 4.2. The standard deviations of the amounts, calculated by calibrating with the first standard, ranged from 0.2% for indeno[1,2,3-cd]pyrene and benzo[ghi]perylene to 4.1% for dibenzo[a,i]pyrene. A lower precision is expected for the later eluting compounds due to broadening of the chromatographic peaks. The standard deviation of the retention times ranged from 0.002 min for dibenzothiophene and perylene to 0.018 min for dibenzo[a,h]pyrene.

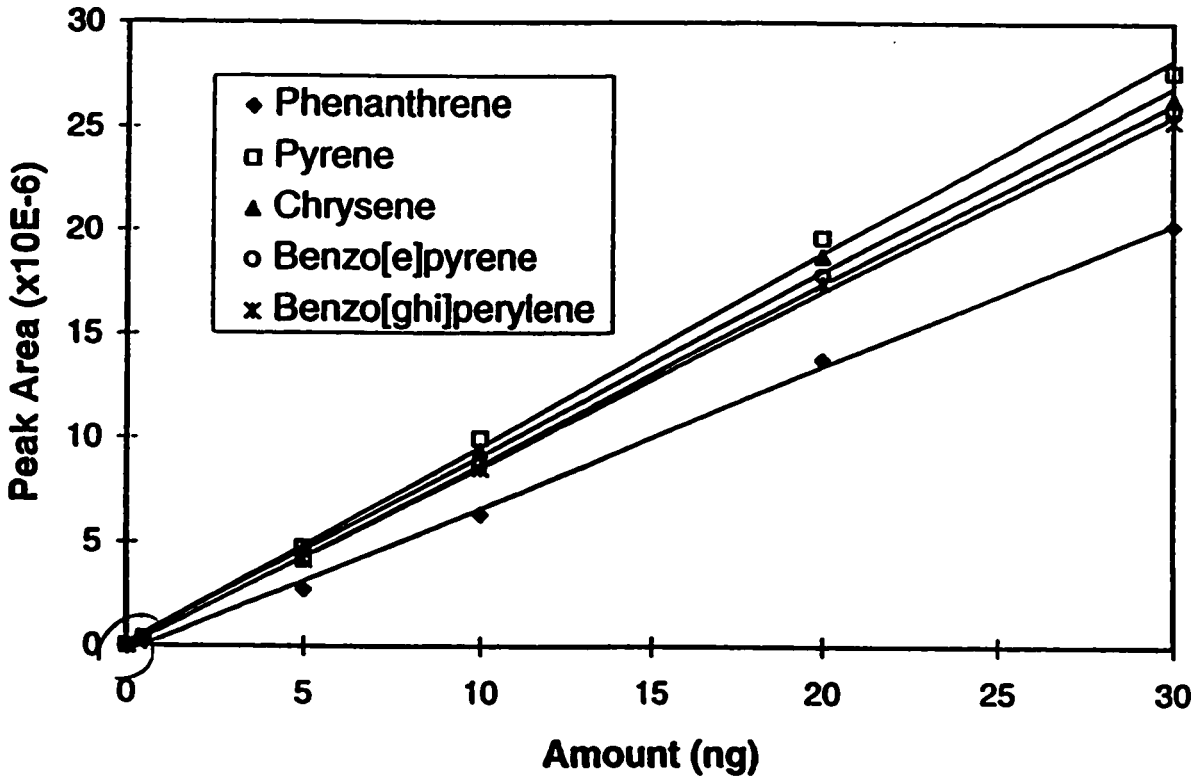

Figure 4.5. Calibration plots for selected PAH.

Table 4.2. Amounts and retention times for eight replicate analyses of a PAH calibration standard. GC/MS Conditions B.

Amount (ng)										
	1	2	3	4	5	6	7	8	Average	% RSD
Dibenzothiophene	6.04	6.04	6.08	6.08	6.12	6.10	6.08	6.07	6.08	0.5
Phenanthrene	8.00	8.01	8.01	7.92	7.94	7.89	7.81	7.80	7.92	1.0
Anthracene	9.82	9.86	10.05	9.98	10.12	10.17	10.18	10.16	10.04	1.4
Fluoranthene	6.84	6.89	6.90	6.92	6.95	6.94	6.94	6.93	6.91	0.5
Pyrene	7.35	7.41	7.35	7.32	7.29	7.27	7.16	7.16	7.29	1.2
B[b]N[2,1-d]thiophene	2.21	2.17	2.18	2.17	2.19	2.18	2.17	2.17	2.18	0.7
B[b]N[2,3-d]thiophene	4.53	4.48	4.48	4.48	4.51	4.49	4.48	4.46	4.49	0.5
Benz[a]anthracene	6.90	6.80	6.78	6.79	6.80	6.80	6.74	6.72	6.79	0.8
Chrysene	7.61	7.52	7.50	7.49	7.55	7.53	7.52	7.53	7.53	0.5
Benzo[b]fluoranthene	6.47	6.61	6.60	6.55	6.49	6.45	6.48	6.44	6.51	1.0
Benzo[k]fluoranthene	4.75	4.77	4.82	4.81	4.87	4.89	4.89	4.92	4.84	1.3
Benzo[j]fluoranthene	4.65	4.70	4.72	4.71	4.75	4.76	4.77	4.80	4.73	1.0
Benzo[e]pyrene	6.91	7.07	7.11	7.09	7.08	7.07	7.09	7.09	7.07	0.9
Benzo[a]pyrene	5.27	5.38	5.38	5.35	5.36	5.39	5.39	5.40	5.37	0.8
Perylene	5.99	6.08	6.13	6.07	6.07	6.07	6.09	6.10	6.08	0.7
Indeno[1,2,3-cd]pyrene	3.32	3.32	3.33	3.32	3.32	3.33	3.34	3.34	3.33	0.2
Dibenz[ac]anthracene	7.45	7.45	7.50	7.46	7.48	7.52	7.50	7.53	7.49	0.4
Picene	2.06	1.99	1.99	1.96	1.94	1.91	1.92	1.89	1.96	2.8
Benzo[ghi]perylene	6.33	6.35	6.38	6.35	6.35	6.35	6.37	6.36	6.36	0.2
Coronene	4.29	4.18	4.21	4.16	4.18	4.17	4.19	4.17	4.19	1.0
Dibenzo[a,e]pyrene	4.42	4.29	4.30	4.26	4.23	4.22	4.22	4.19	4.27	1.7
Dibenzo[a,i]pyrene	4.52	4.31	4.30	4.23	4.18	4.10	4.05	3.97	4.21	4.1
Dibenzo[a,h]pyrene	5.09	4.88	4.85	4.81	4.77	4.75	4.79	4.78	4.84	2.3

Retention time										
	1	2	3	4	5	6	7	8	Average	Std. Dev.
Dibenzothiophene	30.70	30.69	30.69	30.69	30.69	30.69	30.70	30.70	30.695	0.002
Phenanthrene	31.76	31.76	31.75	31.75	31.75	31.75	31.76	31.76	31.755	0.003
Anthracene	31.95	31.95	31.95	31.94	31.94	31.94	31.94	31.95	31.946	0.003
Fluoranthene	42.79	42.79	42.79	42.78	42.78	42.78	42.78	42.79	42.786	0.004
Pyrene	45.25	45.24	45.24	45.24	45.23	45.23	45.24	45.24	45.237	0.004
B[b]N[2,1-d]thiophene	54.23	54.23	54.22	54.23	54.23	54.23	54.23	54.23	54.228	0.003
B[b]N[2,3-d]thiophene	55.92	55.91	55.91	55.91	55.91	55.92	55.92	55.92	55.915	0.004
Benz[a]anthracene	56.47	56.46	56.46	56.46	56.46	56.46	56.46	56.46	56.463	0.003
Chrysene	57.24	57.23	57.23	57.23	57.23	57.23	57.23	57.23	57.229	0.004
Benzo[b]fluoranthene	66.13	66.13	66.12	66.13	66.12	66.12	66.13	66.13	66.126	0.004
Benzo[k]fluoranthene	66.35	66.34	66.34	66.34	66.34	66.34	66.34	66.34	66.341	0.003
Benzo[j]fluoranthene	66.68	66.67	66.67	66.67	66.67	66.67	66.67	66.67	66.671	0.005
Benzo[e]pyrene	69.05	69.05	69.05	69.05	69.04	69.05	69.05	69.05	69.049	0.003
Benzo[a]pyrene	69.42	69.41	69.40	69.41	69.41	69.41	69.41	69.42	69.411	0.004
Perylene	70.46	70.45	70.45	70.45	70.45	70.45	70.45	70.45	70.452	0.002
Indeno[1,2,3-cd]pyrene	77.56	77.56	77.56	77.56	77.57	77.58	77.58	77.58	77.569	0.009
Dibenz[ac]anthracene	77.64	77.64	77.63	77.63	77.63	77.63	77.63	77.64	77.635	0.004
Picene	79.20	79.20	79.19	79.20	79.20	79.21	79.21	79.21	79.202	0.007
Benzo[ghi]perylene	79.77	79.77	79.76	79.77	79.77	79.77	79.77	79.77	79.769	0.003
Coronene	90.34	90.33	90.31	90.32	90.33	90.34	90.34	90.35	90.332	0.010
Dibenzo[a,e]pyrene	90.25	90.24	90.23	90.24	90.25	90.26	90.26	90.27	90.252	0.012
Dibenzo[a,i]pyrene	91.82	91.82	91.81	91.82	91.84	91.85	91.84	91.86	91.831	0.017
Dibenzo[a,h]pyrene	92.83	92.83	92.82	92.83	92.85	92.86	92.86	92.87	92.844	0.018

4.5 GC Column Selection and Determination of Retention Index Values

The chemical composition of GC stationary phases, particularly those developed for use with mass spectrometers, has changed somewhat from the original formulations developed by General Electric, Ohio Valley and other manufacturers. The authors of the first retention index papers used older stationary phase formulations to prepare home-made glass capillary columns. Modern, commercial columns are prepared using direct covalent coupling of the stationary phase to the silica walls of the capillary. The chemical formulations of modern silicone phases are slightly different than the phases made two decades ago. It is probable that modern GC phases will have retention index values that will show some differences from the values reported for home-made phases.

Since no thorough evaluation of PAH separations or retention index determinations had been reported in many years, I conducted a study to compare the performance of some modern GC stationary phases. The GC columns examined are listed in Table 4.3. Columns were 30 meters in length and 0.25 mm internal diameter. All columns have relatively high temperature limits because I wanted to be able to determine retention index values for high mass PAH (276-302 amu). The more polar phases would require higher temperatures for elution of these compounds. All columns had high temperature limits in excess of 300°C, which enabled the determination of retention indices as high as 500.

PAH retention index values are based on the use of four PAH standards which have been assigned the following retention index values: naphthalene, 200; phenanthrene, 300; chrysene, 400; and picene, 500. A retention index (RI) for a given compound (x) is

Table 4.3. Properties of columns and temperature programs used for retention index determinations.

Column ID	Phase (methylpolysiloxane)	Film Thickness	Temperature Program
DB-5ms	5% phenyl	0.25 μm	40-300C@2.5C/min
DB-35ms	35% phenyl	0.25 μm	50-300C@1.6C/min
DB-17ms	50% phenyl	0.25 μm	60-300C@1.6C/min
DB-17ht	50% phenyl	0.15 μm	40-300C@2.5C/min
Rtx-200	trifluoropropyl	0.25 μm	40-300C@2.5C/min

determined by comparing its retention time to the retention times of the two nearest reference standards according to the following formula:

$$RI = \left[100 \times \frac{(t_{R_x} - t_{R_z})}{(t_{R_{z+1}} - t_{R_z})} \right] + 100z$$

where z and z+1 are the numbers of aromatic rings in the bracketing standards and t_R is the retention time.

Retention indices were determined for 49 homocyclic PAH and 66 thia-arenes (PASH) on the five columns. Each RI value (listed in Tables 4.4 and 4.6, respectively) is the mean of six individual determinations. Standard deviations of retention index values averaged 0.02 retention index (RI) units and ranged from 0.01 to 0.04 RI units. Retention indices for most compounds on the different phases varied by up to 4 RI units. These results are consistent with a previous study on retention behaviour of PAH on different stationary phases [72]. This study also laid out the criteria for temperature programs required for accurate and reproducible retention indices. These criteria were taken into account when developing the temperature program for each column.

One of the goals of this study was to identify stationary phases that would resolve closely eluting isomeric components. Since isomeric PAH cannot always be readily differentiated by their mass spectra, it is important to resolve them chromatographically in order to quantify them. The average retention index differences (ΔRI) needed to achieve a 50% valley between two peaks on the five columns were determined to be: 0.45 (DB-5ms); 0.32 (DB-35ms); 0.33 (DB-17ms); 0.39 (DB-17ht); 0.39 (Rtx-200). As a rule of thumb, RI differences of 1 RI unit or greater are sufficient to effect the separation of

Table 4.4. Retention indices for polycyclic aromatic compounds (PAC).

No.	Compound	Mol. Wt.	DB-5ms	DB-35ms	DB-17ms	DB-17ht	Rtx-200
1	**Naphthalene**	**128**	**200.00**	**200.00**	**200.00**	**200.00**	**200.00**
2	2-Methylnaphthalene	142	220.62	218.09	216.23	216.99	219.37
3	1-Methylnaphthalene	142	223.32	221.64	220.27	221.14	221.25
4	Biphenyl	154	235.95	233.88	232.47	234.06	229.33
5	Acenaphthylene	152	247.48	247.67	247.38	248.56	249.66
6	Acenaphthene	154	253.28	252.44	251.53	252.67	247.97
7	Fluorene	166	270.04	268.33	266.88	267.70	266.59
8	**Phenanthrene**	**178**	**300.00**	**300.00**	**300.00**	**300.00**	**300.00**
9	Anthracene	178	301.98	301.60	301.16	300.86	301.62
10	*o*-Terphenyl	230	318.25	314.52	315.33	317.41	294.09
11	Anthraquinone	208	331.12	336.25	335.89	336.29	343.23
12	Fluoranthene	202	344.66	343.90	343.65	343.50	346.96
13	Pyrene	202	352.37	352.81	353.15	353.03	353.11
14	*m*-Terphenyl	230	359.16	353.65	353.09	354.14	345.57
15	*p*-Terphenyl	230	364.50	360.43	359.72	360.52	351.28
16	Benzo[*a*]fluorene	216	366.69	365.39	364.32	364.18	363.05
17	Retene	234	367.45	358.11	355.30	355.75	361.78
18	Benzo[*b*]fluorene	216	369.34	367.50	366.47	366.21	366.44
19	Benzo[*ghi*]fluoranthene	226	390.44	389.56	389.63	389.80	392.70
20	Benzo[*c*]phenanthrene	228	390.95	390.49	390.99	391.16	386.98
21	Cyclopenta[*cd*]pyrene	226	397.39	398.16	398.57	398.61	400.98
22	Benz[*a*]anthracene	228	398.88	397.65	397.21	397.01	399.44
23	**Chrysene**	**228**	**400.00**	**400.00**	**400.00**	**400.00**	**400.00**
24	Benzanthrone	230	405.00	410.18	410.93	411.44	418.77
25	2-Nitrofluoranthene	247	412.21	414.51	411.95	412.43	431.33
26	Benz[*a*]anthracene-7,12-dione	258	419.28	422.01	421.20	421.72	425.41
27	1-Nitropyrene	247	420.61	425.64	425.41	426.24	440.11
28	2-Nitropyrene	247	423.78	428.77	427.61	428.23	442.79
29	Benzo[*b*]fluoranthene	252	443.33	441.61	440.86	440.56	446.64
30	Benzo[*j*]fluoranthene	252	443.60	442.89	442.97	442.90	447.50
31	Benzo[*k*]fluoranthene	252	444.44	442.68	441.86	441.44	447.61
32	Benzo[*a*]fluoranthene	252	447.08	445.93	445.69	445.72	450.55
33	Benzo[*e*]pyrene	252	453.10	453.51	453.89	453.61	455.14
34	Benzo[*a*]pyrene	252	454.92	455.52	455.67	455.41	456.49
35	Perylene	252	458.18	459.61	460.32	460.04	459.56
36	3-Methylcholanthrene	268	469.81	466.46	465.33	465.45	467.22
37	Benzo[*c*]chrysene	278	488.99	488.36	488.90	488.81	483.51
38	Indeno[1,2,3-*cd*]pyrene	276	493.99	493.21	492.82	492.58	498.20
39	Dibenz[*a,c*]anthracene	278	496.05	493.55	492.98	492.65	498.17
40	Dibenz[*a,h*]anthracene	278	496.16	494.46	494.10	493.93	497.75
41	Benzo[*b*]chrysene	278	499.10	498.29	498.10	497.94	500.00
42	**Picene**	**278**	**500.00**	**500.00**	**500.00**	**500.00**	**500.00**
43	Benzo[*ghi*]perylene	276	(501.80)	(502.46)	(502.83)	(502.56)	(504.69)
44	Anthanthrene	276	(505.75)	(506.97)	(507.27)	(507.13)	(508.40)
45	Dibenzo[*a,l*]pyrene	302	(536.57)	(542.62)	(544.12)	(537.89)	(533.78)
46	Coronene	300	(546.27)	(558.56)	(559.29)	(549.86)	(548.84)
47	Dibenzo[*a,e*]pyrene	302	(547.30)	(558.52)	(558.80)	(549.33)	(548.91)
48	Dibenzo[*a,i*]pyrene	302	(551.35)	(567.56)	(568.04)	(556.55)	(551.36)
49	Dibenzo[*a,h*]pyrene	302	(553.59)	(572.46)	(573.70)	(560.91)	(553.09)

any two compounds on any of these phases.

4.5.1 Homocyclic PAH Retention Indices

Differences in retention indices, or residuals, were calculated by subtracting the retention index value for a given PAH or PAC on the least polar phase, DB-5ms, from the retention index value on each of the four other phases (Table 4.5). A value of zero means that the retention index on that stationary phase is identical to the retention index determined on DB-5ms.

The retention of a given molecule depends on the interactions between the molecule and the stationary phase of the column. Larger variations are observed for PAC containing polar functional groups (carbonyl and nitro groups), the terphenyl isomers, and retene. Retention of polar compounds increases as the polarity of the stationary phase increases, leading to large negative residuals. Polar compounds, such as nitro- and ketone-containing PAC had the largest increases in retention indices on polar phases (relative to the 5% phenyl phase). Phenyl-substituted compounds (biphenyl and the terphenyls), which are less polarizable than fused-ring PAH, had lower retention indices on all phases relative to the 5% phenyl phase. Residuals as large as 24 RI units are found for the trifluoropropyl phase, the most polar phase.

Some general trends were observed for the parent PAH compounds. Increasing polarity of the phase had relatively little effect on the retention of parent PAH. The largest residuals for PAH were observed for the non-planar PAH, benzo[*c*]phenanthrene (compound 20), and benzo[*c*]chrysene (compound 37) on the trifluoropropyl phase.

Table 4.5. List of residuals from DB-5ms retention indices for PAC.

No.	Compound	Mol. Wt.	DB-35ms	DB-17ms	DB-17ht	Rtx-200
1	**Naphthalene**	**128**	**0.00**	**0.00**	**0.00**	**0.00**
2	2-Methylnaphthalene	142	-2.54	-4.39	-3.64	-1.25
3	1-Methylnaphthalene	142	-1.68	-3.05	-2.18	-2.07
4	Biphenyl	154	-2.07	-3.48	-1.88	-6.62
5	Acenaphthylene	152	0.19	-0.10	1.08	2.18
6	Acenaphthene	154	-0.84	-1.75	-0.61	-5.31
7	Fluorene	166	-1.71	-3.16	-2.34	-3.45
8	**Phenanthrene**	**178**	**0.00**	**0.00**	**0.00**	**0.00**
9	Anthracene	178	-0.38	-0.82	-1.11	-0.35
10	*o*-Terphenyl	230	-3.73	-2.92	-0.84	-24.16
11	Anthraquinone	208	5.13	4.76	5.17	12.11
12	Fluoranthene	202	-0.76	-1.01	-1.16	2.30
13	Pyrene	202	0.44	0.79	0.66	0.75
14	*m*-Terphenyl	230	-5.52	-6.08	-5.03	-13.60
15	*p*-Terphenyl	230	-4.07	-4.79	-3.99	-13.23
16	Benzo[*a*]fluorene	216	-1.30	-2.37	-2.52	-3.65
17	Retene	234	-9.35	-12.15	-11.71	-5.67
18	Benzo[*b*]fluorene	216	-1.84	-2.86	-3.13	-2.89
19	Benzo[*ghi*]fluoranthene	226	-0.88	-0.81	-0.64	2.25
20	Benzo[*c*]phenanthrene	228	-0.46	0.04	0.22	-3.96
21	Cyclopenta[*cd*]pyrene	226	0.77	1.18	1.22	3.58
22	Benz[*a*]anthracene	228	-1.22	-1.67	-1.87	0.56
23	**Chrysene**	**228**	**0.00**	**0.00**	**0.00**	**0.00**
24	Benzanthrone	230	5.18	5.92	6.44	13.77
25	2-Nitrofluoranthene	247	2.30	-0.26	0.22	19.12
26	Benz[*a*]anthracene-7,12-dione	258	2.73	1.92	2.44	6.13
27	1-Nitropyrene	247	5.03	4.80	5.62	19.50
28	2-Nitropyrene	247	4.99	3.83	4.45	19.01
29	Benzo[*b*]fluoranthene	252	-1.72	-2.47	-2.77	3.31
30	Benzo[*j*]fluoranthene	252	-0.71	-0.63	-0.70	3.90
31	Benzo[*k*]fluoranthene	252	-1.76	-2.58	-3.01	3.17
32	Benzo[*a*]fluoranthene	252	-1.15	-1.40	-1.36	3.46
33	Benzo[*e*]pyrene	252	0.40	0.78	0.51	2.04
34	Benzo[*a*]pyrene	252	0.60	0.75	0.49	1.57
35	Perylene	252	1.43	2.13	1.86	1.38
36	3-Methylcholanthrene	268	-3.35	-4.48	-4.36	-2.59
37	Benzo[*c*]chrysene	278	-0.63	-0.09	-0.18	-5.48
38	Indeno[1,2,3-*cd*]pyrene	276	-0.78	-1.17	-1.40	4.21
39	Dibenz[*a,c*]anthracene	278	-2.50	-3.08	-3.40	2.12
40	Dibenz[*a,h*]anthracene	278	-1.70	-2.06	-2.23	1.59
41	Benzo[*b*]chrysene	278	-0.81	-1.00	-1.15	0.90
42	**Picene**	**278**	**0.00**	**0.00**	**0.00**	**0.00**
43	Benzo[*ghi*]perylene	276	-0.66	-1.03	-0.76	-2.89
44	Anthanthrene	276	-1.22	-1.52	-1.38	-2.65

Non-planar PAH were previously reported to elute earlier than planar PAH of the same molecular mass on SE-52 [45]. The same effect was observed for all phases in the present study, with the largest effect associated with the trifluoropropyl phase.

For most homocyclic PAH containing 5-membered rings, retention indices decreased with increasing phenyl content of the stationary phase. The trifluoropropyl phase was the exception in that retention indices decreased for PAH containing 5-membered rings fused on two sides, but increased for PAH containing 5-membered rings fused on three sides, with the exception of acenaphthylene (compound 5). Acenaphthylene contains a 5-membered ring fused only on two sides but contains no CH_2 moiety.

The differences in retention index performance for three stationary phases (DB-5ms, DB-17ms and Rtx-200) can be shown graphically by plotting the residuals for the two more polar phases against each other. The residuals for the trifluoropropyl phase (Rtx-200) are plotted against the residuals for the 50% phenyl phase (DB-17ms) for all PAH and PAC in Table 4.5 (compounds 1-49, Figure 4.6). Retene (compound 17) eluted much earlier on the DB-17ms column than on the DB-5ms column and was not included in this figure for the sake of clarity. Compounds with specific functional groups that showed consistent large residuals tended to cluster in the same region of the figure. Three such clusters are circled and identified.

The plotted range of residuals for Rtx-200 was about three times greater than the range of residuals for DB-17ms. The trifluoropropyl phase provides a unique selectivity for certain PAH species compared to the phenyl phases, but generally, the 50% phenyl

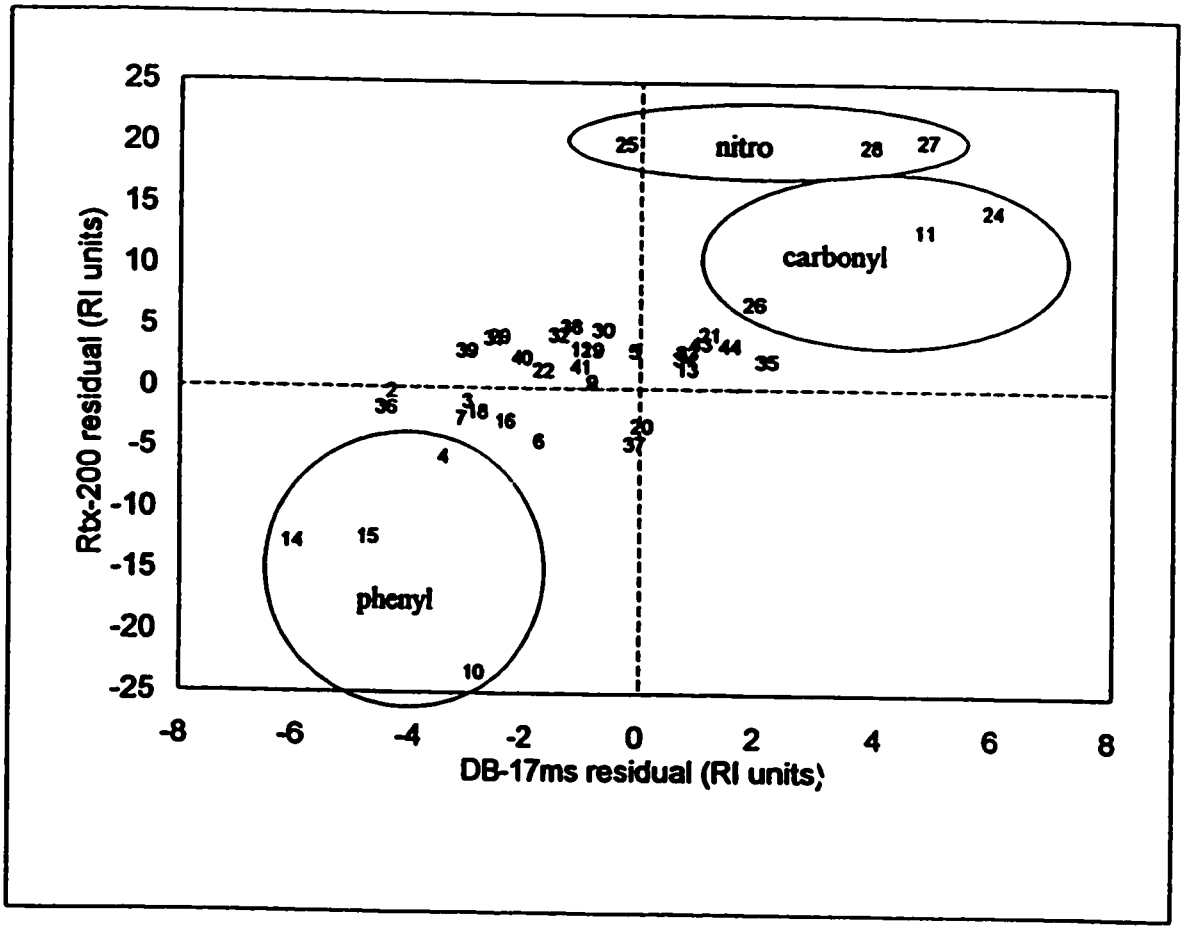

Figure 4.6. Relationship between PAC retention indices on DB-5ms, DB-17ms and Rtx-200 stationary phases. Numbers refer to compounds listed in Tables 4.4 and 4.5.

phase provides the best overall separation between PAH isomers. For example, the 50% phenyl phase is the only phase that provides adequate separation of all seven 252 amu isomers (Compounds 29-35).

A comparison of the relative separation of the 252 amu isomers on four stationary phases is illustrated using a coal tar extract reference material (NIST SRM 1597) (Figure 4.7). All four benzofluoranthene isomers (Compounds 29-32) are resolved only on the DB-17ms and DB-17ht columns. The 278 amu isomers, dibenz[*a,c*]anthracene and dibenz[*a,h*]anthracene are also resolved on this phase, but coelute on the 5% phenyl and trifluoropropyl phases; the 35% phenyl phase gives poorer but adequate resolution. The ability to differentiate between these 252 and 278 amu isomers is important because they show different mutagenic activities and carcinogenic risk factors. The separation and quantification of three benzofluoranthenes (the *b*, *j*, and *k* isomers, Compounds 29, 30 and 31) is an important requirement for PAH analyses by the US EPA; only the 50% phenyl phases resolve these isomers. From a practical standpoint, the higher temperature column (DB-17ht) provides separation equivalent to the DB-17ms column, but allows a faster analysis due to a thinner film coating (0.15 μm compared to 0.25 μm).

4.5.2 Thia-arene Retention Indices

Retention indices for 66 thia-arenes on all five stationary phases are listed in Table 4.6. These standards include four 184 amu isomers, one 208 amu isomer, all 13

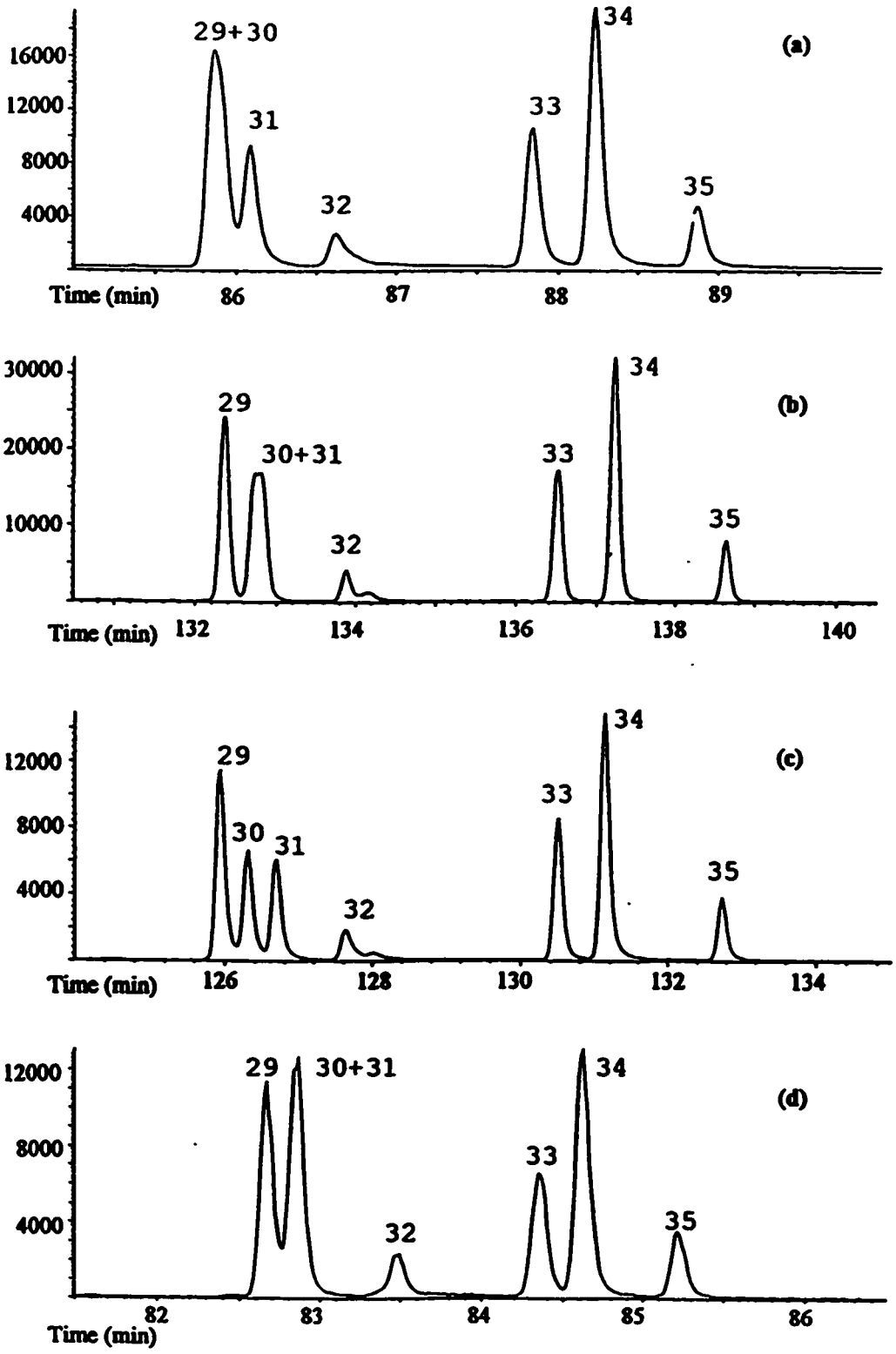

Figure 4.7. Ion 252 chromatograms of Coal Tar Standard Reference Material (SRM 1597) analyzed on (a) DB-5ms, (b) DB-35ms, (c) DB-17ms and (d) Rtx-200. Peak numbers refer to compounds listed in Tables 4.3 and 4.4.

Table 4.6. Retention indices for thia-arenes (PASH).

No.	Compound	Mol. Wt.	DB-5ms	DB-35ms	DB-17ms	DB-17ht	Rtx-200
50	Naphtho[1,2-*b*]thiophene	184	295.63	296.49	297.08	297.46	294.41
51	Dibenzothiophene	184	295.80	295.92	295.99	296.22	293.35
52	Naphtho[2,1-*b*]thiophene	184	299.62	301.59	302.44	302.69	298.73
53	Naphtho[2,3-*b*]thiophene	184	304.70	306.76	307.30	307.17	303.37
54	4-Methyldibenzothiophene	198	312.22	309.70	308.74	308.80	306.98
55	8-Methylnaphtho[1,2-*b*]thiophene	198	314.78	313.07	312.83	313.09	313.15
56	2-Methyldibenzothiophene	198	315.55	312.64	311.59	311.62	312.65
57	3-Methyldibenzothiophene	198	315.78	313.81	312.72	312.86	313.23
58	4-Methylnaphtho[1,2-*b*]thiophene	198	316.56	315.68	315.45	315.53	314.26
59	4-Methylnaphtho[2,1-*b*]thiophene	198	317.63	316.83	316.55	316.57	314.74
60	2-Methylnaphtho[2,1-*b*]thiophene	198	318.35	316.75	316.23	316.30	316.97
61	8-Methylnaphtho[2,1-*b*]thiophene	198	319.34	317.81	317.49	317.64	318.09
62	7-Methylnaphtho[2,1-*b*]thiophene	198	319.72	318.99	318.62	318.63	318.30
63	5-Methylnaphtho[2,1-*b*]thiophene	198	322.42	322.80	322.92	322.94	320.47
64	1-Methylnapho[2,1-*b*]thiophene	198	322.88	323.23	323.57	323.86	319.99
65	6-Methylnaphtho[2,1-*b*]thiophene	198	323.32	323.45	323.63	323.77	320.62
66	3-Ethyldibenzothiophene	212	327.20	322.66	321.38	321.80	319.14
67	4-Ethyldibenzothiophene	212	327.29	322.71	321.46	321.82	319.11
68	4,6-Dimethyldibenzothiophene	212	328.36	323.71	322.18	322.16	321.33
69	2-Ethyldibenzothiophene	212	331.39	325.65	324.10	324.63	326.19
70	2,6-Dimethyldibenzothiophene	212	331.63	326.41	324.41	324.37	326.84
71	3,6-Dimethyldibenzothiophene	212	331.95	327.52	325.53	325.43	327.33
72	2,8-Dimethyldibenzothiophene	212	334.96	329.09	327.07	326.92	331.82
73	3,7-Dimethyldibenzothiophene	212	335.16	331.37	329.24	328.93	333.17
74	1,6-Dimethyldibenzothiophene	212	335.35	331.75	330.57	330.71	327.82
75	1,8-Dimethyldibenzothiophene	212	335.58	331.22	329.90	330.06	331.13
76	1,3-Dimethyldibenzothiophene	212	337.42	334.57	333.36	333.44	332.83
77	3,4-Dimethyldibenzothiophene	212	337.66	333.79	332.35	332.37	332.97
78	1,7-Dimethyldibenzothiophene	212	338.19	334.90	333.44	333.54	333.35
79	Phenaleno[6,7-*bc*]thiophene	208	354.02	356.42	357.65	357.89	352.56
80	Benzo[*b*]naphtho[2,1-*d*]thiophene	234	389.23	388.46	388.20	388.24	386.45
81	Benzo[*b*]naphtho[1,2-*d*]thiophene	234	392.34	392.15	392.53	392.90	389.64
82	Phenanthro[9,10-*b*]thiophene	234	394.70	395.37	395.92	396.16	394.05
83	Phenanthro[4,3-*b*]thiophene	234	394.96	395.74	396.65	396.88	393.81
84	Anthra[1,2-*b*]thiophene	234	395.32	395.13	395.30	395.34	394.12
85	Phenanthro[1,2-*b*]thiophene	234	395.98	396.73	397.29	397.42	394.71
86	Benzo[*b*]naphtho[2,3-*d*]thiophene	234	396.08	395.31	394.95	394.78	393.84
87	Phenanthro[3,4-*b*]thiophene	234	396.21	397.69	398.84	399.22	393.80
88	Anthra[2,1-*b*]thiophene	234	399.13	399.62	400.00	400.04	398.88
89	Phenanthro[2,1-*b*]thiophene	234	400.55	402.62	403.52	403.66	399.58
90	Phenanthro[3,2-*b*]thiophene	234	402.06	403.26	403.81	403.73	401.42
91	Phenanthro[2,3-*b*]thiophene	234	402.42	403.78	404.41	404.37	402.09
92	Anthra[2,3-*b*]thiophene	234	408.16	409.85	410.08	409.84	407.12

Table 4.6. (cont'd)

No.	Compound	Mol. Wt.	DB-5ms	DB-35ms	DB-17ms	DB-17ht	Rtx-200
93	Benzo[2,3]phenanthro[4,5-*bcd*]thiophene	258	443.77	443.53	443.52	443.52	440.74
94	Pyreno[4,5-*b*]thiophene	258	447.27	448.62	449.47	449.44	447.53
95	Benzo[1,2]phenaleno[3,4-*bc*]thiophene	258	448.38	449.48	450.16	450.39	447.27
96	Triphenyleno[4,5-*bcd*]thiophene	258	448.91	449.38	449.89	449.95	446.70
97	Pyreno[1,2-*b*]thiophene	258	450.41	451.98	452.73	452.57	450.31
98	Chryseno[4,5-*bcd*]thiophene	258	451.43	452.49	452.81	452.71	448.43
99	Pyreno[2,1-*b*]thiophene	258	456.16	458.88	459.89	459.67	456.57
100	Benzo[4,5]phenaleno[1,9-*bc*]thiophene	258	456.70	459.20	460.24	460.21	456.00
101	Benzo[4,5]phenaleno[9,1-*bc*]thiophene	258	457.93	460.53	461.76	462.48	457.11
102	Dinaphtho[2,1-*b*:1',2'-*d*]thiophene	284	472.00	472.10	473.27	473.33	460.59
103	Dinaphtho[1,2-*b*:2',1'-*d*]thiophene	284	482.52	480.53	479.99	480.22	479.65
104	Dinaphtho[1,2-*b*:1',2'-*d*]thiophene	284	486.40	485.04	484.95	484.98	483.06
105	Benzo[*b*]phenanthro[9,10-*d*]thiophene	284	486.63	484.87	484.84	484.92	484.02
106	Benzo[*b*]phenanthro[3,4-*d*]thiophene	284	488.54	486.70	486.07	485.95	485.55
107	Anthra[1,2-*b*]benzo[*d*]thiophene	284	488.65	486.77	486.12	485.88	485.62
108	Benzo[*b*]phenanthro[2,1-*d*]thiophene	284	489.16	488.23	487.87	487.77	486.02
109	Dinaphtho[1,2-*b*:2',3'-*d*]thiophene	284	489.29	488.23	487.71	487.57	486.85
110	Benzo[*b*]phenanthro[3,2-*d*]thiophene	284	491.34	489.14	488.57	488.28	489.97
111	Benzo[*b*]phenanthro[1,2-*d*]thiophene	284	492.35	491.85	492.11	492.14	488.83
112	Triphenyleno[2,1-*b*]thiophene	284	493.68	494.89	496.29	496.32	490.27
113	Dinaphth[2,3-*b*:2',3'-*d*]thiophene	284	495.71	494.36	493.71	493.03	493.49
114	Anthra[2,3-*b*]benzo[*d*]thiophene	284	498.46	497.66	497.08	496.75	496.05
115	Triphenyleno[2,3-*b*]thiophene	284	499.98	(500.05)	(500.58)	(500.40)	(500.77)

stable 234 amu isomers and a selection of 258 and 284 amu isomers. Twelve monomethyl and 13 dimethyl or ethyl substituted 184 amu thia-arenes are included in this listing. The listing of retention index residuals is provided in Table 4.7.

4.5.2.1 Separation of Alkylated Thia-Arenes

Standards were not available for all monomethyl and dimethyl 184 amu thia-arene isomers, but some general conclusions can be drawn from the isomers analyzed. The ranges of retention indices for these monomethyl and dimethyl isomers increase only slightly as the phenyl content of the stationary phase increases; little difference was observed in separations comparing the 35% and 50% phenyl phases. The largest range of retention indices was observed for the trifluoropropyl column. The four parent 184 amu thia-arenes showed the greatest range of retention indices on the 50% phenyl phase. These results indicate that increasing phenyl content of the stationary phase aids in separating the unsubstituted thia-arenes while the trifluoropropyl phase shows a greater selectivity for the position of alkyl substituents. Polar phases have previously been shown to separate alkylbenzothiophene isomers over a larger range than non-polar phases [44].

The residuals for the three-ring thia-arenes and the available alkylated derivatives on the trifluoropropyl phase are plotted against the residuals on the 50% phenyl phase (Figure 4.8). The parent thia-arenes, the monomethylated isomers and the dimethyl/ethyl isomers show a steady trend across Figure 4.8 and can be divided into three distinct regions with minimal overlap. Retention of thia-arenes is decreased (negative residuals)

Table 4.7. List of residuals from DB-5ms indices for thia-arenes.

No.	Compound	Mol. Wt.	DB-35ms	DB-17ms	DB-17ht	Rtx-200
50	Naphtho[1,2-*b*]thiophene	184	0.86	1.45	1.83	-1.22
51	Dibenzothiophene	184	0.12	0.18	0.41	-2.45
52	Naphtho[2,1-*b*]thiophene	184	1.97	2.82	3.07	-0.90
53	Naphtho[2,3-*b*]thiophene	184	2.07	2.60	2.48	-1.33
54	4-Methyldibenzothiophene	198	-2.52	-3.48	-3.42	-5.24
55	8-Methylnaphtho[1,2-*b*]thiophene	198	-1.71	-1.95	-1.69	-1.62
56	2-Methyldibenzothiophene	198	-2.91	-3.96	-3.93	-2.90
57	3-Methyldibenzothiophene	198	-1.97	-3.06	-2.92	-2.55
58	4-Methylnaphtho[1,2-*b*]thiophene	198	-0.88	-1.12	-1.04	-2.30
59	4-Methylnaphtho[2,1-*b*]thiophene	198	-0.80	-1.09	-1.06	-2.89
60	2-Methylnaphtho[2,1-*b*]thiophene	198	-1.61	-2.12	-2.05	-1.38
61	8-Methylnaphtho[2,1-*b*]thiophene	198	-1.53	-1.85	-1.70	-1.25
62	7-Methylnaphtho[2,1-*b*]thiophene	198	-0.74	-1.10	-1.09	-1.42
63	5-Methylnaphtho[2,1-*b*]thiophene	198	0.37	0.50	0.52	-1.95
64	1-Methylnapho[2,1-*b*]thiophene	198	0.36	0.69	0.99	-2.89
65	6-Methylnaphtho[2,1-*b*]thiophene	198	0.12	0.31	0.45	-2.71
66	3-Ethyldibenzothiophene	212	-4.54	-5.82	-5.41	-8.06
67	4-Ethyldibenzothiophene	212	-4.58	-5.83	-5.47	-8.18
68	4,6-Dimethyldibenzothiophene	212	-4.65	-6.18	-6.20	-7.03
69	2-Ethyldibenzothiophene	212	-5.73	-7.28	-6.76	-5.20
70	2,6-Dimethyldibenzothiophene	212	-5.22	-7.22	-7.26	-4.79
71	3,6-Dimethyldibenzothiophene	212	-4.43	-6.41	-6.52	-4.62
72	2,8-Dimethyldibenzothiophene	212	-5.86	-7.89	-8.04	-3.14
73	3,7-Dimethyldibenzothiophene	212	-3.80	-5.92	-6.23	-1.99
74	1,6-Dimethyldibenzothiophene	212	-3.60	-4.77	-4.63	-7.52
75	1,8-Dimethyldibenzothiophene	212	-4.36	-5.68	-5.52	-4.45
76	1,3-Dimethyldibenzothiophene	212	-2.84	-4.05	-3.97	-4.59
77	3,4-Dimethyldibenzothiophene	212	-3.87	-5.31	-5.29	-4.69
78	1,7-Dimethyldibenzothiophene	212	-3.29	-4.75	-4.65	-4.84
79	Phenaleno[6,7-*bc*]thiophene	208	2.41	3.64	3.87	-1.46
80	Benzo[*b*]naphtho[2,1-*d*]thiophene	234	-0.77	-1.03	-0.99	-2.79
81	Benzo[*b*]naphtho[1,2-*d*]thiophene	234	-0.19	0.19	0.57	-2.69
82	Phenanthro[9,10-*b*]thiophene	234	0.67	1.22	1.46	-0.65
83	Phenanthro[4,3-*b*]thiophene	234	0.78	1.69	1.92	-1.14
84	Anthra[1,2-*b*]thiophene	234	-0.19	-0.02	0.03	-1.20
85	Phenanthro[1,2-*b*]thiophene	234	0.75	1.30	1.44	-1.27
86	Benzo[*b*]naphtho[2,3-*d*]thiophene	234	-0.77	-1.13	-1.30	-2.24
87	Phenanthro[3,4-*b*]thiophene	234	1.48	2.63	3.01	-2.41
88	Anthra[2,1-*b*]thiophene	234	0.49	0.87	0.90	-0.26
89	Phenanthro[2,1-*b*]thiophene	234	2.07	2.97	3.11	-0.97
90	Phenanthro[3,2-*b*]thiophene	234	1.20	1.75	1.68	-0.63
91	Phenanthro[2,3-*b*]thiophene	234	1.37	1.99	1.95	-0.33
92	Anthra[2,3-*b*]thiophene	234	1.69	1.92	1.68	-1.04

Table 4.7. (cont'd)

No.	Compound	Mol. Wt.	DB-35ms	DB-17ms	DB-17ht	Rtx-200
93	Benzo[2,3]phenanthro[4,5-*bcd*]thiophene	258	-0.24	-0.25	-0.25	-3.03
94	Pyreno[4,5-*b*]thiophene	258	1.35	2.20	2.18	0.26
95	Benzo[1,2]phenaleno[3,4-*bc*]thiophene	258	1.10	1.78	2.01	-1.12
96	Triphenyleno[4,5-*bcd*]thiophene	258	0.46	0.97	1.04	-2.21
97	Pyreno[1,2-*b*]thiophene	258	1.57	2.31	2.16	-0.10
98	Chryseno[4,5-*bcd*]thiophene	258	1.06	1.38	1.28	-3.01
99	Pyreno[2,1-*b*]thiophene	258	2.73	3.74	3.51	0.41
100	Benzo[4,5]phenaleno[1,9-*bc*]thiophene	258	2.51	3.55	3.51	-0.69
101	Benzo[4,5]phenaleno[9,1-*bc*]thiophene	258	2.60	3.83	4.55	-0.82
102	Dinaphtho[2,1-*b*:1',2'-*d*]thiophene	284	0.10	1.26	1.32	-11.41
103	Dinaphtho[1,2-*b*:2',1'-*d*]thiophene	284	-1.99	-2.53	-2.30	-2.87
104	Dinaphtho[1,2-*b*:1',2'-*d*]thiophene	284	-1.36	-1.44	-1.41	-3.33
105	Benzo[*b*]phenanthro[9,10-*d*]thiophene	284	-1.77	-1.79	-1.71	-2.61
106	Benzo[*b*]phenanthro[3,4-*d*]thiophene	284	-1.84	-2.48	-2.59	-2.99
107	Anthra[1,2-*b*]benzo[*d*]thiophene	284	-1.89	-2.54	-2.77	-3.04
108	Benzo[*b*]phenanthro[2,1-*d*]thiophene	284	-0.93	-1.29	-1.39	-3.14
109	Dinaphtho[1,2-*b*:2',3'-*d*]thiophene	284	-1.07	-1.59	-1.72	-2.45
110	Benzo[*b*]phenanthro[3,2-*d*]thiophene	284	-2.20	-2.78	-3.06	-1.38
111	Benzo[*b*]phenanthro[1,2-*d*]thiophene	284	-0.50	-0.25	-0.22	-3.53
112	Triphenyleno[2,1-*b*]thiophene	284	1.21	2.61	2.64	-3.41
113	Dinaphth[2,3-*b*:2',3'-*d*]thiophene	284	-1.35	-2.01	-2.68	-2.22
114	Anthra[2,3-*b*]benzo[*d*]thiophene	284	-0.80	-1.38	-1.71	-2.41

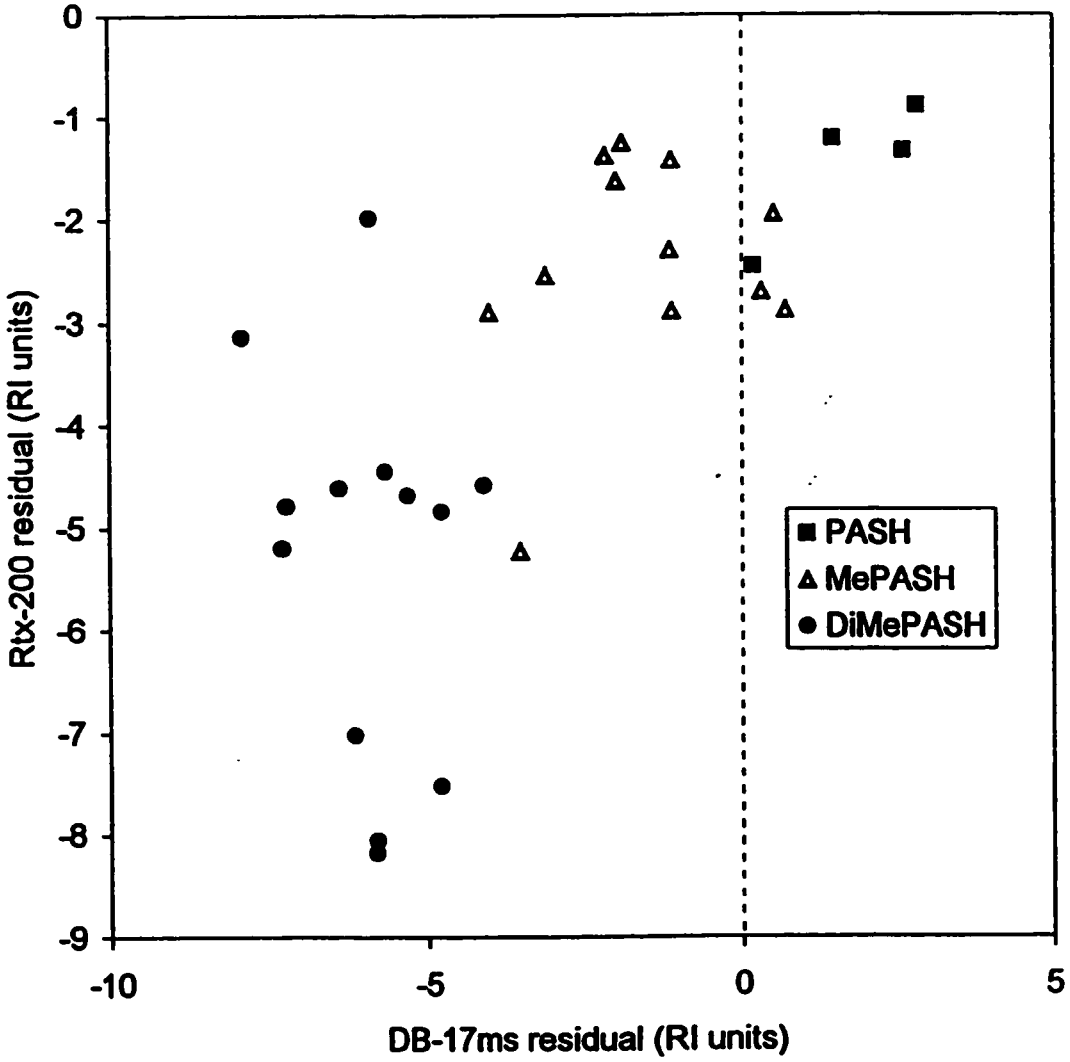

Figure 4.8. Retention index residuals for parent and alkylated three-ring thia-arenes.

on the trifluoropropyl phase compared to the 5% phenyl phase, the largest difference being observed for the dimethyl or ethyl isomers (212 amu). Previous studies have reported increased retention of thia-arenes on more polar phases [24,62]. While increased retention is observed for the unsubstituted 3-ring thia-arenes on the 50% phenyl phase, relative to the 5% phenyl phase, the majority of the alkyl derivatives have lower retention indices.

Analysis of a diesel exhaust reference material (NIST SRM 1650) showed that the DB-17ms and DB-17ht columns provided the best separation of the unsubstituted, monomethylated (Figure 4.9) and dimethylated/ethylated (Figure 4.10) thia-arenes. The 50% phenyl phases (i.e., the DB-17 phases) provided not only excellent separation between 2- and 3-methyldibenzothiophene (compounds 56 and 57, Figure 4.9), compounds that coelute on the 5% phenyl phase, but also afforded the greatest number of resolved dimethyl dibenzothiophenes (Figure 4.10).

Isomers with methyl substituents located in the position closest to the sulfur atom have the lowest retention indices of all the monosubstituted compounds. On each of the phases, 4-methyldibenzothiophene (compound 54) elutes earlier than either 2- or 3-methyldibenzothiophene (compounds 56 and 57, Figure 4.9), and 2- and 4-methylnaphtho[2,1-*b*]thiophene elute earlier than the other naphtho[2,1-*b*]thiophene isomers (Table 4.6). A similar observation was reported by Andersson [44] where 2- and 7-methylbenzothiophene eluted before the other methylbenzothiophene isomers. Andersson reported that disubstituted compounds with two methyl groups located adjacent to each other tend to have longer retention times. Only one dimethyl standard in

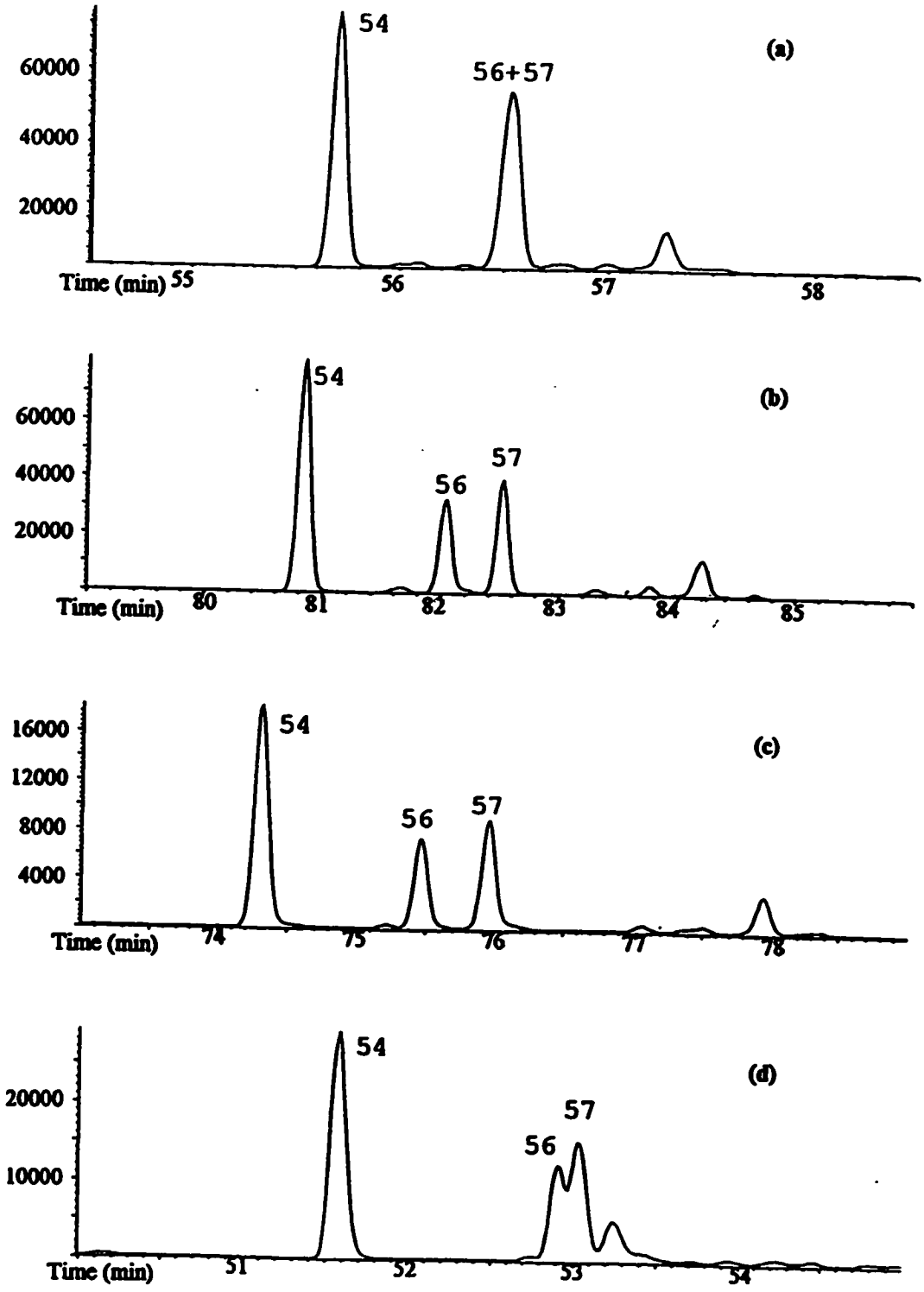

Figure 4.9. Mass chromatograms of the m/z 198 ion from the analyses of Diesel Exhaust Particulate Standard Reference Material (SRM 1650) analyzed on (a) DB-5ms, (b) DB-35ms, (c) DB-17ms and (d) Rtx-200. Peak nos. refer to compounds listed in Table 4.6.

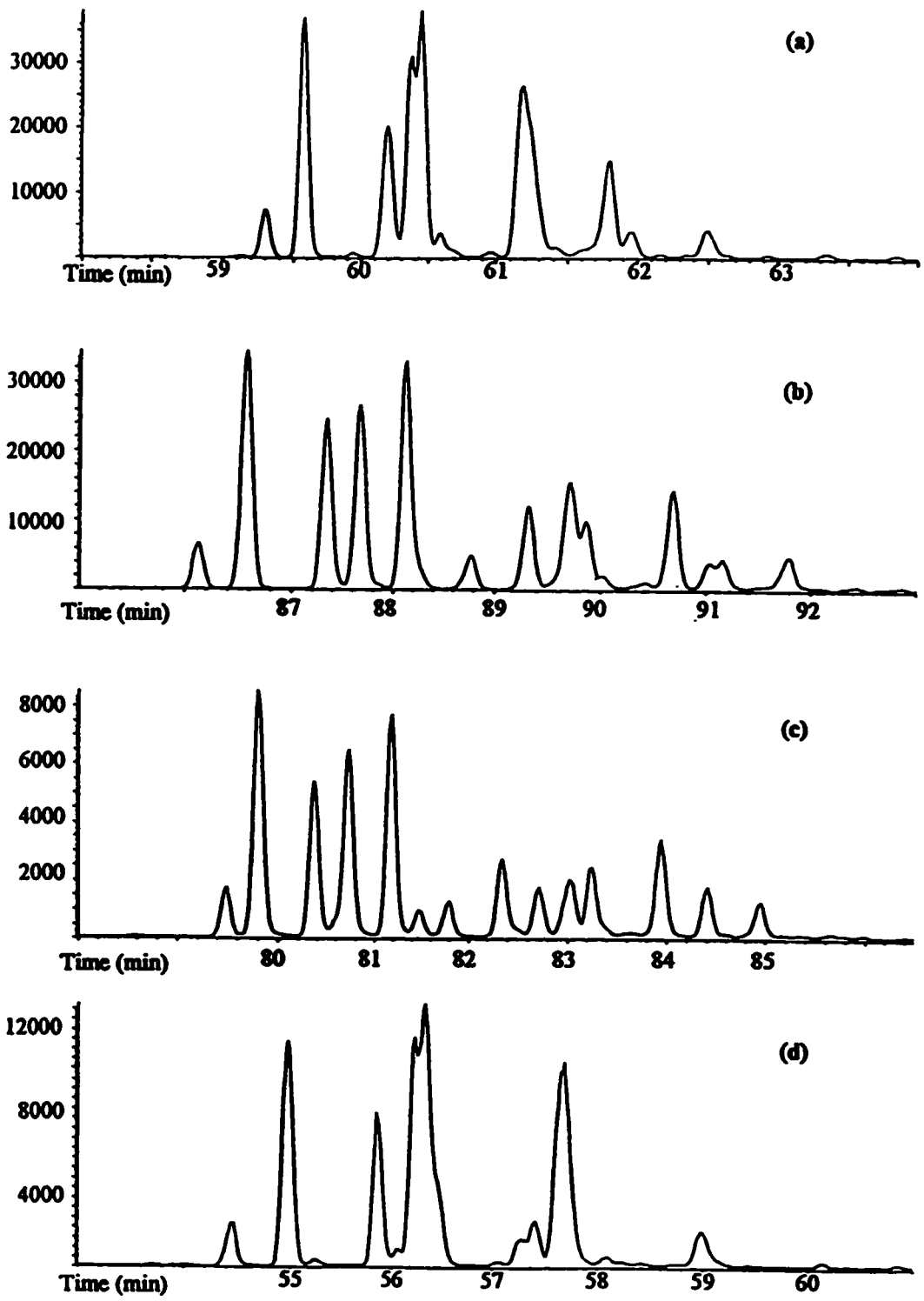

Figure 4.10. Mass chromatograms of the m/z 212 ion from the analyses of Diesel Exhaust Particulate Standard Reference Material (SRM 1650) analyzed on (a) DB-5ms, (b) DB-35ms, (c) DB-17ms and (d) Rtx-200. Peak nos. refer to compounds in Table 4.6.

the present study, 3,4-dimethyldibenzothiophene, was available with two adjacent methyl substituents. This compound is the second or third last dimethyldibenzothiophene isomer to elute on all five columns. The polarity of the column does not appear to have a large effect on the relative retention of this compound.

4.5.2.2 Separation of Parent Thia-Arenes

Recently, Andersson [24] reported that a polar cyanopropyl stationary phase was found to increase the retention, relative to a biphenyl phase, of the three-ring thia-arenes containing a terminal thiophene ring. In the present work, we found that retention indices for the three-ring thia-arenes are lowest for the trifluoropropyl phase, the most polar phase examined, and highest for the 50% phenyl phase (Table 4.6). Decreased retention of thia-arenes relative to the PAH is also observed for many of the four- and five-ring thia-arene isomers on the trifluoropropyl phase (see table of residuals, Table 4.7). The trifluoropropyl phase and the 50% phenyl phase are both suitable for the separation of the four 184 amu thia-arene isomers, but dibenzothiophene and naphtho[1,2-*b*]thiophene coelute on the DB-5 column.

As with the 3-ring unsubstituted thia-arenes, the majority of the 234 amu and 258 amu thia-arenes are more strongly retained with increasing phenyl content in the stationary phase. The same trend is not observed, however, for the 284 amu isomers (Tables 4.6 and 4.7). The effect of increased retention for thiophene-containing compounds, relative to the PAH reference standards, was previously reported to decrease with increasing size of the molecule [24]. Decreased retention indices were also

observed for the PAH in the same elution range. The separation of the 234 amu thia-arene isomers on four stationary phases (which will form the basis for part of the next source apportionment method discussed in Chapters 5-7) is shown in Figure 4.11. The DB-17 phases outperformed all other phases in this analysis (Tables 4.6 and 4.7). Only phenanthro[2,1-*b*]thiophene and phenanthro[3,2-*b*]thiophene (compounds 89 and 90) were found to coelute on the 50% phenyl phase, however, these two isomers are resolved on both the 5% phenyl and trifluoropropyl phases. The separation of the 258 amu thia-arenes was also found to be the best on the 50% phenyl phases (DB-17, Tables 4.6 and 4.7).

4.6 Selection of the Optimum GC Stationary Phase

Based on the observations of PAH and thia-arene separation presented in Sections 4.2 to 4.4 above, it was concluded that the DB-17 phases (50% phenyl phases) provided the best compromise of separation, peak width and overall retention of all compounds examined. The trifluoropropyl phase had the widest range of retention indices of all the phases, however, for resolving specific isomers, the performance of this phase was poorer than that of the 50% phenyl phase.

This work may be useful for practitioners of two-dimensional GC separations. Comprehensive two-dimensional GC methods have recently been developed [175-177]. These methods interface a non-polar first column with a moderately polar second column to achieve separation in two dimensions. A combination of the characteristics of both of these phases could be a very useful avenue to explore.

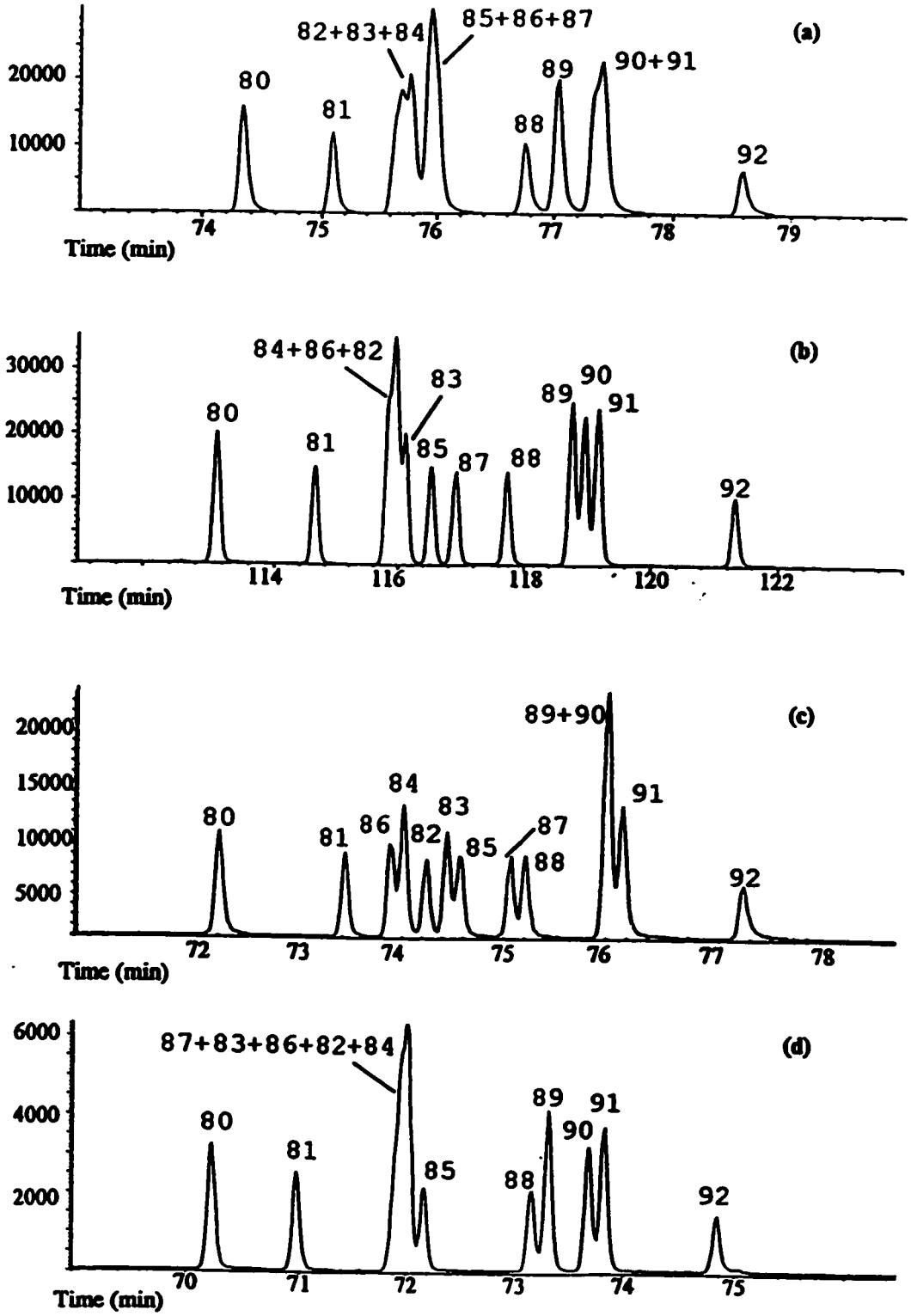

Figure 4.11. Mass chromatograms of the m/z 234 ion from analyses of a mixture of 234 amu thia-arene isomers analyzed on: (a) DB-5ms, (b) DB-35ms, (c) DB-17ms and (d) Rtx-200 columns. Peak numbers refer to compounds listed in Table 4.5.

4.7 Effect of Film Thickness of DB-17 Phase on Analyses

The DB-17ms and DB-17ht columns have similar stationary phase compositions but different film thicknesses (0.25 μm versus 0.15 μm, respectively). Similar, and in many cases identical, retention indices for PAH and thia-arenes were obtained for the two columns (Tables 4.4 and 4.6). Retention indices below 300 were not as consistent as the values between 300 and 500. The starting temperature used for the DB-17ms program was slightly higher to allow picene to elute during the temperature program. Retention indices below 300 are quite dependent on the initial temperature and temperature program rate, as has been noted previously [178]. Between retention index values of 300 and 500, approximately two-thirds of the compounds had values that differed by less than 0.2 RI units on the two phases. Retention indices greater than 500 were calculated by linear extrapolation and were not consistent from column to column, due to differences in temperature programming.

The film thickness of the stationary phase has a direct influence on retention and capacity, and a lesser impact on separation efficiency, inertness and thermal stability [30]. Elution temperatures were on average approximately 9°C higher for the 0.25 μm film than for the 0.15 μm film, consistent with results that found elution temperatures to increase by 16°C with a doubling of the film thickness [30]. The resolution was marginally greater for the thicker film; an average of 0.33 RI units difference was required for two peaks to be 50 % resolved on the 0.25 μm film compared to an average of 0.39 RI units for the 0.15 μm film. Overall, the thinner film column was favoured

because of the lower retention times. Thus, the DB-17ht column was selected for the following analyses in Chapters 5 to 7.

4.8 Analytical Work in Support of New Source Apportionment Method

The alkylated dibenzothiophene isomers were shown to be useful as source tracers in air particulate in Hamilton and in harbour sediments (Chapter 3). Since these compounds were rather volatile and only a small percentage in air was associated with the particulate phase, additional source indicators were sought that would be more appropriate or more suitable for particulate samples. Higher mass thia-arene isomers (234 and 258 amu) were examined in the hope there would also be differences in their profiles as there had been for the 184 amu series of thia-arenes. The m/z 234 and m/z 258 thia-arene profiles of two representative samples, coke oven condensate and diesel exhaust particulate (SRM 1650), were examined. The 234 amu thia-arene isomers in coke oven condensate and diesel exhaust particulate are compared in Figure 4.12. Similarly, the 258 amu thia-arene isomers in coke oven condensate and diesel exhaust particulate are compared in Figure 4.13. The appearance of the coke oven condensate chromatograms is strikingly different from the appearance of the diesel exhaust chromatograms. In Chapter 6, statistical methods will be employed to identify the most suitable chromatographic peaks from these chromatograms for use in source apportionment methodology.

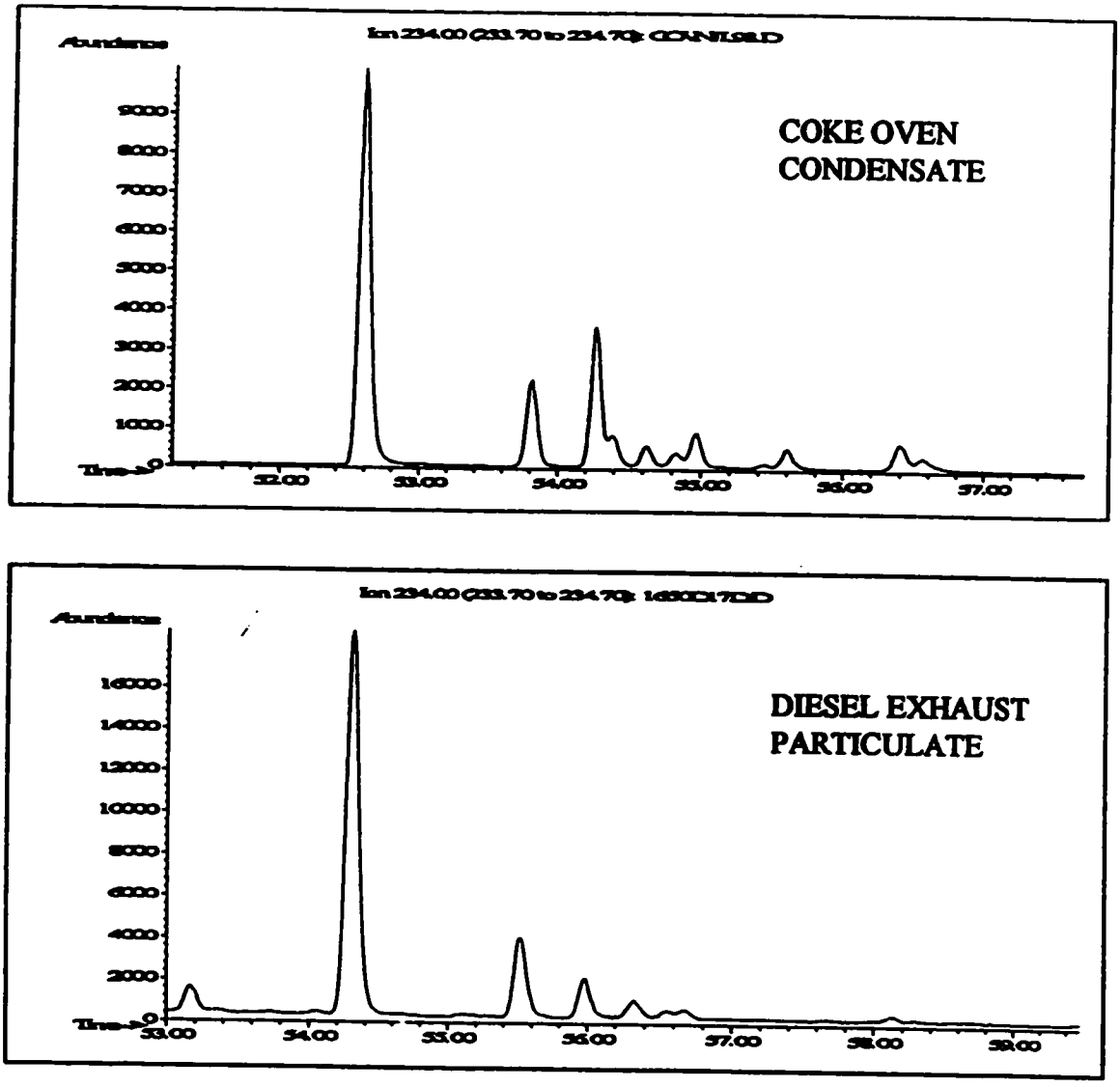

Figure 4.12. Mass chromatograms of the m/z 234 ion for the analysis of coke oven condensate and diesel exhaust particulate extracts.

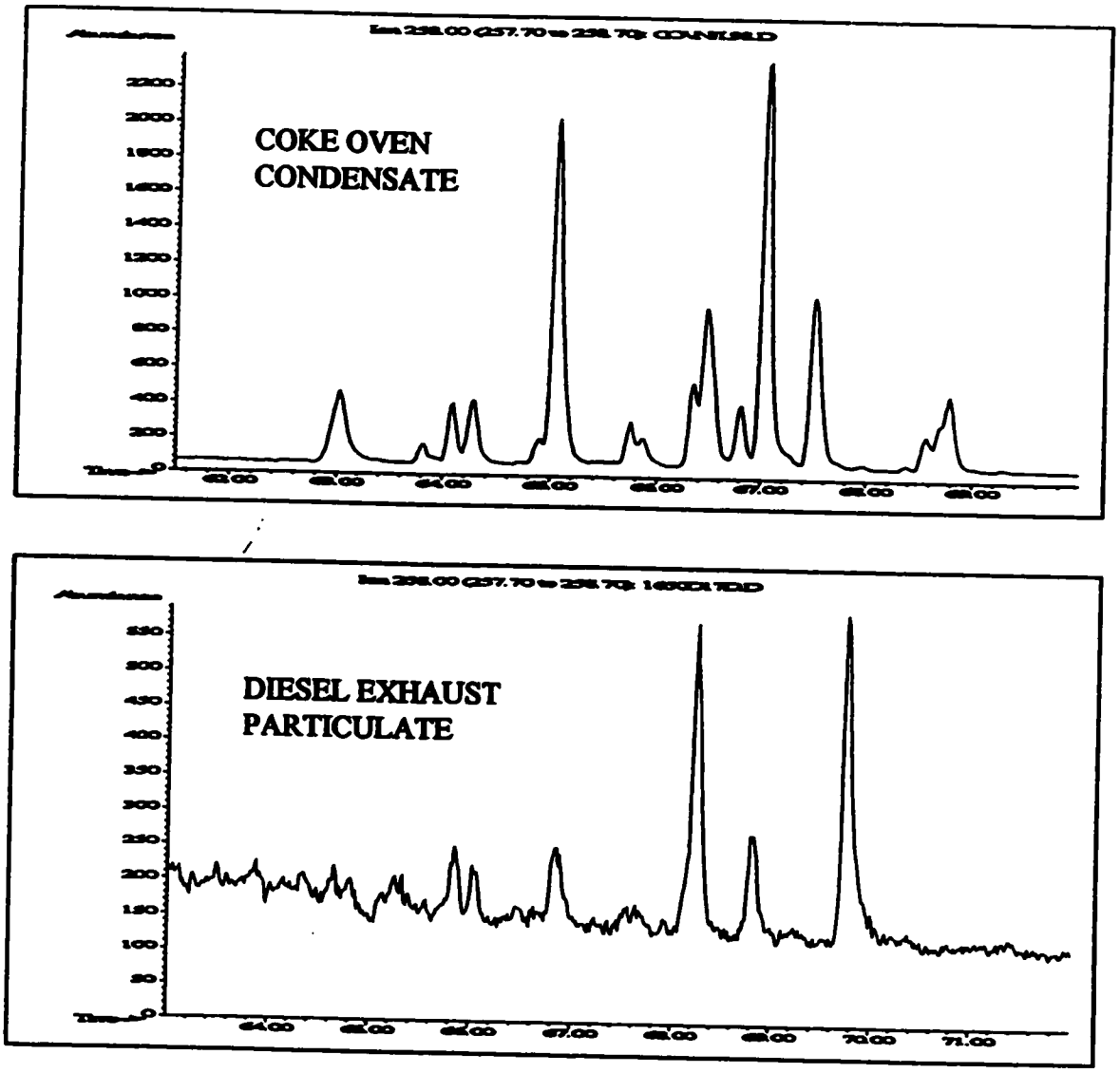

Figure 4.13. Mass chromatograms of the m/z 258 ion for the analysis of coke oven condensate and diesel exhaust particulate extracts.

4.9 Site Selection for Air Particulate Sampling

The work of Dr. A. E. Legzdins had shown that significant impacts from coke ovens could be observed some distance from the steel mills at the downtown Hamilton sampling station (MOE Station 29000). In order to determine coke oven impacts at sites closer to the steel mills, a multi-site sampling campaign was undertaken in July and August, 1995. Anderson PM_{10} high volume samplers were either installed or were made available to us for a six-week sampling period.

A map of the air particulate sampling sites selected in Hamilton was shown in Chapter 2 (Map 2.1). Station 29000 is an MOE air monitoring station; the same location that was used in the 1990-1991 study of Legzdins. We sampled at this station in the 1995 study because the results would be directly comparable to those from the previous study. Stations 29113, 29547 and 29102 were also MOE air monitoring stations. These sites provided sample collections closer to the steel mills and were already established so they were easy to access and provided protection for sample integrity. Stations 29531 and 29557 were established by our lab group. Station 29531 is located close to a current MOE monitoring site so the MOE station number was used to refer to this site. The MOE set up their own equipment at this Station in the year following this study. For our purposes, a PM_{10} sampler was located on the roof of the Hamilton Harbour Commission building near the end of Hillyard Street. Station 29557 was located on the roof of a one-story building which served as a weigh station for a scrap metal recycling plant. This station was located near a carbon black plant and the bulk of the samples collected at this site were used in another study.

Respirable air particulate (PM_{10}) was collected every day from July 10th to August 20th, 1995 at Stations 29000, 29113, 29557, and 29547, and from July 20th to August 20th, 1995 at Station 29531. The sampler at Station 29102 was shared with the MOE so samples were collected for four sequential days, followed by two days off, from July 10th to August 20th, 1995. At Stations 29547 and 29557, a second sampler used to collect total suspended particulate (TSP) was co-located with the PM_{10} sampler. Some of the samples were invalidated due to power interruptions or instrument failures. A total of 219 valid respirable air particulate filters were obtained with the help of A. R. Boden. This study will focus primarily on a selection of samples collected at Stations 29000, 29113, 29531 and 29547.

5. ANALYSIS OF HAMILTON AIR PARTICULATE (1995)

5.1 Filter Collection and Criteria for Selection

A total of 149 respirable air particulate filters were collected at four locations (Map 5.1) during the period from July 10 to August 20, 1995. Due to time and financial constraints, only a subset of these filters were selected and analyzed by GC/MS for PAH and thia-arenes. Four coke oven batteries operated by the steel industries are expected to be major air pollution sources in Hamilton. Traffic emissions will also contribute to PAH concentrations in Hamilton air. The locations of the coke ovens, major roads and the four sampling stations are indicated on Map 5.1. Stations 29000, 29113, 29547 and 29531 are Ontario Ministry of Environment (MOE) sampling stations. Additional air particulate samplers were installed at these sites for the purpose of this study. Station 29531 was not in operation by the MOE at the time of this study.

Samples were collected for 22 hours (8:00 a.m. to 6:00 a.m.) simultaneously at all locations in order to determine the impact of the coke ovens relative to background sources by comparing air particulate collected upwind and downwind of the coke ovens. Since one cannot predict which site will be downwind of the coke ovens, a large number of samples were collected at all sites for six weeks. After the samples had been collected, wind data for the sampling period (provided by the MOE from Station 29026) was analyzed to select specific filters for extraction and chemical analysis.

Map 5.1. Air particulate sampling stations (⊙) in Hamilton, Ontario.

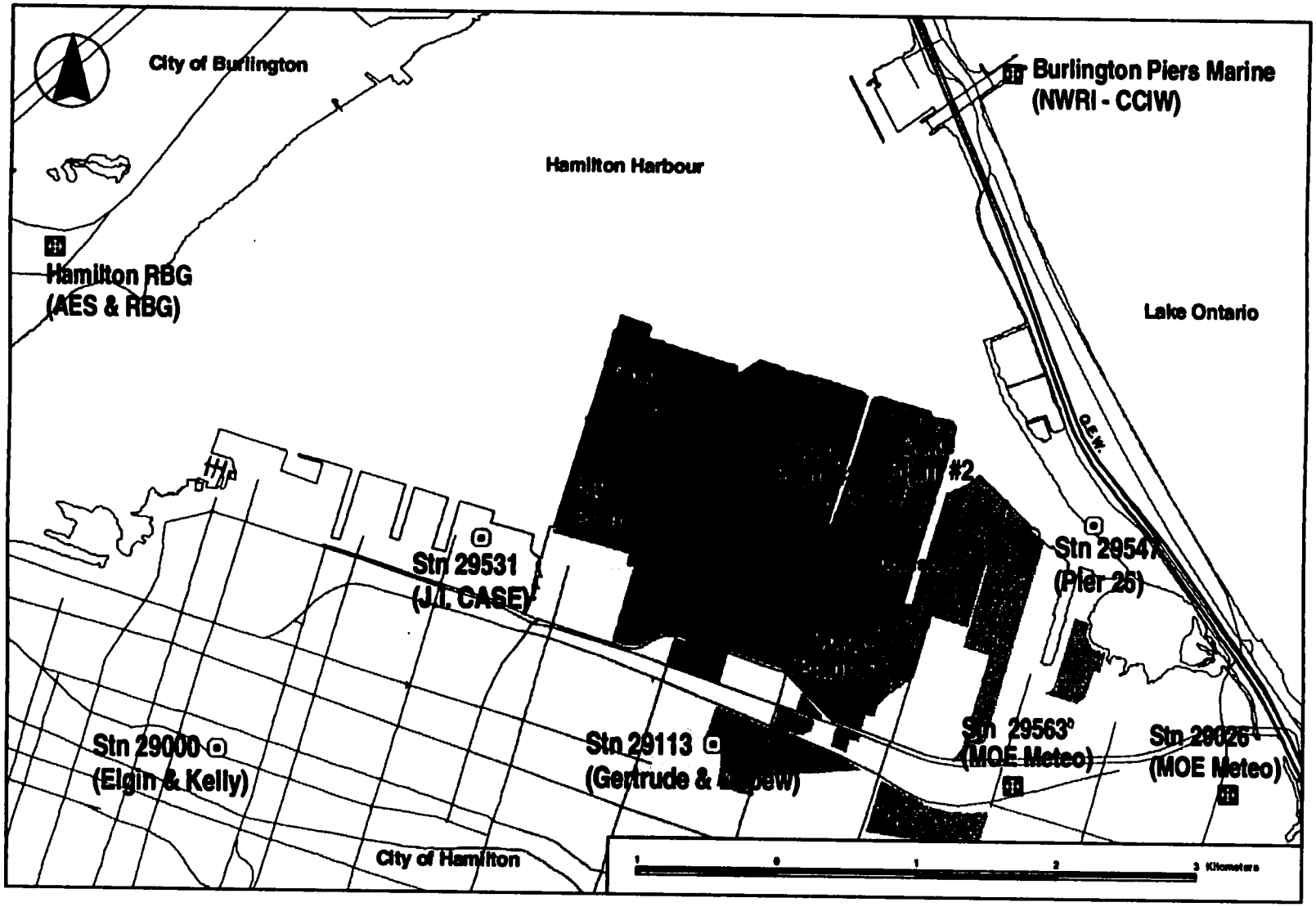

From careful examination of the hourly wind direction and wind speed data specific sampling days were identified that would afford filters from sampling sites with high probabilities of heavy impacts from the coke ovens. These filters were called "downwind" filters. Under these conditions other filters on the same days would probably have experienced little if any impacts from coke oven emissions and these filters were designated as "upwind". On a more quantitative basis, the two criteria for the selection of "upwind" filters were sampling periods during which (a) the wind direction was within 15° of the direction opposite from the coke ovens and (b) the standard deviation of the wind direction during this period was <45°. Conversely, "downwind" filters were selected for sampling periods during which (a) the wind direction was within 15° of the direction of the coke ovens from the sampling site and (b) the standard deviation of the wind direction was also <45°. Furthermore, hourly wind speeds must equal or exceed 3 km/hr for at least 17 hours of the 22 hour sampling period for filters to be considered "upwind" or "downwind" samples.

The coke ovens are located 1 to 3 km from Station 29531 at directions that range from 53 degrees to 102 degrees (Map 5.3). For sampling periods with average wind directions between 38 and 117 degrees, the samples collected at station 29531 were considered to be directly downwind of the coke ovens. Samples collected at station 29531 are considered to be upwind of the coke ovens if the average wind direction was between 218 and 297 degrees. For the other sites, the coke ovens were considered to have significant impacts on sampling sites when the mean wind direction was

Map 5.3. Distances and directions from industrial sources to sampling stn 29531

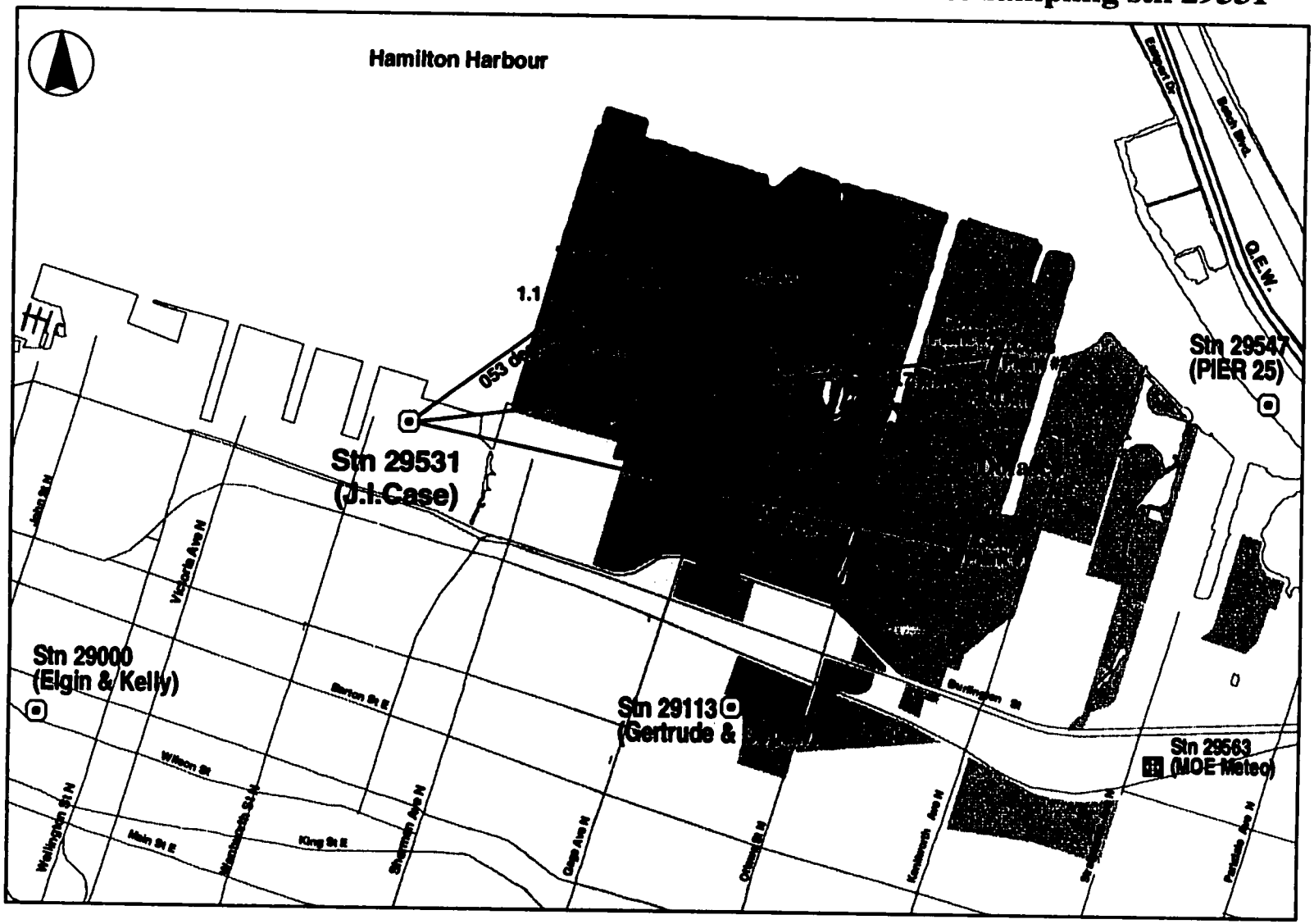

226 to 281 degrees relative to Station 29547 (Map 5.2), 53 to 79 degrees relative to Station 29000 (Map 5.4) and 342 to 55 degrees relative to Station 29113 (Map 5.5).

Filters were classified based on the mean wind direction, the standard deviation of the wind direction and the mean hourly wind speed during the sampling period. Wind data and respirable particulate concentrations are listed in Table 5.1 for all the air particulate filters collected. Hourly wind direction and wind speed data were measured at the Hamilton Sewage Treatment Plant, a location southeast of the sampling sites (Station 29026, Map 5.1) and were kindly provided by the Ontario Ministry of the Environment. The mean values listed in Table 5.1 are 22-hour averages corresponding to the sampling period. Filters were weighed after drying in a desiccator for 5 days before and after sampling. The particulate concentration was calculated by dividing the net weight of particulate by the total air volume sampled.

The average wind direction was plotted against the standard deviation of the wind direction for each of the 42 sampling periods to assist filter selection (Figure 5.1). Areas that are shaded indicate wind direction zones expected to have direct coke oven impacts on one or more sampling stations. The shaded regions are defined by the angles of direct impacts between the coke ovens and each sampling station as defined by the "downwind" criteria. Sampling periods for which filters were selected, extracted and analyzed are represented by filled circles, and sampling periods for which filters were not selected are represented by open circles. Over the course of a calendar year, winds in Hamilton tend to blow primarily from the west and south-west (220-300°) or from the north-east and east (40-100°) about 65% of the time with wind speeds of 3 km/hr or greater. Winds are

Map 5.2. Distances and directions from industrial sources to sampling stn 29547

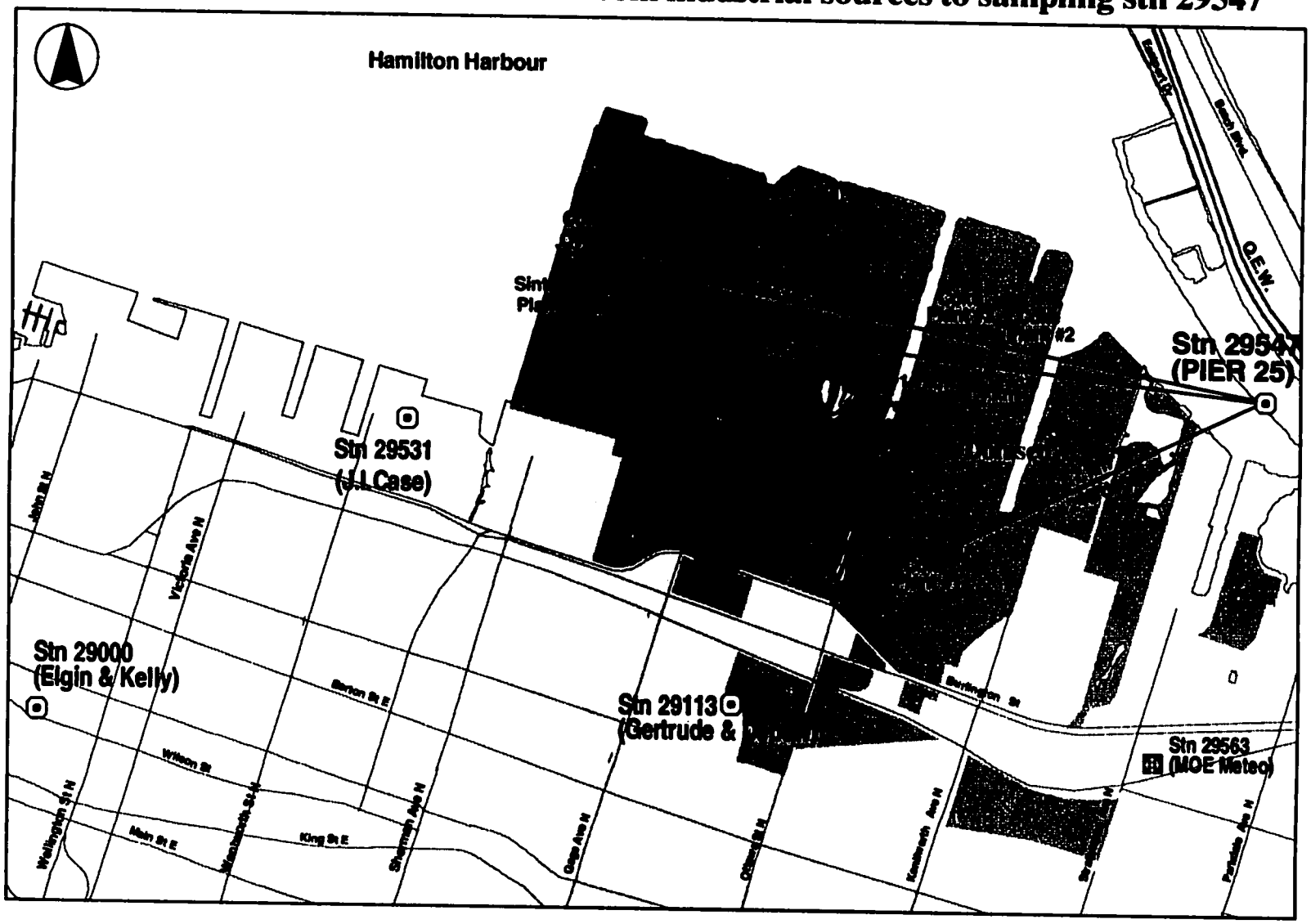

Map 5.4. Distances and directions from industrial sources to sampling stn 29000

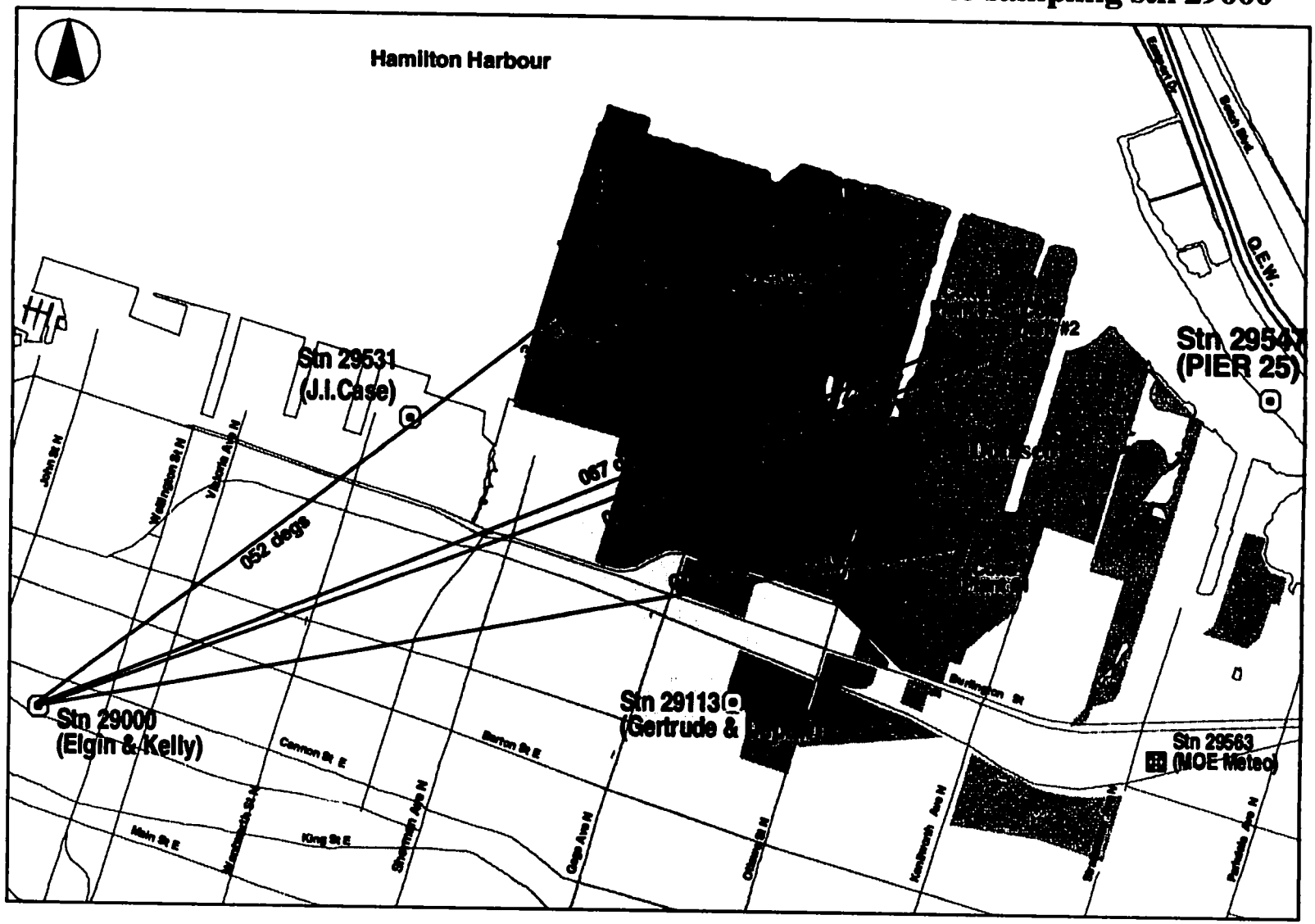

Map 5.5. Distances and directions from industrial sources to sampling stn 29113

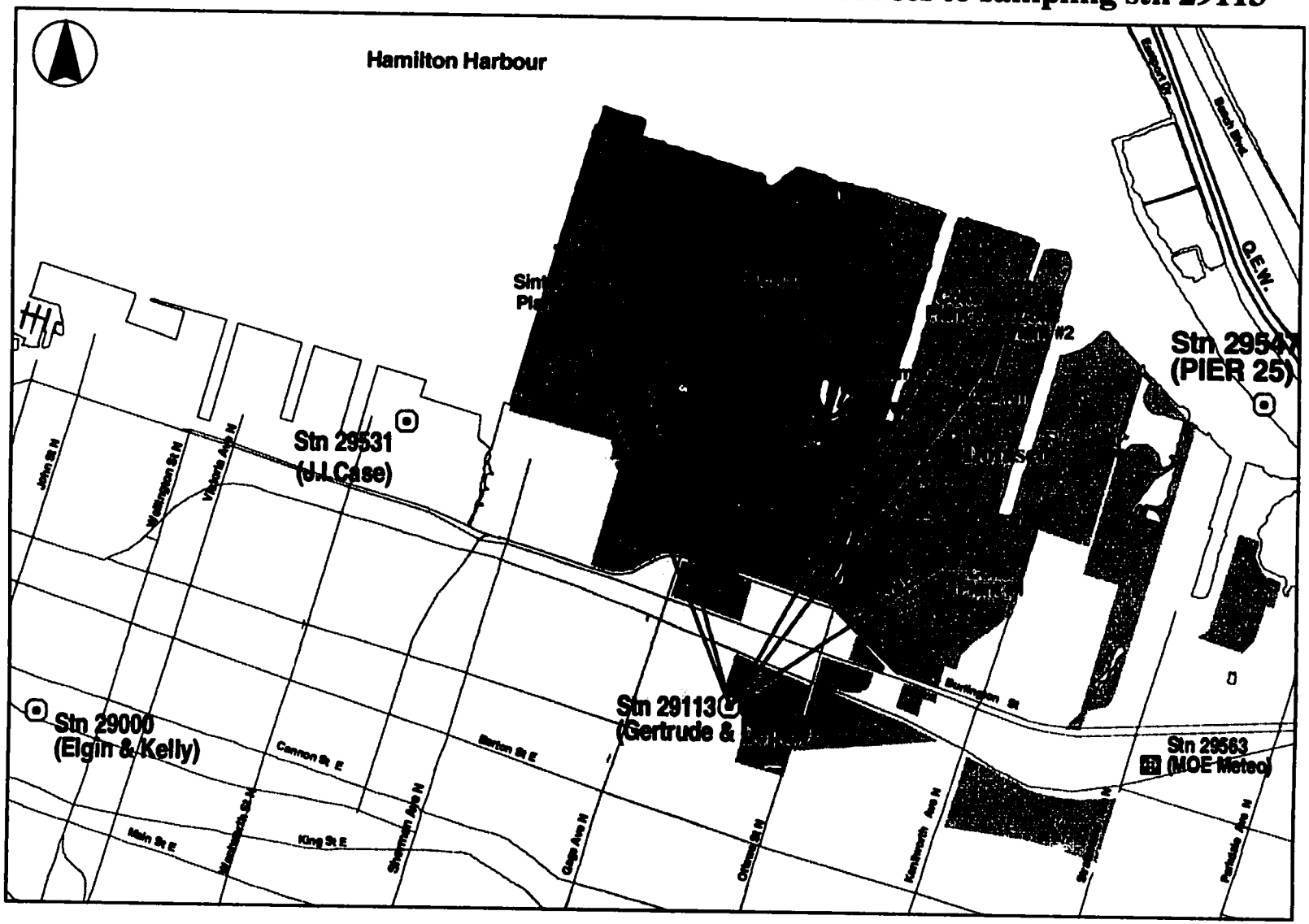

Table 5.1. Wind data and particulate concentrations for all air particulate filters collected in Hamilton in 1995.

Filter #	Date	Wind Direction Avg. (Std. Dev.)	Avg. Wind Speed (km/hr)	# Hours Low Wind Speed[1]	Site[2]	Filter Class[3]	Particulate Conc. (ug/m3)
1	95/07/10	180 (96)	5.2	7	29000		21
2					29113		47
3					29547		44
4	95/07/11	32 (64)	6.3	5	29000		27
5					29113		70
6					29547		43
7	95/07/12	146 (80)	6.8	7	29000		28
8					29113		62
9					29547		53
10	95/07/13	232 (52)	7.1	2	29113		60
11					29547		82
12	95/07/14	250 (33)	8.5	1	29113		44
13					29547		57
14	95/07/15	35 (93)	6.0	8	29113		12
15					29547		7
16	95/07/16	51 (113)	3.7	7	29113		29
17					29547		13
18	95/07/17	246 (25)	7.7	2	29000		16
19					29113		24
20					29547		41
21	95/07/18	272 (12)	11.7	1	29000		13
22					29113		34
23					29547		51
24	95/07/19	254 (35)	6.7	6	29000		19
25					29113		28
26					29547		34
27	95/07/20	238 (7)	10.4	0	29000	UW	26
28					29531	UW	28
29					29113	UW	27
30					29547	DW	42
31	95/07/21	101 (55)	6.5	7	29000		38
32					29531		50
33					29113		50
34					29547		83

Table 5.1. (cont'd)

Filter #	Date	Wind Direction Avg. (Std. Dev.)	Avg. Wind Speed (km/hr)	# Hours Low Wind Speed[1]	Site[2]	Filter Class[3]	Particulate Conc. (ug/m3)
35	95/07/22	147 (78)	4.5	7	29000		33
36					29531		66
37					29113		59
38					29547		54
39	*95/07/23*	*265 (44)*	*8.0*	*5*	*29000*	*S*	*18*
40					*29531*	*S*	*16*
41					*29113*	*S*	*19*
42					*29547*	*S*	*36*
43	95/07/24	74 (41)	2.7	12	29000		52
44					29531		47
45					29113		64
46					29547		39
47	95/07/25	132 (109)	4.8	4	29000		69
48					29531		62
49					29113		68
50					29547		58
51	95/07/26	283 (68)	3.6	12	29000		26
52					29531		31
53					29113		39
54					29547		40
55	*95/07/27*	*71 (37)*	*6.4*	*10*	*29000*	*S*	*43*
56					*29531*	*S*	*49*
57					*29547*	*S*	*38*
58	*95/07/28*	*223 (55)*	*6.4*	*1*	*29000*	*S*	*34*
59					*29531*	*S*	*40*
60					*29547*	*S*	*58*
61	*95/07/29*	*264 (30)*	*7.0*	*6*	*29531*	*S*	*23*
62					*29113*	*S*	*25*
63					*29547*	*S*	*46*
64	95/07/30	123 (63)	5.6	10	29531		47
65					29113		28
66					29547		30
67	95/07/31	176 (64)	6.3	5	29000		41
68					29531		55
69					29113		49
70					29547		132
71	*95/08/1*	*297 (61)*	*6.8*	*2*	*29000*	*S*	*38*
72					*29531*	*S*	*49*
73					*29113*	*S*	*66*
74					*29547*	*S*	*70*

Table 5.1. (cont'd)

Filter #	Date	Wind Direction Avg. (Std. Dev.)	Avg. Wind Speed (km/hr)	# Hours Low Wind Speed[1]	Site[2]	Filter Class[3]	Particulate Conc. (ug/m3)
75	95/08/2	61 (12)	8.2	1	29000	DW	30
76					29531	DW	48
77					29113	S	80
78					29547	UW	28
79	95/08/3	67 (109)	5.4	7	29000		36
80					29531		47
81					29113		56
82					29547		73
83	95/08/4	96 (109)	4.2	8	29000	S	29
84					29531	S	35
85					29113	S	28
86					29547	S	38
87	95/08/5	256 (76)	5.1	4	29000	S	18
88					29531	S	17
89					29113	S	19
90					29547	S	23
91	95/08/6	71 (20)	13.1	0	29000	S	16
92					29531	S	35
93					29113	S	20
94					29547	S	9
95	95/08/7	96 (29)	12.3	0	29000	S	21
96					29531	DW	48
97					29113	S	19
98					29547	UW	15
99	95/08/8	104 (45)	9.6	8	29000	S	28
100					29531	S	49
101					29113	S	42
102					29547	S	50
103	95/08/9	85 (46)	8.1	6	29000	S	38
104					29531	S	51
105					29113	S	34
106					29547	S	35
107	95/08/10	131 (69)	5.3	9	29000	S	63
108					29531	S	72
109					29113	S	58
110					29547	S	58
111	95/08/11	226 (26)	6.4	0	29000	UW	20
112					29531	UW	23
113					29113	UW	23
114					29547	DW	36

Table 5.1. (cont'd)

Filter #	Date	Wind Direction Avg. (Std. Dev.)	Avg. Wind Speed (km/hr)	# Hours Low Wind Speed[1]	Site[2]	Filter Class[3]	Particulate Conc. (ug/m3)
115	**95/08/12**	**326 (45)**	**6.5**	**6**	**29000**	**S**	**15**
116					**29531**	**S**	**15**
117					**29113**	**S**	**20**
118					**29547**	**S**	**15**
119	**95/08/13**	**46 (56)**	**7.0**	**3**	**29000**	**S**	**20**
120					**29531**	**S**	**32**
121					**29113**	**S**	**25**
122					**29547**	**S**	**15**
123	**95/08/14**	**59 (113)**	**4.5**	**6**	**29531**	**S**	**54**
124					**29113**	**S**	**62**
125					**29547**	**S**	**124**
126	**95/08/15**	**296 (60)**	**5.1**	**5**	**29000**	**S**	**22**
127					**29531**	**S**	**55**
128					**29113**	**S**	**34**
129					**29547**	**S**	**32**
130	**95/08/16**	**51 (36)**	**4.3**	**9**	**29000**	**S**	**66**
131					**29531**	**S**	**53**
132					**29113**	**S**	**53**
133					**29547**	**S**	**125**
134	**95/08/17**	**58 (19)**	**5.1**	**3**	**29000**	**DW**	**83**
135					**29531**	**DW**	**67**
136					**29113**	**DW**	**65**
137					**29547**	**UW**	**121**
138	**95/08/18**	**76 (40)**	**5.9**	**3**	**29000**	**DW**	**85**
139					**29531**	**DW**	**64**
140					**29113**	**DW**	**70**
141					**29547**	**UW**	**105**
142	**95/08/19**	**45 (69)**	**6.8**	**6**	**29000**	**S**	**52**
143					**29531**	**S**	**60**
144					**29113**	**S**	**58**
145					**29547**	**S**	**49**
146	**95/08/20**	**26 (93)**	**6.1**	**4**	**29000**	**S**	**37**
147					**29531**	**S**	**38**
148					**29113**	**S**	**45**
149					**29547**	**S**	**43**

[1]low wind speed defined as < 3.0 km/hr

[2]for site location, refer to Map 5.1

[3]UW = upwind of the coke ovens; DW = downwind of the coke ovens; S = selected for analysis, but not classified as either upwind or downwind

Note: Boldface samples were extracted and analyzed by GC/MS.

calm (i.e., wind speed less than 3 km/hr) about 25 % of the time [179]. This pattern is reflected in the wind direction plot (Figure 5.1) that summarizes this information for the 42 days sampled in 1995. The sampling periods with low standard deviations had average wind directions located within the shaded regions for a particular sampling station (Stations 29531, 29000 or 29547). Many of the filters collected during these sampling periods were classified as upwind or downwind samples. Station 29113 was rarely located downwind of the coke ovens. Four sampling periods with average wind directions in the 250-270° range that would have had substantial impacts on Station 29547 were not selected because a corresponding upwind sample was not available from Station 29531.

Filters selected for analysis are indicated in boldface type in Table 5.1. Selected filters are labeled upwind (UW), downwind (DW) or selected but not classified as upwind or downwind (S). A number of "unclassified" filters (S) were chosen that were expected to contain varying amounts of coke oven emissions. Any of the remaining samples would fall into this category so the samples were selected based mainly on sampling date to provide continuity in time to the data set. All filters collected over a 17–day continuous period from August 4 to August 20 were extracted and analyzed. Air particulate samples for all four sites were analyzed for the selected dates, when possible.

The upwind class of samples are expected to represent impacts due primarily to vehicular emissions with little or no impact from the coke ovens while the downwind class of samples should have significant coke oven impacts. Any samples that did not fit

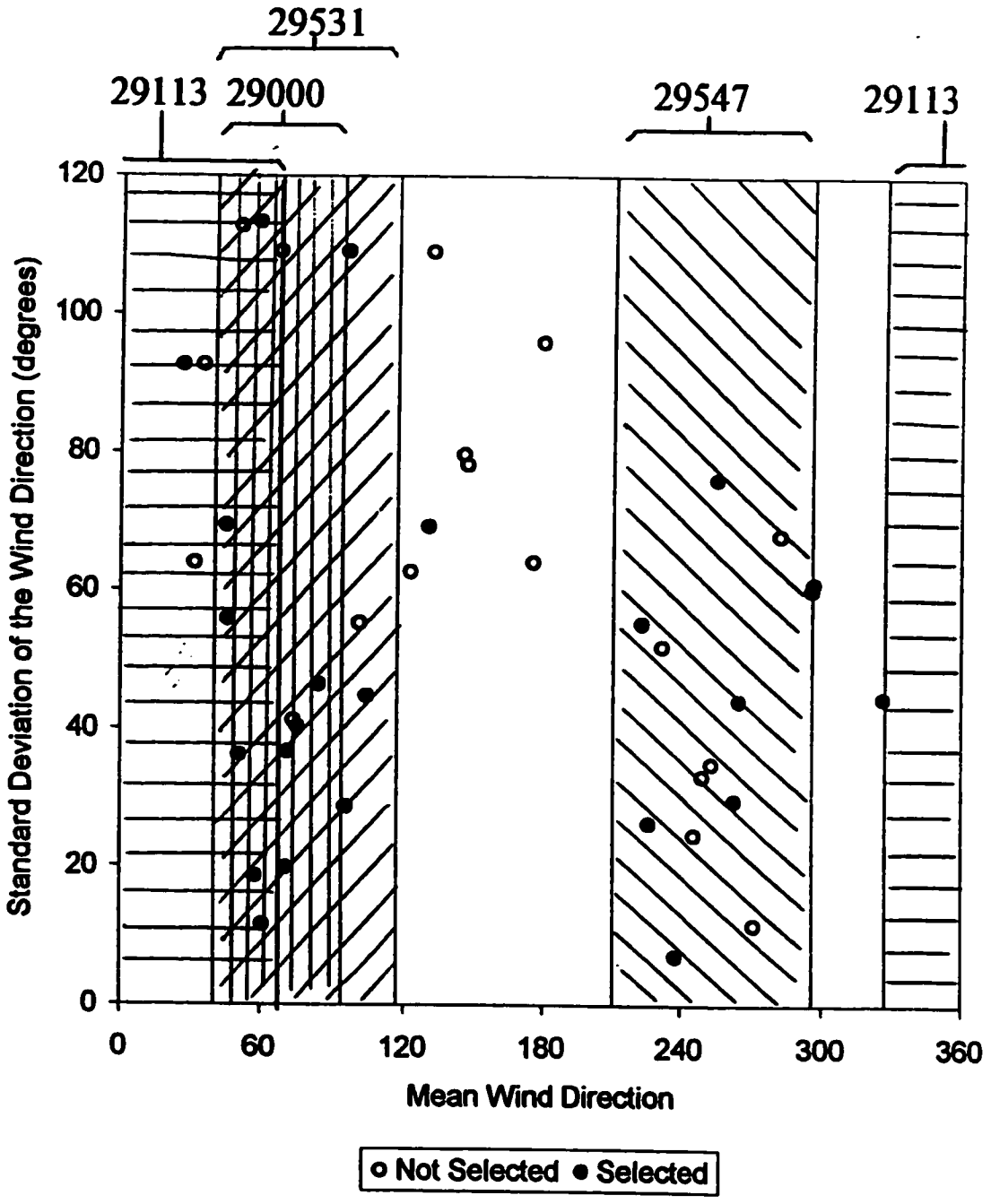

Figure 5.1. Mean wind direction relative to standard deviation of the wind direction for all sampling periods. Shaded regions indicate directions of direct impacts of coke oven emissions on the sampling stations noted at the top of the figure.

either of the first two classes are grouped together as unclassified samples (S). Some of these samples may contain primarily coke oven emissions or primarily vehicle emissions even though one or more of the selection criteria were not met. The proportion of coke oven emissions and vehicular emissions in these samples is not known.

5.2 PAH Analysis

A total of 92 respirable air particulate samples were selected, extracted and cleaned up for GC/MS analysis according to the procedures outlined in the Methods section. These filters are indicated in boldface type in Table 5.1. A former undergraduate student, Sona Mehta, performed the extractions, alumina and Sephadex LH20 chromatography, and GC/MS analysis for 20 of the filters. I extracted, cleaned up and analyzed the remaining 72 filters and was responsible for PAH and thia-arene quantification for all 91 filters.

Total ion current GC/MS chromatograms of the non-polar aromatic fractions of air particulate collected upwind and downwind of the coke ovens on August 2, 1995 are shown in Figure 5.2. The chromatogram of the sample extract from Station 29547 (upwind) was obtained from injection of approximately 20 m^3 of sampled air, while the chromatogram of the sample extract from Station 29531 (downwind) corresponds to approximately 2 m^3 of air injected. The largest peaks in these complex mixtures correspond to PAH. The peak heights in the downwind sample are about twice as intense as in the upwind sample. This means that the corresponding PAH are about 20 times

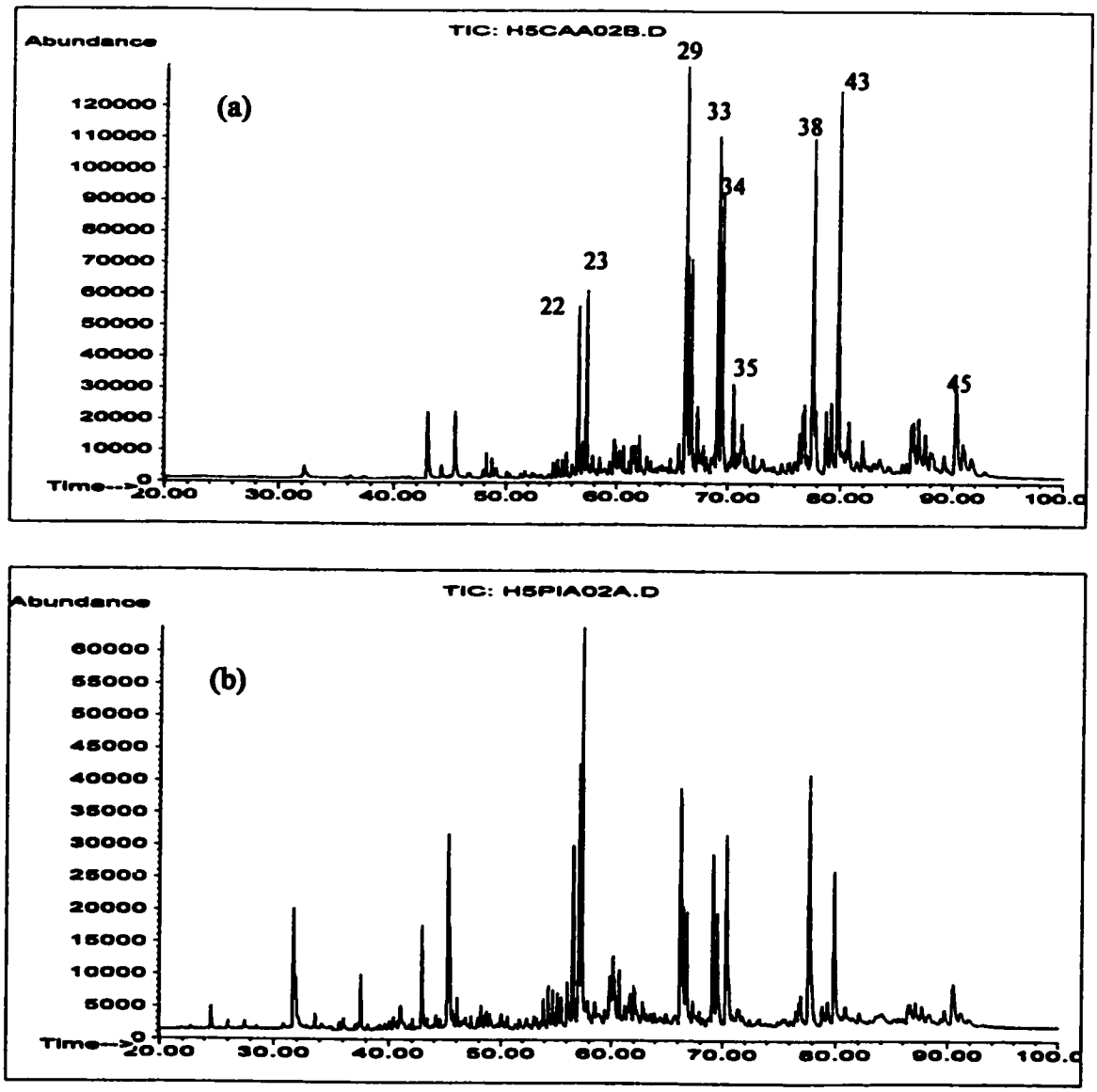

Figure 5.2. Total ion chromatograms of non-polar aromatic fractions prepared from Hamilton air particulate collected on August 2, 1995 (a) downwind of the coke ovens at Station 29531 and (b) upwind of the coke ovens at Station 29547. Samples were analyzed using GC/MS Conditions B.

Table 5.2. List of PAH quantified in Hamilton air particulate. The sum of these individual PAH was calculated and reported as "total concentration of PAH".

Peak No.	Compound	Abbreviation	Molecular Mass
19	Benzo[ghi]fluoranthene	BGF	226
20	Benzo[c]phenanthrene	BCP	228
21	Cyclopenta[cd]pyrene	CPP	226
22	Benz[a]anthracene	BAA	228
23	Chrysene	CHR	228
29	Benzo[b]fluoranthene	BBF	252
30	Benzo[j]fluoranthene	BJF	252
31	Benzo[k]fluoranthene	BKF	252
33	Benzo[e]pyrene	BEP	252
34	Benzo[a]pyrene	BAP	252
35	Perylene	PER	252
38	Indeno[1,2,3-cd]pyrene	IND	276
39	Dibenz[a,c]anthracene	DCA	278
43	Benzo[ghi]perylene	BGP	276
45	Coronene	COR	300

more abundant in the downwind sample. The peaks labeled in the chromatograms are identified in Table 5.2. Peak numbering is consistent with Appendix I.

The distribution patterns of PAH differ in the upwind and downwind samples. The downwind air particulate sample contains a larger proportion of high mass PAH which elute at later retention times than the upwind sample. Similar results were observed for all samples in the upwind and downwind classes.

The PAH listed in Table 5.2 were quantified individually in the air particulate extracts and the concentrations are listed for each sample by station number and date in Appendix II. The total concentration of PAH in a sample is defined as the sum of the concentrations of the 15 compounds listed in Table 5.2. One thia-arene, benzo[b]naphtho[2,1-d]thiophene, was also quantified and the concentration is included with the PAH in Appendix II.

The sum of the concentrations of the PAH compounds is plotted as a function of average wind direction for each sampling station (Figure 5.3). The shaded regions in Figure 5.3 represent the direction of direct impact from the coke ovens. Air particulate samples collected downwind of the coke ovens (in the shaded regions) have higher total concentrations of PAH than air particulate samples collected upwind of the coke ovens. Total concentrations of PAH tend to increase as mean wind directions approach the shaded region for any sampling site.

The total PAH for the upwind samples ranged from 0.44 to 2.1 ng/m^3, while the total PAH for the downwind samples ranged from 17 to 150 ng/m^3. Consistently higher values were determined at Station 29531 than at the other three locations. Two samples

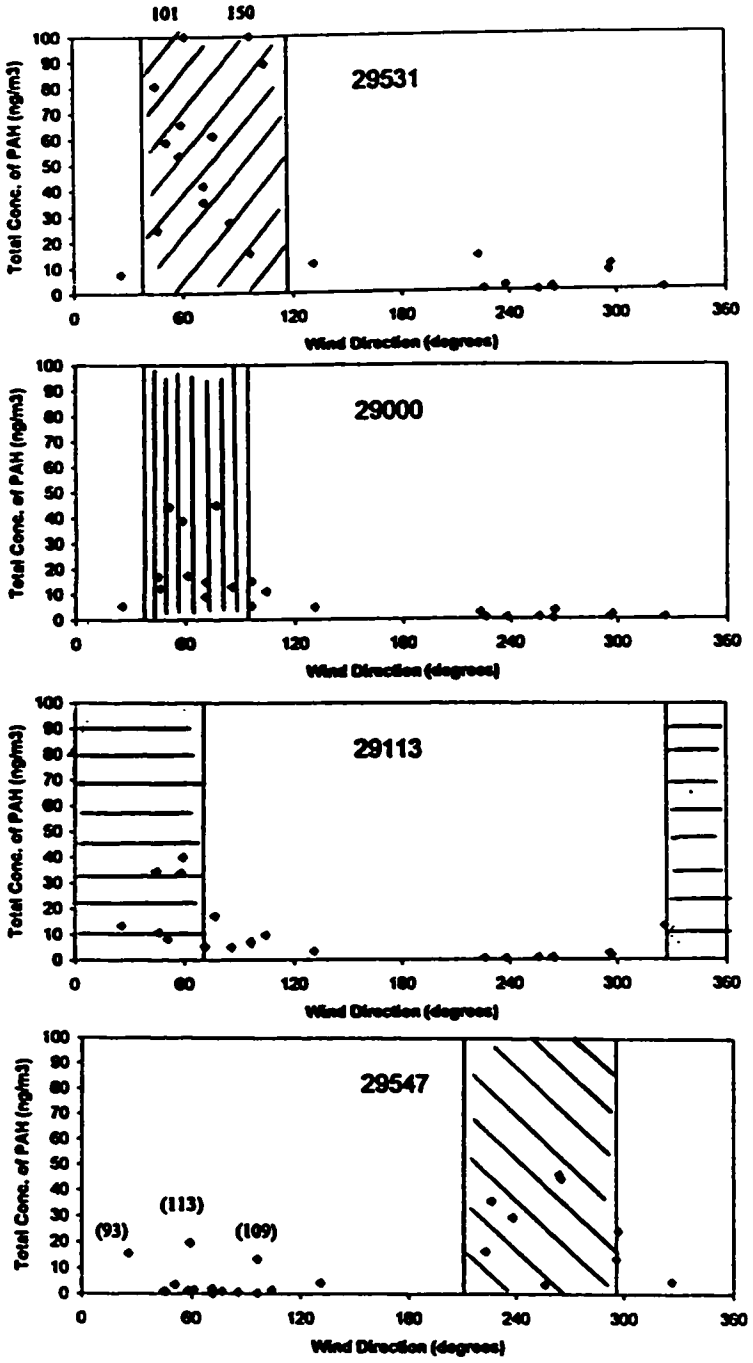

Figure 5.3. Variation of PAH concentration with mean wind direction for each sampling station. Shaded regions indicate wind directions that would result in direct impact of coke oven emissions on the sampling station.

exceeded a total PAH concentration of 100 ng/m^3. The actual total PAH concentration is labeled above the data points for these two samples. Stations 29531, 29547 and 29113 are located approximately equal distances (about 1.7 km) from the nearest coke oven battery. Station 29000 is impacted from the same direction as Station 29531, but Station 29000 is located approximately twice as far from the coke oven battery compared to Station 29531. Total concentrations of PAH are significantly lower at 29000 than at 29531, likely due to increased dispersion of coke oven emissions. A similar range of total PAH concentrations were observed at Stations 29000, 29113 and 29547.

The day-to-day variation of PAH concentrations for the period from August 4 to August 20 is shown for each site (Figure 5.4). Stations 29000, 29113 and 29531 show similar trends, while PAH levels at Station 29547 tend to be opposite to those at 29000, 29113 and 29531 because 29547 is located on the opposite side of the steel mills from the other sites. The day-to-day variability of PAH concentrations can be quite large depending on the direction of the wind.

The total concentrations of PAH for the 92 respirable air particulate samples are plotted as pollution roses on a map of Hamilton (Map 5.6). The lengths of the vectors protruding from the sampling sites correspond to total PAH in ng/m^3, while the direction of the vector corresponds to the mean wind direction for the sample. The longest vectors at each site (greatest PAH concentrations) point in the direction of the coke ovens, indicating the source of the pollutants.

The Ontario Ministry of the Environment (MOE) routinely monitors levels of many PAH compounds because their potential toxic effects are a concern. A provincial

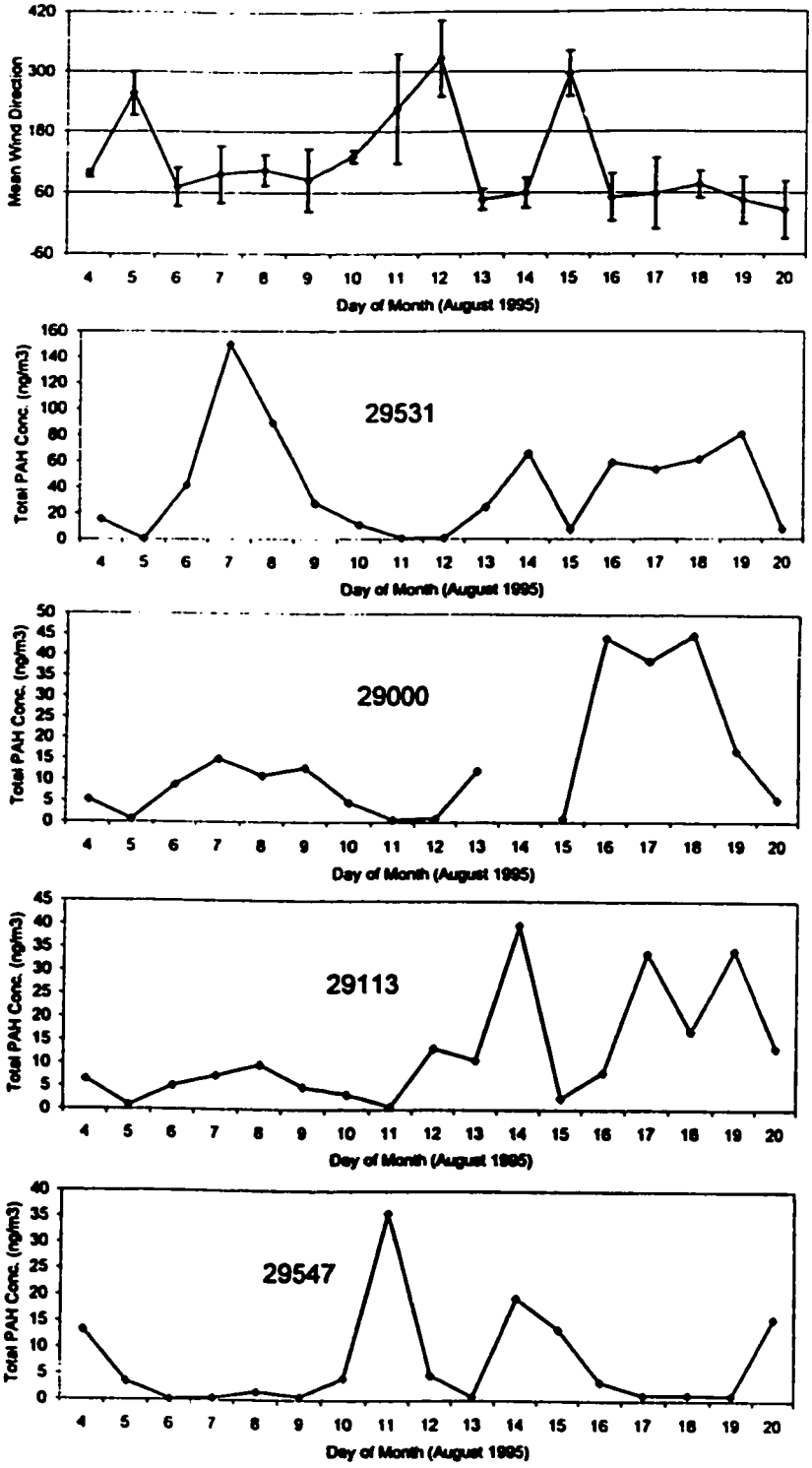

Figure 5.4. Daily variation of PAH concentration for each sampling station.

pling stations for the period of July-August 1995

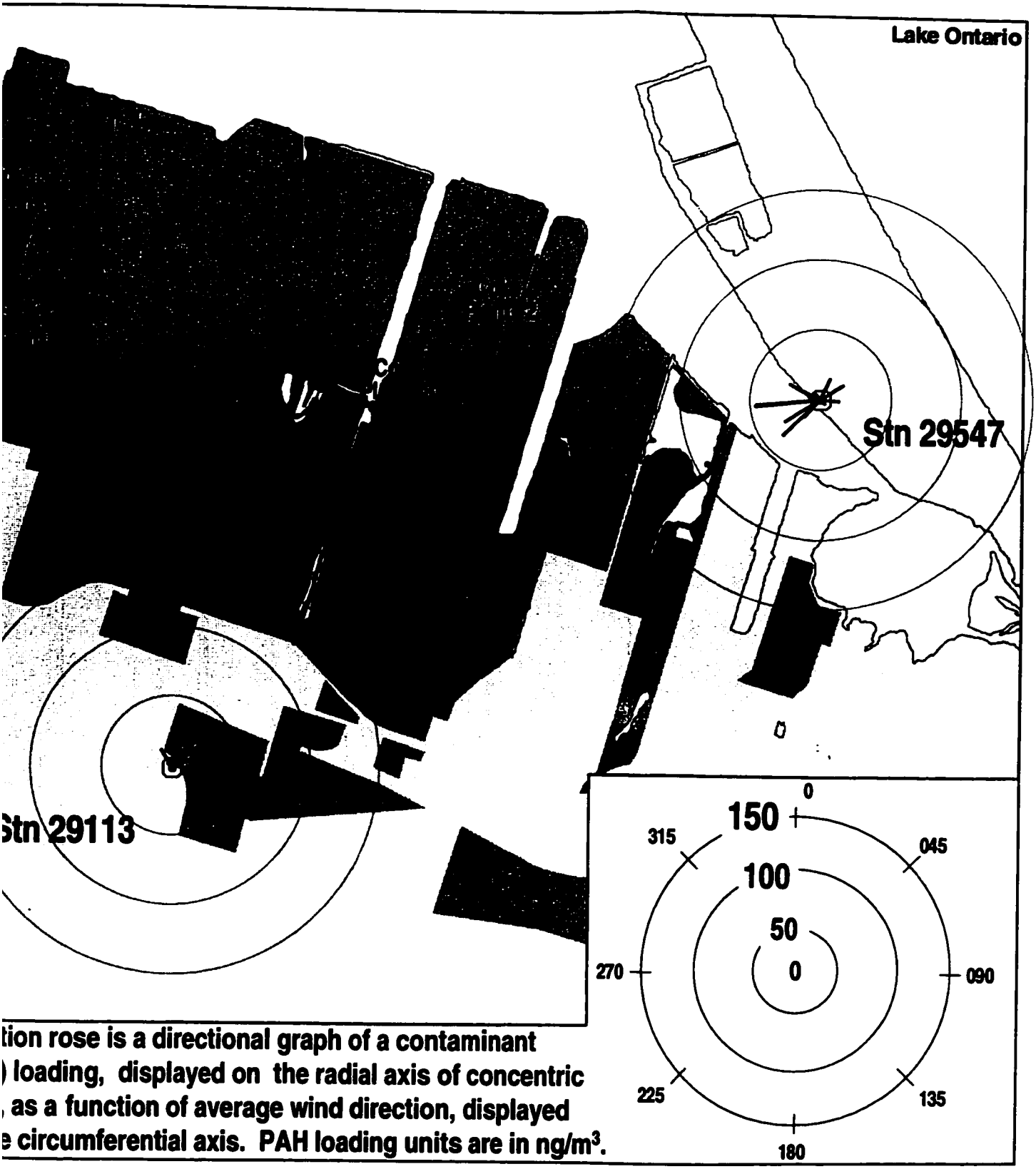

tion rose is a directional graph of a contaminant
) loading, displayed on the radial axis of concentric
, as a function of average wind direction, displayed
e circumferential axis. PAH loading units are in ng/m^3.

Table 5.3. Summary of benzo[a]pyrene (BAP) data for samples collected in this study and data reported by the Ontario Ministry of the Environment (MOE).

Station	Number of Samples Analyzed	Mean B[a]P Concentration (ng/m^3)	Number Exceeding 1.1 ng/m^3	% of Samples Exceeding 1.1 ng/m^3
This Study (1995)				
29547	23	1.4	10	43
29000	23	1.2	11	48
29113	21	1.0	5	24
29531	24	3.4	14	58
MOE Report (1995)[1]				
29547	26	1.8	9	35
29000[2]	23	0.8	5	22
29113	27	0.9	8	30

[1]reference 179

[2]analyzed by Environment Canada

standard has been set for only one compound, BAP. The acceptable 24-hour average concentration of BAP has been set at 1.1 ng/m^3 [179]. This standard was exceeded in 40 of the 91 samples analyzed. The mean BAP concentrations at each sampling station are summarized in Table 5.3. The highest mean concentration of BAP was determined at Station 29531 (3.4 ng/m^3), with 58 % of the 22-hour samples from this site exceeding the 1.1 ng/m^3 standard. The other three stations had mean BAP concentrations ranging from 1.0 to 1.4 ng/m^3. Station 29113, located south of the steel industries had the lowest percentage of samples exceeding 1.1 ng/m^3 (24%).

As part of its regular monitoring program, the MOE analyzed PAH in air samples for 24-hour periods every twelfth day in 1995 at Stations 29547, 29000 and 29113. The mean BAP concentrations reported for these samples are also listed in Table 5.3. At Station 29547, the mean BAP concentration determined by the MOE for 1995 is slightly higher (1.8 ng/m^3) than the mean concentration determined in this study for samples collected in July and August (1.4 ng/m^3), but a similar number of samples exceeded the standard. At Station 29000, a higher mean concentration of BAP (1.2 ng/m^3) was determined in this study than by the MOE (0.8 ng/m^3, analyses performed by Environment Canada). Approximately twice as many of our Station 29000 samples were found to exceed the standard compared to the MOE report.

The small discrepancies between this study and the 1995 Hamilton Air Quality Data Summary are to be expected because sampling times, sampling methods and analytical methods are different. The MOE sampled about twice a month throughout the entire year, while samples in this study were collected in July and August only. Winds

blowing from the northeast were recorded for a greater number of days during the summer than the typical average annual number due to warmer air temperatures in the summer. This wind pattern would tend to increase impacts of coke oven emissions (and thus, PAH concentrations) at Station 29000 and decrease coke oven impacts at Station 29547. This is consistent with the results of the present study. Station 29113 is not usually directly upwind or downwind of the coke ovens so PAH levels at this site would not be expected to change from average values. Results in this study at Station 29113 were consistent with those reported by the MOE.

The MOE has since begun to determine PAH in respirable air particulate at Station 29531, due in part to the high concentrations observed in this study at that location.

5.3 Respirable Air Particulate Data

Levels of respirable particulate in air are a serious public health concern due to the adverse health effects resulting from inhalation of fine particulate. The toxicological effects of the chemicals (e.g., PAH) adsorbed to these particles are a separate issue. The particles alone have also been implicated as a cause of adverse health effects. The MOE has set a guideline of 50 $\mu g/m^3$ for respirable air particulate while other jurisdictions use a value of 100 $\mu g/m^3$.

Concentrations of respirable particulate exceeded 100 $\mu g/m^3$ in four samples out of the 149 filters collected for this study. All four of these samples were collected at Station 29547. A greater number of samples exceed the new MOE guideline of 50

$\mu g/m^3$. This guideline was equaled or exceeded in 52 (35%) of the 149 filters collected. The number of times each site exceeded this guideline are as follows: Station 29547, 17; Station 29113, 16; Station 29531, 14; and Station 29000, 8. Not surprisingly, sites close to the industry had the greatest number of samples exceeding the guideline.

The TSP fraction of air particulate is collected on filters using a high volume sampler. This study has focused on respirable air particulate (PM_{10} <10 μm particle diameter) because it has the most potential effect on human health. From a toxicological perspective, it has been shown that over 95% of the potential mutagens and carcinogens in urban air are associated with respirable particulate [180] and not with gas phase chemicals.

It would be interesting to determine what proportion of the total suspended particulate from steel mill operations is sampled using the respirable particulate (PM_{10}) samplers. At Station 29547, we installed a high volume air sampler (HiVol) alongside the PM_{10} sampler. Particulate concentrations were determined for both the PM_{10} and HiVol samples for 37 days during the sampling period. Only a selection of the PM_{10} samples were analyzed for PAH. On average, the respirable particulate made up 39 % of the total suspended particulate fraction collected at this site. This value agrees well with the 1995 MOE Hamilton Air Quality Data Summary, which states that respirable particulate generally comprised about 40% of the total suspended particulate in Hamilton [179]. On the four days where PM_{10} values exceeded 100 $\mu g/m^3$, the percentage of respirable particulate was lower. When the PM_{10} exceeded 100 $\mu g/m^3$, the respirable particulate accounted for only 21 to 27 % of the total particulate.

The mean, minimum and maximum particulate concentrations were determined for each sampling site (Table 5.4). Station 29547 had the highest mean respirable particulate concentration (50 $\mu g/m^3$). Mean particulate concentrations determined at Stations 29000 (35 $\mu g/m^3$) and 29113 (43 $\mu g/m^3$) are 75% and 30% higher, respectively, than the mean concentrations reported by the MOE for 24-hour samples collected once every six days for the year of 1995 (20 $\mu g/m^3$ at Station 29000 and 33 $\mu g/m^3$ at Station 29113). The maximum particulate concentrations at Stations 29000 and 29113 determined in this study were similar to those reported by the MOE.

5.4 PAH Loadings on Respirable Air Particulate

Concentrations of PAH and respirable air particulate for the upwind (UW) and downwind (DW) subset of the samples in Table 5.1 are listed in Table 5.5. A wide range of PAH concentrations are observed on a given day depending on sampling location. In contrast, a narrower range of particulate concentrations is observed. The loading of PAH ($\mu g/g$) on the particulate was calculated for all samples by dividing the total PAH concentration by the particulate concentration (column 7, Table 5.5). Samples belonging to the downwind classification consistently have much greater PAH loadings than samples belonging to the upwind classification. The average PAH loading downwind of the coke ovens is 867 $\mu g/g$ while the average PAH loading upwind of the coke ovens is only 32 $\mu g/g$. These results indicate that particulate emissions from the coke ovens contain significantly greater amounts of PAH than particulate emissions from background

Table 5.4. Summary of respirable air particulate (PM_{10}) concentrations in $\mu g/m^3$ in Hamilton air.

Station	Number of Samples	Mean Value	Minimum Value	25th Percentile	75th Percentile	Maximum Value
29000	34	35	13	21	40	85
29113	40	43	12	27	60	80
29531	32	45	15	34	55	72
29547-PM10	41	50	7	34	58	132
29547-HiVol	39	150	14	71	159	575
29000-MOE[1]	53	20	---	---	---	88
29113-MOE[1]	52	33	---	---	---	88

[1]Data from reference 179

Table 5.5. List of particulate concentrations, PAH concentrations and PAH loadings for upwind and downwind Hamilton air filters.

Date	Wind Direction Avg. (Std. Dev.)	# Hours Low Wind Speed	Site	Particulate Conc. (ug/m3)	Total PAH Conc. (ng/m3)	PAH Loading (ug/g)	Filter Class
95/07/20	238 (7)	0	29547	42	29	693	DW
95/08/2	61 (12)	1	29000	30	24	823	DW
95/08/2	61 (12)	1	29531	48	17	358	DW
95/08/7	96 (29)	0	29531	48	150	3143	DW
95/08/11	226 (26)	0	29547	36	36	999	DW
95/08/17	58 (19)	3	29000	83	39	468	DW
95/08/17	58 (19)	3	29113	65	34	524	DW
95/08/17	58 (19)	3	29531	67	53	801	DW
95/08/18	76 (40)	3	29000	85	45	533	DW
95/08/18	76 (40)	3	29113	70	17	243	DW
95/08/18	76 (40)	3	29531	64	61	949	DW
95/07/20	238 (7)	0	29000	26	0.65	25	UW
95/07/20	238 (7)	0	29113	27	0.67	25	UW
95/07/20	238 (7)	0	29531	28	2.1	73	UW
95/08/2	61 (12)	1	29547	28	1.6	56	UW
95/08/7	96 (29)	0	29547	15	0.44	29	UW
95/08/11	226 (26)	0	29000	20	0.63	31	UW
95/08/11	226 (26)	0	29113	23	0.65	28	UW
95/08/11	226 (26)	0	29531	23	0.80	34	UW
95/08/17	58 (19)	3	29547	121	1.1	9	UW
95/08/18	76 (40)	3	29547	105	1.0	10	UW

sources. Greater efforts should be made to reduce PAH emissions from coke ovens rather than particulate emissions.

5.5 Evaluation of Thia-Arene Ratios as Source Tracers

To my knowledge, thia-arenes have not previously been evaluated as source apportionment tracers for atmospheric studies. Alkylated dibenzothiophene (3-ring thia-arene) ratios have been used previously in sediment applications and were examined in Hamilton air particulate in Chapter 3. I decided that less volatile source tracers would be more suitable for particulate analyses. Four-ring (234 amu) and five-ring (258 amu) thia-arenes were examined briefly in source samples in Chapter 4. Profiles of the 234 and 258 amu thia-arene isomers were found to differ in coke oven condensate compared to diesel exhaust particulate (see Chapter 4, Figures 4.12 and 4.13, respectively).

The 234 and 258 amu thia-arene isomers were also examined in Hamilton air particulate collected in 1995. Ion chromatograms of the molecular mass 234 thia-arene isomers in downwind and upwind air particulate extracts are shown in Figure 5.5. Criteria for the identification of thia-arenes are discussed in Chapter 4. The thia-arene profile for downwind air particulate (Figure 5.5) is similar to the thia-arene profile for coke oven condensate shown in Figure 4.12. Also, the thia-arene profile for upwind air particulate (Figure 5.5) resembles the thia-arene profile for diesel exhaust particulate (Figure 4.12).

Similarly, ion chromatograms (m/z 258) corresponding to the molecular ions of the 258 amu thia-arene isomers are shown in Figure 5.6 for the downwind and upwind air

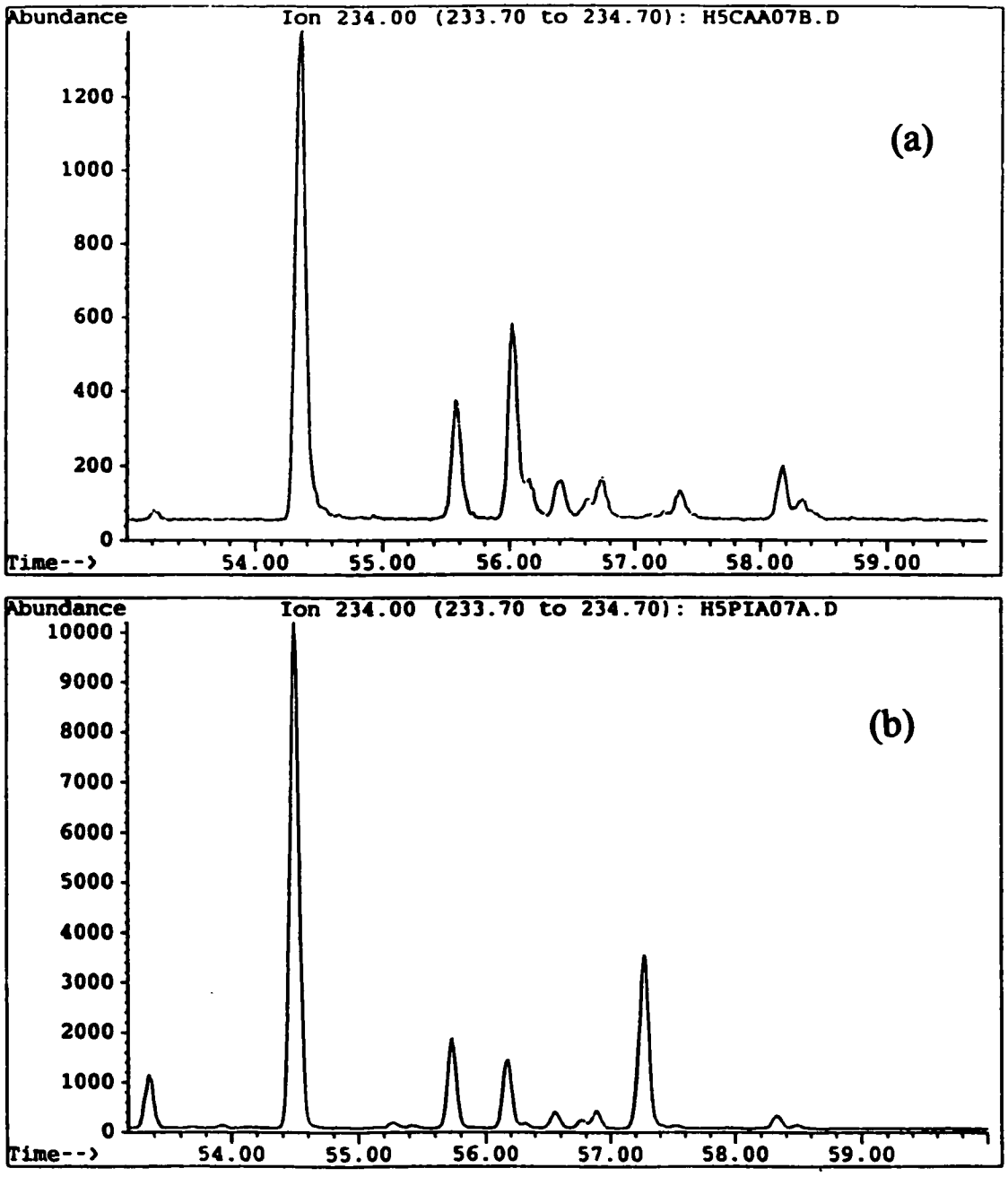

Figure 5.5. Ion chromatograms (m/z 234) of extracts from Hamilton air particulate collected on August 7, 1995 (a) downwind of the coke ovens (Station 29531) and (b) upwind of the coke ovens (Station 29547).

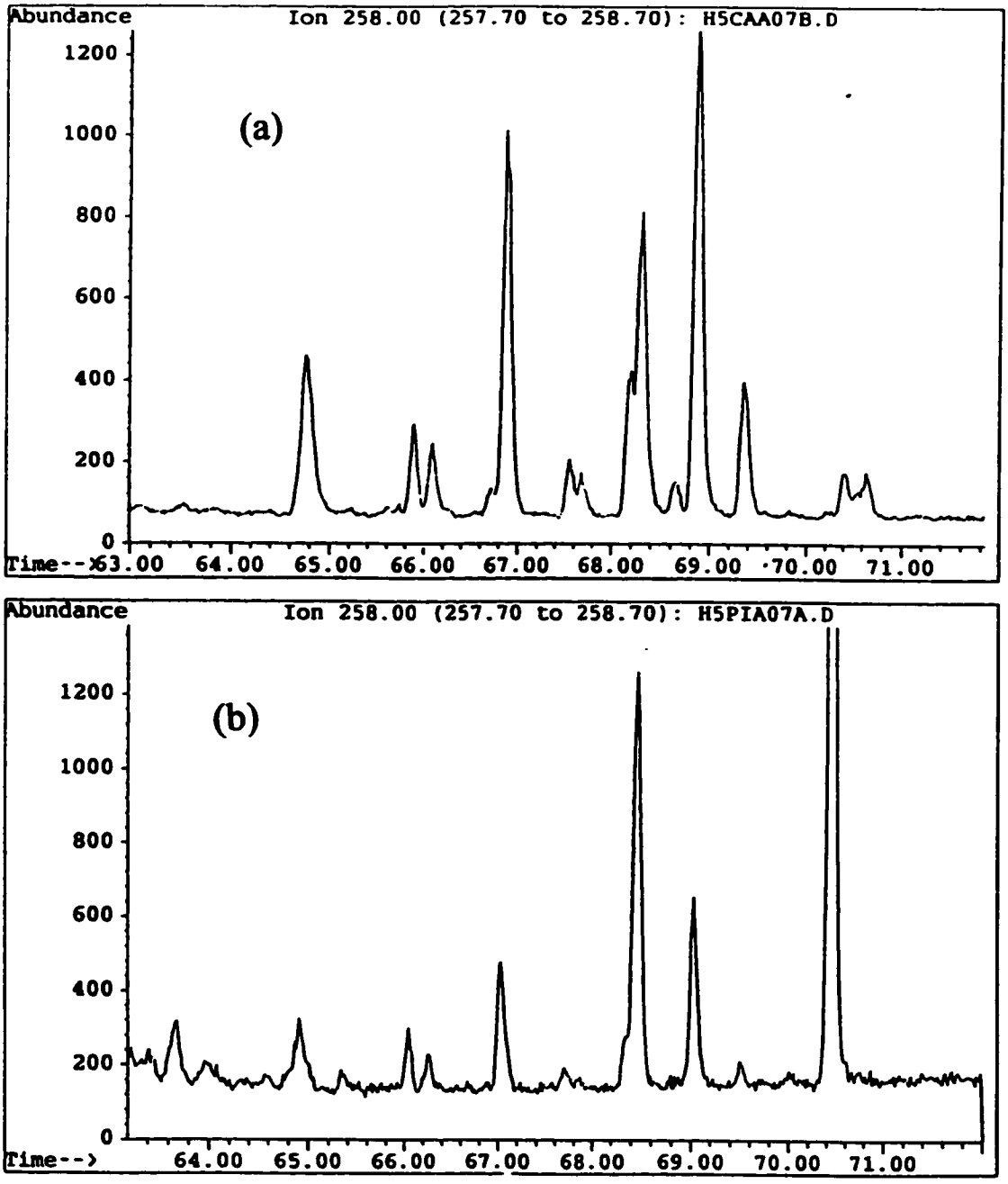

Figure 5.6. Ion chromatograms (m/z 258) of extracts from Hamilton air particulate collected on August 7, 1995 (a) downwind of the coke ovens (Station 29531) and (b) upwind of the coke ovens (Station 29547).

particulate extracts. The m/z 258 thia-arene profile for downwind air particulate (Figure 5.6) is similar to that of coke oven condensate (Figure 4.13), while the m/z 258 thia-arene profile for upwind air particulate (Figure 5.6) is similar to that of diesel exhaust (Figure 4.13). These figures show that ambient air sample profiles are very similar to the relevant source sample profiles.

A large number of thia-arene isomers exist at molecular masses of 234 and 258 amu. It is difficult to determine which isomers should be used for source differentiation by visual inspection only. In the next chapter (Chapter 6), principal component analysis (PCA) will be used as an aid to select useful thia-arene isomers and to help define criteria that can be used to distinguish coke oven emissions from diesel engine emissions. Following PCA, in Chapter 7, the criteria will be further evaluated using the Hamilton air particulate samples collected in the summer of 1995.

6.0 PRINCIPAL COMPONENT ANALYSIS

6.1 Overview

In Chapter 5, differences were observed between thia-arene profiles in coke oven condensate and thia-arene profiles in diesel exhaust particulate by examination of the 234 and 258 amu isomer extracted ion chromatograms. A large number of structural isomers exist for the 234 and 258 amu thia-arenes. It would be useful to know which isomers differ the greatest in the two source samples, but this is not obvious by visual inspection. Principal component analysis (PCA) is a multivariate statistical analysis method that is useful in examining large data sets and finding correlations between variables in that data set. PCA reduces the number of variables needed to explain the variance in a data set. This approach has been applied to source-receptor studies and has been used to determine source emission profiles from ambient air data [37-45]. PCA was used in the present study to identify the thia-arene isomers that provide the most information for source discrimination.

In this chapter, PCA was used for three purposes:

(1) to compare thia-arenes with PAH as source tracers;

(2) to select thia-arene variables for use as source tracers in Chapter 7; and

(3) to examine relationships between various types of environmental samples.

The 1995 Hamilton air particulate data set (89 samples) was analyzed alone and then with source samples using PCA. This analysis was then applied to additional

environmental samples to show the relationships between various samples. The statistics software package used for this work was SPSS version 7.5.

This type of analysis is a sequential and iterative process and requires some intelligent interpretation by the practitioner at different stages of the process. This chapter is organized in sequential format to reflect this process. Toward the end of the chapter, various source samples and other environmental samples that were added to the analysis will be discussed and interpreted.

6.2 Analysis of Hamilton Air Particulate using All PAH and Thia-Arene Data

Eighty-nine Hamilton air particulate samples were used in this section. Peak areas for as many individual 234 and 258 amu thia-arene isomers as possible were determined in all 89 ambient samples. The thia-arene peaks quantified for PCA analysis are labeled on extracted ion chromatograms from a coke oven condensate sample (Figure 6.1). Peak areas for all isomers were normalized and used as variables in the analysis. PCA was then used to extract only the isomers that were useful for differentiating coke oven emissions from diesel emissions.

In several samples, certain thia-arene isomers were below the detection limit or coeluted with interfering compounds such as internal standards. These data were not included in the analysis. Variables B21T, B12T, and B23T represent Compounds 80, 81 and 86, respectively (234 amu thia-arenes, Appendix I). The variables 258A, 258B, and 258C represent the 258 amu isomers and may include Compounds 96 and 98 (Appendix I) in addition to other isomers. Several coeluting 258 amu isomers were not identified

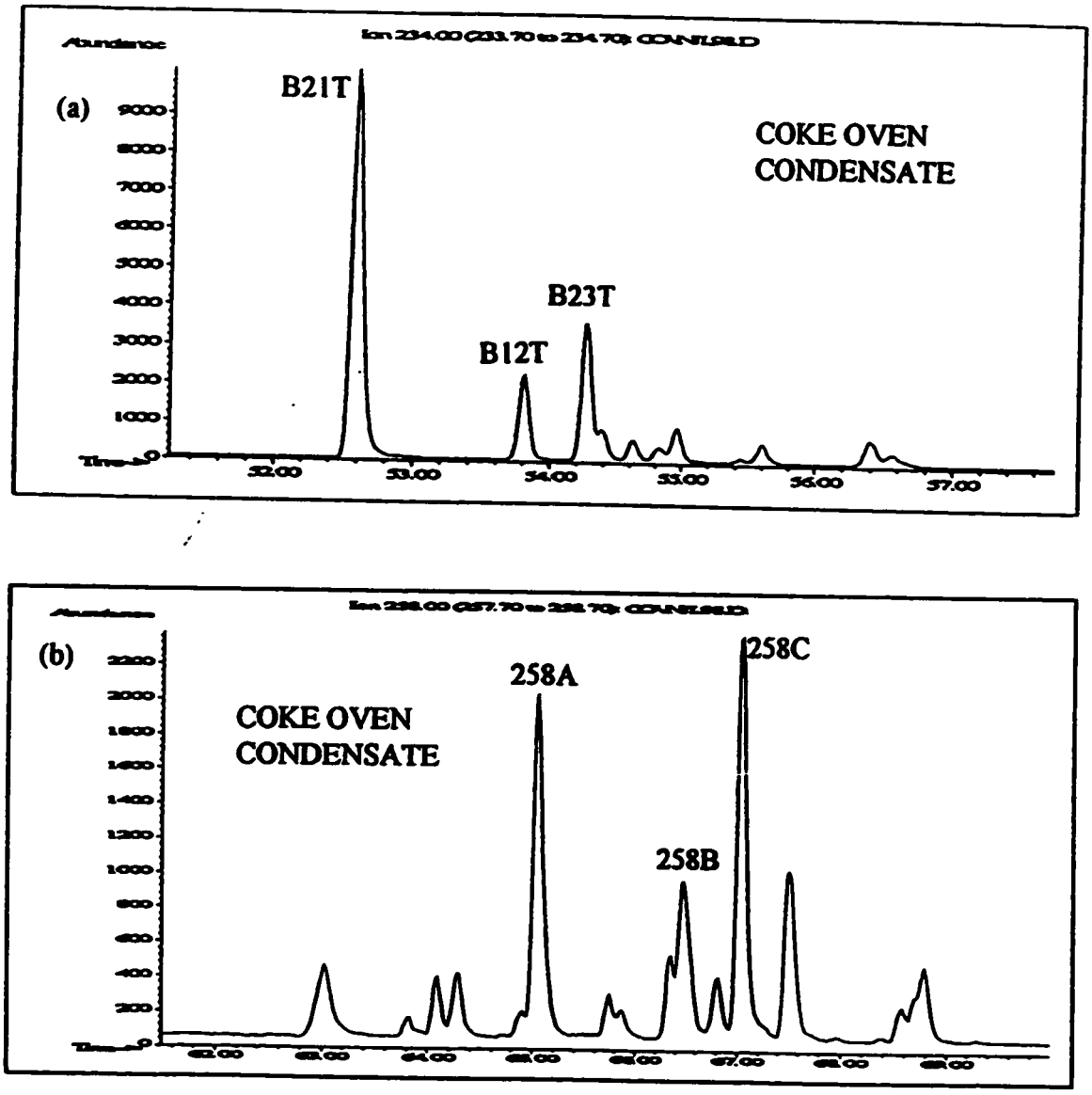

Figure 6.1. Mass chromatograms of the (a) m/z 234 ion and (b) m/z 258 ion from the analysis of coke oven condensate. Labeled peaks are used as variables in PCA.

because authentic standards were not available for all 258 amu isomers. Fifteen PAH compounds that had molecular masses between 226 and 300 amu were also included in the analysis.

The thia-arene peak areas were normalized within each molecular mass group to give a sum of the peak areas equal to 1.0. The 234 amu and 258 amu isomer groups were normalized separately to reduce effects related to compound volatility. All PAH concentrations were normalized in one group to give a total concentration of all 15 PAH equal to 1.0. The PAH were normalized in one group, rather than in separate molecular weight classes, to be consistent with previous studies. Each variable isomer was then mean centered and scaled to unit variance by the following equation:

$$X_{iN} = \left(\frac{X_i - \overline{X_i}}{S_{Xi}} \right)$$

where X_{iN} is the normalized variable, X_i is the original variable value, X_i is the mean of all X_i, and S_{Xi} is the standard deviation of all X_i.

Five significant (eigenvalue >1) components were extracted using PCA, which accounted for a total of 81% of the variance in the data set. This means that the data set containing 21 PAC variables was reduced to 5 "effective" variables or components using linear combinations of the 21 variables. The majority (81%) of the original information in the data set is still maintained in the new set of 5 components.

The factor loadings for the rotated components are listed in Table 6.1. Large absolute values for variable factor loadings indicate a large content of information useful

Table 6.1. List of factor loading values for Varimax rotated components extracted from Hamilton air particulate data using all PAH and thia-arene variables.

	Component				
	1	2	3	4	5
B12T	8.518E-02	-4.3E-02	-1.3E-02	-9.8E-02	.940
B21T	-.843	.298	-8.1E-02	-.179	-.260
B23T	.857	-.300	8.583E-02	.202	9.993E-02
258A	.900	-4.9E-02	-3.7E-02	-.144	-6.3E-02
258B	-.943	8.878E-02	-4.7E-02	.185	-2.6E-02
258C	.901	-.115	.114	-.205	9.846E-02
BAA	.157	.929	-3.6E-02	-2.0E-02	-3.2E-02
BAP	.919	-8.5E-02	.157	7.398E-02	-6.0E-02
BBF	-.383	.186	.765	-.158	.143
BCP	-.414	.808	-5.5E-02	-4.7E-02	5.111E-02
BEP	-1.9E-02	-.217	.818	8.932E-02	.135
BGF	-.633	.673	-.217	.158	-4.8E-02
BGP	-6.8E-02	-.526	-.235	.741	-.124
BJF	.268	4.401E-02	.856	-2.1E-02	-9.7E-02
BKF	.249	-4.8E-02	.820	-.117	-.176
CHR	-.458	.840	6.129E-02	-.157	-8.0E-02
COR	-.526	-.205	-.435	.576	-8.4E-02
CPP	.605	.270	-.221	.433	.239
DAC	.631	-.288	9.850E-02	-6.5E-02	1.024E-02
IND	.245	-.505	-.389	-.654	.150
PER	.445	-6.7E-03	-6.3E-02	-.172	-4.3E-02

for explaining the variance in a data set. In the present analysis, I assumed that at least part of the variance was due to differences in source contributions. The factors that represent variation in source contribution will be determined in Section 6.3.

In Table 6.1, the components are ordered such that the largest amount of variance is accounted for by the first component, then the next largest amount of variance is placed in the second component, and so on. The first component, containing 34% of the variance, contained large factor loadings (> 0.70) for five of the six thia-arene variables and for one PAH, BAP (Compound 34, Appendix I). In the second and third components, which accounted for 17% and 16% of the variance, respectively, large factor loadings were observed for other PAH isomers. In the second component, three 226/228 amu PAH isomers (BCP, Compound 20; BAA, Compound 22; and CHR, Compound 23) had large positive loadings. The third component had large positive loadings for all 252 amu PAH isomers except BAP. The fourth and fifth components, accounting for 8% and 6% of the remaining variance, respectively, contained a large factor loading for only one compound each, IND (Compound 38) in component 4 and B12T (Compound 81) in component 5. Full names and structures for the compound numbers are listed in Appendix I.

One of the functions of PCA in source apportionment is to extract factors from a large data set that, after rotation, represent individual sources of pollution. Previous PCA studies using ambient PAH data have found that factors describe the variation of PAH concentrations due to volatility, rather than different source contributions [40,52]. Consistent with previous studies, results of the present study show PAH variables with

high factor loadings in Components 2 and 3 grouped together by molecular mass or volatility. However, it was shown in Chapter 3 that air particulate collected downwind of the steel industries contains a higher proportion of high mass PAH than air particulate collected upwind of the steel industries. This reflects a difference in source compositions of coke oven emissions compared to vehicular emissions. In the next section, it will be determined whether or not Components 2 and 3 represent different PAH source contributions.

6.3 Selection of Variables useful for Source Differentiation

To determine which factors are useful to distinguish between traffic emissions and coke oven emissions, the sample scores for Component 1 were plotted against the sample scores for Component 2 (Figure 6.2(a)), and the sample scores for Component 3 are plotted against the sample scores for Component 4 (Figure 6.2(b)). Eighty-nine air samples are plotted in each figure and the samples designated as "upwind" of the steel industries (UW) and "downwind" of the steel industries (DW) are indicated with different markers. The classification of upwind and downwind Hamilton air samples was described in detail in Chapter 5. The other Hamilton air particulate samples that were not classified as UW or DW are labeled "HAMAIR" in Figure 6.2 and are represented in the plot by small filled circles.

The downwind samples are well separated from the upwind samples in Figure 6.2(a). It appears that both Component 1 and Component 2 contribute to the separation of the upwind and downwind samples. Downwind samples have higher scores for

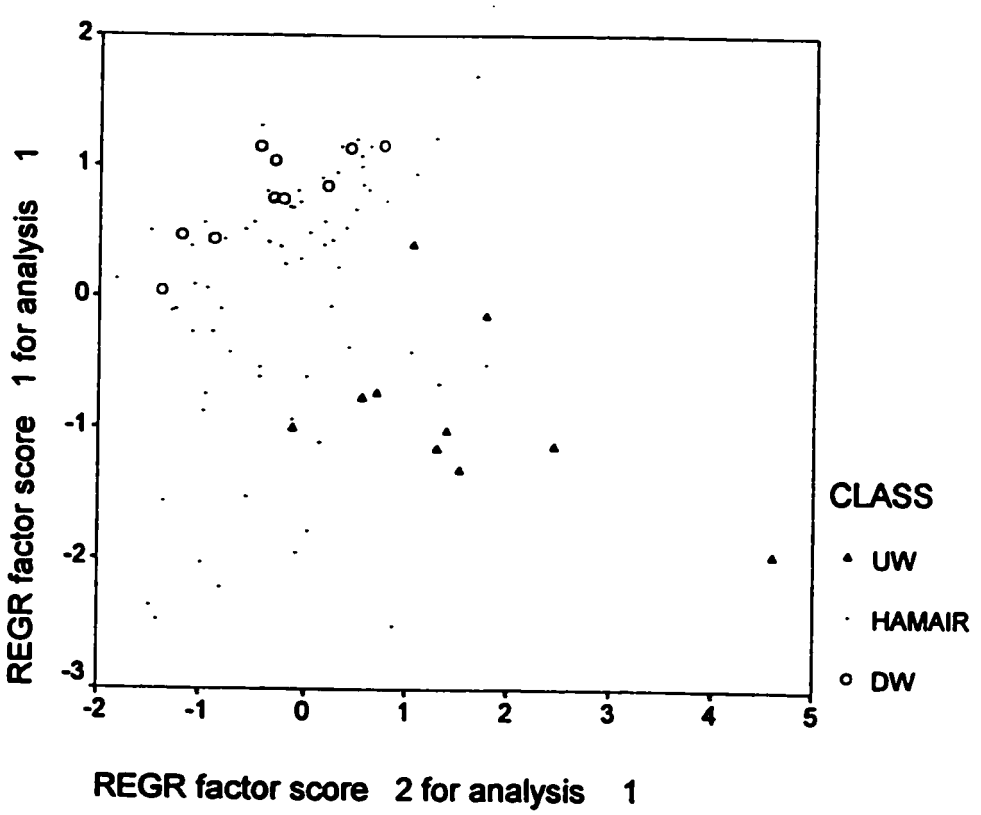

Figure 6.2(a). Hamilton air particulate sample scores on Components 1 and 2 extracted in the analysis using all PAH and thia-arene variables.

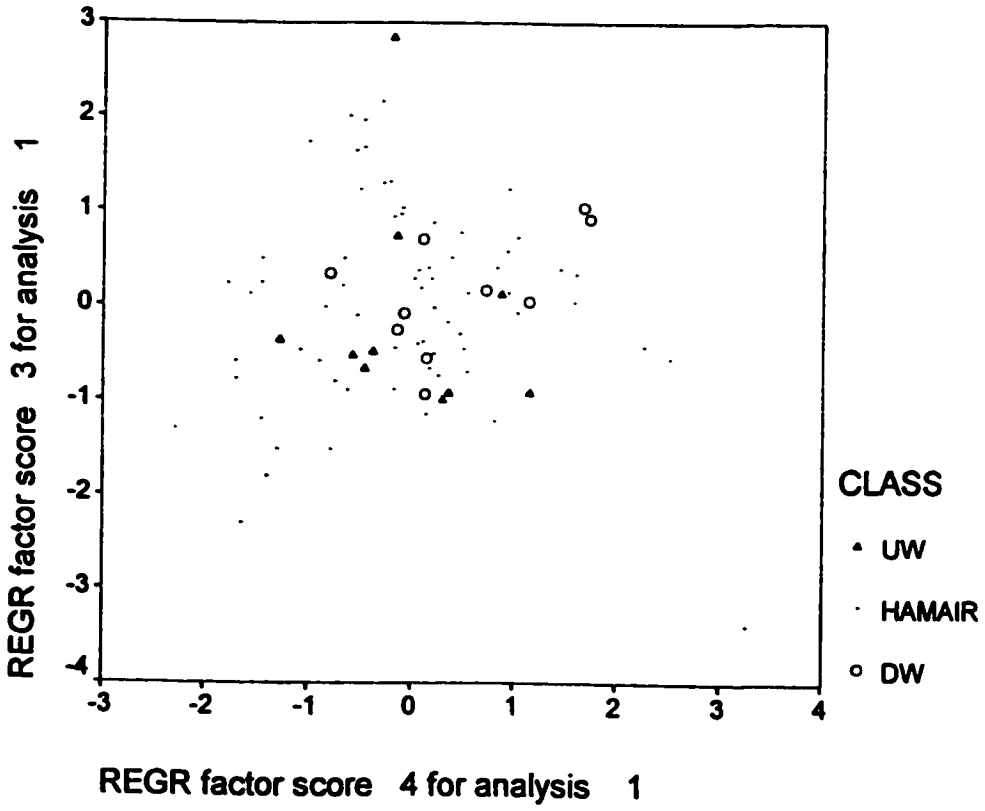

Figure 6.2(b). Hamilton air particulate sample scores on Components 3 and 4 extracted in the analysis using all PAH and thia-arene variables.

Component 1 and lower scores for Component 2, while upwind samples have lower scores for Component 1 and higher scores for Component 2. The upwind samples are spread over a wider range in Figure 6.2(a). As will be shown in Chapter 7, even a small contribution of coke oven emissions to the urban background signature will greatly affect the chemical profile of the upwind or background samples due to the high concentration of PAC in coke oven emissions. It is unlikely that all upwind samples are completely free of impacts from coke oven emissions.

In Figure 6.2(b), the upwind and downwind samples overlap completely. Components 3 and 4 do not appear to be helpful in discriminating between the two pollution sources. A similar observation was made when the sample scores were plotted against Component 5 (data not shown). Only Components 1 and 2 contain significant information for the differentiation of coke oven emissions and vehicular emissions. High factor loadings (>0.7) were observed for variables B21T, B23T, 258A, 258B, 258C and BAP in Component 1; and BAA, BCP and CHR in Component 2. These variables contain information relevant to pollution sources and will be included in the next section.

6.4 Analysis of Hamilton Air Particulate with Reduced Number of Variables

Variables that did not contain much source information were removed from the data set to determine if the additional variables interfered with the analysis. The variables selected were those which showed large factor loadings in Components 1 and 2

in the preliminary analysis. Two 234 amu and three 258 amu thia-arene variables, and four PAH were selected. PCA was repeated with this limited set of variables.

Two significant factors were extracted accounting for 58% (Component 1) and 24% (Component 2) of the variance in the data set. A total of 82% of the variance of the data set is accounted for by these two components. The rotated component coefficient matrix is shown in Table 6.2. High loadings for the thia-arene variables and BAP are observed for Component 1, consistent with results in the previous section. Factor loadings for Components 1 and 2 are illustrated in Figure 6.3. All variables are located far from the origin on either Component 1 or Component 2 axes indicating that all variables for this analysis contain significant information for source discrimination. Loadings for the thia-arenes and BAP are plotted at opposite ends of Component 1, while loadings for the other PAH are plotted together at the positive end of Component 2.

Next, the component 1 and component 2 scores of all 85 ambient air samples were plotted against each other (Figure 6.4). This figure is very similar to Figure 6.2(a), the analysis containing all PAH and thia-arene variables, which shows it was not necessary to eliminate any variables. A larger gap between the majority of the UW and DW samples on the Component 1 axis indicates that Component 1 provides greater discrimination between coke oven emissions and vehicle emissions than the second component. Furthermore, the first component accounted for more than twice the variance in the data set than the second component (58% for Component 1, compared to 24% for Component 2). This analysis shows that ambient concentrations of selected PAH contain useful information about source profiles but the thia-arenes are superior source

Table 6.2. List of factor loading values for Varimax rotated components extracted from Hamilton air particulate data using a reduced number of variables.

	Component	
	1	2
B21T	-.853	.357
B23T	.857	-.357
258A	.911	-5.0E-02
258B	-.967	9.246E-02
258C	.935	-.120
BAP	.908	-.126
BCP	-.368	.835
CHR	-.415	.877
BAA	.177	.926

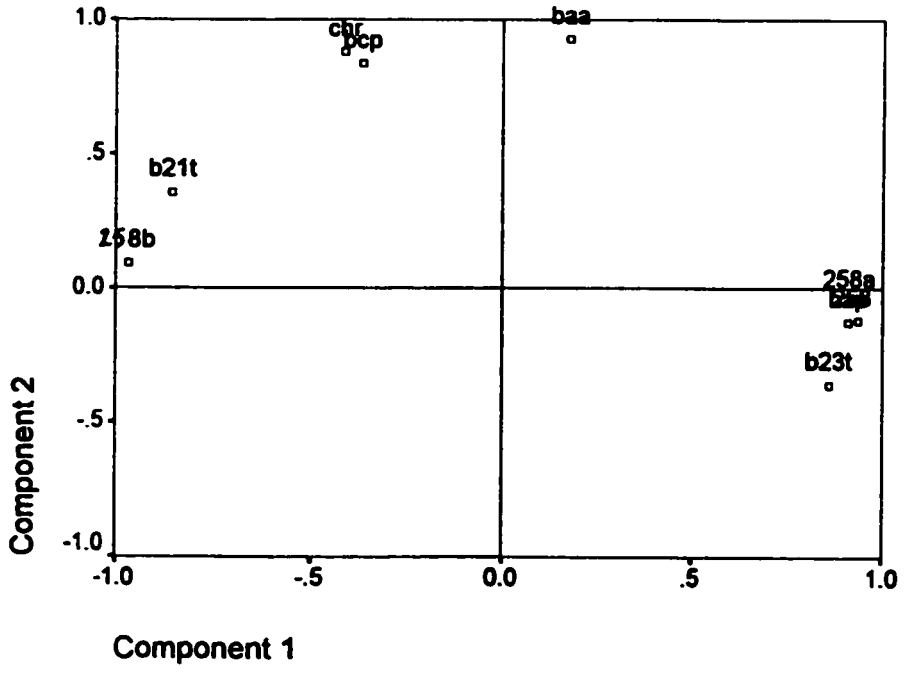

Figure 6.3. Loadings of variables on components 1 and 2. All 89 Hamilton air particulate samples were included in this analysis.

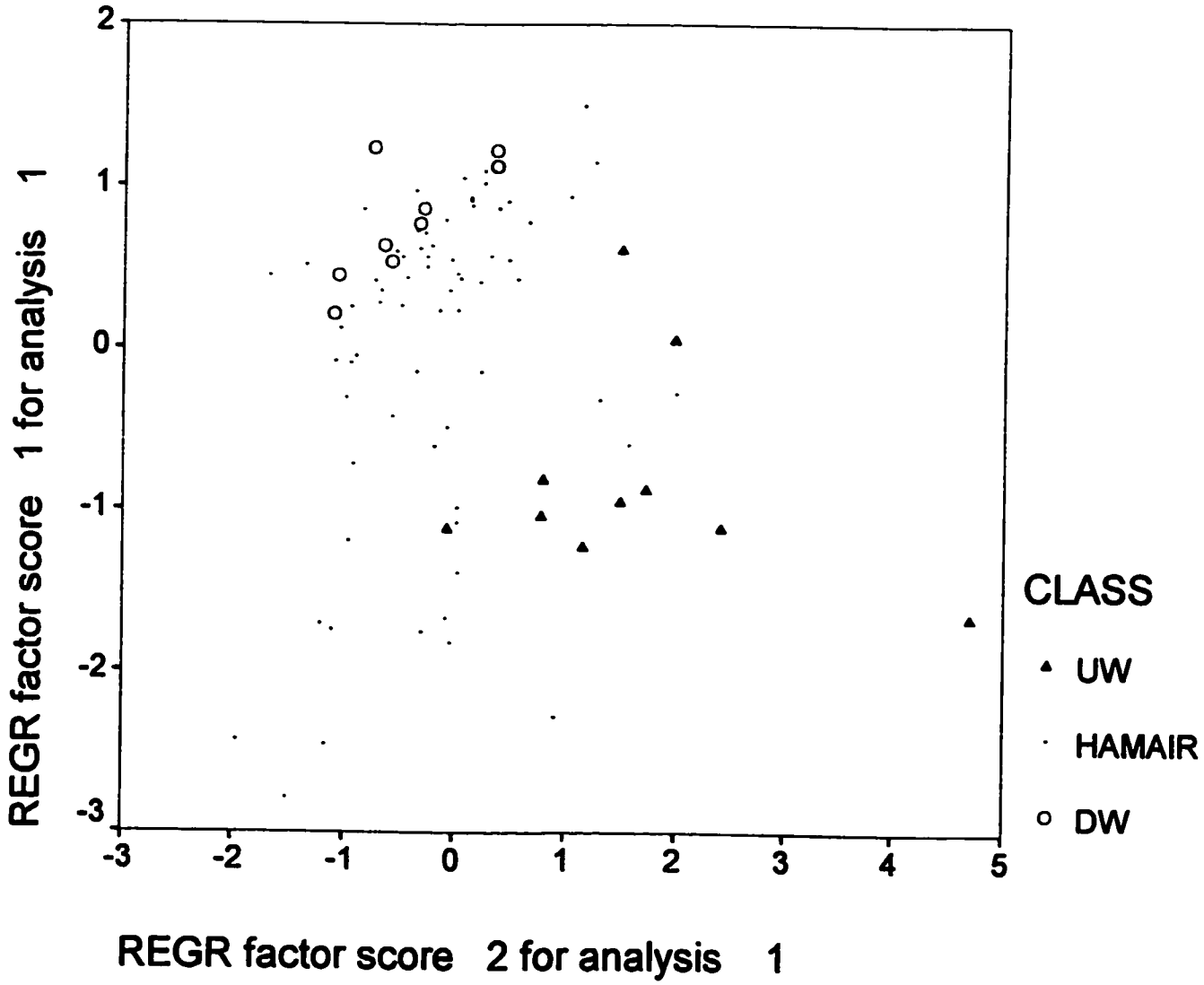

Figure 6.4. Hamilton air particulate sample scores for the two components extracted in the analysis using a reduced number of PAH and thia-arene variables.

apportionment tracers for the differentiation of coal-based emissions and petrogenic emissions. In the subsequent sections, further PCA treatments will include only thia-arene data in the analyses.

6.5 PCA Analysis Including Source Samples

The principal component analyses completed in Sections 6.3 and 6.4 have used only ambient air data and have led to some clear conclusions about which chemical substances are useful in source discrimination. No source samples were used in the first analysis so as not to bias the outcome of the analysis. In this section, source samples were added into the data set to examine their relationship with ambient samples. The PCA method was repeated using the six thia-arene variables included in the original variable list. Only five of the six variables were shown to be useful source indicators. The sixth variable, removed from PCA in Section 6.4, was included in this section for re-examination. It was unclear why this variable was not included in the first components with the other thia-arene variables.

The source samples in this PCA analysis include:

1. Coal Tar Standard Reference Material (SRM 1597)
2. Hamilton coke oven condensate
3. Urban Dust Standard Reference Material (SRM 1649)
4. Diesel Exhaust Particulate Standard Reference Material (SRM 1650)
5. a composite Toronto air particulate extract ("Torair", Toronto Composite B)

Two components were extracted accounting for 67% and 19% of the total variance in the data set. The first component is the dominant component of the two,

accounting for almost four times more of the variance than Component 2. Together the two components account for 88% of the variance in the data set. The rotated component matrix contained large factor loadings in the first component for peaks B21T, B23T, 258A, 258B and 258C (Tables 6.3). Only B12T has a significant loading in the second component. The variable loadings are plotted in Figure 6.5. This figure is similar to the plot of thia-arene variables in Figure 6.3, but B12T was included and the PAH were excluded in the current analysis.

The Component 1 scores are plotted against the Component 2 scores for all ambient and source samples in Figure 6.6. The upwind (UW) and downwind (DW) samples are clearly separated on the Component 1 axis, but not well separated on the Component 2 axis. Component 2 is not useful in distinguishing between the upwind and downwind samples, thus, variables with high loadings only in this component (B12T) will not be useful for the differentiation of coke oven emissions and diesel exhaust emissions.

It is interesting to note the position of the source samples relative to the ambient samples in Figure 6.6. The coke oven condensate (COKEOV) and Coal Tar SRM1597 (COALTAR) source samples are located in a cluster with the air samples collected downwind of the coke ovens in Hamilton (DW). In contrast, Hamilton air particulate samples collected upwind of the coke ovens (UW) are not plotted in the same location as the Urban Dust SRM 1649 (URBAN), Diesel Particulate SRM 1650 (DIESEL) or Toronto air particulate (TORAIR) source samples. The vehicular emission source samples have higher scores on Component 2 than the Hamilton air samples indicating a

Table 6.3. List of factor loading values for Varimax rotated components extracted from Hamilton air particulate and source sample data using thia-arene variables.

	Component	
	1	2
B12T	-4.1E-02	.985
B21T	-.900	-.191
B23T	.906	-1.0E-02
M258A	.897	-.127
M258B	-.957	.114
M258C	.938	-.102

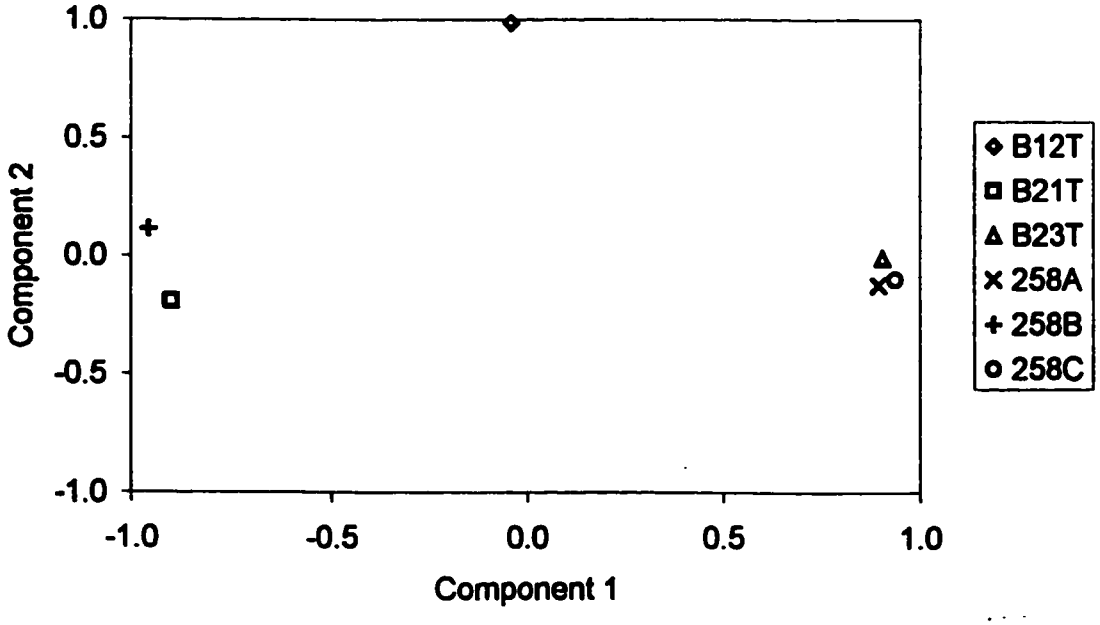

Figure 6.5. Loadings of variables on Components 1 and 2. All 89 Hamilton air particulate samples and five source samples were included in this analysis.

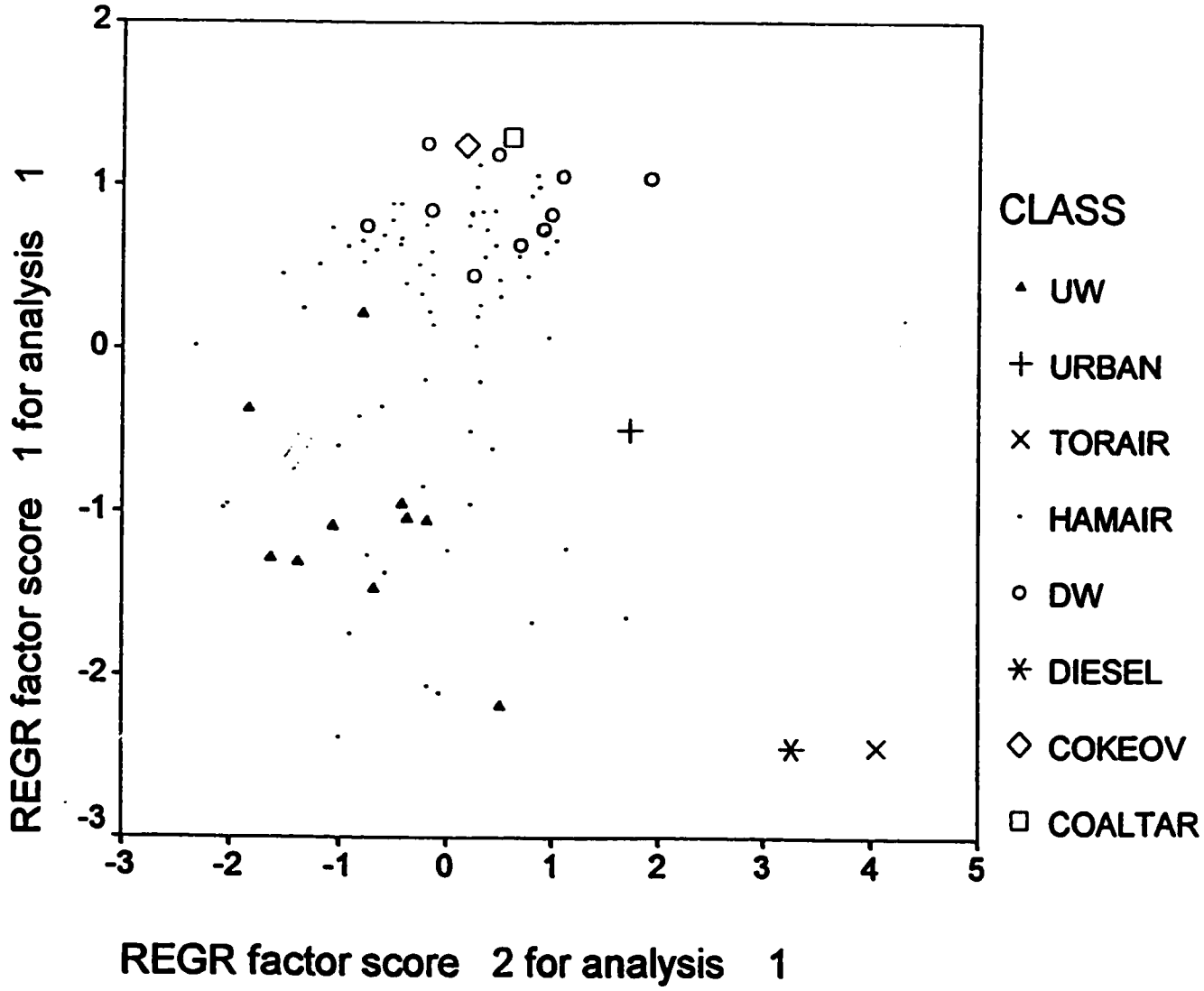

Figure 6.6. Sample scores for ambient and source samples for the two extracted components using thia-arene variables only.

higher relative amount of B12T (Compound 81, Appendix I) in the source samples.

The diesel particulate and Toronto air particulate source samples contain emissions that potentially were exposed to the atmosphere for a shorter length of time than the Hamilton air particulate samples. The Toronto air particulate sampler was located alongside a highway. The majority of vehicular emissions that reached the sampler may have resided in the atmosphere only for moments after their release. In Hamilton, samplers were generally located further from major highways and were more likely to sample a larger proportion of aged vehicular emissions.

It is possible that B12T undergoes transformation in the atmosphere at a faster rate than the other 234 amu thia-arene isomers, altering the thia-arene profile. These results show that B12T is not a useful source apportionment tracer in air particulate. However, if this compound is reactive, it may also degrade readily in other matrices such as crude oil. Previous studies have used profiles of alkylated dibenzothiophenes as maturity indicators for crude oils [121, 122]. Further studies could be conducted to investigate the use of B12T as an alternative indicator for maturity in crude oils.

Another important feature of Figure 6.6 (also observed in Figures 6.2 and 6.4) is the continuity of the data between those samples designated as "upwind" (UW) and those designated as "downwind" (DW). It should be noted that the upwind designation was applied to specific samples based on the estimation that these samples had little or no probability of coke oven impact during the 22-hour sampling period. Even a short period of low wind speeds could result in unexpected coke oven impacts at a given sampling site. Thus, it is not surprising that upwind samples show a range of Component 1 values

from values close to the diesel SRM 1650 and Toronto air samples to values close to the downwind samples.

If this analysis is correct, there are a number of other samples which should be classified as "upwind" based on their Component 1 values alone, i.e., Component 1 values less than –0.5 and certainly less than –1.0. Similarly, there are a large number of samples which have clear "downwind" characteristics, i.e., Component 1 values greater than zero. As Component 1 values approach the highest values (~1.3), the sample profiles are indistinguishable from the coal source samples indicating that coke oven impacts dominate the thia-arene profile.

6.6 Comparison of Various Environmental Samples to Hamilton Air Particulate and Source Samples

PCA using thia-arene variables was applied to a variety of environmental samples from different locations to examine possible source contributions and the applicability of thia-arene source tracers to other matrices and locations. A new data set of samples was assembled, consisting of:

- 3 roadway runoff samples collected under a bridge in Hamilton during rain events
- 5 suspended sediment samples collected from Hamilton creeks during rain events
- 89 Hamilton air particulate samples
- 6 air particulate samples collected next to Highway 404 in Toronto
- 85 Hamilton air particulate samples
- 17 air particulate samples from three sites in the high Arctic Region
- 5 "source" samples

PCA was applied to the data set containing the same six thia-arene variables used in Section 6.5: B21T, B12T, B23T, 258A, 258B and 258C. Two factors were extracted, accounting for 43% and 37% of the variance in the data set after rotation. In this

analysis, high loadings for the thia-arene variables were split between two components (Table 6.4). The variability in the 234 amu thia-arene data is contained primarily within component 2, while the variability in the 258 amu thia-arene data is contained primarily within component 1. In previous analyses, a single component had contained high loadings for 5 of the 6 thia-arene variables.

The variable loadings are plotted in Figure 6.7. Two 234 amu thia-arene variables (B21T and B23T) lie on opposite ends of the Component 2 axis, while the 258 amu variables (258A, 258B and 258C) lie on opposite ends of the Component 2 axis. Again, B12T does not appear to be useful for source differentiation, as indicated by the position of B12T near the origin in Figure 6.7. This analysis has separated the 234 amu variables (Component 2) from the 258 amu variables (Component 1).

The object score plot shows the distribution of the different classes of environmental samples on Components 1 and 2 (Figure 6.8). The coke oven condensate (COKEOV) and coal tar (COALTAR) source samples are clustered at the top of the figure with the Hamilton air particulate collected downwind of the coke ovens (DW). The diesel particulate (DIESEL) and Toronto air composite (TORAIR) samples are located towards the lower left and lower right sides of the figure, respectively. The upwind Hamilton air samples (UW) fall roughly between the coal-based and petroleum-based reference samples.

The roadway runoff samples were collected from the Burlington Skyway Bridge, a large bridge about 3 kilometers northeast of the Hamilton steel mills. These samples may contain vehicle exhaust, road tar, tire crumb, crankcase oil and possibly coal dust

Table 6.4. List of factor loadings for Varimax rotated components extracted from various environmental sample and source sample data using thia-arene variables.

	Component	
	1	2
B12T	-.288	-5.7E-02
B21T	-.223	-.971
B23T	.278	.953
258A	.910	.202
258B	-.952	-.283
258C	.881	.314

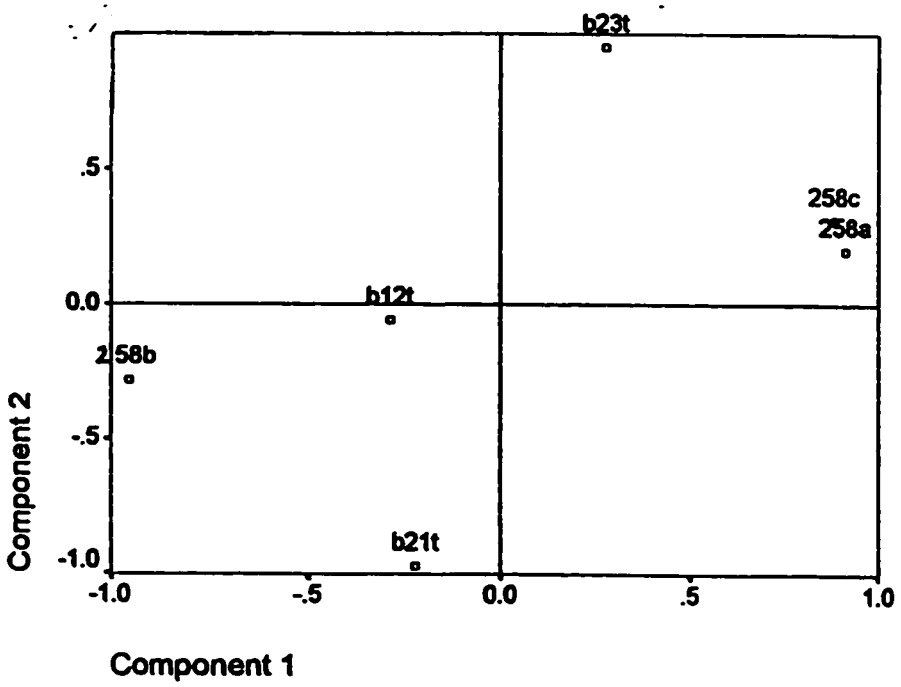

Figure 6.7. Loadings of thia-arene variables on components 1 and 2. A variety of environmental and source samples were included in this analysis.

and coke oven emissions. On the object plot (Figure 6.8), the three roadway runoff samples (ROADRUN) are grouped close together near the urban dust reference standard (URBAN) and close to the upper end of the upwind Hamilton air particulate samples (UW). Coke oven emissions do not appear to be a major contributor to these roadway runoff samples, even though they were collected not far from the steel mills. Roadway runoff may also contain thia-arenes from other sources that have not been examined, such as oils.

The 24-hour collection Toronto air particulate samples (H404) are expected to contain mainly traffic emissions because they were collected beside Highway 404, a busy highway with relatively little diesel truck traffic. These samples were collected in a different location and time from the composite Toronto air sample. The 24-hour Toronto air samples are clustered separately from the Hamilton air particulate collected upwind of the coke ovens, and are located toward the bottom right in Figure 6.8, near the composite Toronto air sample. These results show that the Toronto air particulate samples have a somewhat different thia-arene profile from the upwind Hamilton air particulate samples that are also expected to contain mainly traffic emissions.

It was previously reported that gasoline emissions do not contain detectable levels of thia-arenes [34,42]. As a result, thia-arenes in traffic emissions were expected to originate from diesel engines only. However, atypically high sulfur content of gasoline sold in Southern Ontario (about 350 ppm sulfur) which has recently been publicized may result in measurable emissions of thia-arenes from gasoline-powered vehicles in Ontario. It is also possible that these emissions may have thia-arene profiles that are different from

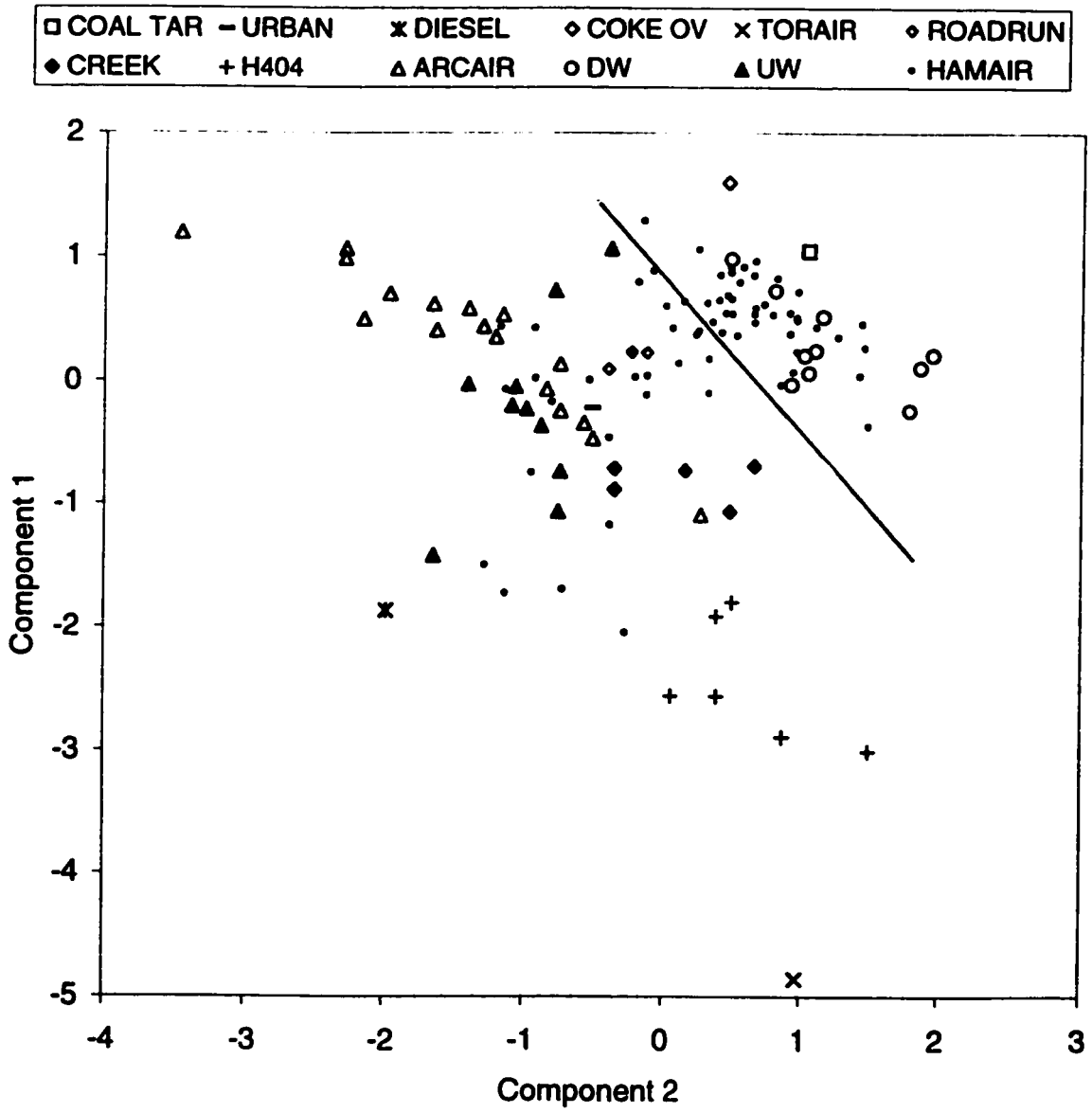

Figure 6.8. Sample scores for various environmental and source samples plotted on Components 1 and 2. All thia-arene variables were included in this analysis.

the profiles in diesel exhaust. In this case, the thia-arene profile would be dependent on the relative content of diesel emissions. Further studies need to be conducted to re-evaluate the content of thia-arenes in gasoline emissions.

The sediments collected from the three major creeks that drain into Hamilton Harbour (Grindstone, Indian and Red Hill Creeks) have low PAH levels (3-8 μg/g) relative to Hamilton Harbour sediments (20-40 μg/g). The main source of PAH contamination in the creek sediments is thought to be roadway runoff from surrounding areas via the watersheds and combined sewer overflow discharges. In addition, drainage from landfill sites may contain used engine oil. The creek sediment samples (CREEK) had similar object scores and were located toward the bottom half of Figure 6.8 between the upwind Hamilton air samples (UW), the roadway runoff samples (ROADRUN) and the Toronto air particulate samples (H404, TORAIR). The creek samples have a thia-arene signature resembling that of diesel emissions indicating an absence of coke oven impacts.

The seventeen air particulate samples collected at three different locations in the high Arctic (Tagish, Yukon; Alert, Ellesmere Island; and Dunai, Russia) are clustered toward the upper left corner of Figure 6.8 (ARCAIR). No differentiation between the three sites was observed in this analysis so all Arctic air samples were assigned identical markers. The Arctic air samples lie close to the upwind Hamilton air particulate samples, Urban Dust Standard Reference Material and the roadway runoff samples. The Arctic air samples are clustered near the top left corner of the plot, whereas the Toronto air samples are clustered near the bottom right of the plot.

The air mass that is transported to the Arctic Region in the winter months originates primarily from the Eurasian land mass (Alert and Dunai) or the Pacific (Tagish). Major industries within the Russian Arctic that may impact the sampling sites include coal and metal ore mining, fossil fuel extraction and metal smelting industries [181]. These samples were analyzed to determine if coal combustion emissions were impacting any of these sites. Figure 6.8 indicates that the thia-arenes in these Arctic samples are not derived from coal combustion emissions because they are well separated from the coal-based samples.

Of all the samples examined, the Arctic samples may be the most problematic for this type of analysis because atmospheric chemical transformations may consume certain thia-arenes preferentially. These air samples have spent several weeks in the air before reaching the Arctic sampling sites. If there is some difference in the rates of reaction of thia-arenes with reactive atmospheric species, then the ratios of thia-arenes may be altered and the usefulness of the approach may be compromised.

A diagonal line was placed on the plot in Figure 6.8 to show the separation between the coal/coke-based emission samples and the samples representing vehicular emissions. Components 1 (258 amu isomers) and 2 (234 amu isomers) both contribute to source differentiation in this analysis. It is not clear what causes the spread among the samples containing vehicular emissions (samples that fall below the diagonal line). The Arctic air samples are well separated from the Toronto air samples. Particulate emissions sampled in the Arctic Region have had a longer residence time in the atmosphere than the particulate emissions from vehicles that were sampled close to the source in Toronto

(beside a major highway). The different thia-arene profiles in these two groups of samples may be the result of atmospheric transformation. Alternatively, there may be variability in the thia-arene profile among different sources of the same type. It would be of interest to examine a greater number of petroleum-based emission source samples to investigate the variability of the thia-arene profile in this source type.

The examination of a variety of different environmental samples from different matrices indicates that thia-arenes are useful for the classification of different pollution sources and different sample types. However, a greater number of thia-arene source profiles may exist than was originally thought. Thia-arene profiles appear to be unique in various sample types and locations, but modifications to the model may be required for areas outside of Hamilton or for weathered samples.

6.8 Summary

PCA has extracted five thia-arene variables that provide useful information for differentiation of coke oven emissions and diesel engine emissions. The first analysis indicated that thia-arenes provide greater source discrimination than most of the PAH isomers, with the exception of BAP. PCA was not designed as a quantitative tool for source apportionment, but rather as a qualitative method of analysis. It also involves complex calculations requiring a large data set. It would be useful to develop simple source apportionment criteria that could be applied to a single ambient sample. In Chapter 7, a source apportionment model will be developed based on the five thia-arene variables, B21T, B23T, 258A, 258B and 258C, identified by PCA as source tracers.

Thia-arene profiles in a variety of environmental samples were examined by PCA in Section 6.6. The impact of pollutant emissions from vehicles is much more widespread than that of coke oven emissions. The coal/coke-based thia-arene profile was dominant only in Hamilton air particulate collected directly downwind of the coke ovens. The vehicular emission thia-arene profile was dominant in all other environmental samples analyzed.

7.0 THIA-ARENE SOURCE APPORTIONMENT MODELLING

7.1 Overview

In Chapter 6, five thia-arene chromatographic peaks (variables B21T, B23T, 258A, 258B, and 258C) were used in PCA to distinguish between air particulate impacted by coke oven emissions and air particulate impacted by diesel engine emissions. A large number of samples are required for PCA analysis, and interpretation of the extracted components can be complicated. A simple approach for the determination of source contributions in a single ambient sample would be useful. In this chapter, a 234 amu thia-arene ratio and a 258 amu thia-arene ratio are determined using the five thia-arene peaks identified by PCA to contain source information. A single thia-arene index is then developed from the combination of the two thia-arene ratios.

7.2 Thia-Arene Ratios in Source Samples (234 and 258 amu)

Chromatographic profiles of the 234 amu and 258 amu thia-arenes in source samples are shown in Figures 7.1 and 7.2, respectively. The thia-arene chromatographic peaks identified by PCA as useful source indicators are labeled on the chromatograms. For peaks consisting of more than one isomer co-eluting, the entire area under the peak is quantified. Authentic standards were available for the identification of all 234 amu isomers and some of the 258 amu isomers.

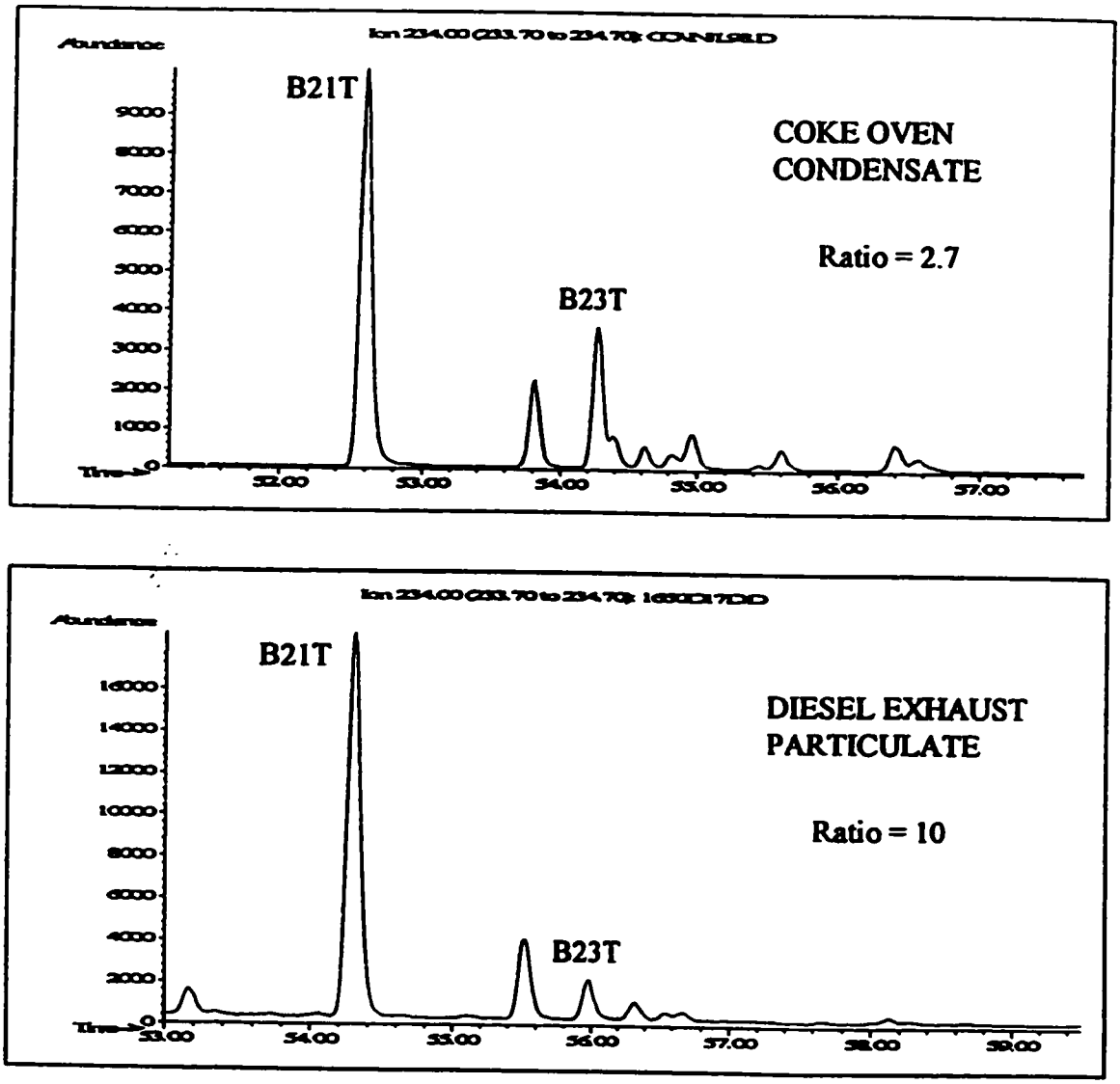

Figure 7.1. Mass chromatograms of the m/z 234 ion for the analysis of coke oven condensate and diesel exhaust particulate. Analyses performed using GC/MS Conditions B. Peaks B21T and B23T are used for source apportionment.

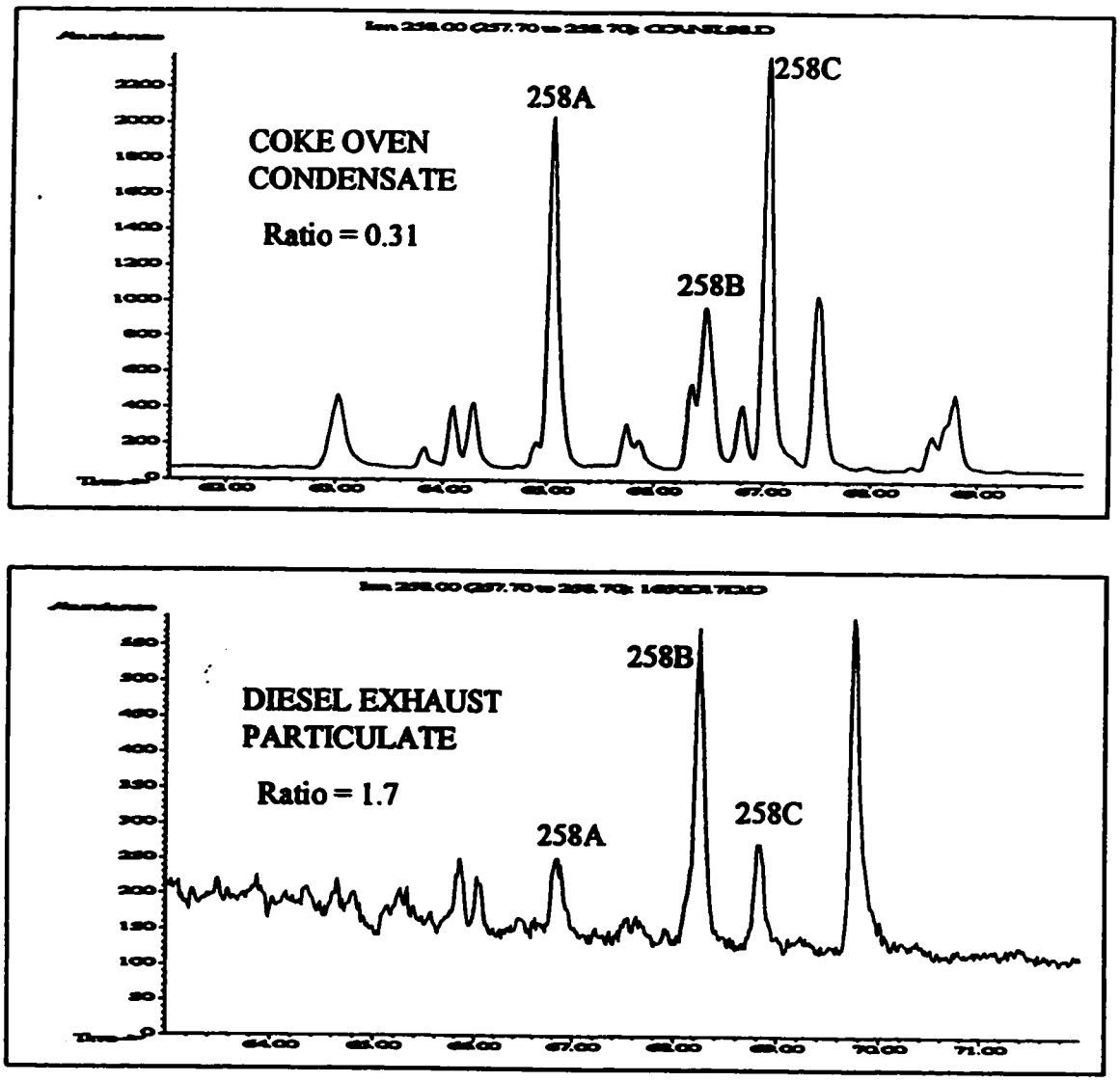

Figure 7.2. Mass chromatograms of the m/z 258 ion for the analysis of coke oven condensate and diesel exhaust particulate. Analyses performed using GC/MS Conditions B. Peaks 258A, 258B and 258C are used for source apportionment.

Differences in the thia-arene profiles were quantified by calculating two ratios: a 234 amu isomer ratio (R234) and a 258 amu isomer ratio (R258). In Chapter 6, variable loadings determined by PCA were used to identify thia-arene source tracers. In Figure 6.7, the variable loadings were plotted on component axes. This plot was used to develop the two ratios. Two of the 234 amu variables were located on opposite ends of the Component 2 axis, while the 258 amu variables were located on opposite ends of the Component 1 axis. Two ratios were developed by placing the areas (A) of the variable(s) with negative loadings in the numerator and areas of variable(s) with positive loadings in the denominator. Equations for the two thia-arene ratios are shown below:

$$R234 = \frac{A_{B21T}}{A_{B23T}}$$

$$R258 = \frac{A_{258B}}{A_{258A} + A_{258C}}$$

Variable B12T wasnot identified as a source tracer in Chapter 6 and was not included in the thia-arene ratios.

Thia-arene ratios were determined in the source samples. The 234 amu thia-arene ratios were determined to be 10 for diesel exhaust particulate and 2.7 for coke oven condensate. The 258 amu thia-arene ratios were determined to be 1.7 for diesel exhaust particulate and 0.31 for coke oven condensate. Thia-arene ratios in five reference and source samples are listed in Table 7.1. The 234 amu and 258 amu thia-arene ratios in Coal Tar (SRM 1597) are similar to the thia-arene ratios in coke oven condensate. The

Table 7.1. Thia-arene ratios determined for five source samples.

Sample	234 amu ratio	Designation (234 ratio)[1]	258 amu ratio	Designation (258 ratio)[1]	Thia-arene Index
Coal Tar (SRM 1597)	2.4	C	0.35	C	0.65
Urban Dust (SRM 1649)	4.2	D	0.68	D	1.2
Diesel Exhaust (SRM 1650)	10	D	1.4	D	2.7
Coke Oven Condensate	2.7	C	0.31	C	0.66
Toronto Air	3.4	D	3.4	D	3.2

1"D"="Diesel", 234 ratio > 3.1, or 258 ratio > 0.63; "C"="Coke oven", 234 ratio<=3.1, or 258 ratio <=0.63

234 amu and 258 amu thia-arene ratios in Urban Dust (SRM 1649) and the composite Toronto air sample are greater than the thia-arene ratios in coke oven condensate and coal tar, but are not as large as the values for Diesel Exhaust Particulate (SRM 1650). The "designation" and "thia-arene index" columns in Table 7.1 will be discussed later in Section 7.7. The new thia-arene ratios were used to examine respirable air particulate extracts from the 89 samples collected in Hamilton in the summer of 1995. PAH and particulate concentrations for these samples were discussed in Chapter 5..

7.3 Thia-arene Ratios in Ambient Samples

The 234 amu and 258 amu ratios were determined for 89 of the 92 Hamilton air particulate extracts analyzed. The 258 amu thia-arene isomers were below the detection limit for three samples at Station 29000 (July 29, August 4 and August 10) so these samples were excluded from the analysis. The thia-arene ratios for the air particulate samples are listed in order of increasing total concentration of PAH in Table 7.2. The "designation" and "thia-arene index" columns also listed in this table will be discussed in Section 7.7.

Data obtained for four individual sampling periods are examined first to show the dependence on wind direction. The data are illustrated by plotting the total PAH concentrations and thia-arene ratios for each day on a separate map (Maps 7.1 to 7.4). The directional frequencies of the wind are also plotted at each sampling station and are estimated by interpolating wind data from the Hamilton met tower (Station 29026), the RBG Station, Station 29563, Station 44015 and the NWRI-CCIW station. Maps 7.1 to

Table 7.2. Thia-arene ratios and total concentrations of PAH for 89 Hamilton air particulate samples listed in order of increasing PAH concentration.

Date	Station	Total PAH (ng/m3)	Class	234 amu ratio	Designation (234 ratio)[1]	258 amu ratio	Designation (258 ratio)[1]	Thia-arene Index
6-Aug	29547	0.17		5.0	D	1.5	D	1.9
5-Aug	29531	0.28		4.3	D	1.1	D	1.5
7-Aug	29547	0.44	UW	6.4	D	1.3	D	2.0
23-Jul	29113	0.52		3.8	D	1.1	D	1.4
23-Jul	*29531*	*0.54*		*3.3*	*D*	*0.73*	*D*	*1.1*
11-Aug	29000	0.63	UW	3.8	D	1.1	D	1.4
20-Jul	29000	0.65	UW	4.0	D	1.2	D	1.5
11-Aug	29113	0.65	UW	4.1	D	0.89	D	1.3
9-Aug	29547	0.65		4.7	D	0.77	D	1.3
20-Jul	29113	0.67	UW	4.2	D	0.88	D	1.3
12-Aug	29531	0.69		3.8	D	1.10	D	1.5
5-Aug	29000	0.72		3.8	D	0.86	D	1.3
13-Aug	29547	0.72		4.9	D	1.2	D	1.7
11-Aug	29531	0.80	UW	4.5	D	0.85	D	1.4
5-Aug	*29113*	*0.90*		*3.2*	*D*	*0.76*	*D*	*1.1*
12-Aug	29000	0.91		3.2	D	1.0	D	1.3
15-Aug	29000	0.92		5.0	D	1.5	D	1.9
29-Jul	29113	1.00		3.5	D	2.4	D	2.4
19-Aug	29547	1.0		3.7	D	1.14	D	1.5
18-Aug	29547	1.0	UW	4.4	D	0.79	D	1.3
17-Aug	29547	1.1	UW	4.6	D	0.89	D	1.4
29-Jul	29531	1.4		3.9	D	1.4	D	1.7
8-Aug	29547	1.6		4.1	D	0.79	D	1.3
2-Aug	***29547***	***1.6***	***UW***	***3.6***	***D***	***0.64***	***C***	***1.1***
1-Aug	*29000*	*1.6*		*2.9*	*C*	*0.59*	*C*	*0.92*
1-Aug	29113	1.80		5.1	D	1.1	D	1.7
27-Jul	29547	2.0		4.0	D	0.68	D	1.2
20-Jul	***29531***	***2.1***	***UW***	***3.3***	***D***	***0.49***	***C***	***0.90***
15-Aug	*29113*	*2.6*		*3.3*	*D*	*0.67*	*D*	*1.0*
28-Jul	29000	2.6		2.6	C	0.51	C	0.81
10-Aug	*29113*	*3.3*		*3.8*	*D*	*0.71*	*D*	*1.1*
23-Jul	29000	3.3		2.5	C	0.52	C	0.80
5-Aug	*29547*	*3.6*		*3.1*	*C*	*0.62*	*C*	*1.0*
16-Aug	*29547*	*3.6*		*3.3*	*D*	*0.65*	*D*	*1.0*
10-Aug	29547	4.2		3.0	C	0.52	C	0.87
12-Aug	29547	4.8		2.7	C	0.44	C	0.76
9-Aug	29113	4.9		2.3	C	0.58	C	0.81
6-Aug	29113	5.2		2.7	C	0.55	C	0.85
20-Aug	29000	5.4		3.0	C	0.46	C	0.82
4-Aug	*29113*	*6.5*		*2.9*	*C*	*0.58*	*C*	*0.91*
7-Aug	29113	7.3		2.7	C	0.50	C	0.82
20-Aug	29531	7.6		2.6	C	0.47	C	0.77
15-Aug	29531	7.6		4.7	D	0.63	C	1.2
16-Aug	*29113*	*8.2*		*3.0*	*C*	*0.55*	*C*	*0.90*
6-Aug	29000	9.0		2.5	C	0.47	C	0.75

Table 7.2. (cont'd)

Date	Station	Total PAH (ng/m3)	Class	234 amu ratio	Designation (234 ratio)[1]	258 amu ratio	Designation (258 ratio)[1]	Thia-arene Index
8-Aug	*29113*	*9.7*		*3.1*	*C*	*0.53*	*C*	*0.90*
1-Aug	*29531*	*10*		*3.1*	*C*	*0.62*	*C*	*1.0*
13-Aug	29113	11		2.8	C	0.49	C	0.82
8-Aug	29000	11		2.4	C	0.47	C	0.75
10-Aug	*29531*	*11*		*3.1*	*C*	*0.56*	*C*	*0.92*
13-Aug	29000	12		2.4	C	0.48	C	0.75
9-Aug	29000	13		2.5	C	0.50	C	0.78
12-Aug	29113	13		2.4	C	0.45	C	0.73
4-Aug	29547	13		2.9	C	0.52	C	0.85
20-Aug	29113	13		2.7	C	0.46	C	0.78
15-Aug	29547	14		2.7	C	0.46	C	0.78
28-Jul	29531	14		2.2	C	0.47	C	0.72
27-Jul	29000	15		2.6	C	0.47	C	0.77
7-Aug	29000	15		2.5	C	0.50	C	0.78
4-Aug	29531	16		2.9	C	0.53	C	0.86
20-Aug	29547	16		2.9	C	0.47	C	0.81
28-Jul	29547	16		2.5	C	0.54	C	0.81
19-Aug	29000	17		2.5	C	0.51	C	0.79
18-Aug	29113	17	DW	3.0	C	0.52	C	0.87
2-Aug	29000	17	DW	1.9	C	0.48	C	0.67
14-Aug	29547	19		2.7	C	0.48	C	0.80
1-Aug	29547	24		2.8	C	0.50	C	0.84
13-Aug	29531	25		2.6	C	0.54	C	0.82
9-Aug	29531	28		2.6	C	0.59	C	0.86
20-Jul	29547	29	DW	2.6	C	0.45	C	0.75
17-Aug	29113	34	DW	2.4	C	0.43	C	0.71
19-Aug	29113	34		2.6	C	0.44	C	0.75
27-Jul	29531	36		2.5	C	0.43	C	0.73
11-Aug	29547	36	DW	2.5	C	0.46	C	0.74
17-Aug	29000	39	DW	2.5	C	0.60	C	0.86
14-Aug	29113	40		2.7	C	0.49	C	0.80
6-Aug	29531	42		2.3	C	0.46	C	0.72
16-Aug	29000	44		2.4	C	0.43	C	0.72
23-Jul	29547	45		2.5	C	0.47	C	0.75
18-Aug	29000	45	DW	2.4	C	0.49	C	0.77
29-Jul	29547	46		2.2	C	0.46	C	0.70
17-Aug	29531	53	DW	2.5	C	0.54	C	0.81
16-Aug	29531	59		2.4	C	0.46	C	0.74
18-Aug	29531	61	DW	2.5	C	0.50	C	0.78
14-Aug	29531	66		2.6	C	0.48	C	0.78
19-Aug	29531	81		2.2	C	0.53	C	0.76
8-Aug	29531	89		3.0	C	0.52	C	0.88
2-Aug	29531	101	DW	2.0	C	0.49	C	0.69
7-Aug	29531	150	DW	2.2	C	0.51	C	0.74

1"D"=234 ratio > 3.1, or 258 ratio > 0.63; "C"=234 ratio<=3.1, or 258 ratio <=0.63

7.4 and the interpolated wind plots were created by N. Finkelstein using ArcView software.

On July 20, 1995, southwest winds were recorded so it is estimated that only Station 29547 would be significantly impacted by coke oven emissions (Map 7.1). This is supported by higher particulate (PM10) and PAH concentrations and lower thia-arene ratios (R234 and R258) at Station 29547 than at the other three stations. The data profiles for Stations 29000 and 29113 are almost identical and show no impact from coke oven emissions. At Station 29531, however, PAH concentration is slightly higher than at Stations 29000 and 29113 and thia-arene ratios are somewhat lower than at Stations 29000 and 29113, indicating that some coke oven emissions impacted this site. Although the wind direction indicates that coke oven emissions would be carried away from Station 29531, this sampling site is close enough to the coke ovens that it is not surprising to observe some impact of coke oven emissions. The wind direction estimated for this site is interpolated from data recorded at other locations and thus is expected to contain some error.

Steady westerly winds were recorded on July 23, predicting again that only Station 29547 would be impacted by coke oven emissions (Map 7.2). Particulate and PAH concentrations were much higher and thia-arene ratios were much lower at Station 29547 than at Stations 29113 and 29531 indicating a major impact of coke oven emissions at Station 29547, but not at Stations 29113 or 29531. At Station 29000, the particulate concentration was similar to particulate concentrations determined at Stations 29113 and 29531. The PAH concentration was approximately 6-fold higher at Station

Map 7.1. Air particulate data at four sampling stations for July 20, 1995

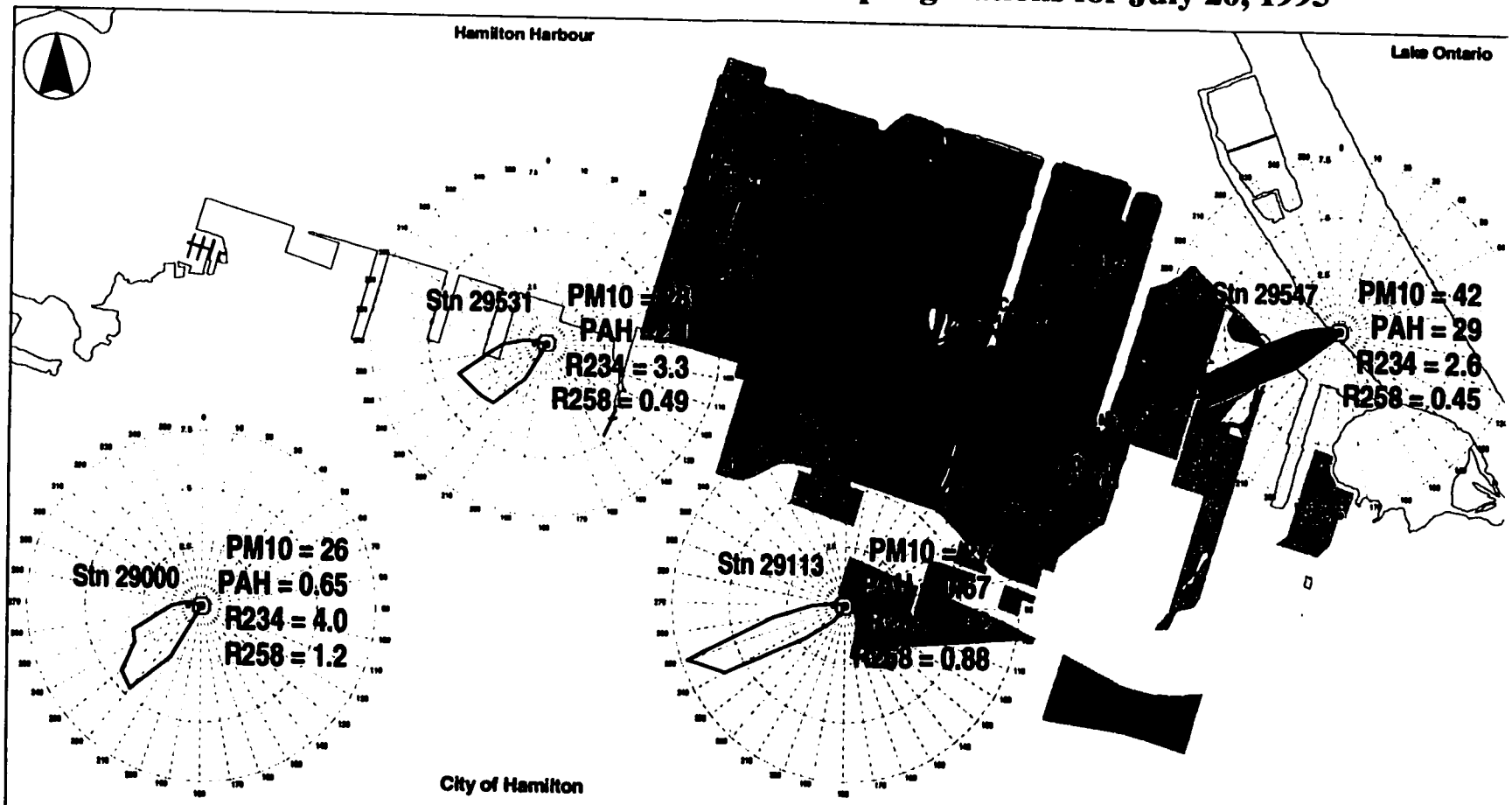

PM10 = respirable air particulate (<10 µm) in µg/m³

PAH = total concentration of PAH in ng/m³

R234 = 234 amu thia-arene ratio

R258 = 258 amu thia-arene ratio

Stn = sampling location (MOE station number); predicte (interpolated) wind frequency distributions (in hours) are also shown at sampling locations as wind roses.

Map 7.2. Air particulate data at four sampling stations for July 23, 1995

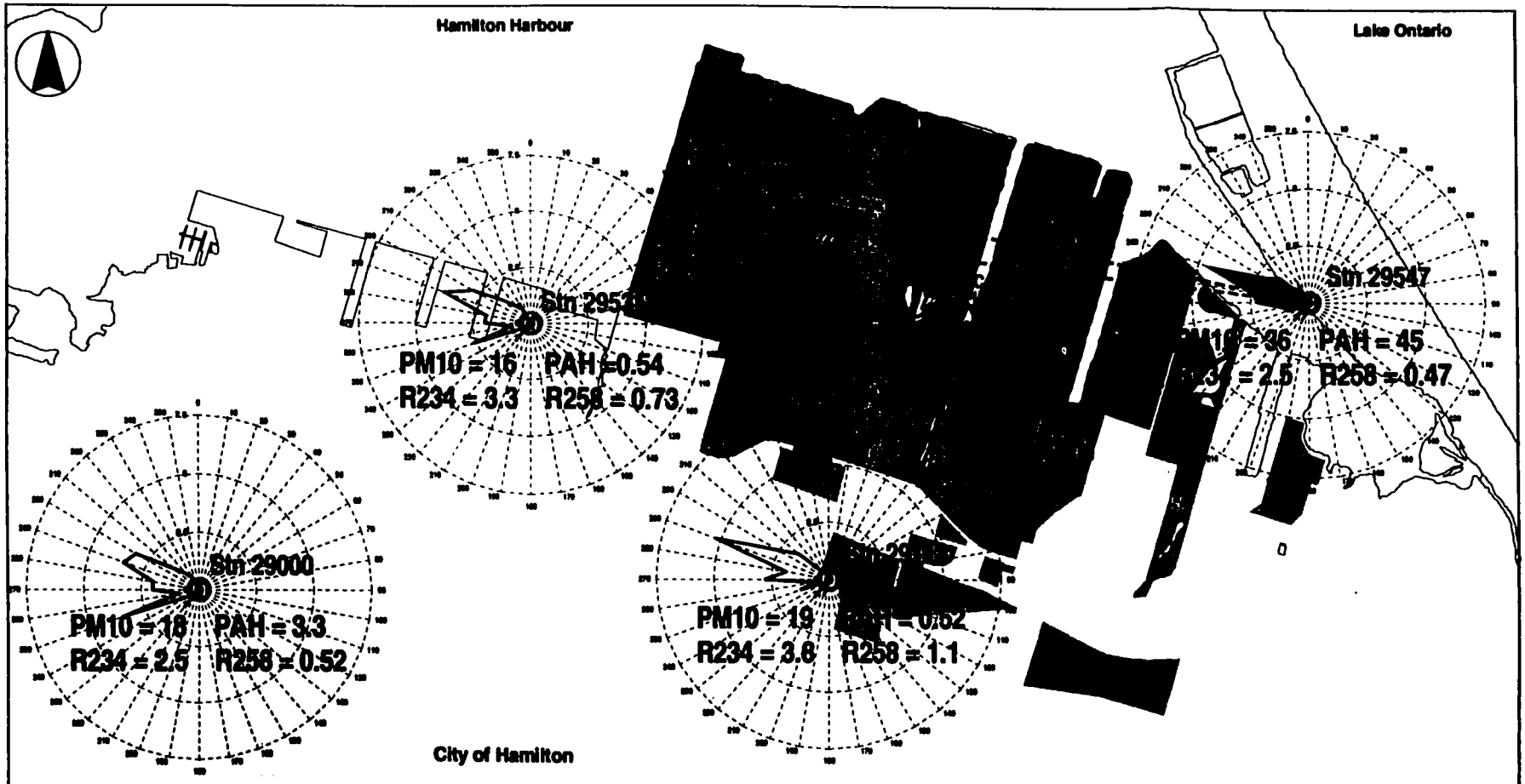

PM10 = respirable air particulate (<10 µm) in µg/m³

PAH = total concentration of PAH in ng/m³

R234 = 234 amu thia-arene ratio

R258 = 258 amu thia-arene ratio

Stn = sampling location (MOE station number); predicted (interpolated) wind frequency distributions (in hours) are also shown at sampling locations as wind roses.

29000 than at Stations 29113 and 29531 (upwind of the coke ovens), but approximately 14-fold lower than the PAH concentration at Station 29547 (downwind of the coke ovens). The R234 ratio at Station 29000 is identical to that at Station 29547, while the R258 ratio at Station 29000 is slightly greater than that at Station 29547. Thia-arene ratios indicate that an impact from coke ovens occurred at Station 29000 during the sampling period on July 23, 1995, although particulate and PAH concentrations indicate that the impact was minor. Particulate concentrations at the three upwind sites on July 23 were lower than the particulate concentrations at upwind sites on July 20, 1995. This may be due to lower estimated motor vehicle emissions on weekend days (e.g., Sunday, July 23) compared to weekdays (e.g., Thursday, July 20). The average PM10 particulate concentration at all stations from Monday to Friday was 49 $\mu g/m^3$. The average PM_{10} particulate concentrations determined for the filters collected on Saturday and Sunday were 33 $\mu g/m^3$ and 27 $\mu g/m^3$, respectively.

On August 2, 1995, northeasterly winds were recorded, and coke oven emissions were expected to impact Stations 29000, 29531 and to a lesser degree 29113. Chemical data were not available for Station 29113 for this sampling period. PAH concentrations are higher and thia-arene ratios are lower downwind of the coke ovens (Stations 29000 and 29531) than upwind of the coke ovens (Station 29547) (Map 7.3). Thia-arene ratios at Stations 29000 and 29531 are almost identical. Particulate and PAH concentrations are lower at Station 29000 than at Station 29531, likely due to dispersion of the coke oven emissions with increased distance from the coke ovens.

at four sampling stations for August 2, 1995

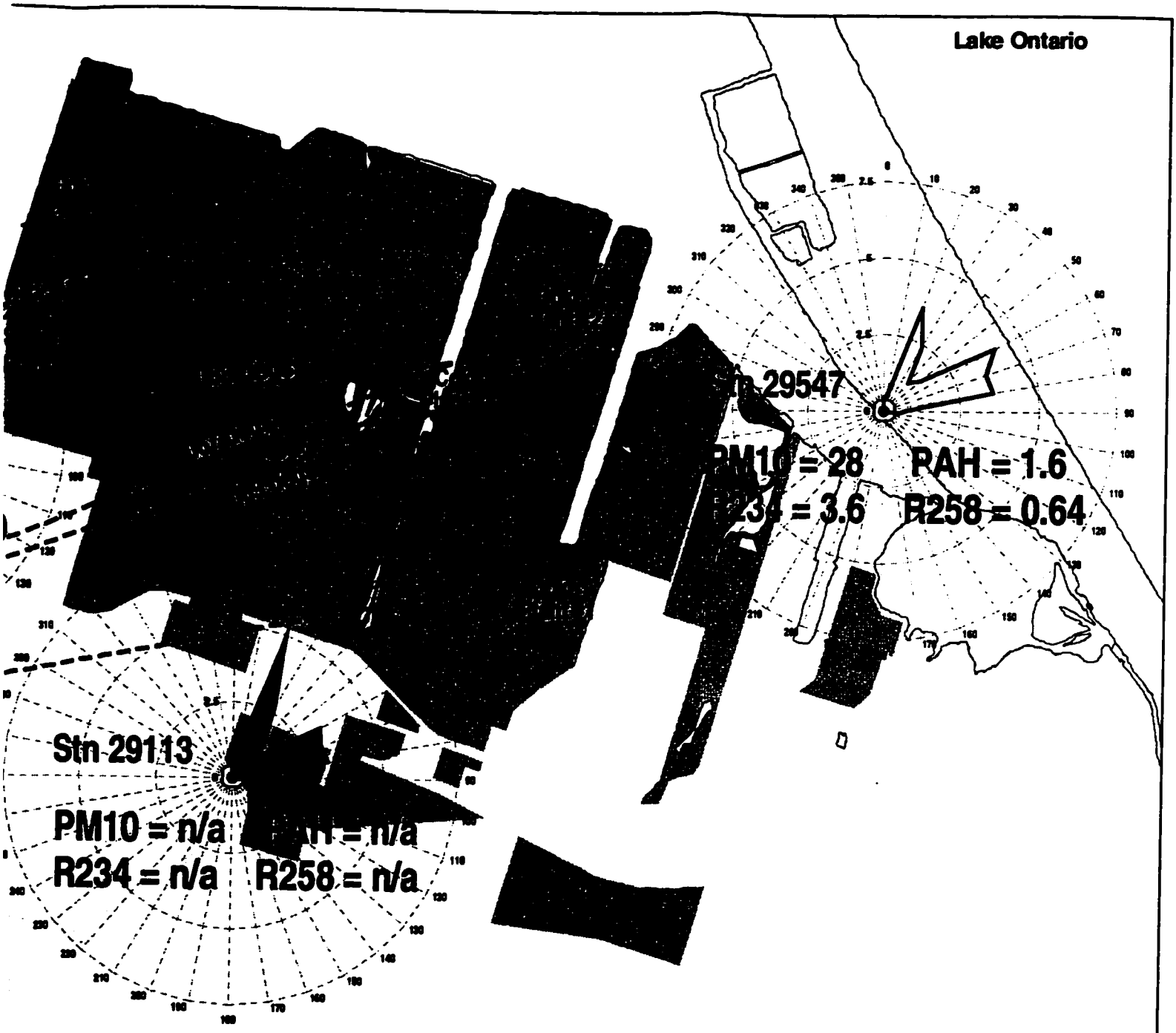

amu thia-arene ratio amu thia-arene ratio	Stn = sampling location (MOE station number); predicted (interpolated) wind frequency distributions (in hours) are also shown at sampling locations as wind roses.

On August 16th it was predicted by the wind direction that Stations 29000, 29531 and 29113 would be impacted by coke oven emissions. High PAH concentrations and low thia-arene ratios at Stations 29000 and 29531 indicate a significant coke oven emission impact (Map 7.4). PAH concentration and thia-arene ratios at Station 29113 are intermediate between the PAH concentrations and thia-arene ratios at Stations 29547 (upwind) and Stations 29000 and 29531 (downwind) indicating a minor coke oven impact at Station 29113. For this sampling period, particulate concentrations were actually lower downwind of the coke ovens (Stations 29531 and 29000) than upwind of the coke ovens (Station 29547). As discussed in the previous section, particulate concentrations alone are not good source markers for coke oven emissions because too many other significant sources of particulate exist in the industrial area. Thia-arene ratios, on the other hand, agree well with expected source contributions based on wind direction.

In Table 7.2, samples identified as upwind (UW) and downwind (DW) samples (classification based on wind data as discussed in Chapter 5) are indicated to show their relative position in the data set. The selected upwind samples have low total PAH concentrations (0.44 - 2.1 ng/m^3) and are found at the top of the list while the downwind samples have high total PAH concentrations (17 – 150 ng/m^3) and are listed near the bottom of Table 7.2. Thia-arene ratios decrease as total PAH concentrations increase.

The range of PAH concentrations for the downwind samples is due to variability in wind direction, wind speed, variable dispersion of coke oven emissions and distance of the sampling site from the industries. Variability in emission rates from the coke ovens is

insignificant because these batteries are operated continuously at a constant rate. Emissions from motor vehicles are affected by meteorological conditions, time of day and type of day (weekday or weekend). No significant difference was observed in the total PAH concentrations on weekdays compared to weekend days, although traffic patterns can differ. Thus, the total PAH concentration for upwind samples is relatively low and constant. Upwind samples may contain minor amounts of coke oven emissions due to the proximity of the sampler to coking operations.

In Figure 7.3, the 234 amu thia-arene ratio is plotted against the 258 amu thia-arene ratio for the upwind and downwind air particulate extracts. The downwind samples are grouped close together in the bottom left corner of the plot. The upwind air particulate samples are well separated from the downwind samples and are spread over a larger area of the Figure. A linear relationship was observed between the 234 amu ratio and the 258 amu ratio with a good correlation coefficient (R = 0.88). Figure 7.3 demonstrates that the upwind and downwind samples can be differentiated based on thia-arene profiles alone.

The full data set of 89 air particulate extracts and 5 source sample extracts is plotted in the same manner (Figure 7.4). A linear best-fit line (solid line, slope = 0.26) for the Hamilton air particulate samples (excluding the sources) is shown in the Figure. Vertical and horizontal dashed lines are drawn on the plot to divide the data into two groups. Samples fall almost exclusively into two quadrants. The top right quadrant contains the diesel exhaust particulate, Toronto air, urban dust and upwind Hamilton air

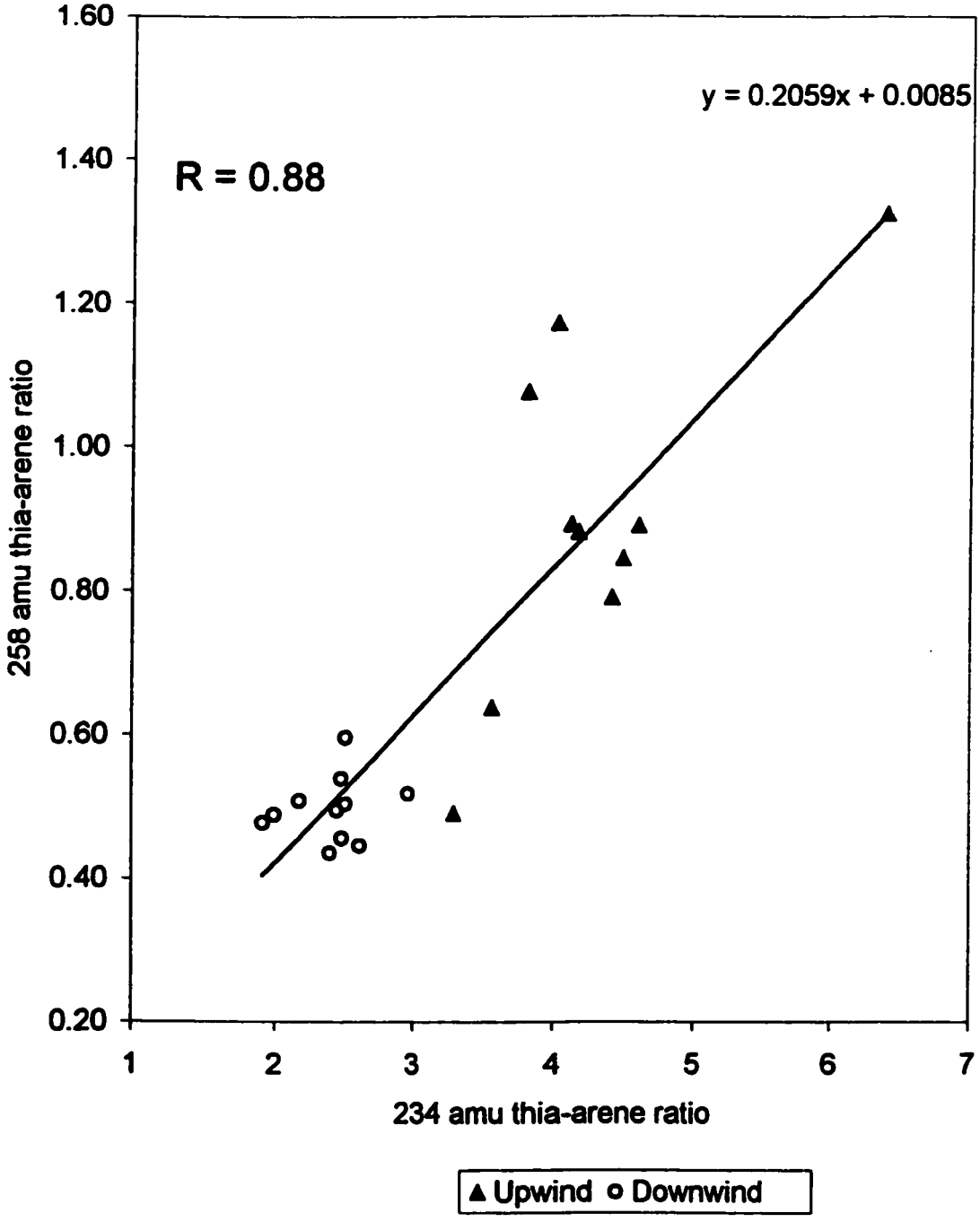

Figure 7.3. Relationship between 234 amu and 258 amu thia-arene ratios in air particulate collected upwind and downwind of the coke ovens in Hamilton. Correlation coefficient = 0.88).

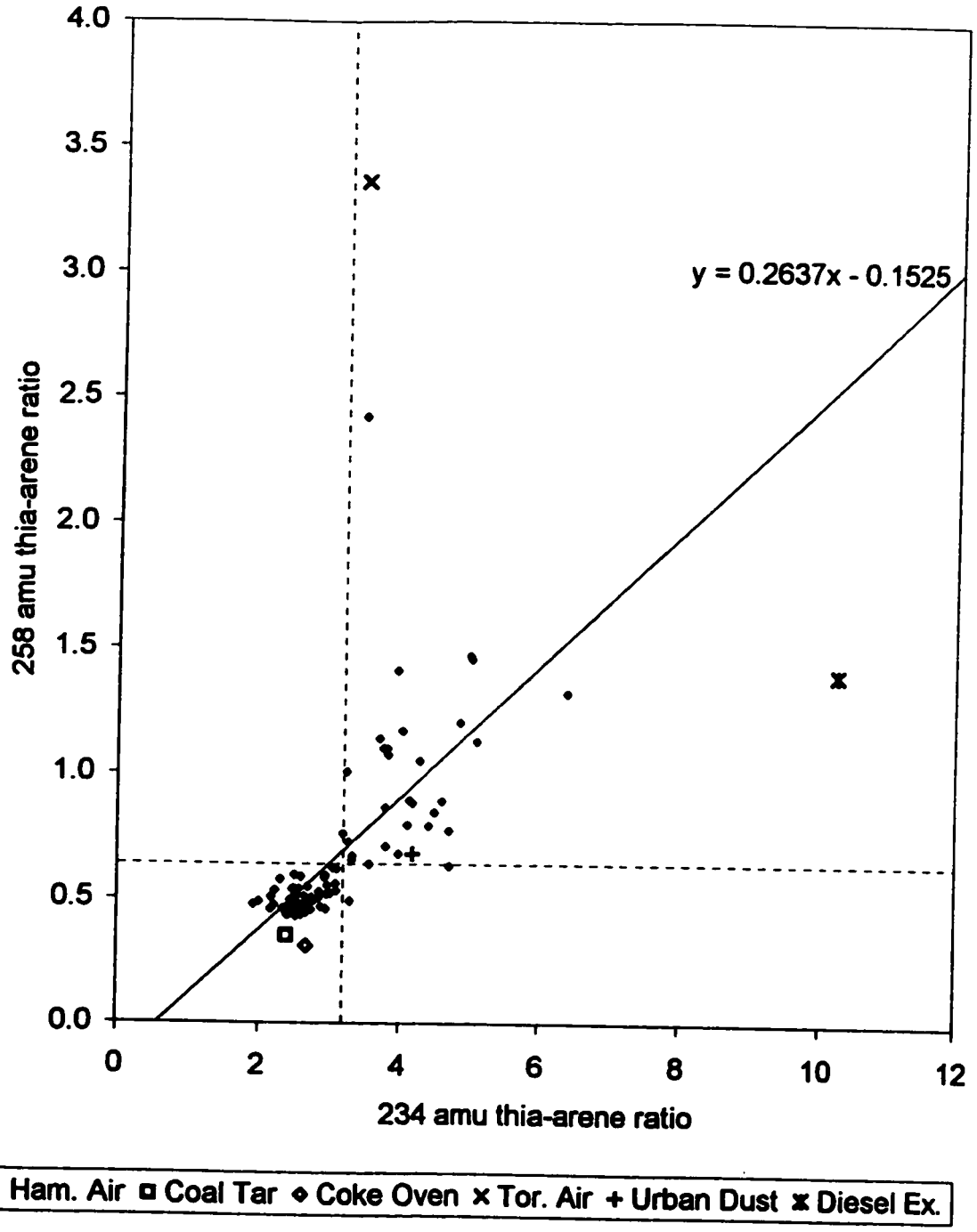

Figure 7.4. Relationship between 234 amu and 258 amu thia-arene ratios in 89 Hamilton air particulate samples and five source samples. Dashed lines separate the data into two groups.

samples, while the bottom left quadrant contains the coal tar, coke oven condensate and downwind Hamilton air samples.

The two dashed lines in Figure 7.4 intersect at a 234 amu thia-arene ratio of 3.2 and a 258 amu thia-arene ratio of 0.64. In Table 7.2, samples that have a 234 amu ratio greater than or equal to 3.2 have been assigned the designation "D" for diesel emissions, while samples that have a 234 amu ratio less than 3.2 have been assigned the designation "C" for coke oven emissions. Similarly, samples that have a 258 amu ratio greater than or equal to 0.64 have been assigned the designation "D" while samples that have a 258 amu ratio less than 0.64 have been assigned the designation "C". Only three samples have a 234 amu designation that is different from the 258 amu designation. These samples are highlighted with bold-face type in Table 7.2. These same three samples fall just outside of the top right and bottom left quadrants (dashed lines) in Figure 7.4. However, these samples can be considered to belong to either the top right or bottom left quadrant within the error for the determination of thia-arene ratios.

Legzdins reported relative standard deviations (RSD) of peak areas ranging from 5.4 to 9.7 % for 228-276 amu PAH in Hamilton air particulate [174]. The mean RSD was determined to be 7.6% for these compounds. If each thia-arene peak area is assumed to have an RSD of 7.6 %, the ratio of the peak areas will have an RSD of approximately 11% (the square root of the sum of the squares of the RSDs for each peak area). Assuming an RSD of 11% for both the 234 and 258 amu thia-arene ratios, the quadrant divisions are at a 234 amu ratio of 3.2 ± 0.4 and a 258 amu ratio of 0.64 ± 0.07. The

samples that fall just outside the lines on the graph belong to one of the two divisions within the 11% RSD error.

Samples with diesel designations are found at the top of Table 7.2, while samples with coke oven designations are found near the bottom of the table. A range of samples on the first page of the table between total PAH concentrations of 1.6 and 3.6 ng/m^3 is bracketed by two dotted lines. Between the two lines, the D and C designations alternate frequently indicating an uncertain, or mixed source composition. Between a total PAH concentration of 1.6 ng/m^3 to 3.6 ng/m^3, coke oven emissions begin to dominate the thia-arene profile for Hamilton air particulate. One exception is the sample collected at Station 29531 on August 15. A high 234 amu ratio indicates that the sample is dominated by diesel engine emissions, however, an atypically high total PAH concentration of 7.6 ng/m^3 was determined for this sample. It is possible that this sampling site was impacted by unusually high concentrations of diesel emissions, or that another source of PAH not normally present contributed to the high total PAH concentration.

The relationship between the thia-arene ratios and total PAH for all Hamilton air samples is explored in Figure 7.5. The 234 amu thia-arene ratios are plotted against total PAH concentration (Figure 7.5(a)) and against the log of the total PAH concentration (Figure 7.5(b)). A non-linear relationship is observed in both plots. A similar pair of figures for the 258 amu thia-arenes are shown in Figures 7.6(a) and 7.6(b). Thia-arene ratios decrease rapidly with increasing PAH concentration to about 5 ng/m^3 PAH. At total PAH concentrations above 5 ng/m^3 there is no apparent change in thia-arene ratios.

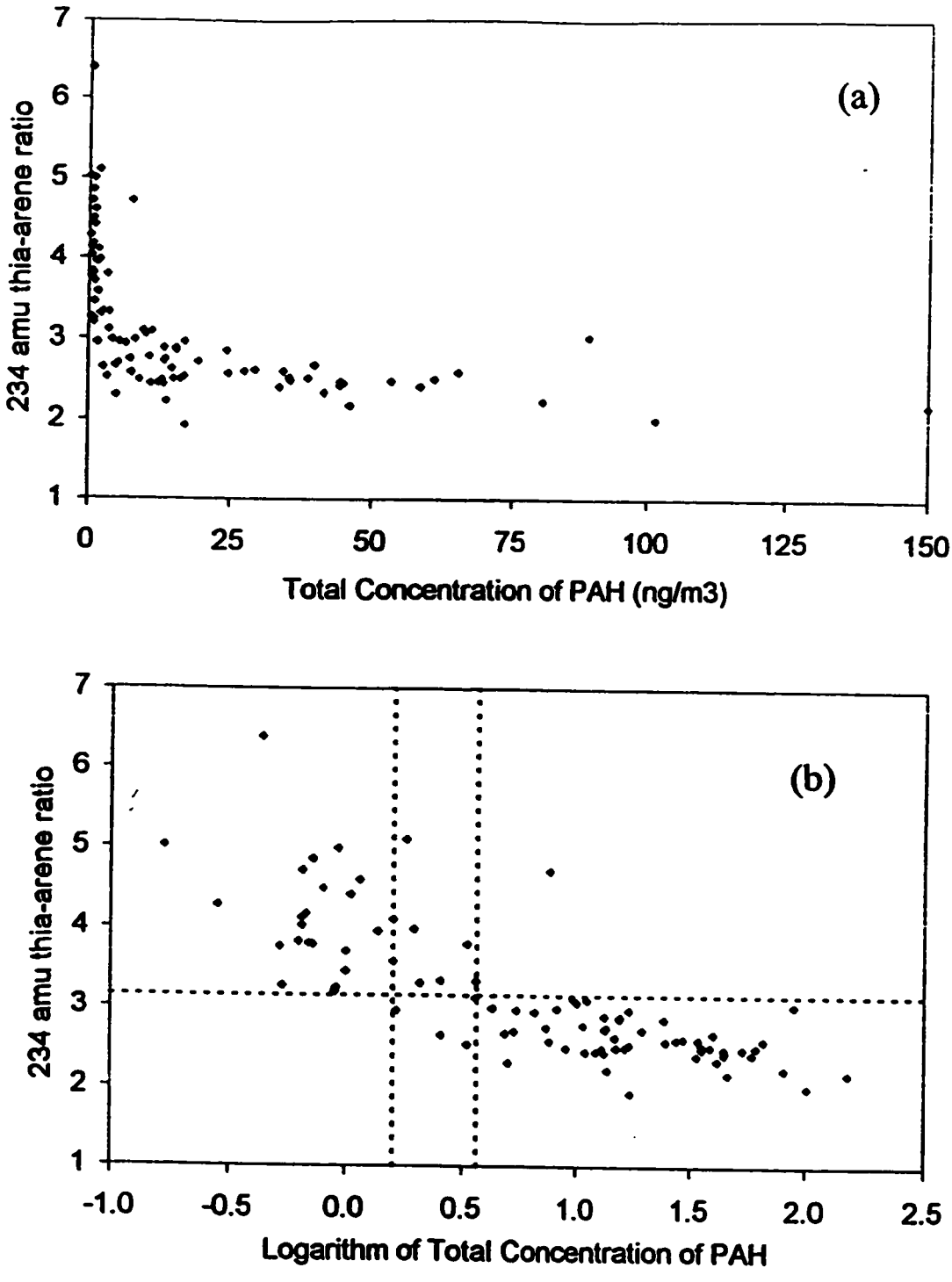

Figure 7.5. Relationship between 234 amu thia-arene ratio and (a) total concentration of PAH and (b) the logarithm of the total concentration of PAH for 89 Hamilton air particulate samples. The horizontal dashed line was determined in Figure 7.4. Vertical dashed lines bracket samples with mixed source contributions.

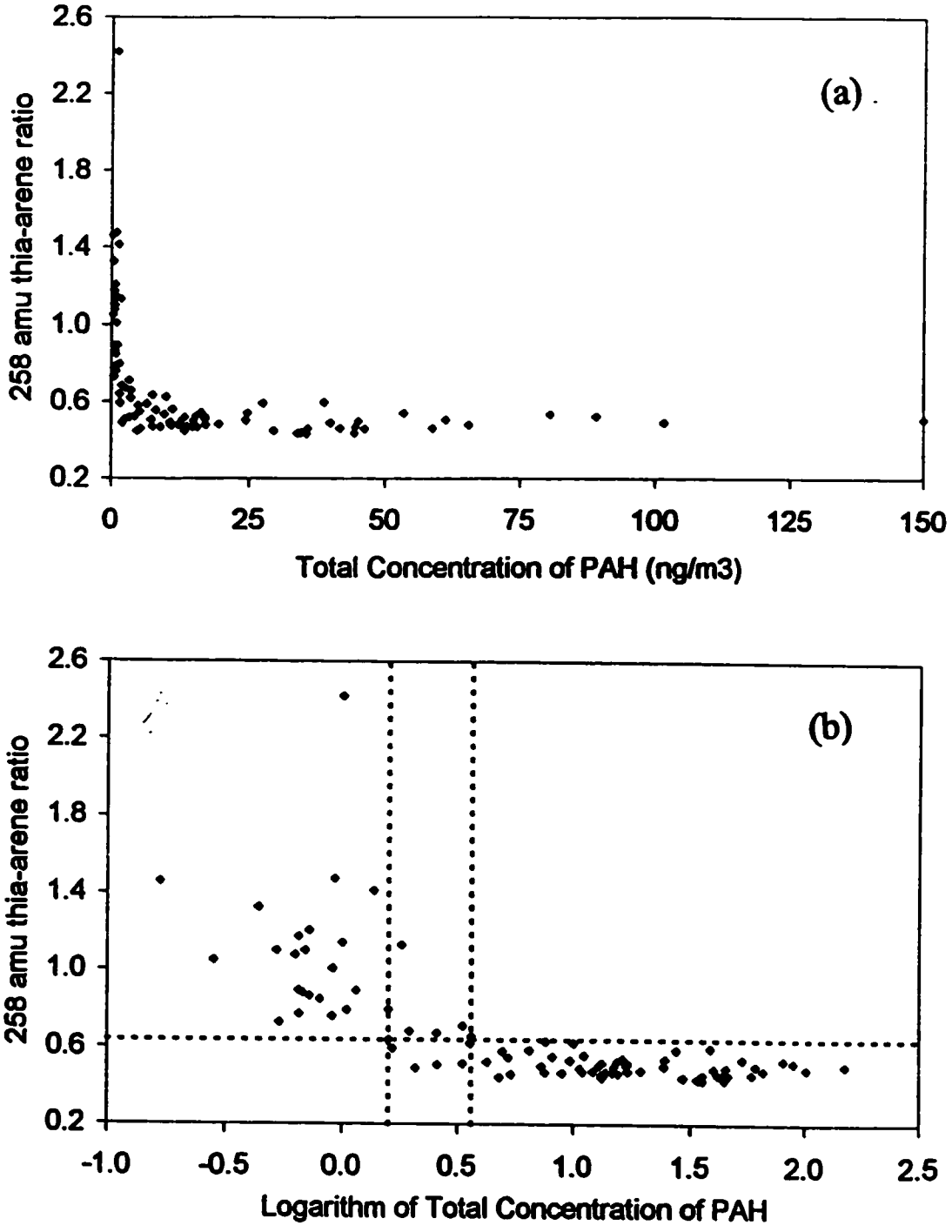

Figure 7.6. Relationship between 234 amu thia-arene ratio and (a) total concentration of PAH and (b) the logarithm of the total concentration of PAH for 89 Hamilton air particulate samples. The horizontal dashed line was determined in Figure 7.4. Vertical dashed lines bracket samples with mixed source contributions.

This is consistent with the observation from Table 7.2 that indicated a dominance of coke oven emissions, based on thia-arene designation, above a total PAH concentration of about 3.6 ng/m^3.

The lowest 234 amu thia-arene ratios observed in Hamilton air particulate are similar to the ratio for the coke oven condensate source sample, 2.7. The highest 234 amu thia-arene ratios fell short of the value determined for the diesel exhaust source sample, 10, but are closer in value to the ratio for the Urban Dust SRM, 4.2. The 258 amu thia-arene ratios for the diesel exhaust particulate (1.4) and the coke oven condensate (0.31) bracketed the values for the ambient data extremely well.

7.4 Thia-arene Index

The thia-arene ratio data in Table 7.2, which was plotted in Figure 7.4, demonstrated that all 89 samples could be classified (within error) as either coke oven-impacted or diesel-impacted by both thia-arene ratio criteria. In this section, a thia-arene index is proposed which combines both the 234 amu thia-arene ratio and the 258 amu thia-arene ratio. The intersection of the dashed lines at a 234 amu ratio = 3.2 and a 258 amu ratio = 0.64 will be assigned a thia-arene index value of 1.0.

Thia-arene ratios for each sample were normalized by dividing the 234 amu ratio by 3.2 and dividing the 258 amu ratio by 0.64. The sum of the normalized thia-arene ratios was divided by 2 to calculate the thia-arene index. The following equation

describes the calculation of the thia-arene index (TI):

$$TI = \left(\frac{R_{234}}{3.2} + \frac{R_{258}}{0.64} \right) \div 2$$

where R_{234} and R_{258} are the 234 and 258 amu thia-arene ratios, respectively. This equation will assign a thia-arene index of 1.0 to the intersecting point of the quadrants defined in Figure 7.4. The relative error is estimated to be 11%, so a point at the intersection of Figure 7.4 is assigned a thia-arene index of 1.0 ± 0.11. An index value greater than 1.1 indicates an impact predominately by diesel engine emissions, while an index value less than 0.89 indicates an impact predominately by coke oven emissions. Thia-arene indices were determined for all 89 Hamilton air particulate extracts and listed in the last column of Table 7.2.

Thia-arene index is plotted against the logarithm of the total PAH concentration for all 89 Hamilton air particulate samples (Figure 7.7). The shape of the data in this figure is similar to that of Figures 7.5(b) and 7.6(b). Samples with low concentrations of total PAH (<1.6 ng/m^3) have thia-arene indices greater than 1.0, while samples with high concentrations of total PAH (>3.6 ng/m^3) have thia-arene indices less than 1.0. Only one sample out of 89 has a thia-arene ratio greater than 1.0 and a high concentration of total PAH. The majority of samples with intermediate concentrations of PAH (1.6-3.6 ng/m^3) also have intermediate thia-arene ratios (near 1.0), indicating that these samples contain a mixture of diesel engine emissions and coke oven emissions.

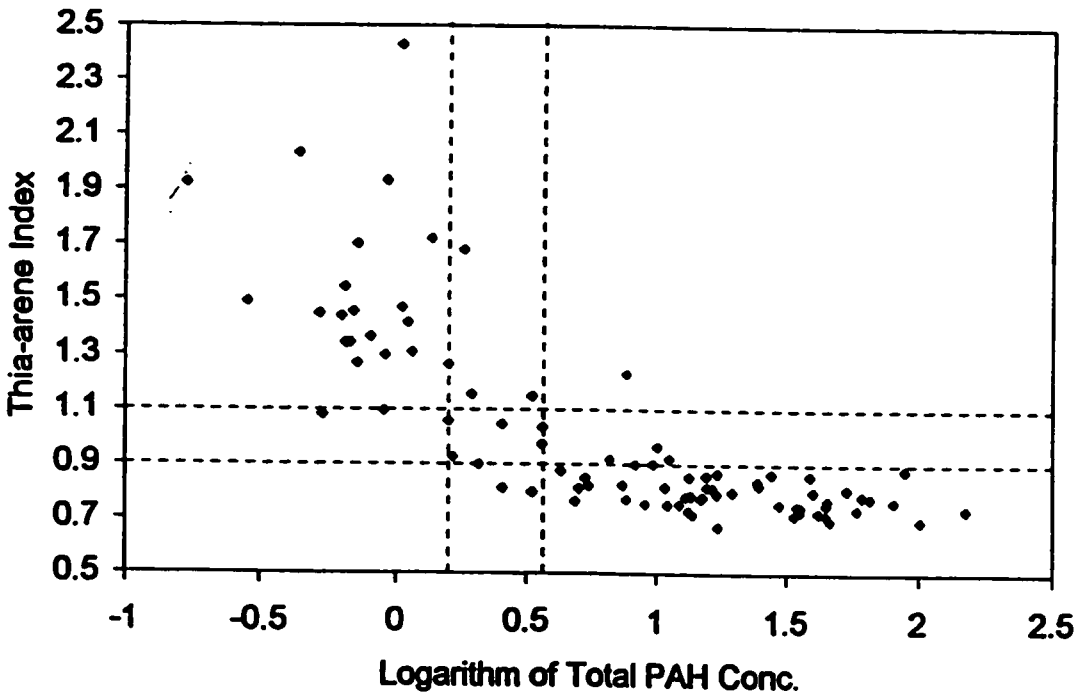

Figure 7.7. Relationship between thia-arene index and the logarithm of the total PAH concentration for 89 Hamilton air particulate samples. The square in the center of the dashed lines encloses samples with an uncertain or mixed source composition.

The relationship between the thia-arene index and the PCA analysis performed in Chapter 6 was examined. In Section 6.5, a data set containing the Hamilton air particulate samples and five source samples was analyzed by PCA using only thia-arene variables. Upwind Hamilton air samples were separated from downwind Hamilton air samples on Component 1 (Figure 6.6). In Figure 7.8, the Component 1 scores are plotted with the thia-arene index for the Hamilton air particulate samples. A strong correlation is observed between component scores and thia-arene indices. This shows that essentially the same information that was obtained by principal component analysis can be obtained by a simple calculation of isomer ratios.

Thia-arene indices (TI) determined for the source samples (Table 7.1) are in agreement with the ambient data set. Coke oven condensate (TI = 0.66) and coal tar (TI = 0.65) bracket the low end of the ambient data. Toronto air (TI = 3.2) and diesel exhaust particulate (TI = 2.7) bracket the high end of the ambient data. The Toronto air "source" sample is a composite air particulate sample collected on Bay Street in downtown Toronto. Additional 24-hour air particulate samples were collected alongside Highway 404 in Toronto in the summer of 1994. These samples are expected to contain primarily vehicle emissions. Thia-arene indices determined for the Hwy. 404 samples were all well above 1.0 (1.4 – 1.9, n=6), supporting the thia-arene index criteria for distinguishing vehicle emissions from coke oven emissions.

Thia-arene indices for the Highway 404 Toronto air, roadway runoff, creek sediment and Arctic air samples are listed in Table 7.3. These samples were examined in Chapter 6 using PCA. Component scores of these samples, relative to source samples,

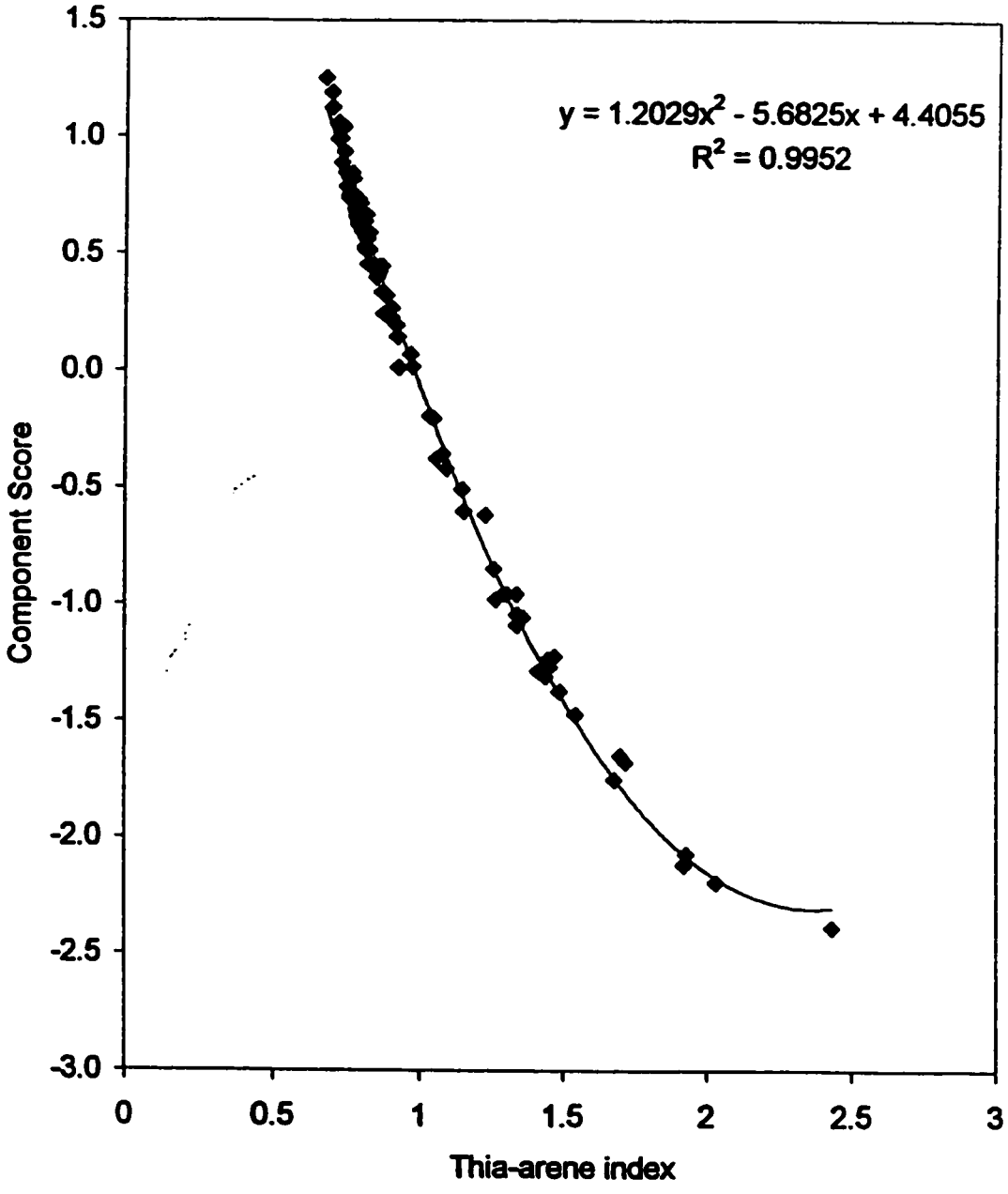

Figure 7.8. Relationship between thia-arene index and Component 1 score calculated in Section 6.5.

Table 7.3. Thia-arene ratios and thia-arene indices determined for various environmental samples.

Sample Type	Sample ID	234 amu ratio	Designation (234 ratio)[1]	258 amu ratio	Designation (258 ratio)[1]	Thia-arene Index
Roadway Runoff	1	3.5	D	0.72	D	1.1
	2	3.2	D	0.64	D	1.0
	3	3.3	D	0.65	D	1.0
Hamilton Creek Sediment	83	2.8	C	0.79	D	1.0
	84	3.1	D	0.84	D	1.1
	86	3.6	D	0.92	D	1.3
	88	3.0	C	0.92	D	1.2
	89	3.8	D	0.94	D	1.3
Toronto Air 24-hr, Hwy404	116	3.5	D	1.8	D	1.9
	19	2.7	C	1.4	D	1.5
	30	3.0	C	1.6	D	1.7
	73	3.3	D	1.2	D	1.5
	84	3.5	D	1.5	D	1.7
	93	3.2	D	1.1	D	1.4
Arctic Air	AA05	5.1	D	0.61	C	1.3
	AA06	5.1	D	0.61	C	1.3
	AA07	5.9	D	0.67	D	1.4
	AA08	6.6	D	0.73	D	1.6
	AA09	5.6	D	0.68	D	1.4
	AA10	13.5	D	0.69	D	2.7
	AA11	4.0	D	0.70	D	1.2
	AA12	4.4	D	0.70	D	1.2
	AD06	4.7	D	0.59	C	1.2
	AD07	6.3	D	0.63	D	1.5
	AD09	6.4	D	0.65	D	1.5
	AD10	4.5	D	0.60	C	1.2
	AD11	4.9	D	0.65	D	1.3
	AD12	4.6	D	0.68	D	1.3
	AY07	5.8	D	0.61	C	1.4
	AY08	5.0	D	0.62	C	1.3
	AY09	4.8	D	0.63	D	1.3

[1] "D"=234 ratio > 3.1, or 258 ratio > 0.63; "C"=234 ratio<=3.1, or 258 ratio <=0.63

indicated that petroleum-based emissions were more dominant than coal/coke-based emissions (Figure 6.8). Indices for Toronto air and Arctic air samples were all greater than 1.1, indicating dominant vehicular emission thia-arene profiles. The three roadway runoff samples and two of the Hamilton creek sediment samples had thia-arene indices between 1.0 and 1.1 indicating an uncertain or mixed thia-arene profile. These samples were collected in the Hamilton are and may contain a significant contribution of coke oven emissions. The roadway runoff samples were collected below a bridge approximately 2 kilometers from the steel industries, so it is likely they may contain coke oven emissions.

Thia-arene ratios are expected to decrease rapidly with increasing impact from coke oven emissions because higher levels of PAH and thia-arenes were observed downwind of the coke ovens. A linear relationship was observed between the concentration of benzo[b]naphtho[2,1-d]thiophene (Compound 80) and the total concentration of PAH (Figure 7.9). Coke oven emissions impacting the sampling sites in this study, even for a short period of time, should have a significant impact on the thia-arene profile of air particulate collected at the site.

7.5 Comparison of Thia-Arene Index and PAH Ratios for Source Apportionment

A new subset of samples was identified solely on the basis of total PAH concentration by examining a cumulative frequency plot for the logarithm of the total PAH (Figure 7.10). A curved section at the low end of the logarithmic plot shows a number of samples with nearly constant PAH concentrations. A horizontal line is drawn

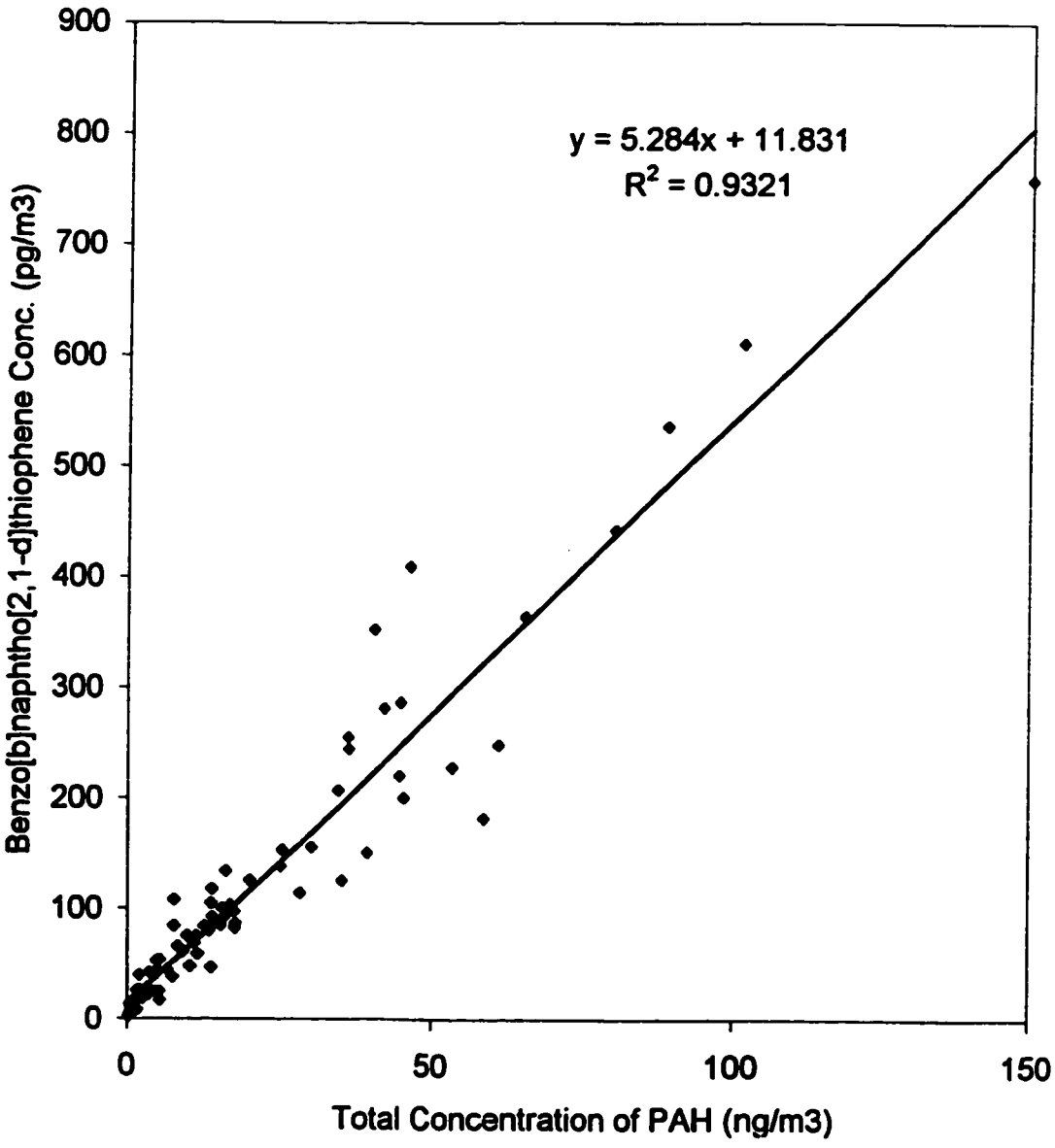

Figure 7.9. Relationship between concentration of benzo[b]naphtho[2,1-d]thiophene (B21T) and total concentration of PAH in 89 Hamilton air particulate samples.

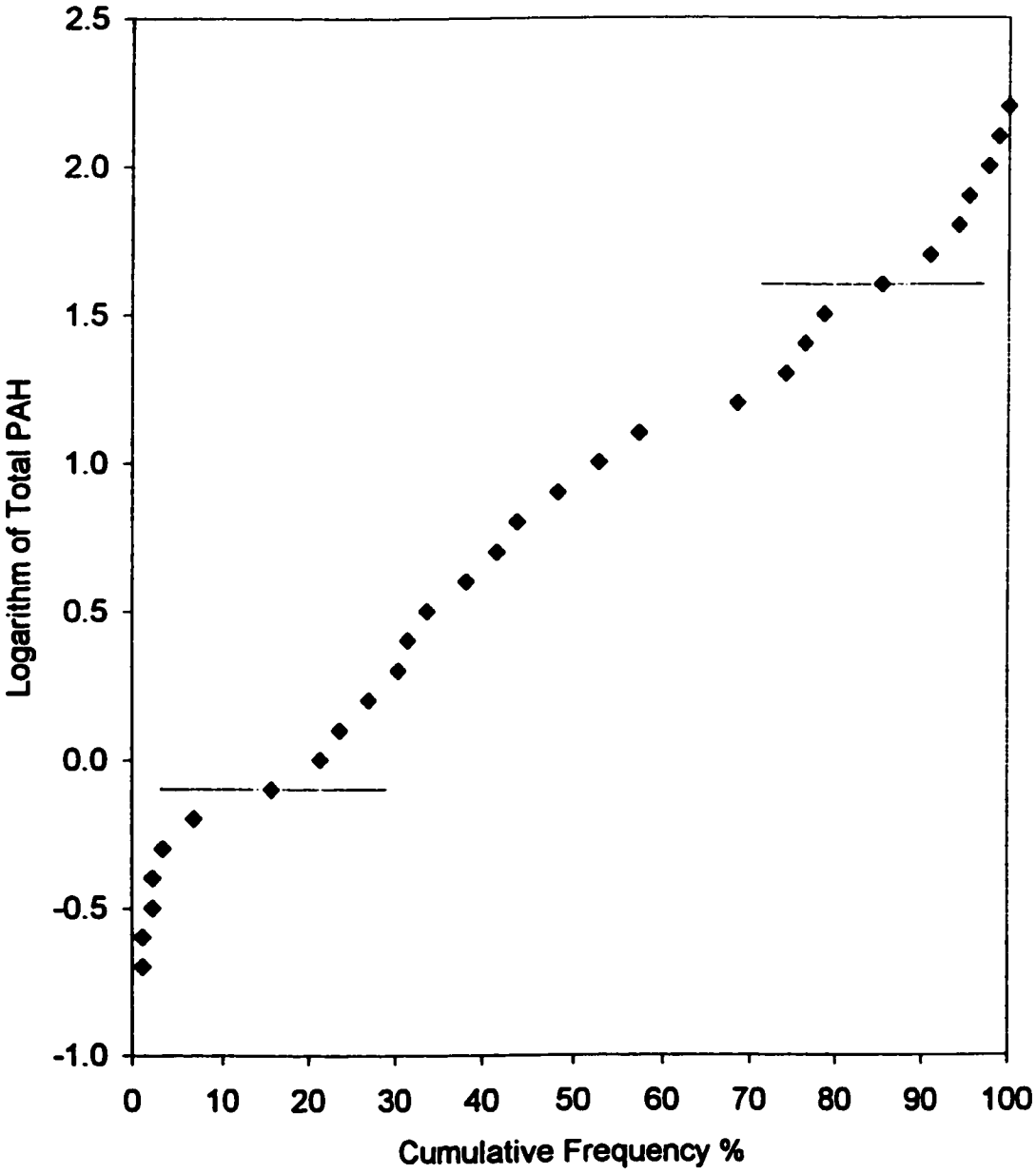

Figure 7.10. Cumulative frequency plot for the logarithm of the total concentration of PAH for 89 respirable air particulate samples collected in Hamilton.

at the end of this curved segment at log (PAH) = -0.1. Thirteen samples with a PAH concentration equal to or less than 0.8 ng/m^3 (log (PAH) = -0.1) belong to the new "low PAH" subset. A curved section at the high end of the plot shows a number samples with nearly constant PAH concentrations at the high end of the PAH scale. A horizontal line is drawn at the beginning of this curved section at log (PAH) = 1.6. Fourteen samples with a PAH concentrations greater than 40 ng/m^3 (log (PAH) = 1.6) belong to this new "high PAH" subset. The total PAH concentrations and thia-arene criteria are listed for these samples which represent the upper 16% and the lower 16% of the PAH distribution (Table 7.4).

The 27 filters identified in the above selection procedure were plotted as a 234 amu thia-arene ratio vs. 258 amu thia-arene ratio plot (Figure 7.11). Figure 7.11 is similar to Figure 7.3 which contained the upwind and downwind subsets. This exercise shows that selection of upwind/downwind samples based on wind direction or selection of the upper and lower PAH segments of the same data leads to similar results. The new subset was defined to identify a group of samples impacted by coke oven emissions and a group of samples impacted by vehicle emissions to compare the thia-arene index with selected PAH ratios previously suggested as source tracers in the literature.

For several years, PAH have been used as source apportionment tracers. Many individual PAH or PAH ratios have been suggested as source tracers as were summarized in Chapter 1. New criteria continue to appear in the literature due to the limitations associated with current source apportionment models, and there is no general consensus as to the best criteria to use for PAH-based source apportionment models.

Table 7.4. PAH and thia-arene data for the low PAH and high PAH Hamilton air particulate sample subsets.

Date	Station	Total PAH (ng/m3)	234 amu ratio	Designation (234 ratio)[1]	258 amu ratio	Designation (258 ratio)[1]	Thia-arene Index
Low PAH (<0.8 ng/m3)							
08/06/95	29547	0.17	5.0	D	1.5	D	1.9
08/05/95	29531	0.28	4.3	D	1.1	D	1.5
08/07/95	29547	0.44	6.4	D	1.3	D	2.0
07/23/95	29113	0.52	3.8	D	1.1	D	1.4
07/23/95	29531	0.54	3.3	D	0.73	D	1.1
08/11/95	29000	0.63	3.8	D	1.1	D	1.4
07/20/95	29000	0.65	4.0	D	1.2	D	1.5
08/11/95	29113	0.65	4.1	D	0.89	D	1.3
08/09/95	29547	0.65	4.7	D	0.77	D	1.3
07/20/95	29113	0.67	4.2	D	0.88	D	1.3
08/12/95	29531	0.69	3.8	D	1.1	D	1.5
08/05/95	29000	0.72	3.8	D	0.86	D	1.3
08/13/95	29547	0.72	4.9	D	1.2	D	1.7
08/11/95	29531	0.80	4.5	D	0.85	D	1.4
High PAH (>40 ng/m3)							
08/14/95	29113	40	2.7	C	0.49	C	0.80
08/06/95	29531	42	2.3	C	0.46	C	0.72
08/16/95	29000	44	2.4	C	0.43	C	0.72
07/23/95	29547	45	2.5	C	0.47	C	0.75
08/18/95	29000	45	2.4	C	0.49	C	0.77
07/29/95	29547	46	2.2	C	0.46	C	0.70
08/17/95	29531	53	2.5	C	0.54	C	0.81
08/16/95	29531	59	2.4	C	0.46	C	0.74
08/18/95	29531	61	2.5	C	0.50	C	0.78
08/14/95	29531	66	2.6	C	0.48	C	0.78
08/19/95	29531	81	2.2	C	0.53	C	0.76
08/08/95	29531	89	3.0	C	0.52	C	0.88
08/02/95	29531	101	2.0	C	0.49	C	0.69
08/07/95	29531	150	2.2	C	0.51	C	0.74

[1]"D"=234 ratio > 3.1, or 258 ratio > 0.63; "C"=234 ratio<=3.1, or 258 ratio <=0.63

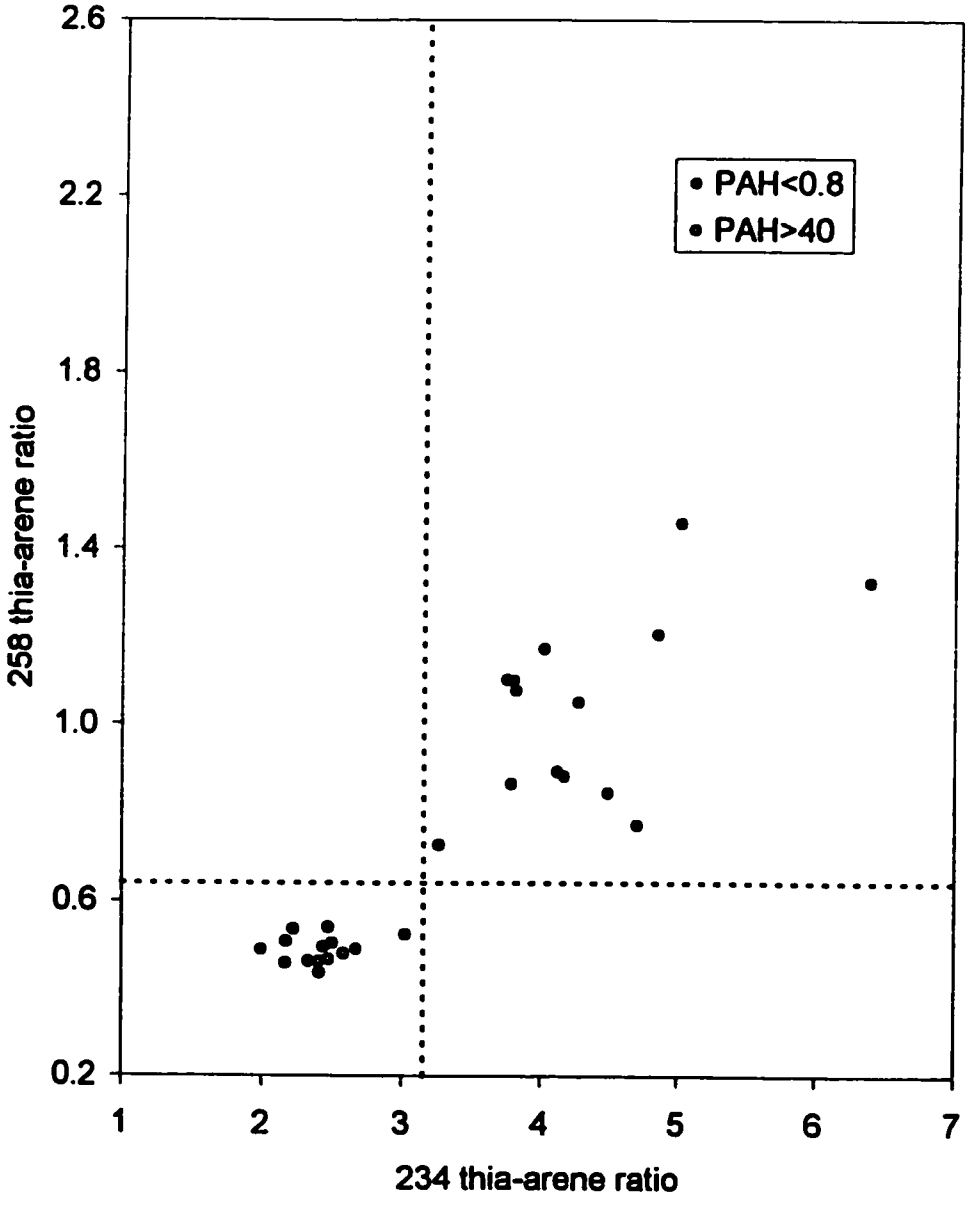

Figure 7.11. Relationship between 234 amu and 258 amu thia-arene ratios in low PAH and high PAH Hamilton air particulate sample subsets (samples listed in Table 7.3).

A 1986 review [22] suggested several ratios for use with specific sources, based on the examination of several published PAH source inventories. In this review, the BAP:BEP, BGP:BEP and BCP:BEP ratios were proposed as indicators to differentiate coke oven emissions from traffic emissions while the BKF:BEP ratio was suggested as an indicator for coal combustion. The BGP:BAP ratio was identified in another study to distinguish traffic emissions from coal combustion emissions [32].

These five PAH ratios were selected as the best available PAH ratio criteria for source apportionment relevant to the present study and these ratios were calculated for each of the samples in the "low PAH" and "high PAH" subsets. The five ratios (BGP:BEP, BKF:BEP, BGP:BAP, BAP:BEP and BCP:BEP) were plotted alongside the thia-arene index for the corresponding samples (Figure 7.12). The thia-arene indices for the two subsets do not overlap at all, consistent with Figure 7.11. The PAH ratios, on the other hand, show modest to complete overlaps of these sample sets. The thia-arene ratios are clearly superior source apportionment tracers to the PAH ratios for distinguishing coke oven emissions from motor vehicle emissions in Hamilton, Ontario.

Benzo[a]pyrene (BAP) and benzo[e]pyrene (BEP) are two compounds that are determined by all environmental agencies which monitor PAH so there is a very large database of BAP and BEP determinations. Only one low PAH sample overlapped with the high PAH samples for the BAP:BEP ratio (Figure 7.12). If only PAH data is available this may be the best ratio to estimate source contributions. The BAP:BEP ratio for all 89 samples was plotted against the thia-arene index (Figure 7.13). The dashed line at thia-arene index = 1.0 separates the coke oven impacted samples from the diesel-

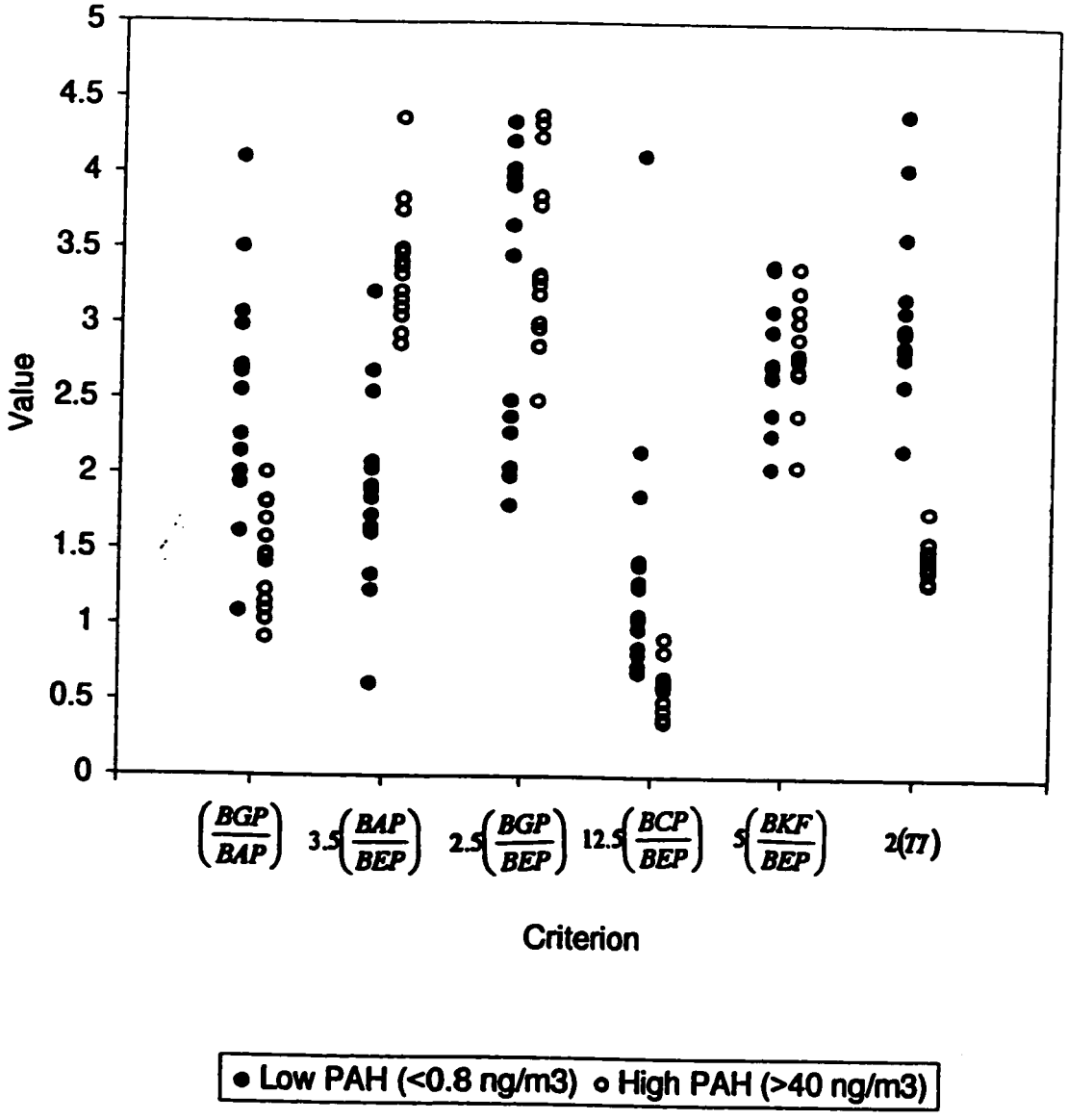

Figure 7.12. Selected PAH ratios and thia-arene index in Hamilton air particulate collected upwind and downwind of the coke ovens. Sample classification based on highest (downwind) and lowest (upwind) PAH concentrations.

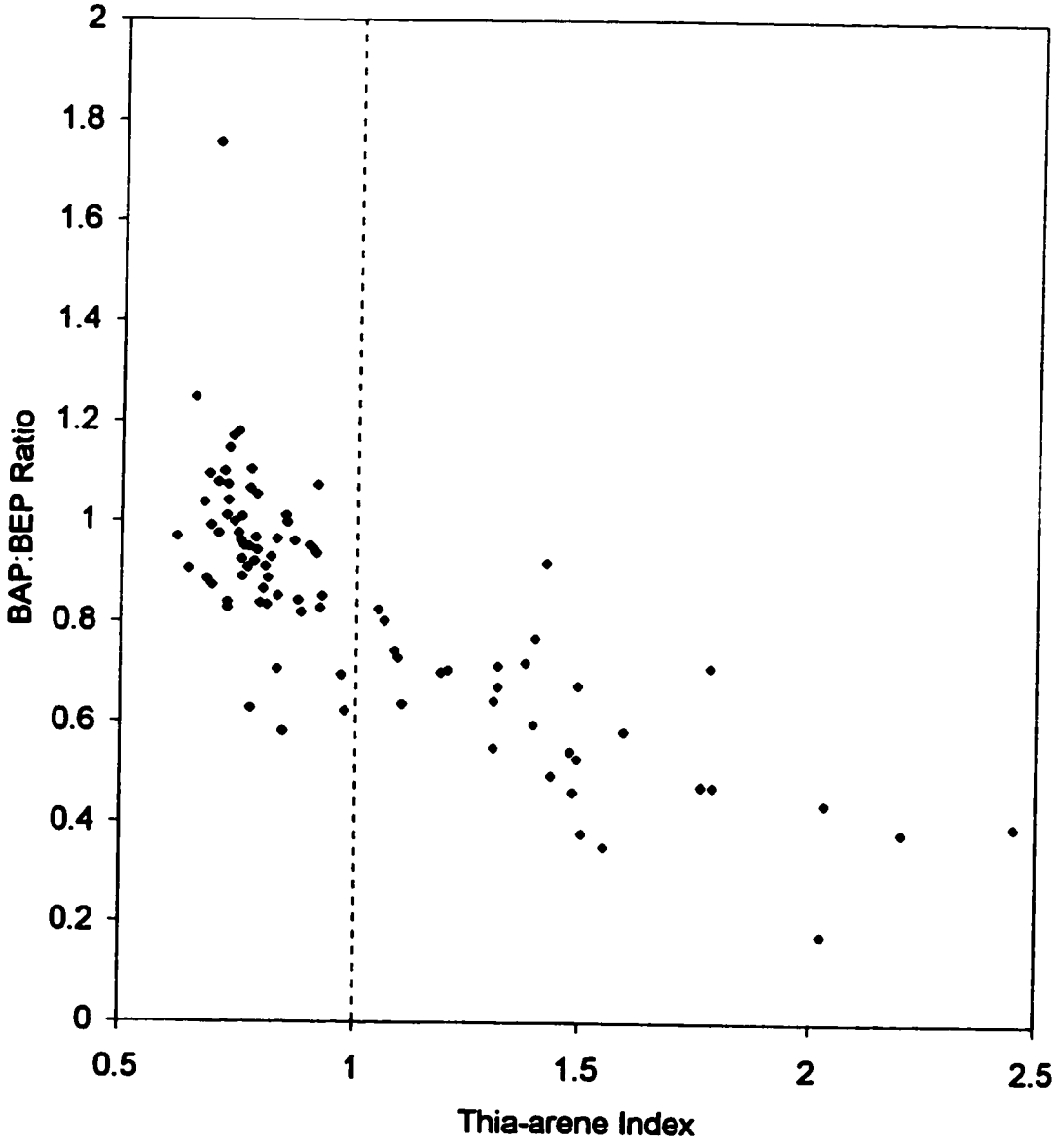

Figure 7.13. Relationship between BAP:BEP ratio and thia-arene index for 89 Hamilton air particulate samples.

impacted samples. These two groups are fairly well separated by BAP:BEP ratio, divided by a value of approximately 0.75. Three samples with thia-arene index well below 1.0 significantly overlap with the diesel-impacted samples (thia-arene index > 1.0). The BAP:BEP ratio ranged from 0.85 to 1.2 for the downwind samples. This range of values compares favourably to the BAP:BEP ratio of 1.0 reported for ambient air in an area with coke oven emissions [22]. BAP:BEP ratios in upwind samples range from 0.18 to 1.1. A similar range of values (0.3-1.4) was reported for spark-ignition engine exhaust [22]. The BAP:BEP ratios determined in this study are consistent with the literature, however, the use of BAP as a source tracer has been strongly discouraged due to the reactivity of the compound [25,28]. The reactivity of BAP may be the cause of the few overlapping samples in Figure 7.13.

The frequency distributions of the BAP:BEP ratio and the thia-arene index are plotted in Figures 7.14(a) and 7.14(b). The highest frequencies of BAP:BEP ratios are in the center of the distribution and it is difficult to see separation of two groups of samples impacted by different sources. Two distributions can be seen for the plot of thia-arene index frequencies. A narrow range of high frequencies is observed for the low thia-arene index samples (coke oven impact). This group is clearly separated from a second group (diesel impact) with a wider distribution. The frequency distributions also show a clearer separation of source impacts using the thia-arene source apportionment criteria. The ability of the thia-arene index to distinguish coke oven emissions from diesel emissions surpasses previous PAH source apportionment methodology.

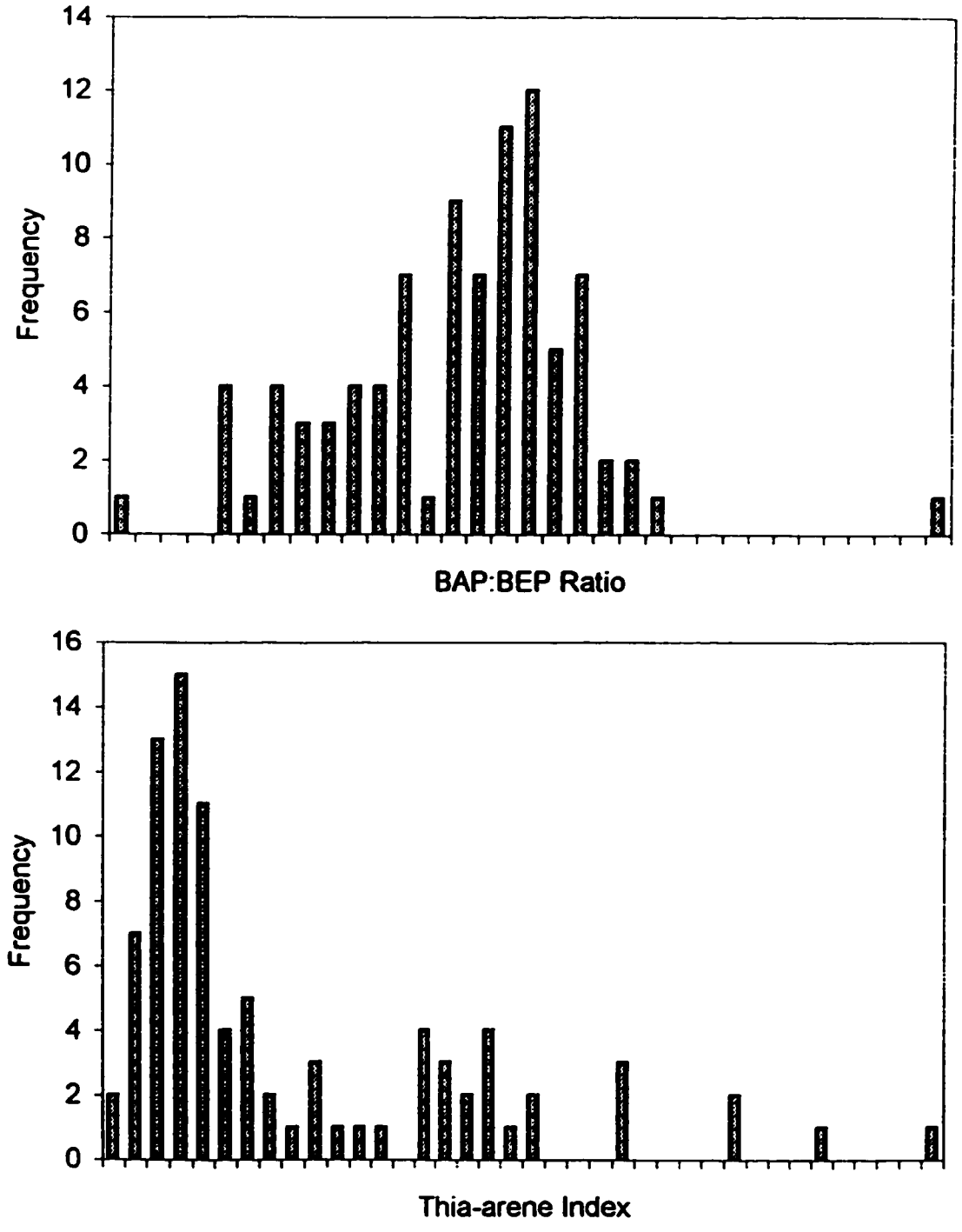

Figure 7.14. Frequency distributions for (a) BAP:BEP ratio and (b) thia-arene index.

8.0 CONCLUSIONS AND FUTURE WORK

A large number of samples were collected in Hamilton at different locations and during a variety of meteorological conditions. Even with the large data set, only a few of the samples could be classified as upwind or downwind based on wind data. Sampler location and wind conditions must be just right to get useful information. This set of data is the most extensive air particulate data set available for the city of Hamilton. Government agencies typically sample one day out of every 6 or 12 calendar days at fewer sites surrounding the industries. Days with the appropriate meteorological conditions for classification of samples would often be missed due to the occasional sampling strategy for routine monitoring.

One of the sampling locations (Station 29531) had not previously been used for the collection of ambient air particulate. Samples obtained at this site contained the highest average concentrations of PAH of all the locations in this study. Station 29531 is located very close to the coke ovens and northeasterly winds carry emissions from the industry to impact this site. The ambient levels of PAH at this location are a concern because residential housing is also located in the area. PAH concentrations observed at Station 29531, a result of the present study, prompted the Ontario Ministry of the Environment to begin regular monitoring of ambient air at this site.

PAH levels in air particulate vary widely from day to day and from site to site. Up to 340-fold higher total concentrations of PAH were detected downwind of the steel industries than upwind of the industries (August 7, 1995). The steel industries contribute

the large majority of PAH in Hamilton air particulate collected downwind of the coke ovens. This is consistent with the work of Legzdins' [174], but in the present study, a second sampler was also located upwind of the steel industries to confirm that elevated PAH concentrations in air particulate did not originate from another source upwind of the steel industries. Upwind of the coke ovens, traffic emissions are a significant source of PAH in Hamilton. In Toronto, Ontario and the Arctic Region, thia-arene profiles in air particulate indicated that no significant amount of coke/coal-based emissions impacted these regions. Pollution from coke oven emissions in Hamilton appears to be a local problem that does not significantly impact areas distant from the steel industries. In contrast, thia-arene profiles in these other areas indicate that vehicular/petroleum-based emissions are a widespread pollution problem.

Particulate is another type of pollutant in ambient air identified as a health hazard. The concentrations of particulate emissions from the steel mills, measured at a site downwind of the coke ovens, were not significantly greater than background levels of particulate in Hamilton. In some cases, particulate levels were higher upwind of the coke ovens than downwind of the coke ovens. Particulate deposits on the properties of Hamilton residents are a major complaint. The results of this study show that the coke ovens are not the only major source of particulate emissions in Hamilton. In fact, the highest particulate concentrations in this study were observed upwind of the coke ovens at Station 29547. The impact that vehicular emissions have on particulate levels in the city is evident by the pattern of lower particulate concentrations throughout the sampling area on Saturdays and Sundays when the volume of traffic is likely reduced. Overall

higher particulate levels at Station 29547 indicate an additional local source. Due to health concerns associated with air particulate, future studies in Hamilton should aim to identify all major particulate sources.

Few studies have focused on the analysis of thia-arenes, particularly higher molecular mass isomers (258 amu). The analytical method used in the present study was modified to optimize conditions for thia-arene analysis. The DB-17ht (50% phenylmethylpolysiloxane) GC column was selected for the separation of thia-arene isomers. This column performed significantly better than DB-5ms that is conventionally used for PAH analysis. This is the only commercially available phase that was found to provide adequate and reproducible resolution of al the 252 and 278 amu PAH isomers. Previously, analysts have abandoned gas chromatographic methods and relied on high performance liquid chromatography for the analysis of these PAH isomers. This is no longer necessary.

Retention indices reported for four different stationary phases, including DB-17ht, will be useful to other scientists for identification of thia-arenes when standards are not available, or for the development of two-dimensional chromatography methods. Improved separation of thia-arene isomers using the DB-17 stationary phase was also recently reported by Mossner and Wise [142]. They did not however report retention indices and the range of thia-arenes evaluated was limited to isomers of molecular mass no greater than 248. Mossner and Wise [142] also report a unique separation of selected thia-arenes using a liquid crystalline stationary phase. This phase could also be evaluated

in the future for the selectivity toward the 258 amu thia-arene isomers. Several possible 258 amu thia-arene compounds were found to co-elute even on the DB-17ht column.

Profiles of alkylated dibenzothiophene isomers, 234 amu isomers and 258 amu isomers were characterized in a variety of source and ambient samples. Differences in the thia-arene profiles of air particulate collected upwind and downwind of the coke ovens were determined. The different profiles observed in ambient samples were also compared to thia-arene profiles in source samples. This gives some indication of the stability of the profile or the variability in the source profile. Thia-arene profiles observed in ambient samples contaminated by coke oven emissions were found to be consistent with thia-arene profiles in the source samples. Greater variability was observed in the thia-arene profiles of samples contaminated by diesel emissions. Further investigation of the thia-arene profile variation in diesel or background urban emissions should be conducted in the future.

The 234 amu and 258 amu thia-arene profiles in source samples more closely resembled the profiles in ambient samples than the alkylated dibenzothiophene profiles previously used as source tracers in sediments. This led to the use of the 234 amu and 258 amu compounds in the development of a thia-arene index for source classification. To my knowledge, this is the first time 234 amu and 258 amu isomer thia-arene profiles have been used in an atmospheric source apportionment study.

The most suitable thia-arene isomers to use as source tracers were identified in Hamilton air particulate using principal component analysis (PCA). This information was later used to derive a thia-arene index for the classification of individual samples.

PCA is a popular tool for receptor modeling because the factors extracted in the analysis are often related to emission source profiles. Discriminant partial least squares (PLS) analysis has also been used to assess emission source contributions in ambient air samples [182]. This technique works well with similar source emission profiles (often found with PAH compounds) because this method maximizes the differences between source classes. In the future, a PLS analysis could be performed using the data from the present study and compared to the results in this study.

The thia-arene criteria proposed in this study provide a clear separation of samples contaminated by coke oven emissions and samples contaminated by diesel exhaust emissions. In comparison to PAH ratios used in the past, the thia-arene criteria show greater differentiation between samples upwind and downwind of the coke ovens. No criterion in the literature offers sufficient differentiation of upwind and downwind samples in the Hamilton air particulate data set. The thia-arene source apportionment approach provides a simple, reliable and sensitive method for identifying coke oven emissions in urban air. This study focused mainly on air particulate pollution sources but the method can be applied to any environmental sample. In future studies, a greater number and wider variety of emission sources should be characterized to expand this thia-arene source apportionment model.

REFERENCES

1. Cecilione, V. *Can. J. Pub. Health*, **1976** *67*, 53-58.
2. Shannon, H. S.; Hertzman, C.; Julian, J. A.; Hayes, M. V.; Henry, N,; Charters, J.; Cunningham, I.; Gibson, E. S.; Sackett, D. L. *Can. J. Pub. Health* **1988**, *79*, 255-259.
3. Levy, D.; Gent, M.; Newhouse, M. T. *Am. Rev. Respir. Disease* **1977**, *116*, 167-173.
4. Grimmer, G. *Profile Analysis of Polycyclic Aromatic Hydrocarbons in Air;* Ch. 4.
5. Katz, M.; Chan, C. *Environ. Sci. Technol.* **1980**, *14*, 838-843.
6. Katz, M.; Sakuma, T.; Ho, A. *Environ. Sci. Technol.* **1978**, *12*, 909-915.
7. Morris, W. A.; Versteeg, J. K.; Bryant, D. W.; Legzdins, A. E.; McCarry, B. E.; Marvin, C. H. *Atmos. Environ.* **1995**, *29*, 3441-3450.
8. Legzdins, A. E.; McCarry, B. E.; Bryant, D. W. *Polycyclic Aromatic Compounds* **1994**, *5*, 157-165.
9. Legzdins, A. E.; McCarry, B. E.; Marvin, C. H.; Bryant, D. W. *Intern. J. Environ. Anal. Chem.* **1995**, *60*, 79-94.
10. Marvin, C. H.; Allan, L.; McCarry, B. E.; Bryant, D. W. *Environ. Molec. Mutagen.* **1993**, *22*, 61-70.
11. Bates, T. S.; Carpenter, R. *Geochim. Cosmochim. Acta* **1979**, *43*, 1209-1221.
12. Pettersen, H.; Naf, C.; Broman, D. Mar. Pollut. Bull. **1997**, 34, 85-95.
13. Canadian Environmental Protection Act: Strategic Options for the Management of Toxic Substances from the Steel Manufacturing Sector, Report of Stakeholder Consultations, Environment Canada, December 30, 1996.
14. Benarie, M. M. *Urban Air Pollution Modelling*, MIT Press: Cambridge, 1980; p 13.
15. Gordon, G. E. *Environ. Sci. Technol.*, **1988**, *22*, 1132-1140.
16. Edgerton, S. A.; Holdren, W. A. *Environ. Sci. Technol.*, **1987**, *21*, 1102-1110.
17. Cooper, J. A.; Watson, Jr., J. G. *J. Air Pollut. Control Assoc.* **1980**, *30*, 1116-1125.
18. Gordon, G. E. *Environ. Sci. Technol.*, **1988**, *22*, 1132-1140.
19. Friedlander, S. K. *Environ. Sci. Technol.*, **1973**, *7*, 235-240.

20. Gordon, R. J.; Bryan, R. J. *Environ. Sci. Technol.* **1973**, *7*, 1050-1053.

21. Greenberg, A.; Bozzelli, J. W.; Cannova, F.; Forstner, E.; Giorgio, P.; Stout, D.; Yokoyama, R. *Environ. Sci. Technol.* **1981**, *15*, 566-569.

22. Daisey, J. M.; Cheney, J. L.; Lioy, P. J. *JAPCA* **1986**, *36*, 17-33.

23. Venkataraman, C.; Lyons, J. M.; Friedlander, S. K. *Environ. Sci. Technol.* **1994**, *28*, 555-562.

24. Hering, S. V.; Miguel, A. H.; Dod, R. L. *Sci. Total Environ.* **1984**, *36*, 39-45.

25. Cretney, J. R.; Lee, H. K.; Wright, G. J.; Swallow, W. H.; Taylor, M. C. *Environ. Sci. Technol.* **1985**, *19*, 397-404.

26. Daisey, J. M.; Miguel, A. H.; de Andrade, J. B.; Pereira, P. A. P.; Tanner, R. L. *J. Air Pollut. Control Assoc.* **1987**, *37*, 15-23.

27. Benner, B. A., Jr.; Wise, S. A.; Currie, L. A.; Klouda, G. A.; Klinedinst, D. B.; Zweidinger, R. B.; Stevens, R. K.; Lewis, C. W. *Environ, Sci. Technol.* **1995**, *29*, 2382-2389.

28. Miguel, A. H.; Pereira, P. A. P. *Aerosol Sci. Technol.* **1989**, *10*, 292-295.

29. Li, C. K.; Kamens, R. M. *Atmospheric Environment*, **1993**, *27A*, 523-532.

30. 30. Lee, M. L.; Prado, G. P.; Howard, J. B.; Hites, R. A. *Biomed. Mass Spectrom.* **1977**, *4*, 182-186.

31. Miguel, A. H. *Sci. Total Environ.* **1984**, *36*, 305-311.

32. Daisey, J. M.; Kneip, T. J.; Ming-xing, W.; Li-xin, R.; Wei-xiu, L. *Aerosol Sci. Technol.* **1983**, *2*, 407-415.

33. Grimmer, G.; Naujack, K.-W.; Schneider, D. *Fres. Z. Anal. Chem.* **1982**, *311*, 475-484.

34. Grimmer, G.; Naujack, K.-W.; Schneider, D. In *Polynuclear Aromatic Hydrocarbons: Chemistry and Biological Effects*; Bjorseth, A.; Dennis, A. J., Eds.; Battelle Press: Columbus, OH, 1980; pp 107-125.

35. Wild, S. R.; Jones, K. C. *Environ. Pollut.* **1995**, *88*, 91-108.

36. Brown, J. R.; Field, R. A.; Goldstone, M. E.; Lester, J. N.; Perry, R. *Sci. Total Environ.* **1996**, *177*, 73-84.

37. Edgerton, S. A.; Holdren, M. W. *Environ. Sci. Technol.* **1987**, *21*, 1102-1107.

38. Sweet, C. W.; Vermette, S. J. *Environ. Sci. Technol.* **1992**, *26*, 165-173.

39. Harrison, R. M.; Smith, D. J. T.; Luhana, L. *Environ. Sci. Technol.* **1996**, *30*, 825-832.

40. de Raat, W. K.; de Meijere, F. A. *Sci. Total Environ.* **1991**, *103*, 1-17.

41. Armanino, C.; Forina, M.; Bonfanti, L.; Maspero, M. *Anal. Chim. Acta* **1993**, *284*, 79-89.

42. Alsberg, T.; Hakansson, S.; Strandell, M.; Westerholm, R. *Chemomet. Intell. Lab. Sys.* **1989**, *7*, 143-152.

43. Westerholm, R.; Li, H. *Environ. Sci. Technol.* **1994**, *28*, 965-972.

44. Rachdawong, P.; Christensen, E. R. *Environ. Sci. Technol.* **1997**, *31*, 2686-2691.

45. Baldasano, J. M.; Delgado, R.; Calbo, J. *Environ. Sci. Technol.* **1998**, *32*, 405-412.

46. Gordon, G. E. *Environ. Sci. Technol.* **1988**, *22*, 1132-1142.

47. Henry, R. C.; Lewis, C. W.; Hopke, P. K.; Williamson, H. J. *Atmos. Environ.* **1984**, *18*, 1507-1515.

48. Roscoe, B. A.; Hopke, P. K.; Dattner, S. L.; Jenks, J. M. *J. Air Pollut. Control Assoc.* **1982**, *32*, 637-642.

49. Wold, S.; Esbensen, K.; Geladi, P. *Chemom. Intell. Lab. Syst.* **1987**, *2*, 37-52.

50. Howard, P. J. A. *An Introduction to Environmental Pattern Analysis*; Parthenon Publishing Group Ltd.: Park Ridge, NJ, USA,1991; ch 5.

51. Hopke, P. K. *Receptor Modeling in Environmental Chemistry*; John Wiley & Sons, Inc.: New York, NY, USA, 1985; ch 7.

52. de Raat, W. K.; Kooijman, S. A. L. M.; Gielen, J. W. J. *Sci. Total Environ.* **1987**, *66*, 95-114.

53. Sexton, K.; Liu, K.-S.; Hayward, S. B.; Spengler, J. D. *Atmos. Environ.* **1985**, *19*, 1225-1236.

54. Greenberg, A.; Darack, F.; Harkov, R.; Lioy, P.; Daisey, J. *Atmos. Environ.* **1985**, *19*, 1325-1339.

55. Simcik, M. F.; Eisenreich, S. J.; Golden, K. A.; Liu, S.-P.; Lipiatqu, E.; Swackhamer, D. L.; Long, D. T. *Environ. Sci. Technol.* **1996**, *30*, 3039-3046.

56. Candeli, A.; Mastrandrea, V.; Morozzi, G.; Toccaceli, S. *Atmos. Environ.* **1974**, *8*, 693-705.

57. Christensen, E. R.; Zhang, X. *Environ. Sci. Technol.* **1993**, *27*, 139-146.

58. Youngblood, W. W.; Blumer, M. *Geochim. et Cosmochim. Acta* **1975**, *39*, 1303-1314.

59. Dominguez, A.; Alvarez, R.; Blanco, C. G.; Diez, M. A. *J. Chromatogr. A* **1996**, *719*, 181-194.

60. Baek, S. O.; Goldstone, M. E.; Kirk, P. W. W.; Lester, J. N.; Perry, R. *Sci. Tot. Environ.* **1992**, *111*, 169-199.

61. Tancell, P. J.; Rhead, M. M.; Trier, C. J.; Bell, M. A.; Fussey, D. E. *Sci. Tot. Environ.* **1995,** *162,* 179-186.

62. Kamens, R. M.; Guo, Z.; Fulcher, J. N.; Bell, D. A. *Environ. Sci. Technol.* **1988,** *22,* 103-108.

63. Jang, M.; McDow, S. R. *Environ. Sci. Technol.* **1995,** *29,* 2654-2660.

64. Pistikopoulos, P.; Masclet, P.; Mouvier, G. *Atmos. Environ.* **1990,** *24A,* 1189-1197.

65. Pitts, Jr., J. N.; Paur, H. –R.; Zielinska, B.; Arey, J.; Winer, A. M.; Ramdahl, T.; Mejia, V. *Chemosphere* **1986,** *15,* 675-685.

66. Van Vaeck, L.; Van Cauwenberghe, K. *Atmos. Environ.* **1984,** *18,* 323-328.

67. Nielsen, T. *Environ. Sci. Technol.* **1984,** *18,* 157-163.

68. Pitts, Jr.,J. N.; Sweetman, J. A.; Zielinska, B.; Winer, A. M.; Atkinson, R. *Atmos. Environ.* **1985,** *19,* 1601-1608.

69. Behymer, T. D.; Hites, R. A. *Environ. Sci. Technol.* **1988,** *22,* 1311-1319.

70. Patton, G. W.; Walla, M. D.; Bidleman, T. F.; Barrie, L. A. *J. Geophysical Res.* **1991,** *96,* 10867-10877.

71. Greenberg, A.; Stein, S. E.; Brown, R. L. *Sci. Tot. Environ.* **1984,** *40,* 219-230.

72. John, W.; Hering, S.; Reischl, G.; Sasaki, G. *Atmos. Environ.* **1983,** *17,* 115-119.

73. Baek, S. O.; Field, R. A.; Goldstone, M. E.; Kirk, P. W.; Lester, J. N.; Perry, R. *Wat. Air Soil Pollut.* **1991,** *60,* 279-300.

74. Andersson, J. T.; Sielex, K. *J. High Resol. Chromatogr.* **1996,** *19,* 49-53.

75. Hunt, D. F.; Shabanowitz, J. *Anal. Chem.* **1982,** *54,* 574-578.

76. Grimmer, G.; Jacob, J.; Naujack, K. –W. *Fres. Z. Anal. Chem.* **1983,** *314,* 29-36.

77. Sinkkonen, S. *J. Chromatogr.* **1989,** *475,* 421-425.

78. Nishioka, M.; Bradshaw, J. S.; Lee, M. L.; Tominaga, Y.; Tedjamulia, M.; Castle, R. N. *Anal. Chem.* **1985,** *57,* 309-312.

79. Palmentier, J. –P. F.; Britten, A. J.; Charbonneau, G. M.; Karasek, F. W. *J. Chromatogr.*, **1989,** *469,* 241-251.

80. Andersson, J. T.; Schmid, B. *J. Chromatogr. A.*, **1995,** *693,* 325-338.

81. Willey, C.; Iwao, M.; Castle, R. N.; Lee, M. L. *Anal. Chem.*, **1981,** *53,* 400-407.

82. Nishioka, M.; Whiting, D. G.; Campbell, R. M.; Lee, M. L. *Anal. Chem.* **1986,** *58,* 2251-2255.

83. Peaden, P. A.; Lee, M. L.; Hirata, Y.; Novotny, M. *Anal. Chem.* **1980,** *52,* 2268-2271.

84. Lee, M. L.; Hites, R. A. *Anal. Chem.* **1976**, *48*, 1890-1893.

85. Colmsjo, A. L.; Zebuhr, Y. U.; Ostman, C. E. *Anal. Chem.* **1982**, *54*, 1673-1677.

86. Nishioka, M.; Chang, H. –C.; Lee, M. L. *Environ. Sci. Technol.* **1986**, *20*, 1023-1027.

87. Tong, H. Y.; Karasek, F. W. *Anal. Chem.* **1984**, *56*, 2129-2134.

88. Mason, G.; Gustafsson, J. –A.; Westerholm, R. N.; Li, H. *Environ. Sci. Technol.* **1992**, *26*, 1635-1638.

89. Schmid, E. R.; Bachlechner, G.; Varmuza, K.; Klus, H. *Fresenius Z. Anal. Chem.* **1985**, *322*, 213-219.

90. Kong, R. C.; Lee, M. L.; Tominaga, Y.; Pratap, R.; Iwao, M.; Castle, R. N.; Wise, S. A. *J. Chromatogr. Sci.* **1982**, 20, 502-510.

91. Gryglewicz, G.; Jasienko, S. *Fuel Process. Technol.* **1988**, *19*, 51-59.

92. Kong, R. C.; Lee, M. L.; Tominaga, Y.; Pratap, R.; Iwao, M.; Castle, R. N.; Wise, S. A. *J. Chromatogr. Sci.* **1982**, 20, 502-510.

93. Boudou, J. P.; Boulegue, J.; Malechaux, L.; Nip, M.; de Leeuw, J. W.; Boon, J. J. *Fuel* **1987**, *66*, 1558-1568.

94. White, C. M.; Lee, M. L. *Geochim. et Cosmochim. Acta* **1980**, *44*, 1825-1832.

95. Chang, H. –C. K.; Skelton, Jr., R. J.; Markides, K. E.; Lee, M. L. *Polycyclic Aromatic Compounds* **1990**, *1*, 251-264.

96. Nishioka, M.; Lee, M. L.; Castle, R. N. *Fuel* **1986**, *65*, 390-396.

97. Wise, S. A.; Benner, B. A.; Byrd, G. D.; Chesler, S. N.; Rebbert, R. E.; Schantz, M. M. *Anal. Chem.*, **1988**, *60*, 887-894.

98. Cullis, C. F.; Hirschler, M. M. *Atmos. Environ.* **1980**, *14*, 1263-1278.

99. Chang, H. –C., K.; Bartle, K. D.; Markides, K. E.; Lee, M. L. in *Advances in Coal Spectroscopy*, Meuzelaar, H. L. C., Ed.; Plenum Press: New York, 1992, ch.7.

100. Nishioka, M.; Lee, M. L. in *Advances in Chemistry Series No. 217: Polymuclear Aromatic Compounds*, Ebert, L. B., Ed.; American Chemical Society, 1988, ch. 14.

101. Burchill, P.; Herod, A. A.; Pritchard, E. *J. Chromatogr.* **1982**, *242*, 65-76.

102. Nishioka, M.; Campbell, R. M.; West, W. R.; Smith, P. A.; Booth, G. M.; Lee, M. L. *Anal. Chem.* **1985**, *57*, 1868-1871.

103. Grimmer, G.; Jacob, J.; Dettbarn, G.; Naujack, K.-W. *Fresenius Z. Anal. Chem.* **1985**, *322*, 595-602.

104. Knobloch, T.; Engewald, W. *HRC* **1993**, *16*, 239-242.

105. Thomas, D.; Crain, S. M.; Sim, P. G.; Benoit, F. M. *J. Mass Spectrom.* **1995,** *30,* 1034-1040.

106. Bates, T. S.; Carpenter, R. *Anal. Chem.* **1979,** *51,* 551-554.

107. Vassilaros, D. L.; Eastmond, D. A.; West, W. R.; Booth, G. M.; Lee, M, L. in *Polynuclear Aromatic Hydrocarbons: Sixth International Symposium on Physical and Biological Chemistry,* Bjorseth, A., Ed.; Battelle Press: Columbus, OH, 1981, p.845-857.

108. Canton, L.; Grimalt, J. O. *J. Chromatogr.* **1992,** *607,* 279-286.

109. McCarry, B. E.; Allan, L. M.; Legzdins, A. E.; Lundrigan, J. A.; Marvin, C. H.; Bryant, D. W. *Polycyclic Aromatic Compounds* **1996,** *11,* 75-82.

110. Colucci, J. M.; Begeman, C. R. *Environ. Sci. Technol.* **1971,** *5,* 145-150.

111. Tilak, B. D. *Tetrahedron,* **1960,** *9,* 76-95.

112. Eastmond, D. A.; Booth, G. M.; Lee, M. L. *Arch. Environ. Contam. Toxicol.,* **1984,** *13,* 105-111.

113. Ames, B. N.; McCann, J.; Yamasaki, E. *Mutation Res.* **1975,** *31,* 347-364.

114. Ames, B. N. *Science* **1979,** *204,* 587-593.

115. Pelroy, R. A.; Stewart, D. L.; Tominaga, Y.; Iwao, M.; Castle, R. N.; Lee, M. L. *Mutation Res.*, **1983,** *117,* 31-40.

116. McFall, T.; Booth, G. M.; Lee, M. L.; Tominaga, Y.; Pratap, R.; Tedjamulia, M.; Castle, R. N. *Mutation Res.*, **1984,** *135,* 97-103.

117. Nishioka, M.; Smith, P. A.; Booth, G. M.; Lee, M. L.; Kudo, H.; Muchiri, D. R.; Castle, R. N.; Klemm, L. H. *Fuel* **1986,** *65,* 711-714.

118. Damste, J. S. S.; Kohnen, M. E. L.; de Leeuw, J. W. *Nature* **1990,** *345,* 609-611.

119. Sporstol, S.; Gjos, N.; Lichtenthaler, R. G.; Gustavsen, K. O.; Urdal, K.; Oreld, F.; Skei, J. *Environ. Sci. Technol.* **1983,** *17,* 282-286.

120. Yunker, M. B.; Snowdon, L. R.; Macdonald, R. W.; Smith, J. N.; Fowler, M. G.; Skibo, D. N.; McLaughlin, F. A.; Danyushevskaya, A. I.; Petrova, V. I.; Ivanov, G. I. *Environ. Sci. Technol.* **1996,** *30,* 1310-1320.

121. Damste, J. S. S.; Rijpstra, W. I. C.; de Leeuw, J. W.; Schenck, P. A. *Geochim. Cosmochim. Acta* **1989,** *53,* 1323-1341.

122. Budzinski, H.; Garrigues, P.; Connan, J.; Lee, M. L.; Andersson, J.; Bellocq, J. In *Organic Geochemistry: Advances and Applications in the Natural Environment*; Manning, D. A. C., Ed.; Manchester University Press: New York, USA, 1991; pp 619-623.

123. Douglas, G. S.; Bence, A. E.; Prince, R. C.; McMillen, S. J.; Butler, E. L. *Environ. Sci. Technol.* **1996,** *30,* 2332-2339.

124. Peltonen, K.; Kuljukka, T. *J. Chromatogr. A.*, **1995**, *710*, 93-108.

125. Kirton, P. J.; Crisp, P. T. *Fuel* **1990**, *69*, 633-638.

126. Poster, D. L.; Hoff, R. M.; Baker, J. E. *Environ. Sci. Technol.* **1995**, *29*, 1990-1997.

127. Venkataraman, C.; Friedlander, S. K. *Environ. Sci. Technol.* **1994**, *28*, 563-572.

128. Allen, J. O.; Dookeran, N. M.; Smith, K. A.; Sarofim, A. F.; Taghizadeh, K.; Lafleur, A. L. *Environ. Sci. Technol.* **1996**, *30*, 1023-1031.

129. Miguel, A. H.; Kirchstetter, T. W.; Harley, R. A.; Hering, S. V. *Environ. Sci. Technol.* **1998**, *32*, 450-455.

130. Vo-Dinh, T. *Chemical Analysis of Polycyclic Aromatic Compounds*; Wiley Interscience: New York, 1988, ch. 3.

131. Wise, S. A.; Sander, L. C.; May, W. E. *J. Chromatogr.* **1993**, *642*, 329-349.

132. Sander, L. C.; Wise, S. A. *J. High Resol. Chromatogr. & Chromatogr. Commun.* **1988**, *11*, 383-387.

133. Lee, M. L.; Wright, B. W. *J. Chromatogr. Sci.* **1980**, *18*, 345-358.

134. Lee, M. L.; Novotny, M.; Bartle, K. D. *Anal. Chem.* **1976**, *48*, 1566-1572.

135. Grimmer, G.; Naujack, K. –W.; Schneider, D. *Fres. Z. Anal. Chem.* **1982**, *311*, 475-484.

136. May, W. E.; Wise, S. A. *Anal. Chem.* **1984**, 56, 225-232.

137. Wise, S. A.; Benner, B. A.; Chesler, S. N.; Hilpert, L. R.; Vogt, C. R.; May, W. E. *Anal. Chem.* **1986**, *58*, 3067-3077.

138. Escriva, C.; Viana, E.; Molto, J. C.; Pico, Y.; Manes, J. *J. Chromatogr. A* **1994**, *676*, 375-388.

139. Lee, H. K. *J. Chromatogr. A* **1995**, *710*, 79-92.

140. Naikwadi, K. P.; Charbonneau, G. M.; Karasek, F.W.; Clement, R. E. *J. Chromatogr.* **1987**, *467*, 227-237.

141. Wise, S. A.; Campbell, R. M.; May, W. E.; Lee, M. L.; Castle, R. N. in *Polynuclear Aromatic Hydrocarbons: Seventh International Symposium on Formation, Metabolism and Measurement*, Cooke, M. W., Dennis, A.J., Eds.; Battelle Press, Columbus, OH, 1982, p.1247-1265.

142. Mossner, S. G.; Wise, S. A. *Anal. Chem.* **1999**, *71*, 58-69.

143. Lee, M.L.; Vassilaros, D. L.; White, C. M.; Novotny, M. *Anal. Chem.*, **1979**, *51*, 768-773.

144. Engkvist, O.; Borowski, P.; Berngard, A.; Karlstrom, G.; Lindh, R.; Colmsjo, A. *J. Chem. Inf. Comput. Sci.* **1996**, *36*, 1153-1161.

145. Elizalde-Gonzalez, M. P.; Huttlieli, M.; Hedden, K. *J. High Resol. Chromatogr.* **1996,** *19,* 345-351.

146. Palmentier, J. –P. F.; Britten, A. J.; Charbonneau, G. M.; Karasek, F. W. *J. Chromatogr.*, **1989**, *469*, 241-251.

147. Campbell, R. M.; Lee, M. L. *Anal. Chem.*, **1984**, *56*, 1026-1030.

148. Andersson, J. T. *J. Chromatogr.*, **1986**, *354*, 83-98.

149. Drushel, H. V.; Sommers, A. L. *Anal. Chem.*, **1967**, *39*, 1819-1827.

150. Madesclaire, M. *Tetrahedron*, **1986**, *42*, 5459-5495.

151. Joyce, W. F.; Uden, P. C. *Anal. Chem.*, **1983**, *55*, 540-547.

152. Andersson, J. T. *Anal. Chem.*, **1987**, *59*, 2207-2209.

153. Davis, F. A.; Sheppard, A. C. *Tetrahedron*, **1989**, *45*, 5703-5742.

154. Davis, F. A.; Chattopadhyay, S.; Towson, J. C.; Lal, S.; Reddy, T. *J. Org. Chem.*, **1988**, *53*, 2087-2089.

155. Liu, G. H.; Fu, P. R. *Chromatographia*, **1989,** *27*, 159-167.

156. Efer, J.; Maurer, T.; Engewald, W. *Chromatographia*, **1990**, *29*, 115-122.

157. Sye, W. F.; Zhao, Z. X.; Lee, M. L. *Chromatographia*, **1992**, *33*, 507-514.

158. Shearer, R. L. *Anal. Chem.*, **1992**, 6, 2192-2199.

159. Albro, T. G.; Dreifuss, P. A.; Wormsbecher, R. F. *HRC*, **1993**, *16*, 13-17.

160. J. Jacob, *Sulfur Analogues of Polycyclic Aromatic Hydrocarbons (Thiaarenes)*, Cambridge University Press: Cambridge, 1990.

161. Scheutzle, D.; Jensen, T. E.; Ball, J. C. *Environ. Int.* **1985,** *11*, 169-181.

162. McCalla, D. R.; Quilliam, M. A.; Kaiser-Farrell, C.; Tashiro, C.; Hoo, K.; Gibson, E. S.; Lockington, N. J.; Kerr, A.A.; Sheldrake, C. in *Carcinogenic and Mutagenic Responses to Aromatic Amines and Nitroarenes*, King, C. M.; Romano, L. J.; Schuetzle, D., Eds.; Elsevier Science Publishing Co., Inc.: New York, 1988, p. 47-63.

163. Later, D. W.; Lee, M. L.; Bartle, K. D.; Kong, R. C.; Vassilaros, D. L. *Anal. Chem.* **1981,** *53*, 1612-1620.

164. Marvin, C. H.; Allan, L.; McCarry, B. E.; Bryant, D. W. *Environ. Molec. Mutagen.* **1993**, *22*, 61-70.

165. Nikolaou, K.; Masclet, P.; Mouvier, G. Sci. Tot. Environ. **1984,** 32, 103-132.

166. Neff, J. M. Polycyclic Aromatic Hydrocarbons in the Aquatic Environment: Sources, Fates and Biological Effects; Applied Science Publishers Ltd.: London, 1979.

167. Kropp, K. G.; Andersson, J. T.; Fedorak, P. M. *Environ. Sci. Technol.* **1997,** *31,* 1547-1554.

168. Hinchee, R. E.; Alleman, B. C.; Hoeppel, R. E.; Miller, R. N. *Hydrocarbon Bioremediation;* CRC Press, Inc.:Boca Raton, FL, 1994.

169. Hinchee, R. E.; Leeson, A.; Semprini, L.; Ong, S. K. *Bioremediation of Chlorinated and Polycyclic Aromatic Hydrocarbon Compounds;* CRC Press Inc.,: Boca Raton, FL, 1994.

170. Garrigues, P.; De Vazelhes-De Sury, R.; Angelin, M. L.; Ewald, M.; Oudin, J. L.; Connan, J. *Org. Geochem.* **1984,** *6,* 829-837.

171. Garrigues, P.; Parlanti, E.; Radke, M.; Bellocq, J.; Willsch, H.; Ewald, M. *J. Chromatogr.* **1987,** *395,* 217-228.

172. Wang, Z.; Fingas, M. Environ. Sci. Technol. **1995,** 29, 2842-2849.

173. Marvin, C. H. A Multi-media Bioassay-Directed Investigation of the Hamilton Harbour Area of Western Lake Ontario; Ph.D. Thesis, McMaster University, 1994.

174. Legzdins, A. E. *Chemical and Biological Characterization of Southern Ontario Urban Air Particulate;* Ph.D. Thesis, McMaster University, 1996.

175. Liu, Z.; Sirimanne, S. R.; Patterson, Jr., D. G.; Needham, L. L.; Phillips, J. B. *Anal. Chem.* **1994,** *66,* 3086-3092.

176. Schomburg, G. *J. Chromatogr. A* **1995,** *703,* 309-325.

177. Phillips, J. B.; Xu, J. *J. Chromatogr. A* **1995,** *703,* 327-334.

178. Lioy, P. J.; Daisey, J. M. *Environ. Sci. Technol.* **1986,** *20,* 8-14.

179. Ontario Ministry of Environment and Energy *1995 Air Quality Data Summary Regional Municipality of Hamilton-Wentworth;* Queen's Printer for Ontario, 1997.

180. Lewtas. J.

181. Halsall, C. J.; Barrie, L. A.; Fellin, P.; Muir, D. C. G.; Billeck, B. N.; Lockhart, L.; Rovinsky, F. YA.; Kononov, E. YA.; Pastukhov, B. *Environ. Sci. Technol.* **1997,** *31,* 3593-3599.

182. Vong, R.; Geladi, P.; Wold, S.; Esbensen, K. *J. Chemometrics* **1988,** *2, 281-296.*

APPENDIX I. Identities and structures of PAH and thia-arenes.

No.	Compound	Mol. Wt.
1	Naphthalene	128
2	2-Methylnaphthalene	142
3	1-Methylnaphthalene	142
4	Biphenyl	154
5	Acenaphthylene	152
6	Acenaphthene	154
7	Fluorene	166
8	Phenanthrene	178
9	Anthracene	178
10	*o*-Terphenyl	230
11	Anthraquinone	208
12	Fluoranthene	202
13	Pyrene	202
14	*m*-Terphenyl	230
15	*p*-Terphenyl	230
16	Benzo[*a*]fluorene	216
17	Retene	234
18	Benzo[*b*]fluorene	216
19	Benzo[*ghi*]fluoranthene	226
20	Benzo[*c*]phenanthrene	228
21	Cyclopenta[*cd*]pyrene	226
22	Benz[*a*]anthracene	228
23	Chrysene	228
24	Benzanthrone	230
25	2-Nitrofluoranthene	247
26	Benz[*a*]anthracene-7,12-dione	258
27	1-Nitropyrene	247
28	2-Nitropyrene	247
29	Benzo[*b*]fluoranthene	252
30	Benzo[*j*]fluoranthene	252
31	Benzo[*k*]fluoranthene	252
32	Benzo[*a*]fluoranthene	252
33	Benzo[*e*]pyrene	252
34	Benzo[*a*]pyrene	252
35	Perylene	252
36	3-Methylcholanthrene	268
37	Benzo[*c*]chrysene	278
38	Indeno[1,2,3-*cd*]pyrene	276
39	Dibenz[*a,c*]anthracene	278
40	Dibenz[*a,h*]anthracene	278
41	Benzo[*b*]chrysene	278
42	Picene	278
43	Benzo[*ghi*]perylene	276
44	Anthanthrene	276

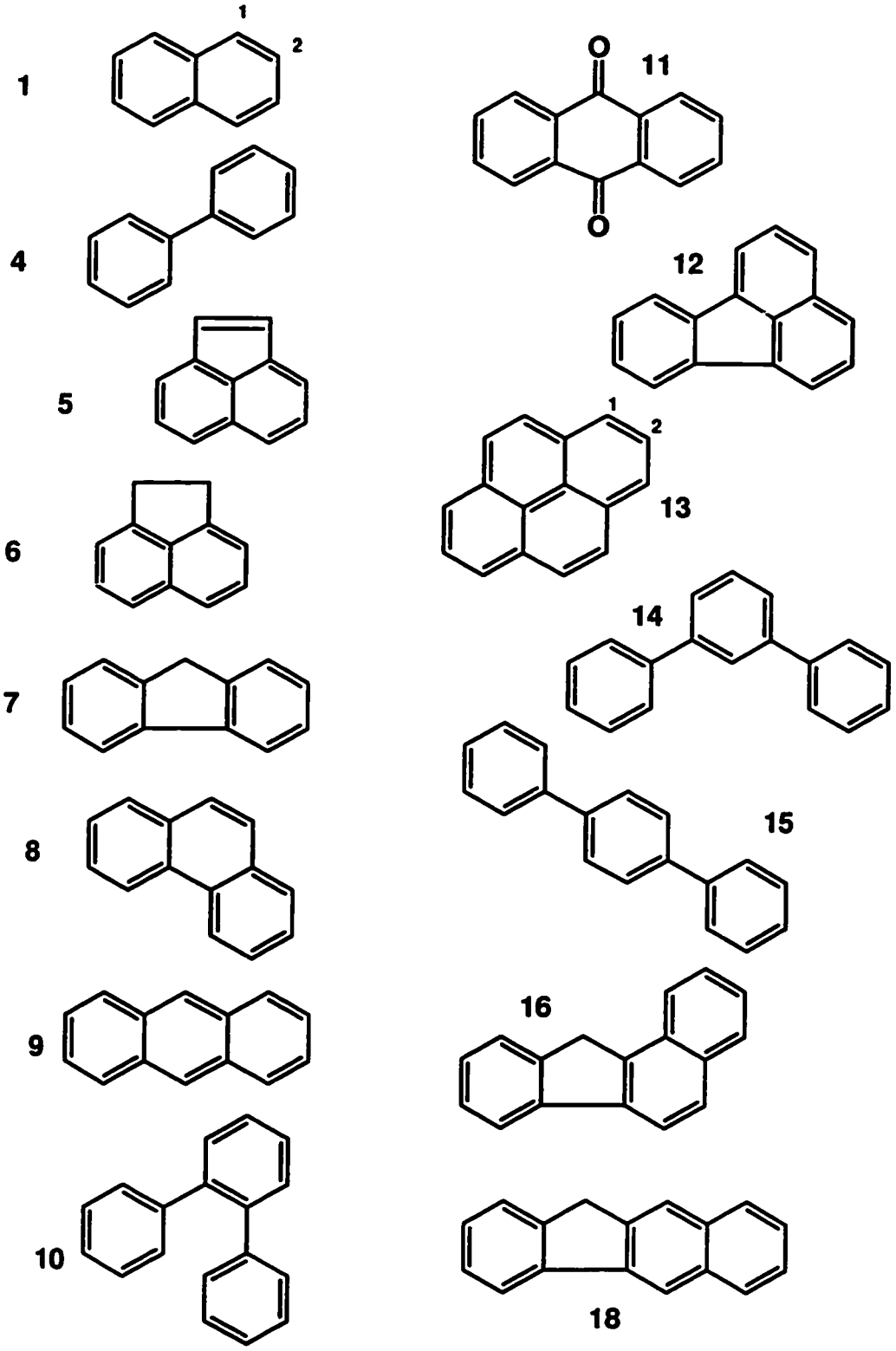
1
1
2
4
5
6
7
8
9
10
O
O
11
12
1
2
13
14
15
16
18

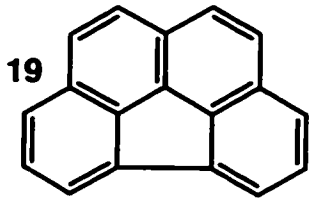

19

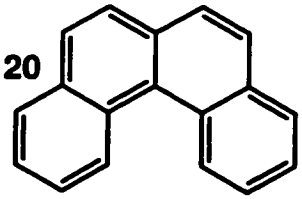

20

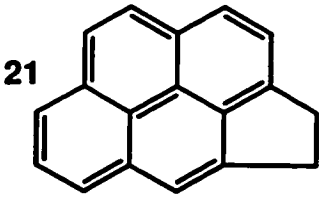

21

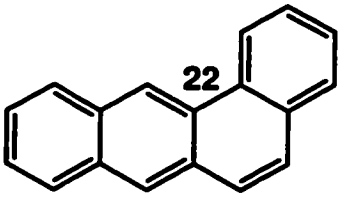

22

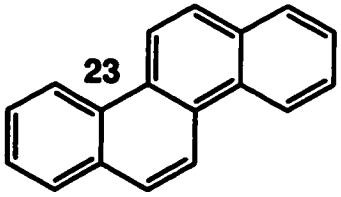

23

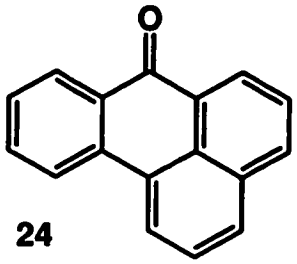

24

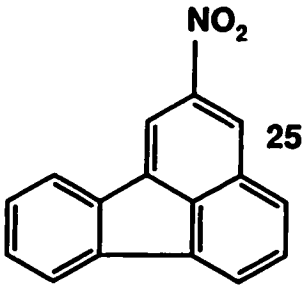

25

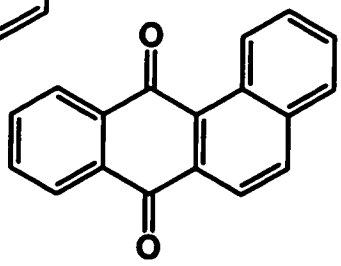

26

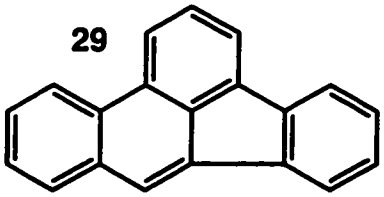

29

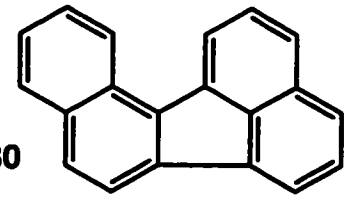

30

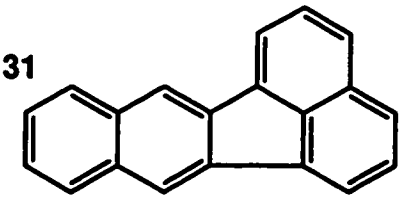

31

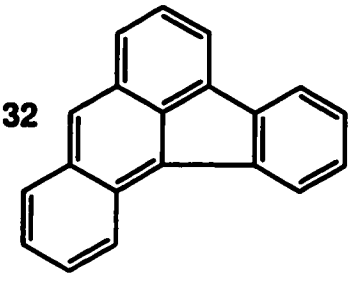

32

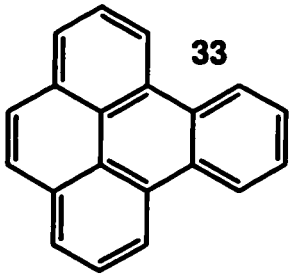

33

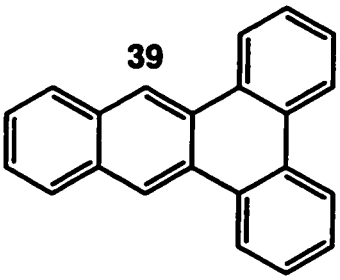

39

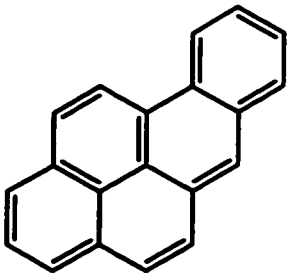

34

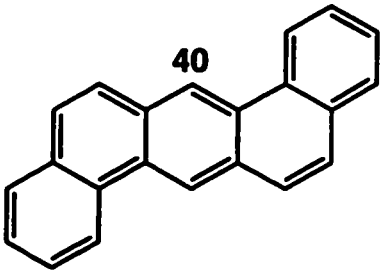

40

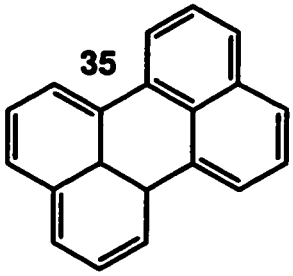

35

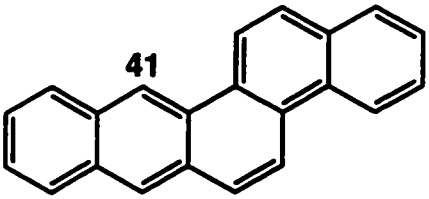

41

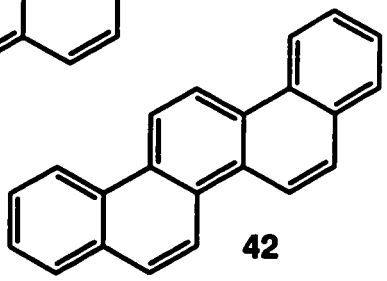

42

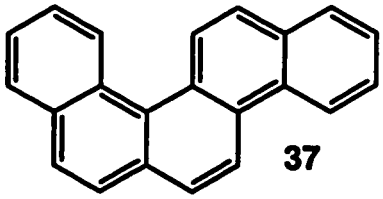

37

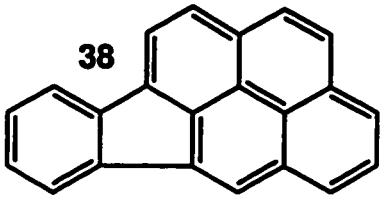

38

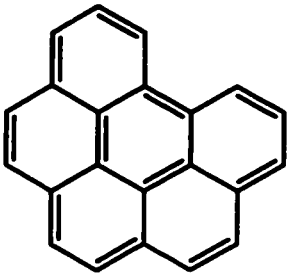

43

No.	Compound	Mol. Wt.
50	Naphtho[1,2-*b*]thiophene	184
51	Dibenzothiophene	184
52	Naphtho[2,1-*b*]thiophene	184
53	Naphtho[2,3-*b*]thiophene	184
54	4-Methyldibenzothiophene	198
55	8-Methylnaphtho[1,2-*b*]thiophene	198
56	2-Methyldibenzothiophene	198
57	3-Methyldibenzothiophene	198
58	4-Methylnaphtho[1,2-*b*]thiophene	198
59	4-Methylnaphtho[2,1-*b*]thiophene	198
60	2-Methylnaphtho[2,1-*b*]thiophene	198
61	8-Methylnaphtho[2,1-*b*]thiophene	198
62	7-Methylnaphtho[2,1-*b*]thiophene	198
63	5-Methylnaphtho[2,1-*b*]thiophene	198
64	1-Methylnapho[2,1-*b*]thiophene	198
65	6-Methylnaphtho[2,1-*b*]thiophene	198
66	3-Ethyldibenzothiophene	212
67	4-Ethyldibenzothiophene	212
68	4,6-Dimethyldibenzothiophene	212
69	2-Ethyldibenzothiophene	212
70	2,6-Dimethyldibenzothiophene	212
71	3,6-Dimethyldibenzothiophene	212
72	2,8-Dimethyldibenzothiophene	212
73	3,7-Dimethyldibenzothiophene	212
74	1,6-Dimethyldibenzothiophene	212
75	1,8-Dimethyldibenzothiophene	212
76	1,3-Dimethyldibenzothiophene	212
77	3,4-Dimethyldibenzothiophene	212
78	1,7-Dimethyldibenzothiophene	212
79	Phenaleno[6,7-*bc*]thiophene	208

APPENDIX I. Structures of thia-arenes.

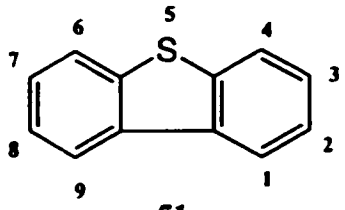

51

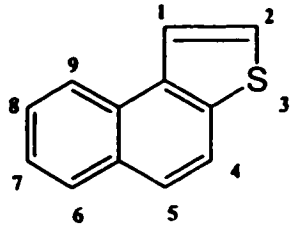

52

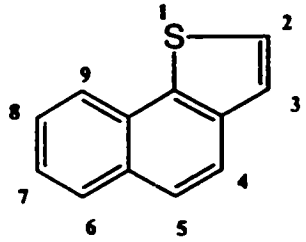

50

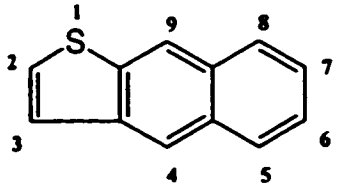

53

79

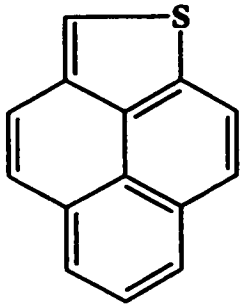

No.	Compound	Mol. Wt.
80	Benzo[*b*]naphtho[2,1-*d*]thiophene	234
81	Benzo[*b*]naphtho[1,2-*d*]thiophene	234
82	Phenanthro[9,10-*b*]thiophene	234
83	Phenanthro[4,3-*b*]thiophene	234
84	Anthra[1,2-*b*]thiophene	234
85	Phenanthro[1,2-*b*]thiophene	234
86	Benzo[*b*]naphtho[2,3-*d*]thiophene	234
87	Phenanthro[3,4-*b*]thiophene	234
88	Anthra[2,1-*b*]thiophene	234
89	Phenanthro[2,1-*b*]thiophene	234
90	Phenanthro[3,2-*b*]thiophene	234
91	Phenanthro[2,3-*b*]thiophene	234
92	Anthra[2,3-*b*]thiophene	234
93	Benzo[2,3]phenanthro[4,5-*bcd*]thiophene	258
94	Pyreno[4,5-*b*]thiophene	258
95	Benzo[1,2]phenaleno[3,4-*bc*]thiophene	258
96	Triphenyleno[4,5-*bcd*]thiophene	258
97	Pyreno[1,2-*b*]thiophene	258
98	Chryseno[4,5-*bcd*]thiophene	258
99	Pyreno[2,1-*b*]thiophene	258
100	Benzo[4,5]phenaleno[1,9-*bc*]thiophene	258
101	Benzo[4,5]phenaleno[9,1-*bc*]thiophene	258
102	Dinaphtho[2,1-*b* :1',2'-*d*]thiophene	284
103	Dinaphtho[1,2-*b* :2',1'-*d*]thiophene	284
104	Dinaphtho[1,2-*b* :1',2'-*d*]thiophene	284
105	Benzo[*b*]phenanthro[9,10-*d*]thiophene	284
106	Benzo[*b*]phenanthro[3,4-*d*]thiophene	284
107	Anthra[1,2-*b*]benzo[*d*]thiophene	284
108	Benzo[*b*]phenanthro[2,1-*d*]thiophene	284
109	Dinaphtho[1,2-*b* :2',3'-*d*]thiophene	284
110	Benzo[*b*]phenanthro[3,2-*d*]thiophene	284
111	Benzo[*b*]phenanthro[1,2-*d*]thiophene	284
112	Triphenyleno[2,1-*b*]thiophene	284
113	Dinaphth[2,3-*b* :2',3'-*d*]thiophene	284
114	Anthra[2,3-*b*]benzo[*d*]thiophene	284

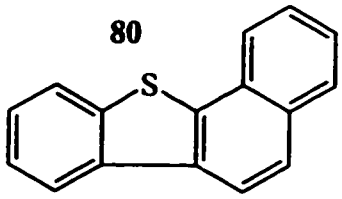
80
S

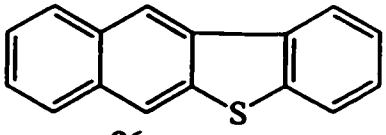
S
86

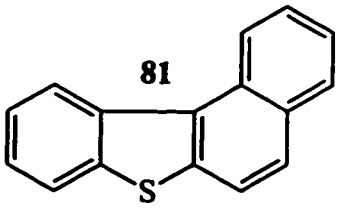
81
S

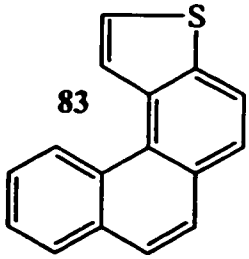
S
83

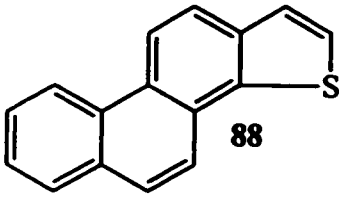
S
88

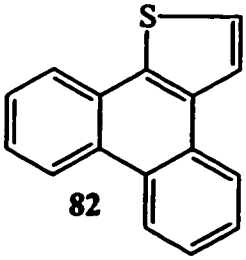
S
82

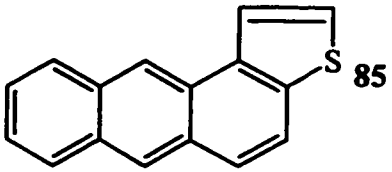
S
85

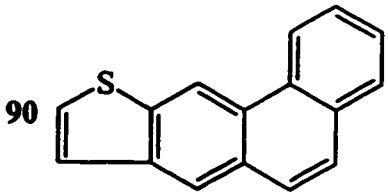
90
S

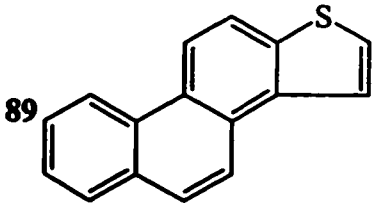
S
89

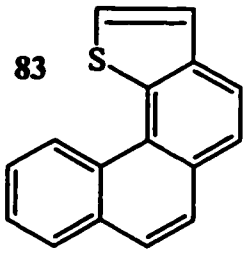
83
S

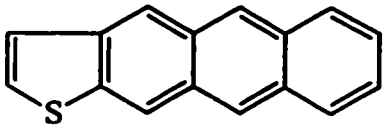
S
92

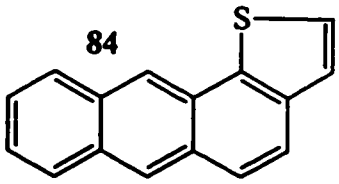
84
S

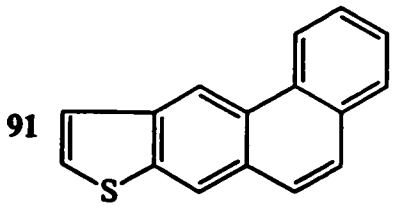
91
S

93

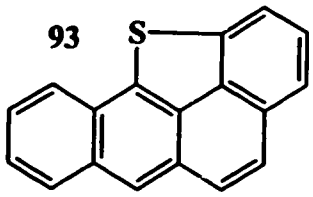

97

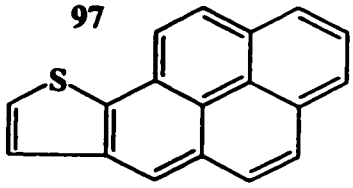

94

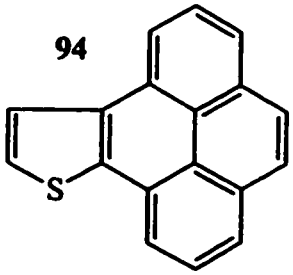

98

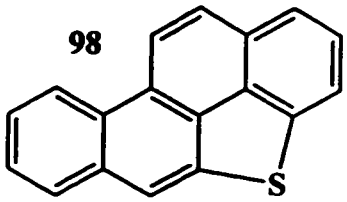

99

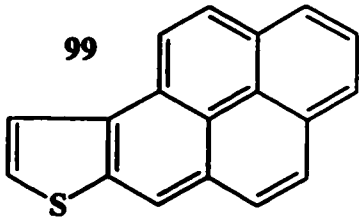

95

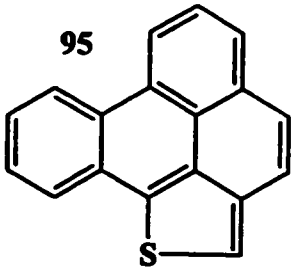

100

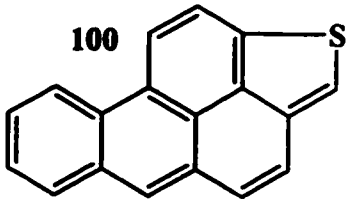

96

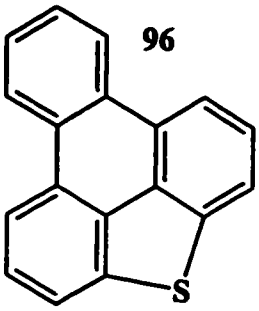

101

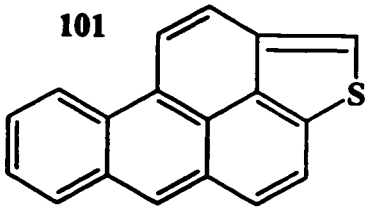

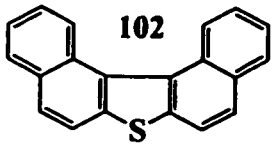
102
S

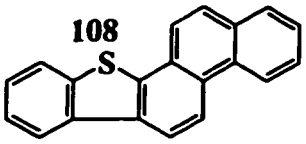
108
S

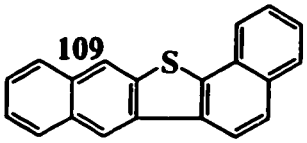
109
S

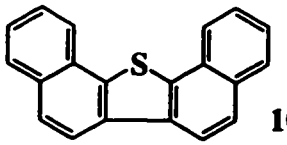
S
103

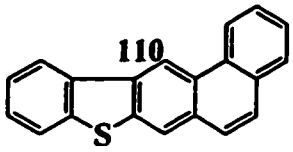
110
S

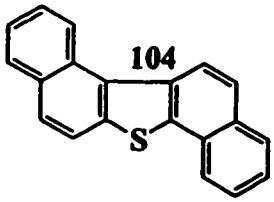
104
S

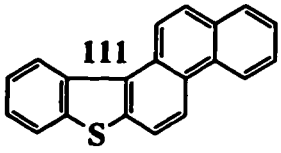
111
S

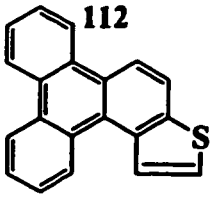
112
S

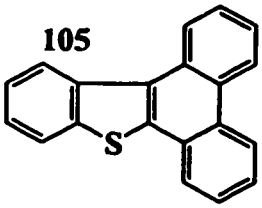
105
S

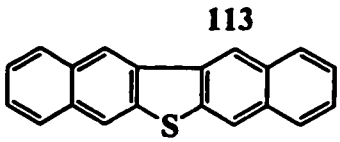
113
S

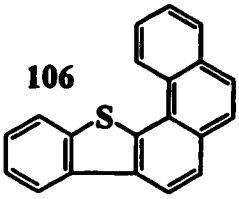
106
S

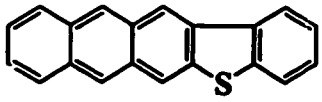
S
114

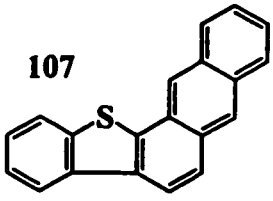
107
S

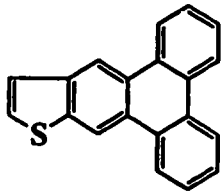
S
115

APPENDIX II. Lists of PAH concentrations for each day at each Station.

SITE 29000, PAH Concentrations in pg/m3												
Compound Name	20-Jul	23-Jul	27-Jul	28-Jul	29-Jul	1-Aug	2-Aug	4-Aug	5-Aug	6-Aug	7-Aug	8-Aug
Benzo[ghi]fluoranthene	25.7	42.9	150.2	31.9	11.5	16.6	146.6	32.9	14.7	88.3	169.1	145.7
Benzo[c]phenanthrene	10.3	19.2	65.7	16.9	4.6	6.1	7.0	11.8	4.7	45.2	105.0	63.5
Benz[a]anthracene	56.9	209.0	659.4	120.4	23.3	53.8	863.6	128.4	35.7	527.9	913.0	602.2
Cyclopenta[cd]pyrene	7.9	41.8	189.8	33.6	1.2	8.7	251.4	32.7	4.9	131.3	279.4	252.2
Chrysene	105.0	279.1	1020.5	213.0	62.7	100.5	1014.9	216.7	73.8	669.2	1117.2	817.2
Benzo[b]fluoranthene	82.4	438.9	1704.0	355.4	40.7	240.0	2139.0	823.6	91.0	1110.5	1919.4	1351.4
Benzo[k]fluoranthene	31.8	215.1	955.9	163.3	19.1	120.4	1089.3	325.2	43.1	555.3	943.0	669.9
Benzo[j]fluoranthene	31.7	220.6	944.1	161.0	16 2	117.4	1113.2	253.3	41.6	551.8	964.1	668.4
Benzo[e]pyrene	59.8	360.1	1586.1	272.1	25.8	196.5	2194.5	598.2	69.5	1036.3	1673.3	1193.6
Benzo[a]pyrene	34.8	397.2	1600.2	227.7	9.8	162.5	2127.9	427.9	38.1	1188.0	1606.8	1207.1
Perylene	7.8	104.5	242.9	57.4	1.9	46.7	572.1	134.4	8.0	331.6	447.3	327.0
Indeno[1,2,3-cd]pyrene	36.5	266.5	2084.2	386.0	16.9	228.2	1540.6	1091.0	83.8	870.4	1331.6	1084.4
Dibenz[a,c]anthracene	5.4	51.9	334.4	56.3	1.8	36.7	313.9	138.2	12.3	183.3	247.6	163.6
Benzo[ghi]perylene	93.8	465.3	2235.5	347.7	31.8	234.5	2904.9	774.5	117.1	1336.5	2464.5	1780.9
Coronene	55.7	203.5	1023.2	120.6	22.4	76.7	929.7	327.7	79.6	342.2	849.3	668.4
Total PAH (ng/m3)	0.65	3.3	15	2.6	0.29	1.6	17	5.3	0.72	9.0	15	11
Benzo[b]naphtho[2,1-d]thiophene	15.4	25.0	84.8	17.9	4.6	8.7	86.4	16.7	6.9	61.0	100.1	75.2

SITE 29000, PAH Concentrations in pg/m3 Compound Name	9-Aug	10-Aug	11-Aug	12-Aug	13-Aug	15-Aug	16-Aug	17-Aug	18-Aug	19-Aug	20-Aug
Benzo[ghi]fluoranthene	133.0	55.5	17.1	13.4	132.2	22.1	411.4	248.1	375.7	164.1	79.3
Benzo[c]phenanthrene	56.6	17.2	7.1	5.1	68.7	4.2	181.7	128.7	158.4	91.0	45.2
Benz[a]anthracene	590.4	172.3	39.5	32.4	668.4	28.3	1980.7	1330.8	1868.3	833.2	270.7
Cyclopenta[cd]pyrene	176.1	33.2	7.3	9.9	177.4	11.3	459.9	206.1	408.2	243.2	62.0
Chrysene	852.2	272.3	95.3	57.4	964.2	75.3	2749.1	1841.4	2668.9	1046.1	485.3
Benzo[b]fluoranthene	1877.2	530.6	95.4	111.8	1514.5	125.6	5635.4	4371.0	4553.4	1806.9	641.4
Benzo[k]fluoranthene	872.6	255.2	34.6	44.4	674.1	43.7	2697.6	2220.7	2423.0	845.9	330.6
Benzo[j]fluoranthene	883.3	257.1	37.0	50.6	669.3	48.1	2640.0	2188.5	2310.1	852.0	264.2
Benzo[e]pyrene	1617.5	464.2	63.4	95.8	1257.4	94.0	4625.7	4529.4	4513.8	1699.2	530.5
Benzo[a]pyrene	1494.0	388.4	34.3	61.5	1309.5	41.0	5062.7	3852.5	4513.0	1540.7	492.4
Perylene	430.8	102.8	10.0	17.3	333.2	9.1	1151.3	780.2	955.8	377.8	89.0
Indeno[1,2,3-cd]pyrene	1192.9	991.4	38.0	74.4	2083.2	49.1	8641.7	7744.9	8935.1	3526.0	1035.6
Dibenz[a,c]anthracene	239.5	238.4	6.2	13.5	321.9	5.8	840.8	703.8	750.9	208.8	87.4
Benzo[ghi]perylene	1909.1	655.0	87.6	216.0	1496.5	202.8	5565.9	6158.1	7653.7	2698.8	652.7
Coronene	614.4	256.3	54.2	106.5	560.8	161.6	1735.5	2443.0	2993.3	1083.1	309.5
Total PAH (ng/m3)	13	4.7	0.63	0.91	12	0.92	44	39	45	17	5.4
Benzo[b]naphtho[2,1-d]thiophene	79.7	25.5	10.2	6.7	84.0	9.0	221.1	150.8	200.8	97.5	53.2

SITE 29113, PAH Concentrations in pg/m3 Compound Name	20-Jul	23-Jul	29-Jul	1-Aug	4-Aug	5-Aug	6-Aug	7-Aug	8-Aug	9-Aug	10-Aug
Benzo[ghi]fluoranthene	13.1	7.0	17.9	27.8	71.7	9.2	31.5	49.1	98.0	47.8	40.1
Benzo[c]phenanthrene	5.3	3.3	6.5	11.4	32.6	4.3	18.7	27.4	60.1	24.2	19.1
Benz[a]anthracene	28.3	15.1	32.8	79.8	317.7	29.9	173.8	279.8	497.9	228.1	151.6
Cyclopenta[cd]pyrene	6.5	4.2	6.8	10.8	86.4	7.3	25.2	38.6	61.8	9.5	17.0
Chrysene	66.8	30.7	77.1	175.0	500.5	59.9	259.8	380.4	678.0	360.0	272.6
Benzo[b]fluoranthene	71.5	66.8	126.7	213.1	823.3	129.8	784.5	924.2	1314.8	721.0	454.9
Benzo[k]fluoranthene	34.2	23.2	45.6	80.7	394.4	59.4	391.0	506.2	644.2	283.8	236.7
Benzo[j]fluoranthene	37.7	26.6	54.9	94.2	426.3	55.9	341.7	531.6	658.9	298.8	219.9
Benzo[e]pyrene	62.3	56.5	146.9	170.9	710.7	99.9	644.8	845.3	902.0	539.6	346.6
Benzo[a]pyrene	47.8	26.0	58.0	121.2	665.3	63.5	454.4	748.2	852.5	338.6	241.9
Perylene	10.9	6.2	12.3	27.1	190.0	16.9	135.2	244.3	263.7	97.6	61.0
Indeno[1,2,3-cd]pyrene	101.1	90.9	133.9	435.3	930.1	129.0	1011.9	1025.4	1583.0	1182.0	692.3
Dibenz[a,c]anthracene	6.5	8.9	16.5	20.4	113.9	9.5	57.5	251.7	237.6	105.2	56.8
Benzo[ghi]perylene	108.1	91.2	190.0	227.1	888.3	145.4	876.0	1092.0	1287.3	544.1	374.4
Coronene	73.1	65.1	112.4	120.6	350.6	81.2	23.5	371.8	547.5	155.6	123.8
Total PAH (ng/m3)	0.67	0.52	1.0	1.8	6.5	0.90	5.2	7.3	9.7	4.9	3.3
Benzo[b]naphtho[2,1-d]thiophene	7.8	4.0	11.7	21.3	45.1	5.3	24.9	38.4	75.3	44.6	28.8
% Phenanthrene-d_{10}	78	70	76	na	75	9	21	5	65	79	76
% Chrysene-d_{12}	84	81	92	na	111	50	42	70	63	75	83
% Dibenz[ah]anthracene-d_{14}	82	79	88	na	92	38	46	71	91	62	76

na=not added

SITE 29113, PAH Concentrations in pg/m3 Compound Name	11-Aug	12-Aug	13-Aug	14-Aug	15-Aug	16-Aug	17-Aug	18-Aug	19-Aug	20-Aug
Benzo[ghi]fluoranthene	17.2	101.0	104.7	514.9	29.7	96.0	290.1	108.2	183.6	156.6
Benzo[c]phenanthrene	8.8	37.9	47.3	291.9	11.7	45.2	150.7	44.2	87.2	96.6
Benz[a]anthracene	47.7	485.4	452.1	2893.0	108.1	449.9	2179.5	588.1	447.3	590.1
Cyclopenta[cd]pyrene	4.7	251.7	158.9	674.6	25.1	87.2	329.8	129.0	44.4	159.5
Chrysene	90.9	665.8	701.0	3873.0	166.7	703.0	2646.1	866.4	1305.8	1163.6
Benzo[b]fluoranthene	79.9	1521.1	1416.6	5069.1	281.0	1064.9	5341.2	1885.9	5425.4	1300.8
Benzo[k]fluoranthene	31.4	724.6	397.7	2471.8	118.6	483.9	2021.0	1283.9	2681.6	580.7
Benzo[j]fluoranthene	34.7	780.2	649.8	2654.4	128.0	543.8	1799.9	1145.5	2579.5	592.9
Benzo[e]pyrene	59.0	915.6	1107.4	4422.2	228.7	900.4	3895.9	1886.1	4543.5	1045.8
Benzo[a]pyrene	35.1	1606.8	1007.1	4274.3	183.5	857.4	3446.2	1811.2	3755.8	993.1
Perylene	7.2	577.3	307.6	1213.4	49.1	224.9	1040.3	508.6	591.6	226.4
Indeno[1,2,3-cd]pyrene	64.5	1961.5	1840.9	5261.4	609.7	975.0	5423.7	3343.4	5998.0	3925.9
Dibenz[a,c]anthracene	5.4	335.3	215.4	794.9	33.2	192.1	979.5	376.3	774.9	209.9
Benzo[ghi]perylene	93.8	2446.8	1579.8	4409.5	351.2	1063.9	3233.8	2434.7	4825.3	1608.6
Coronene	66.8	891.9	736.3	1071.8	228.5	487.3	1029.7	646.1	1215.3	746.0
Total PAH (ng/m3)	0.65	13	11	40	2.6	8.2	34	17	34	13
Benzo[b]naphtho[2,1-d]thiophene	13.5	46.9	68.4	353.0	17.9	65.6	207.3	82.7	125.6	117.7
% Phenanthrene-d_{10}	75	80	77	72	na	na	na	na	na	na
% Chrysene-d_{12}	87	89	85	110	na	na	na	na	na	na
% Dibenz[ah]anthracene-d_{14}	92	87	89	101	na	na	na	na	na	na

na=not added

SITE 29547, PAH Concentrations in pg/m3												
Compound Name	20-Jul	23-Jul	27-Jul	28-Jul	29-Jul	1-Aug	2-Aug	4-Aug	5-Aug	6-Aug	7-Aug	8-Aug
Benzo[ghi]fluoranthene	232.6	436.5	49.7	121.3	605.0	176.4	33.9	164.9	35.1	4.6	25.0	26.6
Benzo[c]phenanthrene	108.0	235.2	21.5	63.6	332.2	74.8	11.8	93.4	19.4	2.1	13.2	9.9
Benz[a]anthracene	1428.5	2556.9	143.6	725.2	3583.0	1013.3	127.5	700.9	159.7	10.7	41.3	71.2
Cyclopenta[cd]pyrene	401.5	830.1	15.8	125.6	1240.5	279.7	12.9	191.9	20.1	nd	4.2	11.1
Chrysene	1754.5	3078.4	337.2	1063.7	4472.9	1348.9	286.8	1150.7	255.1	26.4	108.7	177.8
Benzo[b]fluoranthene	2938.5	5246.0	282.4	2287.2	5459.9	2963.4	231.0	1733.3	576.0	39.2	65.7	210.2
Benzo[k]fluoranthene	2004.0	2483.8	112.0	1098.0	2925.1	1523.9	109.8	763.8	270.6	12.4	19.3	76.5
Benzo[j]fluoranthene	1878.0	2619.1	117.0	1104.0	2989.0	1359.3	104.1	860.2	265.5	10.0	23.0	77.1
Benzo[e]pyrene	2894.3	4484.0	192.8	1963.1	4542.6	2439.9	164.1	1454.5	454.5	21.0	40.1	142.4
Benzo[a]pyrene	3389.5	4811.6	135.7	1849.7	5663.4	2353.6	121.8	1472.2	282.9	3.7	15.3	95.5
Perylene	917.8	1331.5	21.6	578.7	1552.1	653.1	21.5	382.9	85.3	0.0	3.2	213.6
Indeno[1,2,3-cd]pyrene	5450.5	7950.0	227.4	2249.4	5158.6	5766.2	102.1	1883.3	569.2	14.4	24.1	256.6
Dibenz[a,c]anthracene	566.8	651.0	21.5	355.2	798.4	505.4	15.8	222.0	7.2	nd	2.9	12.8
Benzo[ghi]perylene	4298.1	5923.5	182.1	2134.6	5174.1	3165.5	178.7	1737.5	459.3	15.1	32.8	142.6
Coronene	1176.8	1872.1	89.9	593.3	1675.3	795.4	61.2	524.8	132.3	8.2	17.2	58.9
Total PAH (ng/m3)	29	45	2.0	16	46	24	1.6	13	3.6	0.17	0.44	1.6
Benzo[b]naphtho[2,1-d]thiophene	155.6	287.5	40.1	103.0	409.8	138.2	25.7	104.3	22.0	2.2	12.8	18.5
% Phenanthrene-d_{10}	72	66	88	76	77	na	na	71	31	3	2	83
% Chrysene-d_{12}	86	83	84	86	87	na	na	104	46	33	70	88
% Dibenz[ah]anthracene-d_{14}	122	89	88	90	88	na	na	88	46	36	65	88

nd = not detected, na=not added

SITE 29547, PAH Concentrations in pg/m3 Compound Name	9-Aug	10-Aug	11-Aug	12-Aug	13-Aug	14-Aug	15-Aug	16-Aug	17-Aug	18-Aug	19-Aug	20-Aug
Benzo[ghi]fluoranthene	14.7	42.1	340.3	71.0	10.4	171.7	133.2	60.5	23.6	25.4	15.3	173.9
Benzo[c]phenanthrene	6.5	15.3	188.3	39.8	5.1	86.0	53.1	21.2	7.6	8.6	5.5	117.2
Benz[a]anthracene	45.6	283.7	2168.0	358.2	31.2	969.6	672.8	187.3	67.0	67.4	27.1	307.1
Cyclopenta[cd]pyrene	4.6	23.2	469.2	87.1	5.5	190.5	208.3	47.9	11.4	11.9	4.6	19.6
Chrysene	97.1	443.8	2776.9	456.9	92.6	1390.4	878.9	376.8	160.5	152.1	100.5	1186.9
Benzo[b]fluoranthene	83.5	651.6	4577.4	545.1	127.6	2641.8	1449.0	434.4	110.5	139.9	213.3	2364.1
Benzo[k]fluoranthene	38.5	248.5	2359.7	244.8	42.0	1228.8	627.3	206.4	62.9	61.7	68.8	1200.5
Benzo[j]fluoranthene	37.3	275.3	2461.2	274.4	43.6	1399.2	620.7	219.4	63.0	65.6	66.9	1167.2
Benzo[e]pyrene	57.0	425.8	4032.3	450.6	92.5	2300.9	1215.8	384.1	124.7	112.5	147.2	1868.6
Benzo[a]pyrene	52.4	358.5	4432.4	531.4	43.5	2425.2	1295.0	316.9	83.8	80.9	55.5	1556.6
Perylene	11.0	99.0	1283.7	149.1	9.6	696.1	387.3	70.3	19.7	19.5	11.1	194.9
Indeno[1,2,3-cd]pyrene	116.5	841.2	4478.4	756.7	83.3	2641.8	3741.5	488.2	163.9	174.9	139.2	2432.5
Dibenz[a,c]anthracene	8.3	68.6	797.0	103.1	8.0	381.3	223.4	57.6	16.7	15.8	12.4	178.7
Benzo[ghi]perylene	56.8	355.5	4329.7	528.3	84.4	2393.8	1612.7	541.3	145.4	142.5	123.6	2133.9
Coronene	20.6	103.4	972.9	191.3	39.6	575.4	446.8	214.8	66.5	65.8	54.5	718.7
Total PAH (ng/m3)	0.65	4.2	36	4.8	0.72	19	14	3.6	1.1	1.1	1.0	16
Benzo[b]naphtho[2,1-d]thiophene	11.2	39.1	245.2	52.6	12.7	125.4	92.1	42.1	14.2	17.4	10.2	133.6
% Phenanthrene-d_{10}	82	73	61	88	79	72	na	na	na	na	na	na
% Chrysene-d_{12}	82	82	88	98	89	112	na	na	na	na	na	na
% Dibenz[ah]anthracene-d_{14}	83	73	94	94	91	95	na	na	na	na	na	na

SITE 29531, PAH Concentrations in pg/m3 Compound Name	20-Jul	23-Jul	27-Jul	28-Jul	29-Jul	1-Aug	2-Aug	4-Aug	5-Aug	6-Aug	7-Aug	8-Aug
Benzo[ghi]fluoranthene	38.7	9.3	402.8	149.2	49.9	70.4	1060.8	154.5	4.8	407.4	1218.5	1072.6
Benzo[c]phenanthrene	22.8	4.3	207.8	82.8	5.9	38.4	562.3	75.6	2.1	231.0	777.7	487.6
Benz[a]anthracene	141.5	24.3	1979.7	750.1	28.7	353.0	6752.8	787.1	11.7	2600.9	7581.9	4651.7
Cyclopenta[cd]pyrene	8.4	6.1	810.2	312.9	7.8	110.9	2116.0	235.9	1.5	719.7	2531.8	2527.6
Chrysene	236.2	43.4	2662.2	962.7	64.1	530.0	8096.1	1171.8	35.1	3210.4	9232.1	5893.1
Benzo[b]fluoranthene	245.0	69.6	4373.2	1720.1	104.6	1352.9	14545.1	2087.7	58.6	5460.4	18259.5	12488.9
Benzo[k]fluoranthene	128.9	28.6	2066.5	857.7	39.5	470.8	7157.9	1043.9	21.5	3088.2	9253.7	5906.3
Benzo[j]fluoranthene	126.8	32.2	2142.7	893.3	46.2	549.2	7012.4	1121.5	20.3	2823.1	9515.1	6036.1
Benzo[e]pyrene	192.9	52.2	3601.4	1445.7	84.6	1032.6	11543.3	1769.3	31.8	4564.9	15290.0	10536.0
Benzo[a]pyrene	207.1	38.0	3883.1	1501.5	39.9	715.8	10440.4	1765.4	11.2	4527.2	13329.6	8621.5
Perylene	53.2	8.9	1154.7	429.5	9.5	249.9	2800.5	497.2	2.6	1224.3	4017.5	2332.8
Indeno[1,2,3-cd]pyrene	335.5	88.0	6268.6	2046.6	90.7	2891.2	8068.0	2055.0	28.6	5319.0	21794.7	11502.3
Dibenz[a,c]anthracene	38.3	2.0	489.2	276.5	8.8	185.6	1564.3	244.1	3.1	820.3	2848.3	1577.4
Benzo[ghi]perylene	218.6	76.3	4106.2	1763.7	301.6	1141.1	14751.8	1976.0	30.3	5214.2	26787.0	12520.7
Coronene	75.4	52.3	1358.7	561.6	480.3	345.0	5016.4	549.6	19.8	1470.6	7588.6	3050.9
Total PAH (ng/m3)	2.1	0.54	36	14	1.4	10	101	16	0.28	42	150	89
Benzo[b]naphtho[2,1-d]thiophene	26.6	4.8	255.5	86.0	9.5	48.0	610.3	93.0	2.9	282.1	759.1	536.5
% Phenanthrene-d_{10}	72	74	65	76	77	na	na	73	10	40	81	76
% Chrysene-d_{12}	79	79	81	82	86	na	na	111	42	48	92	92
% Dibenz[ah]anthracene-d_{14}	84	82	91	83	92	na	na	92	44	77	114	95

na=not added

SITE 29531, PAH Concentrations in pg/m3												
Compound Name	9-Aug	10-Aug	11-Aug	12-Aug	13-Aug	14-Aug	15-Aug	16-Aug	17-Aug	18-Aug	19-Aug	20-Aug
Benzo[ghi]fluoranthene	202.5	77.5	18.2	12.5	225.0	604.7	157.2	309.7	450.0	384.4	727.5	117.4
Benzo[c]phenanthrene	94.1	32.9	9.7	5.2	121.8	286.3	55.8	158.5	187.9	196.4	428.1	69.7
Benz[a]anthracene	972.5	389.5	48.7	38.3	1237.5	3090.2	506.5	1624.9	2453.1	2032.8	3432.3	410.1
Cyclopenta[cd]pyrene	304.0	93.8	3.5	9.9	440.2	1443.7	85.8	646.8	1004.2	671.8	948.3	134.4
Chrysene	1403.0	625.2	130.0	65.7	1596.8	4150.5	1079.2	2035.1	3132.0	2839.4	5045.5	741.8
Benzo[b]fluoranthene	3538.3	1183.1	172.6	95.3	3106.6	8049.7	856.8	6170.4	6861.7	6373.9	9731.2	960.9
Benzo[k]fluoranthene	1458.0	822.0	63.9	35.3	1380.4	2950.3	204.8	2932.0	2888.9	3539.0	4856.2	441.2
Benzo[j]fluoranthene	1510.4	808.4	67.4	41.3	1491.6	3589.8	467.4	2787.0	3431.6	3446.3	4865.4	445.4
Benzo[e]pyrene	2908.9	1092.6	94.1	66.2	2764.9	7148.8	848.1	5469.9	6008.5	6297.5	8984.5	736.0
Benzo[a]pyrene	1691.0	929.5	46.4	34.8	2389.6	6350.1	603.4	5333.2	5522.1	5988.8	7530.7	718.0
Perylene	432.2	249.5	10.5	8.4	683.8	2036.4	187.4	1544.1	1663.4	1693.7	1726.4	154.2
Indeno[1,2,3-cd]pyrene	7344.1	2952.4	16.1	102.5	4254.5	12545.9	1176.5	17793.4	7984.3	12400.4	11445.1	1171.5
Dibenz[a,c]anthracene	565.6	195.3	7.5	9.0	683.8	1090.0	94.2	1137.5	1377.5	1232.7	1711.1	138.8
Benzo[ghi]perylene	3845.2	1303.6	74.8	104.0	3410.1	9327.1	946.1	8416.5	7997.5	10901.5	13608.6	913.9
Coronene	1272.4	417.5	37.0	65.0	933.2	2839.4	303.7	2323.5	2515.1	3157.7	5619.1	402.1
Total PAH (ng/m3)	28	11	0.80	0.69	25	66	7.6	59	53	61	81	7.6
Benzo[b]naphtho[2,1-d]thiophene	114.4	59.3	13.0	7.5	153.2	364.2	107.8	182.0	228.6	249.1	442.4	84.5
% Phenanthrene-d_{10}	76	81	79	76	75	76	na	na	na	na	na	na
% Chrysene-d_{12}	89	88	93	90	93	92	na	na	na	na	na	na
% Dibenz[ah]anthracene-d_{14}	100	110	91	92	95	101	na	na	na	na	na	na

na=not added